

Univerzita Karlova v Praze
1. lékařská fakulta

Studijní program: Neurovědy



MUDr. Mgr. Helena Janíčková

Cholinergní muskarinová transmise a Alzheimerova choroba

Muscarinic acetylcholine transmission and Alzheimer's disease

Disertační práce

Školitel: MUDr. Vladimír Doležal, DrSc.

Praha, 2013

**Univerzita Karlova v Praze, 1. lékařská fakulta
Kateřinská 32, Praha 2**

**Prohlášení zájemce o nahlédnutí
do závěrečné práce absolventa studijního programu
uskutečňovaného na 1. lékařské fakultě Univerzity Karlovy v Praze**

Jsem si vědom/a, že závěrečná práce je autorským dílem a že informace získané nahlédnutím do zpřístupněné závěrečné práce nemohou být použity k výdělečným účelům, ani nemohou být vydávány za studijní, vědeckou nebo jinou tvůrčí činnost jiné osoby než autora.

Byl/a jsem seznámen/a se skutečností, že si mohu pořizovat výpisy, opisy nebo kopie závěrečné práce, jsem však povinen/a s nimi nakládat jako s autorským dílem a zachovávat pravidla uvedená v předchozím odstavci.

Prohlášení:

Prohlašuji, že jsem disertační práci zpracovala samostatně a že jsem řádně uvedla a citovala všechny použité prameny a literaturu. Současně prohlašuji, že práce nebyla využita k získání jiného nebo stejného titulu.

Souhlasím s trvalým uložením elektronické verze mé práce v databázi systému meziuniverzitního projektu Theses.cz za účelem soustavné kontroly podobnosti kvalifikačních prací.

V Praze, 23.1.2013

HELENA JANÍČKOVÁ

Podpis

Identifikační záznam:

JANÍČKOVÁ, Helena. *Cholinergní muskarinová transmise a Alzheimerova choroba. [Muscarinic acetylcholine transmission and Alzheimer's disease]*. Praha, 2013. 84 s., 6 příloh. Disertační práce (Ph.D.). Univerzita Karlova v Praze, 1. lékařská fakulta. Školitel Doležal, Vladimír.

Poděkování

Ráda bych poděkovala především svému školiteli MUDr. Vladimíru Doležalovi, DrSc. za dlouhodobé odborné vedení, za všechno, co jsem se od něj mohla naučit nejen z hlediska technik a metod, ale také z hlediska přístupu k vědeckým problémům a jejich řešení. Děkuji mimo jiné také za to, že jsem i díky jemu neztratila chuť se vědě i dále věnovat. Děkuji mu za jeho lidský přístup a za schopnost vytvořit pracovní kolektiv, na který budu vždycky ráda vzpomínat.

Za pomoc a všeestrannou podporu děkuji také všem ostatním (bývalým i současným) spolupracovníkům z oddělení Neurochemie, se kterými jsem měla to štěstí se během mého doktorského studia potkat.

Publikace, které jsou součástí této dizertační práce, byly podporovány grantem EU LipiDiDiet (FP7 program, Grant Agreement No 211696) a granty GACR 305/09/0681, GACR P304/12/G069, IAA500110703 a MSMT CR LC554, s podporou na dlouhodobý koncepční rozvoj výzkumné organizace AV0Z50110509 a RVO:67985823.

Obsah

Seznam zkratek	8
Úvod	10
1. Alzheimerova choroba	10
2. Muskarinové receptory	13
3. Cholinergní hypotéza Alzheimerovy choroby	17
4. β -amyloid a amyloidová hypotéza Alzheimerovy choroby	21
5. Současné možnosti léčby Alzheimerovy choroby	24
6. Poškození cholinergní signalizace u zvířecích modelů Alzheimerovy choroby	27
7. β -amyloid a poškození funkce muskarinových receptorů	29
Cíle práce a hypotézy	31
Metody	32
1. Experimentální zvířata a příprava membrán	32
2. Buněčné kultury a příprava membrán	32
3. Vazebné saturační a kompetiční studie	33
4. Vazba ^{35}S -GTP γS	35
5. Měření akumulace inositolfosfátů a inhibice syntézy cAMP	35
6. Stanovení kaspázové aktivity a oxidační aktivity	36
7. Určení stupně agregace A β_{1-42}	37
8. Stanovení proteinů	37
9. Vyhodnocení výsledků	37
Výsledky	40
1. Vliv A β_{1-42} na vazebné vlastnosti jednotlivých podtypů mAChR	40
1.1. Vliv A β_{1-42} na vazebné vlastnosti mAChR pro [^3H]-NMS	40
1.2. Vliv A β_{1-42} na vazebné vlastnosti mAChR pro karbachol	41
2. Vliv chronického působení A β_{1-42} na funkční vlastnosti jednotlivých podtypů mAChR	47
2.1. Vliv chronického působení A β_{1-42} na aktivaci G-proteinů	47
2.2. Vliv chronického působení A β_{1-42} na aktivaci nitrobuněčných signalačních drah M1-M2 mAChR	50
3. Aktivita kaspáz a tvorba volných kyslíkových radikálů v buňkách vystavených chronickému vlivu A β_{1-42}	52

4. Forma β -amyloidu 1-42 přítomného v kultivačním médiu	54
5. Vliv rozpustného amyloidu na aktivaci G-proteinů <i>in vivo</i> v mozkové kůře myší APPswe/PS1dE9	58
6. Vliv nutričně obohaceného média na vazbu [3 H]-NMS a aktivaci G-proteinů prostřednictvím mAChR	59
Diskuze	61
Závěr	69
Souhrn	71
Summary	72
Seznam použité literatury	73
Seznam příloh	84

Seznam zkratek

$\text{A}\beta_{1-42}$	β -amyloid 1-42
AChE	acetylcholinesteráza
APP	amyloid precursor protein (protein prekurzor amyloidu)
B_{\max}	maximální vazba
cAMP	cyklický adenosinmonofosfát
Cdk5	cyklin-dependentní kináza
ChAT	cholinacetyltransferáza
CHO	Chinese hamster ovary (fibroblasty z ovárií zlatého křečka)
DHA	dokosahexaenová kyselina
DMEM	Dulbecco's modified Eagle's medium
EC_{50}	effective concentration 50 (koncentrace vyvovávající polovinu max. odpovědi)
EDTA	ethylendiamintetraoctová kyselina
E_{\max}	maximální stimulace
EPA	eikosapentaenová kyselina
GDP	guanosin difosfát
GPCR	receptory spřažené s G-proteiny (G-protein coupled receptor)
GppHNP	guanosin-5'-($\beta\gamma$ -imino)trifosfát
GSK-3 β	glykogensyntáza-kináza-3 β
GTP	guanosin trifosfát
^{35}S -GTP γ S	radioaktivní izotop guanosin-5'-O-(γ -thio)trifosfátu
[^3H]-NMS	tritiovaná forma N-methylskopolaminu
IC_{50}	half maximal inhibitory concentration (koncentrace, která vytěsní 50% značeného ligandu; případně koncentrace agonisty vyvolávající 50% maximálního inhibičního účinku)
I_{\max}	maximální inhibice
IL-1, IL-6 a IL-10	interleukin-1, -6 a -10
K_d	rovnovážná disociační konstanta (koncentrace, při níž je obsazena polovina vazebných míst)
LTP	dlouhodobá potenciace (long term potentiation)
M1, M2, M3, M4 a M5	jednotlivé podtypy muskarinového receptoru

mAChR	muskarinový acetylcholinový receptor
MCI	mírný kognitivní deficit (mild cognitive impairment)
PAM	pozitivní alosterický modulátor
PBS	Phosphate Buffered Saline
RLU	relativní světelná jednotka (relative light unit)
sAPP	solubilní fragment APP
S.E.M.	střední chyba průměru (standard error of mean)
VAChT	vezikulární transportér acetylcholinu

Úvod

1. Alzheimerova choroba

Alzheimerova choroba je nejčastějším neurodegenerativním onemocněním u člověka. Poprvé byla popsána německým lékařem Aloisem Alzheimerem jako onemocnění nejasného původu, které se klinicky projevuje progresivní demencí, tedy postupným zhoršováním paměti a kognitivních funkcí. Charakteristickým *post mortem* patologickým znakem, který jednoznačně potvrzuje klinickou diagnózu, jsou extracelulární amyloidové plaky tvořené především bílkovinou β -amyloidem a dále intracelulární neurofibrilární klubka tvořená hyperfosforylovaným tau proteinem. Jak amyloidové plaky tak neurofibrilární klubka se nacházejí v mozkové kůře a hipokampu pacientů s Alzheimerovou chorobou. Dalším typickým patologickým znakem Alzheimerovy choroby je ztráta neuronů a neuronových synapsí v mozkové kůře a v hipokampu a dalších podkorových oblastech mozku.

Alzheimerova choroba se vyskytuje ve dvou základních formách – první bývá označována jako dědičná, druhá jako sporadicke forma onemocnění. Dědičná forma se začíná projevovat dříve, například již kolem 40. roku věku, vždy ale před 65. rokem věku. Tvoří přibližně jen asi 3 % všech případů onemocnění. Na druhou stranu mnohem častější forma sporadická se začíná projevovat až po 65. roce věku a s přibývajícím věkem její riziko výrazně stoupá. Alzheimerova choroba se o něco častěji vyskytuje u žen než u mužů.

Etiologie Alzheimerovy choroby je stále neznámá, i když do dnešní doby již byla vyslovena řada hypotéz o příčinách tohoto onemocnění. Od 80. let minulého století, kdy byla na základě pravidelného nálezu poškození cholinergních neuronů při pitvě formulována cholinergní hypotéza Alzheimerovy choroby (Bartus RT. et al., 1982), se zkoumá role cholinergní neurotransmise v etiologii a patogenezi Alzheimerovy choroby. Cholinergní hypotéza byla od chvíle svého vzniku již mnohokrát zpochybňena a v dnešní době všeobecně převládá později vyslovená amyloidová hypotéza (Hardy JA. et Higgins GA., 1992). Základem amyloidové hypotézy je myšlenka, že první příčinou onemocnění je zvýšená hladina amyloidogenních peptidů (zejména fragmentu 1-42; $A\beta_{1-42}$) odštěpovaných z bílkoviny prekurzor amyloidu (APP, amyloid precursor protein) a souhrnně označovaných jako β -amyloid. Ten se může v mozku vyskytovat v různých formách (různá délka fragmentu, agregovaný či rozpustný) a v dnešní době se má za to, že nejvíce škodlivé jsou nepříliš velké rozpustné oligomery amyloidogenních peptidů. Prvotní změny vyvolané těmito neurotoxicckými oligomery jsou skryté a pravděpodobně předcházejí klinickou diagnózu

onemocnění o desítky let. Cholinergní a amyloidová hypotéza Alzheimerovy choroby budou ještě podrobněji zmíněny v samostatné části úvodu této práce.

Na základní myšlence amyloidové hypotézy již bylo postaveno několik léčebných strategií Alzheimerovy choroby, z nichž se však až dosud žádná nesetkala s větším úspěchem. To je také jeden z důvodů, proč neustále probíhají snahy vysvětlit vznik Alzheimerovy choroby jiným mechanismem. Již delší dobu se například hromadí důkazy o spojení mezi Alzheimerovou chorobou a metabolismem cholesterolu. Některé mutace v genech, které kódují proteiny podílející se na metabolismu cholesterolu, byly identifikovány jako rizikové pro vznik sporadické formy Alzheimerovy choroby (Martins IJ. et al., 2009) a porušený metabolismus cholesterolu hráje pravděpodobně významnou roli při tvorbě amyloidových plaků a hyperfosforylace tau proteinu. Epidemiologické studie rovněž ukazují, že zvýšená hladina cholesterolu je rizikovým faktorem pro vznik Alzheimerovy choroby a podle některých údajů mohou dokonce léky snižující hladinu cholesterolu v krvi (statiny) snižovat riziko výskytu Alzheimerovy choroby (Kandiah N. et Feldman HH., 2009; Arvanitakis Z. et al., 2008). Jednou z molekul nejčastěji zmiňovaných v souvislosti s metabolismem cholesterolu a Alzheimerovou chorobou je apolipoprotein E, který je v mozku mimo jiné odpovědný za transport cholesterolu z astrocytů do neuronů, ale ovlivňuje také clearance β -amyloidu vzniklého štěpením APP. Již dlouho je známo, že homozygotní jedinci s alelou ApoE $\epsilon 4$ mají významně zvýšené riziko Alzheimerovy choroby oproti jedincům nesoucím alesy $\epsilon 2$ a $\epsilon 3$ (Evans RM. et al., 2004).

Zvýšená hladina cholesterolu se poměrně často objevuje společně s insulinovou rezistencí a v poslední době se ukazuje, že insulinová rezistence nebo přímo diabetes mellitus 2. typu zvyšují riziko vzniku Alzheimerovy choroby (Cole AR. et al., 2007). Na druhou stranu souvislost mezi insulinovou rezistencí a Alzheimerovou chorobou není natolik zřejmá, aby bylo možné hovořit o jediné společné příčině Alzheimerovy choroby a diabetu mellitus 2. typu. Spíše se zdá, že porucha metabolismu glukózy a insulinová rezistence urychlují progresi neurodegenerativních změn a ztráty synapsí v průběhu onemocnění (Williamson R. et al., 2012).

Za alternativu nebo dokonce protipól amyloidové hypotézy Alzheimerovy choroby je často pokládána teorie, která za hlavní faktor vyvolávající onemocnění považuje hyperfosforylovaný tau protein. Ten tvoří párová helikální filamenta agregující za vzniku intracelulárních neurofibrilárních klubek – vedle amyloidových plaků hlavní patologická známka Alzheimerovy choroby. Párová helikální filamenta je možné pozorovat v dendritech

jako neuropilová vlákna (threads) a v některých axonálních zakončeních obklopujících amyloidové plaky.

Tau protein patří mezi bílkoviny asociované s mikrotubuly. Za fyziologických podmínek podporuje polymerizaci jednotek tubulinu do mikrotubulů a podílí se tak na axonálním transportu, avšak abnormálně hyperfosforylovaný tau protein agreguje do podoby párových helikálních filament a ztrácí schopnost ovlivňovat polymerizaci tubulinu. Na hyperfosforylací tau proteinu se pravděpodobně podílí kinázy cyklin-dependentní kináza (Cdk5) a glykogensyntáza-kináza-3 β (GSK-3 β) (Noble W. et al., 2003).

Některé výsledky ukazují, že patologie tau proteinu a zvýšená produkce β -amyloidu spolu pravděpodobně úzce souvisí. Například syntetický β -amyloid injekčně aplikovaný transgenním myším exprimujícím modifikovaný lidský tau protein významně zvýšil výskyt neurofibrilárních klubek (Götz J et al., 2001). Podobně imunizace β -amyloidem u trojtě transgenního myšího modelu Alzheimerovy choroby měla za následek nejen snížení produkce β -amyloidu, ale také hyperfosforylovaného tau proteinu (Oddo S. et al., 2004). Další výsledky naznačují, že procesy vedoucí k nadprodukci β -amyloidu zároveň zvyšují aktivitu GSK-3 β , která je odpovědná za hyperfosforylací tau proteinu, a tau-kinázy tak mohou být spojujícím prvkem mezi oběma hlavními patologickými znaky Alzheimerovy choroby (Terwel D. et al., 2008).

Vedle již zmíněných teorií o příčinách vzniku a progrese Alzheimerovy choroby se vyskytuje ještě řada dalších. Například skutečnost, že v místě amyloidových plaků se často akumulují buňky mikroglie, vedla k myšlence, že na vzniku Alzheimerovy choroby se významně podílejí zánětlivé a imunologické mechanismy. Buňky mikroglie mají schopnost fagocytovat β -amyloid v reakci na jeho zvýšenou akumulaci (Kitamura Y. et al., 2003) a zvýšená aktivace fagocytózy β -amyloidu mikroglií se také stala jednou z uvažovaných strategií v léčbě Alzheimerovy choroby. Kromě úlohy mikroglie je v souvislosti s patogenezí Alzheimerovy choroby diskutována mimo jiné i role hematoencefalické bariéry, astrocytů, zánětlivých cytokinů (především IL-1, IL-6 a IL-10) nebo volných kyslíkových radikálů (Sardi F. et al., 2011). I když není jasné, nakolik jsou zánětlivé pochody odpovědné za vznik onemocnění a nakolik jsou jen jeho průvodním jevem, je velmi pravděpodobné, že zánětlivý proces hraje při vývoji onemocnění důležitou úlohu.

2. Muskarinové receptory

Muskarinové receptory (mAChR) jsou acetylcholinové receptory spadající do skupiny receptorů spřažených s G-proteiny (GPCR). V organismu jsou mAChR distribuovány jak v mozku tak také v mnoha dalších orgánech a tkáních. Dělí se do pěti podtypů M1 až M5 (Bonner TI. et al., 1987, 1988; Peralta EG. et al., 1987), z nichž vždy liché a sudé podtypy jsou si vzájemně funkčně i strukturně podobné. Acetylcholin jako přirozený ligand mAChR se váže také na nikotinové receptory, které však na rozdíl od mAChR patří do skupiny chemicky řízených iontových kanálů.

Muskarinové receptory se vyskytují prakticky v celém organizmu, například v neuronech centrálního i periferního nervového systému, v srdeční a hladké svalovině, žlázách s vnější i vnitřní sekrecí, ale také v bílých krvinkách nebo endoteliálních buňkách. V centrálním nervovém systému jsou zastoupené především podtypy M1, M2 a M4. Podtyp M4 se nachází na presynaptických i postsynaptických membránách především ve striatu a ovlivňuje funkci dopaminergního systému. Podtypy M1 a M2 se nacházejí ve velkém množství v hipokampu a mozkové kůře. Vzhledem k cholinergním neuronům je zde podtyp M2 převážně presynaptický receptor, který inhibuje uvolňování acetylcholinu, zatímco podtyp M1 je uložen postsynapticky. Distribuce mAChR v periferních tkáních i v centrálním nervovém systému se v minulosti zjišťovala pomocí radioaktivně značených antagonistů, jako jsou například neselektivní ^3H -N-methylskopolamin ($[^3\text{H}]\text{-NMS}$) nebo ^3H -pirenzepin, který vykazuje určitou selektivitu k M1 receptoru. Vazba ligandů byla lokalizována pomocí autoradiografické vizualizace, použité ligandy však neumožňovaly spolehlivě rozlišit jednotlivé podtypy mAChR.

Studie s komplementární RNA schopnou hybridizovat s mRNA jednotlivých podtypů mAChR přinesly o distribuci mAChR detailnější poznatky. Pokud byl však receptor exprimován v neuronech, mohly být výsledky studií s hybridizací mRNA zavádějící. mRNA je totiž produkována v buněčném těle, které může být i značně vzdáleno od výběžků neuronu, kde je nakonec funkční receptor lokalizován. Ještě přesnější určení lokalizace mAChR bylo proto dosaženo pomocí specifických protilátek zaměřených proti $-\text{NH}_2$ konci třetí intracelulární smyčky mAChR, nejvariabilnější části receptorů specifické pro jednotlivé podtypy (Levey AI., 1993).

V mozku potkanů je možné prokázat expresi mRNA pro všechny podtypy mAChR (Krejčí A. et Tuček S., 2002). Nejhojněji je zastoupena mRNA pro M1, zatímco v nejmenším

množství se vyskytuje mRNA pro M5. Mezi oblasti CNS, ve kterých byla prokázána mRNA pro M1 a zároveň také imunoreaktivita pro M1, patří mozková kůra, hipokampus, thalamus, caudatum, putamen a amygdala. V bulbus olfactorius a gyrus dentatus byla nalezena pouze M1 mRNA bez příslušné imunoreaktivity (Caulfield MP., 1993).

Oblastmi bohatými na M2 mRNA a zároveň vykazujícími M2 imunoreaktivitu jsou bazální telencefalon, caudatum, putamen, hipokampus, hypothalamus, amygdala a pontinní jádra. V bulbus olfactorius, habenulech, jádřech retikulární formace a locus coeruleus byla nalezena pouze M2 mRNA (Caulfield MP., 1993).

Podtyp M3 je typickým periferním receptorem, který se v CNS vyskytuje málo. Existuje studie, ve které nebyla pro M3 receptor nalezena imunoreaktivita v žádné ze studovaných oblastí mozku (Levey AI. et al., 1991). Na druhou stranu přítomnost M3 mRNA byla prokázána v mozkové kůře, hipokampu, mediálním thalamu, caudatu, putamen a amygdale (Buckley NJ. et al., 1988; Levey AI. et al., 1991). Jiná studie rovněž prokázala M3 imunoreaktivitu v mozkové kůře a hipokampu (Wall SJ. et al., 1991).

Pro M4 receptor byla nalezena mRNA a také imunoreaktivita v mozkové kůře, hipokampu, thalamu, caudatu a putamen.

Pro M5 receptor, stejně jako pro M3, nebyla podle Leveyho studie zjištěna v mozku žádná imunoreaktivita. Velmi nízká M5 imunoreaktivita však byla podle jiné studie nalezena ve striatu, hipokampu, středním mozku, pontomedulární oblasti a v mozečku (Yasuda RP. et al., 1993). M5 mRNA byla naopak prokázána v hipokampu, substantia nigra, amygdale, thalamu, hypothalamu a laterálních habenulech.

V periferních tkáních potvrdily pokusy s protitlákami i hybridizační mRNA studie přítomnost podtypů M1 a M3 v exokrinních žlázách (především slinných a slzných) (Dörje F. et al., 1991; Levey AI., 1993). V srdeční svalovině byl prokázán pouze M2 receptor. V hladké svalovině tenkého a tlustého střeva, trachey a močového měchýře nejsou výsledky různých studií jednotné, avšak obecně tyto tkáně obsahují především větší či menší množství podtypů M2, M3 a M4. V plicní tkáni byla nalezena převaha podtypů M2 a M4.

Přestože jsou muskarinové receptory v organismu odpovědné za regulaci velkého množství fyziologických dějů, když se na konci devadesátých let minulého století podařilo vytvořit myší knock-outy postrádající jednotlivé geny pro M1, M2, M3, M4 a M5 mAChR (Wess J. et al., 2003), ukázalo se, že tato zvířata nevykazují žádné větší fenotypové odchylky. Myši postrádající jednotlivé podtypy mAChR byly životoschopné, fertilní, nevykazovaly zjevné morfologické abnormality nebo změny v chování a teprve podrobnější studie u jednotlivých mutantních kmenů objevily některé charakteristické rysy (Wess J. et al., 2007).

Studie s knock-out myšmi postrádajícími M1 receptor například zjistila, že na rozdíl od nemutovaných myší a kmenů s vyřazením ostatních podtypů mAChR nebylo možné u M1 knock-outů vyvolat epileptický záchvat pomocí pilokarpinu. To naznačuje, že signalizace M1 receptorů v mozku se podílí na vzniku přinejmenším některých typů epileptických záchvatů (Hamilton SE. et al., 1997). U M1 knock-outů kromě toho dochází například ke ztrátě aktivace MAP kinázové dráhy v korových neuronech (Hamilton SE. et Nathanson NM., 2001) a pyramidových neuronech z CA1 oblasti hipokampu (Berkeley JL. et al., 2001). Protože MAP kinázová signalizace hraje pravděpodobně významnou roli v synaptické plasticitě (Adams JP. et Sweatt JD., 2002), podporují tato pozorování myšlenku, že aktivace M1 mAChR má značný význam pro kognitivní funkce a tvorbu paměťových stop. V souladu s tím je také fakt, že M1 knock-outy vykazují deficit neuronální plasticity v některých oblastech mozku (Zhang Y. et al., 2006). Mezi další změny, které byly zjištěny u M1 knock-out myší, patří zvýšená koncentrace dopaminu ve striatu, ztráta vlivu muskarinových agonistů na vodivost některých typů vápníkových kanálů v sympatických nervových gangliích nebo zvýšená lokomoční aktivita zvířat (Wess J., 2004).

Podrobnější prostudování knock-outů postrádajících další podtypy mAChR odhalilo vícero na první pohled neznatelných odchylek charakteristických pro jednotlivé receptory. Například studie s myšmi postrádajícími M2 receptor ukázaly, že u M2 knock-outu je nejnápadnější vliv na regulaci srdečního rytmu. Zatímco za normálních okolností snižuje aktivace M2 receptorů srdeční frekvenci, u M2 knock-out myší nemá acetylcholin na rytmicitu stahů srdeční svaloviny žádný vliv. Mezi další změny nalezené u M2 knock-outů patří absence oxotremorinem indukovaného třesu a snížení hypotermie indukované oxotremorinem nebo absence muskarinem zprostředkované desenzitizace periferních nociceptorů (Wess J., 2004). Zprvu velmi zajímavé se zdálo zjištění u M3 knock-outů, které měly výrazně sníženou tělesnou hmotnost (přibližně o 25%) i množství tukových zásob, což však bylo posléze vysvětleno jako důsledek sníženého příjmu potravy vlivem nižší tvorby slin (M3 mAChR je většinově zastoupen právě ve slinných žlázách). Další odchylky pozorované u M3 knock-outů byly například větší velikost zornice a distenze močového měchýře (Wess J., 2004). Z výsledků vyplynulo, že M3 mAChR zastoupený především v periferních tkáních obecně zvyšuje kontraktilitu hladké svaloviny a ovlivňuje činnost žláz s vnější sekrecí (Caulfield MP., 1993). U M4 knock-outů byla stejně jako u M1 pozorována zvýšená lokomoční aktivita a dále například snížení vlivu oxotremorinu na uvolňování draslíku ze striatálních řízků (Wess J., 2004). O fyziologických funkcích posledního podtypu mAChR, M5, je toho známo poměrně málo. U M5 knock-outů například nedocházelo k dilataci

mozkových arterií na popud acetylcholinu a stejně jako M4 knock-outy vykazovaly tyto kmeny snížený vliv oxotremorinu na uvolňování draslíku ze striatálních rízků (Wess J., 2004).

V 80. letech minulého století se podařilo naklonovat všech pět podtypů mAChR a postupně byly získány poměrně detailní informace o molekulární struktuře těchto receptorů. Především se ukázalo, že jednotlivé podtypy mAChR jsou si mezi sebou do značné míry podobné a z celkové délky zhruba 500 aminokyselin obsahují 160 invariantních zbytků. Molekulová hmotnost mAChR se pohybuje mezi 51 000 (M1, M2) až 66 000 (M3). Aminokyselinové sekvence mAChR obsahují sedm hydrofobních segmentů v délce 20 – 30 aminokyselin, které tvoří transmembránové domény. Všechny podtypy mAChR jsou u savčích druhů silně konzervované (89 – 98% sekvenční homologie) a většina zjištěných rozdílů se vyskytuje na extracelulárních smyčkách peptidového řetězce a v cytoplazmatické oblasti spojující transmembránové domény V a VI (třetí intracelulární smyčka) na $-\text{NH}_2$ konci pro 15 – 20 posledních aminokyselin. Maximum sekvenční homologie se naopak nachází v oblasti transmembránových domén. Transmembránové domény jsou také nejvíce konzervované mezi členy celé rozsáhlé nadrodiny GPCR (Brann MR. et al., 1993).

Ve struktuře receptoru se aminokyselinové zbytky důležité pro vazbu ligandu nachází na vnitřním povrchu transmembránových helixů, jeden až tři závity od jejich předpokládaného extracelulárního konce (Hulme EC. et al., 1993). Určitá specifita spřahování jednotlivých podtypů mAChR s jejich ortosterickými ligandy je přitom závislá především na druhé, třetí a sedmé transmembránové doméně. Zásadní roli ve vazbě ligandů hraje aspartát ve třetí transmembránové doméně, se kterým interaguje kladně nabité kvartérní amoniová skupina přirozeného ligandu acetylcholinu, která je také součástí většiny dalších muskarinových agonistů.

Transmembránové domény číslo II, IV, V a VI se shlukují kolem domény číslo III a tvoří tak útvar připomínající pravidelný šestistěn. Transmembránová doména číslo I není součástí tohoto šestistěnu a vyčnívá na jeho okraji. Svazek takto shluklých transmembránových domén je na vnitřní straně cytoplazmatické membrány velmi těsně sbalený, avšak směrem ven se poněkud rozevírá a tvoří tak kapsu, do které se pod úrovní povrchu cytoplazmatické membrány zachycuje ligand. Stejně jako u mnoha dalších členů rodiny GPCR, také konformace mAChR je stabilizována disulfidovým můstkem, který spojuje extracelulární konec třetí transmembránové domény a druhou extracelulární smyčku mezi doménami IV a V. Transmembránové domény I–V a domény VI a VII, které jsou vzájemně odděleny dlouhou třetí intracelulární smyčkou, mohou fungovat do jisté míry nezávisle na sobě a v membráně se dokáží spontánně shlukovat. V některých studiích byly

tyto dvě skupiny domén ko-exprimovány nezávisle na sobě, přičemž aktivita receptoru zůstala zachována (Maggio R. et al., 1993).

Jednotlivé podtypy mAChR se specificky spřahují s různými typy G-proteinů. Za specifitu spřahování je přitom odpovědná variabilita -NH₂ konce třetí intracelulární smyčky, jejíž struktura je vždy navzájem podobná mezi lichými a sudými podtypy mAChR. Liché podtypy M1, M3 a M5 se spřahují specificky s G_{q/11} proteiny, které aktivují fosfolipázu C, podílejí se na regulaci fosfatidylinositolového metabolismu a jedním z hlavních důsledků jejich aktivace je uvolnění intracelulárních zásob kalcia do cytoplazmy. Naproti tomu sudé podtypy M2 a M4 se specificky spřahují s G_{i/o} proteiny, které inhibují adenylátcyclázu a snižují tak koncentraci druhého posla cyklického adenosin monofosfátu (cAMP). Specifita spřahování jednotlivých receptorových podtypů s příslušnými G-proteinami však není absolutní a sudé i liché podtypy se vedle preferenčního G-proteinu mohou spřahovat také s dalšími třídami G-proteinů. Při dostatečné koncentraci agonisty a zároveň vysoké hustotě muskarinových receptorů v membráně byla například pozorována aktivace nepreferenčních G_s a G_{q/11} G-proteinů u buněk stabilně exprimujících pouze M2 nebo M4 podtyp mAChR (Michal P. et al., 2001, 2007, 2009).

G-proteiny existují v klidovém stavu jako heterotrimery složené z podjednotek α, β a γ, na podjednotku α váží guanosin difosfát (GDP) a jsou asociovány s transmembránovými receptory nebo s nimi náhodně interagují (Rodbell M., 1997). Navázání agonisty na receptor podnítí konformační změny receptoru, která dále způsobí změnu konformace asociovaného G-proteinu. Ta vede ke snížení afinity G-proteinu pro GDP a k jeho výměně za guanosin trifosfát (GTP). G-protein se následně rozpadá na dimer podjednotek βγ a α podjednotku. Podjednotka α i heterodimer βγ jsou biologicky aktivní a dále ovlivňují buněčné děje. Celý systém se vrací do klidového stavu poté, co je agonista uvolněn z receptoru a GTPázová aktivita vlastní α podjednotce hydrolyzuje GTP zpět na GDP. To nakonec vede k reasociaci jednotlivých podjednotek do původního heterotrimera a možnosti jejich zpětného spřažení s receptorem (Nestler EJ. et Duman RS., 1999).

3. Cholinergní hypotéza Alzheimerovy choroby

Na význam cholinergního systému pro integritu kognitivních funkcí poukázaly jako první studie s anticholinergními látkami, jejichž podání vyvolávalo u pokusných zvířat poruchy paměti (Drachman DA. et Leavitt J., 1974; Longo VG., 1966). Cholinergní hypotéza

Alzheimerovy choroby (postulující, že poškození cholinergního systému je hlavní příčinou vzniku Alzheimerovy choroby) byla pak formulována na přelomu 70. a 80. let minulého století (Bartus RT. et al., 1982). Cholinergní hypotéza byla založena především na výsledcích studií, které zaznamenaly pravidelné poškození cholinergních neuronů v mozcích pacientů s Alzheimerovou chorobou (Davies P. et Maloney AJ., 1976; Perry EK. et al., 1977a,b; Sims NR. et al., 1980, 1981), konkrétně poškození cholinergní projekce z nucleus basalis magnocellularis Meynerti uloženého v předním mozku vedoucí do kůry a hipokampu (Whitehouse PJ. et al., 1981, 1982). Zároveň byla v mozkové kůře a hipokampu pacientů s Alzheimerovou chorobou ve srovnání s věkově odpovídajícími zdravými kontrolami soustavně zjištována snížená aktivita enzymů cholinergního metabolismu, především enzymu cholinacetyltransferázy (ChAT), který je odpovědný za syntézu acetylcholinu z cholinu a acetyl-CoA. V některých případech bylo zjištěno také snížení syntézy acetylcholinu (Bowen DM. et al., 1981), snížené uvolňování acetylcholinu indukované depolarizací a snížení zpětného vychytávání cholinu nervovými zakončeními (Nilsson L. et al., 1986; Rylett RJ. et al., 1983). Tyto změny přitom pozitivně korelovaly nejen s počtem amyloidních plaků v mozku (Perry EK. et al., 1978; Wilcock GK. et al., 1982), ale také s rozsahem kognitivního deficitu u pacientů, a ve srovnání se změnami některých dalších neurotransmitterových systémů byly zjištovány již v době nástupu prvních příznaků demence (Francis PT. et al., 1993; Tsang SW. et al., 2006).

Kromě výše uvedených změn cholinergního systému byl u některých pacientů s Alzheimerovou chorobou zjištěn *post mortem* také úbytek celkového počtu mAChR v určitých oblastech mozku. Ohledně vlivu Alzheimerovy choroby na počet mAChR však různé studie vykazovaly mnohdy velmi rozdílné výsledky. To mohlo být částečně způsobeno tím, že počet mAChR u lidí (stejně jako u experimentálních hlodavců) s věkem přirozeně klesá a Alzheimerova choroba na tento pokles již nemusí mít další vliv. Na druhou stranu poté, co byl objeven způsob, jak měřit selektivně vazbu na jednotlivé podtypy mAChR, bylo zjištěno, že zatímco denzita postsynaptických receptorů (M1, M3) zůstává poměrně stálá, množství presynaptických receptorů (M2) se v mozcích pacientů s Alzheimerovou chorobou přece jen poněkud snižuje.

V průběhu let byly zjištěny také další skutečnosti podporující myšlenku cholinergní hypotézy Alzheimerovy choroby, jako například nižší aktivita pyruvát-dehydrogenázového komplexu, enzymu důležitého pro syntézu acetylcholinu, který je obvykle vysoce aktivní v cholinergních neuronech nucleus basalis Meynerti (Gibson GE. et al., 1988). Bez ohledu na to, že aplikace cholinergní hypotézy přinesla hmatatelné výsledky v podobě symptomatické

léčby Alzheimerovy choroby (inhibitory acetylcholinesterázy – donepezil, rivastigmin, galantamin a tacrin), byla od svého vzniku tato hypotéza již mnohokrát přehodnocena (Bartus RT., 2000; Davis KL. et al., 1999; DeKosky ST. et al., 2002) nebo rovnou zamítnuta. Ukázalo se například, že snížení aktivity ChAT v rozsahu běžně přítomném u Alzheimerovy choroby nemusí být nutně spojeno s kognitivním poškozením. Někteří autoři neprokázali přítomnost cholinergního deficitu u pacientů v časném stádiu onemocnění (Davis KL. et al., 1999) nebo na rozdíl od starších prací zaznamenali zvýšenou aktivitu ChAT (DeKosky ST. et al., 2002). Některé práce u lidí a primátů došly také k závěru, že cholinergní aktivita v mozkové kůře klesá přirozeně v průběhu stárnutí (Smith DE. et al., 1999; Sparks DL. et al., 1992), případně se vyskytuje také u dalších neurodegenerativních onemocnění (Murdoch I. et al., 1998; Perry EK. et al., 1985). Například ve specifickém případě dědičné olivo-ponto-cerebelární atrofie dochází k podstatnému snížení aktivity ChAT, aniž by zároveň došlo k rozvoji demence (Kish SJ. et al., 1989). Navíc další terapeutické pokusy založené na podpoře a obnovení funkcí cholinergního systému (například pomocí prekurzorů acetylcholinu), nepřinesly v léčbě Alzheimerovy choroby vesměs žádný pokrok. Kromě inhibitorů acetylcholinesterázy byly od počátku prováděny pokusy také s léčbou Alzheimerovy choroby pomocí agonistů M1 muskarinových receptorů (jeden z prvních byl například parciální agonista arecolin), avšak až do dnešní doby nebyla vyvinuta látka s tímto účinkem, kterou by bylo možné použít v humánní medicíně (jednou z významných překážek je například nedostatečná selektivita většiny M1 agonistů).

Na druhou stranu je nepochybné, že cholinergní hypotéza přinesla významný pokrok ve výzkumu a poznání podstaty (nejen) Alzheimerovy choroby a do dnešní doby se význam cholinergního systému či přímo mAChR v patogenezi Alzheimerovy choroby intenzivně zkoumá společně s některými dalšími neurotransmitterovými systémy (především glutamátergním). V novější době se objevily například důkazy poškozeného spřahování mezi M1 receptorem, G-proteiny a dalšími molekulami signalační kaskády (Francis PT. et al., 1999; Tsang SW. et al., 2006) v mozcích pacientů s Alzheimerovou chorobou a také známky vlivu mAChR na metabolismus APP. Jedním z důvodů některých nejednotných závěrů a četných zpochybňení cholinergní hypotézy Alzheimerovy choroby byl pravděpodobně fakt, že ačkoli v době jejího vzniku bylo již k dispozici značné množství výsledků, které ji podporovaly, bylo do té doby provedeno jen velmi málo studií porovnávajících nejen mozky pacientů s Alzheimerovou chorobou a mozky starých zdravých kontrol, ale také mozky mladých lidí. Nebylo tak možné od počátku jasně odlišit vliv patologické demence a normálního věkem podmíněného poklesu kognitivních funkcí (Contestabile A., 2011).

Možným spojujícím článkem mezi poškozením cholinergního systému a patogenezí Alzheimerovy choroby jsou právě cholinergní mAChR. Na jejich význam poukázaly například výsledky studie provedené u pacientů trpících Parkinsonovou chorobou a léčených látkami s antimuskarinovým účinkem. Pacienti dlouhodobě léčení těmito léky měli ve srovnání s krátkodobě léčenými nebo neléčenými pacienty významně vyšší výskyt amyloidních plaků a také neurofibrilárních klubek (Perry EK. et al., 2003). Je známo, že mAChR společně s dalšími neurotransmitterovými systémy přímo ovlivňují metabolismus APP, jehož štěpením za určitých podmínek vzniká patologický protein β -amyloid ukládající se v mozích pacientů s Alzheimerovou chorobou ve formě amyloidních plaků (Buxbaum JD. et al., 1992; Nitsch RM. et al., 1992; Nitsch RM., 1996). Zatímco proteolytickým štěpením APP pomocí α - a následně γ -sekretázy vzniká jako produkt molekula α APPs s neuroprotektivními účinky (tzv. neamyloidogenní štěpení) (Lichtenthaler SF., 2011), výsledkem amyloidogenního štěpení β - a γ -sekretázou je neurotoxickej β -amyloid. Již počátkem 90. let bylo prokázáno, že aktivace M1 a M3 mAChR významně ovlivňuje zpracování APP a zvyšuje podíl příznivě působícího neamyloidogenního štěpení (Nitsch RM. et al., 1992; Buxbaum JD. et al., 1992). K podobnému závěru u M1 receptoru došli také autoři novější studie s použitím myší s knock-outem M1 receptoru (Davis AA. et al., 2010). Na druhou stranu sudé podtypy mAChR M2 a M4 uvolňování neuroprotektivního α APPs spíše potlačují (Müller DM. et al., 1997) a napomáhají tak amyloidogennímu štěpení APP. Zatímco tedy neurotoxickej působení β -amyloidu může poškozovat mAChR a funkci celého cholinergního systému, naopak snížená funkce lichých podtypů mAChR přispívá k vyšší produkci škodlivého β -amyloidu, čímž se bludný kruh uzavírá. Avšak i když existují práce dokládající tuto obousměrnou interakci mezi β -amyloidem a mAChR (přehled viz Pákáski M. et Kálmán J., 2008), je třeba uvést, že dokladů o škodlivém působení β -amyloidu na cholinergní systém (včetně muskarinových receptorů) bylo v průběhu let nashromážděno podstatně více než dokladů o způsobu, jakým muskarinové receptory ovlivňují metabolismus APP a produkci β -amyloidu (Roberson MR. et Harrell LE., 1997).

I když cholinergní teorie Alzheimerovy choroby zatím nedokázala přinést žádný větší úspěch v léčbě a její platnost je značně diskutabilní, pokusy o její potvrzení či vyvrácení přinesly celou řadu nových poznatků o patologii a molekulární podstatě demence a zejména Alzheimerovy choroby. Přínosné byly například studie zkoumající přítomnost cholinergního deficitu již v časných fázích onemocnění, které byly provedeny v rámci takzvané „religion-orders study“ (někdy známé také pod názvem „nun-study“) financované mimo jiné

americkým National Institute of Aging a umožněné účastí více než tisícovky členů křesťanských řádů po celých Spojených státech. Účastníci těchto studií podstupovali pravidelné lékařské a psychologické vyšetření a po jejich smrti bylo provedeno důkladné vyšetření patologie mozku a integrity cholinergního systému. Ukázalo se, že ačkoliv cholinergní deficit, stanovený podle snížení aktivity ChAT, je běžně patrný u pacientů s pokročilou formou Alzheimerovy choroby, snížení aktivity ChAT nebylo spolehlivě prokázáno v případech časné diagnózy onemocnění (ve fázi takzvaného mírného kognitivního deficitu) (Davis KL. et al., 1999; Tiraboschi P. et al., 2000; DeKosky ST. et al., 2002). Později byly studie rozšířeny o zhodnocení počtu a stavu neuronů v bazálním mozku zásobujících cholinergní inervaci mozkovou kůru a hipokampus a další četné studie se zaměřily také na zkoumání nervového růstového faktoru a jeho receptorů, jelikož působení nervového růstového faktoru je nezbytné pro udržení a normální funkci cholinergního systému. Výsledky všech těchto studií ukázaly, že i v časných fázích onemocnění může být přítomen cholinergní deficit, který však není doprovázen snížením aktivity ChAT a poškození se nachází primárně v jiných pre- či postsynaptických složkách cholinergního systému (Sarter M. et Bruno JP., 2002; Terry AV. Jr. et Buccafusco JJ., 2003).

V současné době převládá názor, že cholinergní hypotéza Alzheimerovy choroby, tak jak byla původně formulována (tj. že poškození cholinergního systému je primární příčinou vzniku a postupného rozvoje onemocnění), je rozhodně příliš zjednodušená a není možné ji rozumně obhájit (Bartus RT., 2000). Na druhou stranu poškození cholinergního systému je nepochybně důležitou součástí rozvoje a progrese onemocnění a je pravděpodobné, že cholinergní teorie či alespoň její části budou v budoucnu součástí komplexnější teorie o vzniku a patogenezi Alzheimerovy choroby.

4. β -amyloid a amyloidová hypotéza Alzheimerovy choroby

Amyloidová hypotéza Alzheimerovy choroby byla poprvé formulována již před více než dvaceti lety. Podle této hypotézy je příčinou onemocnění bílkovina β -amyloid, která se ukládá v mozku pacientů ve formě plaků. Přesná sekvence β -amyloidu byla poprvé zjištěna v první polovině 80. let minulého století (Glenner GG. et Wong CW., 1984), konkrétně u bílkoviny získané z meningeálních cév pacientů s Alzheimerovou chorobou a Downovým syndromem. Krátce poté byl peptid se stejnou sekvencí identifikován jako hlavní složka senilních (amyloidových) plaků uložených v mozku pacientů s Alzheimerovou chorobou

(Masters CL. et al., 1985). Následovalo naklonování genu pro APP a jeho lokalizace na 21. chromosom (Kang J. et al., 1987), což společně se starším poznatkem, že trisomie chromosomu 21 u Downova syndromu má za následek neuropatologické příznaky obdobné těm u Alzheimerovy choroby, položilo základy amyloidové hypotéze.

Je známo, že β -amyloid, který se skládá ze 38 až 43 aminokyselin, vzniká takzvaným amyloidogenním štěpením bílkoviny prekurzor amyloidu, která se skládá z jedné transmembránové domény, dlouhého extracelulárního $-NH_2$ konce a kratšího intracelulárního $-COOH$ konce. APP je běžně exprimována v neuronech i dalších typech buněk. Produkce β -amyloidu štěpením APP probíhá obecným fyziologickým mechanismem známým jako řízená membránová proteolýsa (regulated intramembrane proteolysis), při němž membránové proteiny nejprve podstoupí odštěpení své extracelulární části prostřednictvím proteáz asociovaných s membránou (sekretáz) a poté je odštěpená část (v případě APP označovaná jako sAPP) uvolněna do extracelulárního prostoru. V membráně zanořený zbytek bílkoviny je dále štěpen uvnitř své transmembránové domény, přičemž dochází k uvolnění malého hydrofobního peptidu (například β -amyloidu v případě APP po odštěpení extracelulární části β -sekretázou). Intracelulární část se uvolňuje do cytoplazmy, kde může mít různé fyziologické funkce například v aktivaci nukleárních signálních drah. Rozdílná délka jednotlivých druhů β -amyloidu (obvykle se uvádí 38 až 43 aminokyselin) je způsobena variabilním místem štěpení na hydrofobním C konci peptidu a tato variabilita propůjčuje jednotlivým druhům β -amyloidu odlišnou schopnost oligomerizace. Komplex γ -sekretázy štěpí APP přinejmenším na třech různých místech transmembránové domény označovaných jako γ , ϵ a ζ . Výsledkem štěpení je β -amyloid o délce 38, 40 nebo 42 aminokyselin. Pouze β -amyloid 1-42 má silnou schopnost oligomerizace *in vivo*.

Při amyloidogenním štěpení je APP postupně štěpen dvěma různými proteázami, β - a γ -sekretázou, a výsledkem tohoto štěpení je β -amyloid. Na druhou stranu, při takzvaném neamyloidogenním štěpení je APP místo β -sekretázy nejprve rozštěpen α -sekretázou, jež štěpí APP uvnitř amyloidové sekvence a tím brání vzniku β -amyloidu při následném štěpení γ -sekretázou. Výsledek štěpení γ -sekretázou, což je ve skutečnosti proteázový komplex tvořený čtyřmi podjednotkami (presenilin-1 nebo presenilin-2, nicastrin, proteiny APH1 a PEN2) tak může být dvojí: při neamyloidogenním štěpení je to solubilní fragment sAPP α společně s krátkým peptidem p3, při amyloidogenním štěpení je to solubilní fragment sAPP β a dále škodlivý fragment označovaný jako β -amyloid. Příčinou vzniku Alzheimerovy choroby podle amyloidové teorie pak může být patologické posílení amyloidogenního štěpení APP a

tím zvýšená akumulace (případně v součinnosti s nedostatečnou clearance) β -amyloidu v mozku.

Amyloidová hypotéza Alzheimerovy choroby byla vždy mimo jiné podporována skutečností, že u dědičných forem onemocnění byly popsány mutace genu pro APP a mutace v genech kódujících enzymy uplatňující se při amyloidogenním štěpení APP (presenilin 1 a presenilin 2, které jsou součástí γ -sekretázy). Mutace v genu pro APP mající za následek dědičnou formu onemocnění se vesměs nacházejí v místech, kde dochází ke štěpení APP proteázami α -, β - a γ - a upřednostňují amyloidogenní štěpení APP (Citron M. et al., 1992). Dalším přesvědčivým důkazem úlohy amyloidogenních peptidů v patogenezi onemocnění je již zmíněný pravidelný výskyt Alzheimerovy choroby u Downova syndromu, kde je příčinou zvýšené tvorby normálního (nemutovaného) amyloidu tzv. gene dosage effect (přítomnost tří kopií normálního genu pro APP, který je umístěn na 21. chromosomu). Exprese genu pro APP je u pacientů s Downovým syndromem asi 1,5 krát vyšší než u zdravých jedinců a tvorba amyloidových plaků předchází tvorbě neurofibrilárních klubek přibližně o 10 let (Mann DM., 1989).

Přestože pro amyloidovou hypotézu dnes existuje řada přesvědčivých argumentů, nikdy nepřestala být zpochybňována relevance amyloidních plaků v patogenezi Alzheimerovy choroby, mimo jiné proto, že množství plaků v mozkové tkáni ne vždy korelovalo s tíží kognitivního deficitu u pacientů (Nagy Z. et al., 1995). Navíc bylo zjištěno, že i u zdánlivě zcela zdravých jedinců se v mozkové kůře nachází nezanedbatelné množství β -amyloidu, i když ten je zpravidla uložen v difuzních placích, které neobsahují amyloidové fibrily, a v jejich okolí se téměř nevyskytují známky neuronálního nebo gliového poškození (Dickson DW., 1997). Řešení všech těchto problémů se objevilo až poměrně nedávno poté, co pomocí zdokonalených metod bylo možno mnohem přesněji zhodnotit množství i specifické vlastnosti zkoumaného β -amyloidu. Tyto novější studie ukázaly, že s tíží kognitivního deficitu mnohem lépe než pouhý počet amyloidových plaků koreluje koncentrace rozpustného β -amyloidu včetně rozpustných oligomerů (Näslund J. et al., 2000; McLean CA. et al., 1999). Postupně bylo zjištěno, že hlavním nositelem synaptické toxicity není agregovaný β -amyloid tvořící plaky, ale podstatně menší molekuly, rozpustné oligomery β -amyloidu (Haass C. et Selkoe DJ., 2007). Navíc nejen u Alzheimerovy choroby, ale i u dalších neurologických onemocnění jsou k dispozici doklady o tom, že rozsáhlé agregáty patologického proteinu jsou buď zcela inertní nebo působí dokonce protektivně (huntingtin u Huntingtonovy choroby, ataxin u spinocerebelární ataxie) (Arrasate M. et al., 2004; Cummings CJ. et al., 1999). Na

druhou stranu je třeba zmínit, že v okolí rozsáhlých plaků fibrilárního β -amyloidu obvykle nacházíme četné známky synaptického poškození. Tyto plaky však mají ve svém okolí také zvýšenou koncentraci rozpustných oligomerů β -amyloidu a je těžké rozlišit, zda poškození okolních synapsí je přímo způsobeno amyloidovými plaky či nikoli. Shrňeme-li současnou situaci, naprostá většina odborníků (pokud rovnou neodmítají amyloidovou hypotézu jako celek) má dnes za to, že principiální roli v patogenezi Alzheimerovy choroby hrají rozpustné oligomery β -amyloidu, přinejmenším v časných nebo dokonce již pre-symptomatických fázích onemocnění.

Jedním z často zmiňovaných mechanismů, kterými β -amyloid může poškozovat paměť a kognitivní funkce, je inhibice dlouhodobé potenciace (long term potentiation, LTP) v hipokampusu. LTP je zesílení synaptického přenosu díky opakováním elektrickým signálům s vysokou frekvencí a LTP v některých synaptických okruzích hipokampusu je odpovědná za synaptickou plasticitu a tedy i schopnost učení a paměti. V několika studiích bylo prokázáno, že jak syntetický β -amyloid tak přirozeně uvolňované oligomery β -amyloidu mají schopnost potlačovat LTP v hipokampusu již při sub-nanomolárních koncentracích (Lambert MP. et al., 1998; Walsh DM. et al., 2002) a tento efekt je specificky inhibován protilátkami proti β -amyloidu *in vivo* (Klyubin I et al., 2005). Jindy zase podání oligomerů β -amyloidu způsobilo rychlou a reverzibilní poruchu učení a paměti u pokusných zvířat (Cleary JP. et al, 2005). Z uvedených výsledků vyplývá, že poruchy paměti mohou být přímo vyvolány izolovanou a biochemicky přesně definovanou formou β -amyloidu, konkrétně jeho rozpustnými oligomery o velikosti přibližně mezi di- až dekamery (Haass C. et Selkoe DJ., 2007).

5. Současné možnosti léčby Alzheimerovy choroby

V současné době se k léčbě Alzheimerovy choroby v klinické praxi využívají léky ze skupiny inhibitorů acetylcholinesterázy (AChE) a dále antagonista NMDA receptorů (memantin). V různém stádiu preklinického a klinického zkoumání je však celá řada dalších přístupů, včetně využití ligandů mAChR (přehled viz Huang Y. et Mucke L., 2012). Vliv léků, které se v současné době používají k léčbě Alzheimerovy choroby, na průběh onemocnění je poměrně malý a pouze přechodný. Přestože tyto látky mohou oddálit nástup těžké demence (především jsou-li používány v kombinaci, Lopez OL. et al., 2009), nedokáží postup onemocnění zastavit nebo zvrátit.

Prvním lékem ze skupiny inhibitorů AChE, který byl schválem americkým Úřadem pro kontrolu potravin a léčiv (Food and Drug Administration, FDA), byl tacrin v roce 1993. Následoval donepezil (1996), rivastigmin (2000) a galantamin (2001). Protože první ze schválených léků, tacrin, má v organismu velmi krátký poločas a rovněž s sebou nese nezanedbatelné riziko hepatotoxicity, v současné se již prakticky nepoužívá.

Všechny inhibitory AChE působí tak, že acetylcholin uvolňovaný z presynaptického zakončení setrvává déle v synapsi a zvyšuje se tak pravděpodobnost jeho interakce s postsynaptickými cholinergními (muskarinovými či nikotinovými) receptory. I když jednotlivé léky ze skupiny inhibitorů AChE se poměrně významně liší svými vlastnostmi (například rivastigmin kromě AChE inhibuje také butyrylcholinesterázu, galantamin alostericky ovlivňuje nikotinové receptory), klinický význam těchto rozdílů je zanedbatelný a žádný z inhibitorů AChE není efektivnější než ostatní léky ze skupiny. Přestože se často uvádí, že jedním zdůvodněním malé účinnosti léků používaných v léčbě Alzheimerovy choroby je jejich nasazení v relativně pozdním stádiu onemocnění, žádná ze studií neprokázala, že by inhibitory AChE mohly být s úspěchem použity v léčbě takzvaného mírného kognitivního deficitu (mild cognitive impairment, MCI), který Alzheimerově chorobě obvykle předchází (Jelic V. et al., 2006; Russ TC. et Morling JR., 2012). Jedním z důvodů může být fakt, že MCI je etiologicky heterogenní a jen 60 až 70 % případů je podmíněno nastupující Alzheimerovou chorobou (Jicha GA. et al., 2006). U inhibitorů AChE jsou běžné nežádoucí účinky na gastrointestinální systém, jako je anorexie, nauzea a váhový úbytek. Vliv na cholinergní systém se může projevovat také bradykardií, která představuje kontraindikaci při podávání inhibitorů AChE.

V současné době se v různé fázi nachází celá řada klinických studií zkoumajících možný efekt dalších potenciálních způsobů léčby Alzheimerovy choroby. Zároveň však mnoho z nich, převážně díky nedostatečně přesvědčivým prvním výsledkům, bylo prakticky zastaveno a nachází se na mrtvém bodě (Aisen PS. et al., 2012). Jednou z intenzivně zkoumaných látek byl například tramiprosat (homotaurin), který se má vázat na β -amyloid a blokovat jeho agregaci a tvorbu fibril. Jeho účinnost při zlepšení kognitivních funkcí se však nepodařilo prokázat (Aisen PS. et al., 2011). Dále byly v nedávných letech vyvíjeny především látky snižující produkci nebo naopak zvyšující clearance β -amyloidu. Tyto látky převážně snižují aktivitu β a γ -sekretázy, které jsou odpovědné za amyloidogenní štěpení APP. V roce 2010 však byla zastavena III. fáze klinických studií jednoho z původně velmi slibných inhibitorů γ -sekretázy, semagacestatu, kvůli nedostatečnému efektu a vážným

nežádoucím účinkům, které zahrnovaly i zhoršení kognitivního deficitu. Jedním z mnoha možných důvodů překvapivě špatných výsledků studie může být fakt, že APP není zdaleka jediným substrátem štěpeným γ -sekretázou a aktivita tohoto enzymu ovlivňuje signalizaci mnoha buněčných drah, mimo jiné i signalizaci prostřednictvím receptoru pro nervový růstový faktor, p75NRT (Schor NF., 2011). Podobně dopadl také potenciální lék tarenflurbil, který měl rovněž snižovat hladinu β -amyloidu skrze modulaci funkce γ -sekretázy (Xia W. et al., 2012).

Snahy o snížení hladiny A β prostřednictvím zvýšené clearance vycházejí z výsledků studií, ve kterých aktivní imunizace proti A β snížila výskyt amyloidních plaků u transgenních myší, avšak následné klinické studie musely být zastaveny kvůli vedlejším účinkům na imunitní systém (Gilman S. et al., 2005). V současnosti probíhají další klinické studie s pasivní imunizací monoklonálními protilátkami, které by měly mít méně nežádoucích účinků. Další možností, jak zvýšit clearance β -amyloidu, je aktivace apolipoproteinu E, který se za normálních podmínek na této clearance významně podílí. V současné době jsou k dispozici poměrně slibné výsledky z preklinických studií, kdy bexaroten, agonista RXR receptoru podporující expresi apolipoproteinu E, dokázal rychle a účinně zvýšit clearance β -amyloidu z mozku transgenních myší (Cramer PE. et al., 2012).

Protože existují četné důkazy o tom, že v průběhu Alzheimerovy choroby dochází k oxidativnímu poškození, zánětlivým změnám a poškození mitochondrií, některé léčebné strategie zahrnují i použití antioxidantů, protizánětlivých léků a látek s ochranným účinkem na mitochondrie (například látka s ochranným účinkem na mitochondrie AC-1204, vitamín E, kurkumin nebo kyselina dokosahexaenová). Nicméně také řada těchto léků se již v průběhu klinických studií ukázala jako neefektivní.

Další z možných léčebných strategií Alzheimerovy choroby je využití ligandů mAChR, které by se svým primárním účinkem na cholinergní systém řadily do skupiny symptomatických léků, podobně jako inhibitory AChE. V léčbě by se mohly uplatnit především selektivní agonisté M1 případně antagonisté M2 mAChR, které by zvýšily uvolňování endogenního acetylcholinu a tím i stimulaci postsynaptických M1 receptorů. Jedním z hlavních problémů případné léčby Alzheimerovy choroby pomocí agonistů stimulujících funkci postsynaptických mAChR je však nedostatečná selektivita těchto látek pro jednotlivé receptorové podtypy. Kromě toho selektivita pozorovaná *in vitro* se nemusí vždy uplatnit také v podmírkách *in vivo*. Do fáze klinických studií se v minulosti dostaly látky (např. xanomelin), které, ačkoliv měly příznivé účinky na kognici pacientů (Bodick NC.

et al., 1997), vykazovaly zároveň vážné nežádoucí účinky na vegetativní nervový systém právě z důvodu nedostatečné selektivity. V současnosti se největší pozornost zaměřuje především na tři skupiny látek: ortosterické a alosterické agonisty M1 receptorů a na pozitivní alosterické modulátory M1 (M1 PAMs). U alosterických agonistů a PAMs je zpravidla možné dosáhnout větší M1 selektivity než u ortosterických agonistů, které se váží do evolučně vysoce konzervovaného vazebného místa. Vyšší selektivitu vykazují někteří antagonisté M2 receptorů, avšak jejich účinek, podobně jako u dnes používaných inhibitorů AChE, je limitován postupně se prohlubující presynaptickou hypofunkcí cholinergních neuronů.

Léčba posilující funkci cholinergního systému je v souvislosti s Alzheimerovou chorobou obvykle vnímána pouze jako symptomatická, neovlivňující podstatu vzniku onemocnění. Protože však aktivace M1 i M3 mAChR podporuje neamyloidogenní štěpení APP a tím snižuje množství vznikajícího β -amyloidu (Nitsch RM. et al., 1992; přehled viz Fisher A., 2012), mohly by M1 selektivní agonisté sehrát pozitivní roli i při řešení samotné příčiny onemocnění. Tuto myšlenku podporují například výsledky studie, kde podávání donepezilu pokusným zvířatům mělo za následek snížení produkce β -amyloidu (Kimura M. et al., 2005). U pacientů s Alzheimerovou chorobou léčených inhibitory AChE byl zase pomocí zobrazovacích technik zjištěn menší rozsah mozkové atrofie než u neléčených kontrol (Rountree SD. et al., 2009). Protože však jiné studie naopak nezjistily žádný vliv inhibitorů AChE na průběh onemocnění, musí být případný takový vliv jen malý a tyto léky mají obecně především symptomatický efekt.

6. Poškození cholinergní signalizace u zvířecích modelů Alzheimerovy choroby

Ke studiu postupných změn v cholinergním systému v průběhu normálního stárnutí a u Alzheimerovy choroby je možné využít transgenní zvířecí modely. Rovněž součástí experimentů obsažených v této disertační práci bylo zhodnocení cholinergní transmise a funkce muskarinových receptorů u transgenního myšího modelu Alzheimerovy choroby APPswe/PS1dE9 (Jankowsky JL. et al., 2004) s takzvanou švédskou mutací v genu pro APP (K670N/M671L) a s delecí 9. exonu v genu pro presenilin 1 (součást γ -sekretázového komplexu).

V minulosti bylo u myšího modelu APPswe/PS1dE9 ve srovnání se zdravými kontrolami zjištěno snížení aktivity AChE a ChAT (Savonenko A. et al., 2005), snížení aktivity butyrylcholinesterázy, snížená koncentrace transportéru pro acetylcholin (vesicular

acetylcholine transporter, VACHT) a také poškozené spřahování mAChR s G-proteiny, určené jako změna vazby ^{35}S -GTP γ S stimulované karbacholem. Porucha spřahování mAChR s G-proteiny a také snížení koncentrace VACHT jsou u transgenních zvířat patrné již ve věku přibližně sedmi měsíců, tedy v době, kdy se v mozku myší teprve začínají hromadit amyloidní plaky (Machová E. et al., 2008).

Zatímco měření vazby $[^3\text{H}]\text{-NMS}$, které nerozlišuje mezi jednotlivými podtypy mAChR, zjistilo celkové snížení jejich denzity u transgenních myší zvyšující se s věkem (Machová E. et al., 2008), měření exprese M1 a M3 receptorů neodhalilo rozdíl v hladině mRNA těchto dvou podtypů mezi transgenními zvířaty a kontrolami stejného věku (Goto Y. et al., 2008). V jiné práci byl zjištován kognitivní deficit a stav cholinergního systému u mladých myší APPswe/PS1dE9 (ve věku 2,5 a 3,5 měsíce). Zatímco u zvířat starých 2,5 měsíce nebyla patrná žádná kognitivní porucha ani rozdíl ve funkci cholinergního systému u transgenních myší a kontrol, u transgenních myší starých 3,5 měsíce se objevily poruchy prostorové paměti doprovázené snížením koncentrace ACh a aktivity ChAT v mozku. Jak koncentrace ACh tak aktivita ChAT negativně korelovaly s tíží kognitivního deficitu u myší (Zhang W. et al., 2012). Mezi další projevy poškození cholinergního systému u transgenních myší APPswe/PS1dE9 patří i zkrácení celkové délky axonů cholinergních neuronů o celkových přibližně 300 m v porovnání s kontrolami stejného věku, které bylo zjištěno stereologicky po imunohistochemickém označení VACHT (Nikolajsen GN. et al., 2011). Dále metodou měření excitačních postsynaptických potenciálů byly u APPswe/PS1dE9 myší zjištěny změny cholinergní modulace glutamátergní transmise a to již u pětiměsíčních zvířat. (Goto Y. et al., 2008).

Ve starších pracích byly jako model Alzheimerovy choroby využívány transgenní myši s mutací v jediném genu, především myši Tg2576 s takzvanou švédskou mutací v genu pro APP, u kterých se amyloidní plaky začínají objevovat až ve věku přibližně deseti měsíců. U těchto myší nebyly v žádném věku zjištěny rozdíly v aktivitách ChAT a AChE mezi transgenními zvířaty a kontrolami, byla však zaznamenána snížená funkce vysokoafinitního přenašeče cholinu a také snížení vazby M1 a později i M2 podtypu mAChR (Apelt J. et al., 2002).

Naopak v současné době se stále častěji využívají trojitě transgenní myši (obvykle kombinující mutaci v genu pro APP, presenilin-1 a tau protein), u kterých rovněž dochází k poruše řady cholinergních markerů. U trojitě transgenních myší APPswe/PS1M146V/tauP301L byly zjištěny například morfologické změny cholinergních axonů zvýrazňující se s věkem, redukce počtu ChAT-pozitivních buněk v některých oblastech

mozku, snížení aktivity ChAT v hipokampu a také změny v koncentraci nervového růstového faktoru a jeho receptorů TrkA a p75NTR (Perez SE. et al., 2011). Na druhou stranu bylo zjištěno také zvýraznění amyloidové a tau patologie v mozku trojité transgenních myší s nedostatečnou funkcí mAChR, konkrétně knock-out M1 mAChR u těchto myší dále zvyšuje počet amyloidových plaků a neurofibrilárních klubek v mozku, zhoršuje synaptické poškození neuronů a zvýrazňuje kognitivní deficit (Medeiros R. et al., 2011).

7. β -amyloid a poškození funkce muskarinových receptorů

Neurotoxicický vliv rozpustných oligomerů β -amyloidu, který pravděpodobně hraje důležitou roli v průběhu Alzheimerovy choroby, je všeobecně přijímán (McLean CA. et al., 1999; Selkoe DJ., 2002; Glabe CG., 2006). Za použití dostatečně vysokých koncentrací lze toxicické účinky β -amyloidu pozorovat také *in vitro*, i když tento přístup může být zavádějící a má své nevýhody: za prvé k dosažení toxicitého účinku je zpravidla nutná vysoká („nefyziologická“) koncentrace syntetického β -amyloidu a za druhé syntetické oligomery β -amyloidu v podmírkách *in vitro* jsou pravděpodobně nestabilní a mohou vytvářet řadu odlišných konformací vzdálených od struktur přítomných *in vivo* (Benilova I. et al., 2012). Bylo navrženo více mechanismů, které by mohly být odpovědné za neurotoxiccké vlastnosti β -amyloidu, například oxidativní stres, změna struktury biomembrán nebo interakce s některými receptory.

Hlavním cílem této dizertační práce bylo prostudovat možný vliv β -amyloidu na funkci jednotlivých podtypů mAChR, které jsou součástí cholinergního systému vykazujícího významné morfologické poškození a funkční deficit u lidí s Alzheimerovou chorobou. Již některé starší práce prováděné *post mortem* na mozcích pacientů s Alzheimerovou chorobou se pokusily důkladněji prostudovat funkční stav mAChR v mozkových řezech. V těchto pracích bylo zjištěno, že v mozcích pacientů s Alzheimerovou chorobou dochází k poklesu vysokoafinitní vazby agonistů u mAChR (agonisté mAChR, na rozdíl od antagonistů, rozeznávají vysokoafinitní konformaci, která odpovídá afinitě receptoru spřaženého s G-proteinem, a nízkoafinitní konformaci, která odpovídá afinitě rozpřaženého receptoru), dále ke snížení karbacholem stimulované vazby ^{35}S -GTP γ S, poklesu aktivity GTPáz a také fosfolipázy C stimulované karbacholem (Flynn DD. et al., 1991). Celková hladina G-proteinů se přitom nelišila u pacientů s Alzheimerovou chorobou a u zdravých věkem odpovídajících kontrol.

Dále bylo u pacientů s Alzheimerovou chorobou pomocí vazby ^3H -pirenzepinu zjištěno stejně množství M1 receptorů jako u zdravých kontrol, zatímco imunohistochemicky bylo M1 receptorů ve srovnání s kontrolami naměřeno méně. To naznačuje, že v průběhu onemocnění může být v mozku přítomná alterovaná forma M1 receptoru s odlišnou konformací (Flynn DD. et al., 1995). Některé výsledky také ukázaly, že rozsah poškození spřahování M1 receptoru s G-proteiny v prefrontální kůře je přímo úměrný rozsahu kognitivního poškození a nepřímo úměrný aktivitě ChAT (Tsang SW. et al., 2006). Podle některých autorů je poškozené spřahování M1 receptoru s G-proteiny způsobeno sekvestrací $\text{G}_{q/11}$ G-proteinů oligomery angiotensinového receptoru AT2 (AbdAlla S. et al., 2009), které v průběhu Alzheimerovy choroby vznikají především důsledkem oxidativního stresu.

Kromě studií na mozcích pacientů s Alzheimerovou chorobou byl toxický vliv β -amyloidu na mAChR studován také na primárních kulturách neuronů, na liniích buněk přirozeně exprimujících mAChR nebo na transfekovaných buňkách heterologně exprimujících pouze jednotlivé podtypy mAChR (Joseph JA. et Fisher DR., 2003). V kultuře potkaních korových neuronů β -amyloid snižoval aktivitu GTPázy, což je známka poškozeného spřahování mAChR s G-proteiny, a zároveň snižoval akumulaci inositolfosfátů a uvolňování intracelulárního kalcia (Kelly JF. et al., 1996; Huang HM. et al., 2000). Oba tyto procesy jsou aktivovány signalizační dráhou spouštěnou $\text{G}_{q/11}$ G-proteiny, se kterými se preferenčně spřahují liché podtypy mAChR. Tento účinek β -amyloidu byl blokován látkami s antioxidačním působením. Nevýhodou uvedených výsledků je skutečnost, že byly vesměs dosaženy s použitím vysokých koncentrací β -amyloidu (cca 10 μM), které jsou velmi vzdálené „fyziologickým“ podmínkám *in vivo*.

Cíle práce a hypotézy

Hlavním cílem této práce bylo zjistit, zda a případně jakým způsobem ovlivňuje rozpustný β -amyloid přenos signálu muskarinovými receptory. Je známo, že v průběhu Alzheimerovy choroby, v jejíž patogenezi hraje β -amyloid významnou úlohu, dochází k poškozování cholinergního systému. Změny funkce některých podtypů mAChR, které jsou významnou součástí cholinergního neurotransmitterového systému, byly zjištěny jak *post mortem* v mozcích pacientů s Alzheimerovou chorobou, tak u dvojitě a trojitě transgenních myších modelů tohoto onemocnění. Význam oslabování cholinergní transmise v patogenezi Alzheimerovy choroby je ještě zvýrazněn skutečností, že interakce mezi β -amyloidem a mAChR je podle všeho oboustranná, tedy nejenže β -amyloid negativně ovlivňuje funkci receptorů, ale naopak i snížená aktivace některých podtypů mAChR se podílí na zvýšeném uvolňování β -amyloidu a tím snad i na urychlení progrese Alzheimerovy choroby.

V předkládané práci jsem vycházela z následujících hypotéz, které jsou založené na dosud známých faktech a celé řadě výsledků, které byly na toto téma až dosud publikovány, především v rámci zkoumání a ověřování „cholinergní hypotézy“ Alzheimerovy choroby:

- β -amyloid 1-42 ($A\beta_{1-42}$) ovlivňuje funkci mAChR (případně jen některých jejich podtypů) v rozpustné formě, bez přítomnosti nerozpustných amyloidních deposit (plaků). Tento vliv by měl být patrný i při relativně nízké koncentraci $A\beta_{1-42}$ a objevuje se již v počátečních fázích rozvoje onemocnění.
- Je možné očekávat diferencovaný účinek $A\beta_{1-42}$ na jednotlivé podtypy mAChR, neboť je známo z literatury (histologické a biochemické výsledky získané na mozcích pacientů *post mortem*), že jednotlivé muskarinové receptory nejsou u Alzheimerovy choroby postiženy stejně.
- Vliv $A\beta_{1-42}$ na funkci mAChR může být přímý ($A\beta_{1-42}$ se přímo váže na mAChR) nebo nepřímý (pokud $A\beta_{1-42}$ ovlivňuje například vlastnosti okolní membrány či další molekuly vstupující do přímé interakce s receptorem, jako jsou například G-proteiny).
- Předpokládaný vliv $A\beta_{1-42}$ na mAChR se může projevovat na úrovni vazby (váže se na receptor a mění vazebné vlastnosti receptoru pro agonisty, antagonisty nebo obojí), na úrovni spřahování receptoru s G-proteinami, na úrovni aktivace G-proteinů a jejich signalizačních drah a koncentrace druhých poslů nebo se může vliv $A\beta_{1-42}$ projevovat jako kombinace výše uvedených možností.

Metody

1. Experimentální zvířata a příprava membrán

Transgenní myši kmene APPswe/PS1dE9 původně pocházející z Johns Hopkins University, Baltimore, MD, USA (D. Borchelt and J. Jankowsky, Dept. Pathology) byly chovány na University of Eastern Finland v Kuopiu (Finsko). Tyto myši exprimují konstrukt vytvořený z lidského genu pro APP s vloženou švédskou mutací (dvojitá záměna v aminokyselinách číslo 670 a 671 - lysin za methionin respektive asparagin za lysin) a z genu pro presenilin 1 s deleční mutací devátého exonu. K pokusům byly vždy použity kontrolní a transgenní samice ze stejného vrhu. Zvířata byla přemístěna letecky do Prahy a zde chována při následujících podmínkách: teplota 22 °C, světlo od 07:00 do 19:00, vzdušná vlhkost 50-60 %, voda i potrava *ad libitum*. Od převozu zvířat do zahájení experimentů uplynuly vždy minimálně dva týdny. Pokusy byly prováděny na dvou skupinách zvířat různého věku, 7–10 týdnů a 5–7 měsíců. Z mozkové kůry pravých hemisfér myší APPswe/PS1dE9 jsem připravila membrány pro měření vazby ^{35}S -GTP γ S. Mozková kůra (přibližně 100 mg) byla homogenizována skleněným homogenizérem na ledu, každý vzorek v 1,5 ml pufru obsahujícího 100 mM NaCl, 10 mM MgCl₂, 20 mM Hepes, 10 mM EDTA, pH 7.4. Homogenáty byly poté centrifugovány 30 minut při 30000 xg a 4 °C. Pelety membrán byly resuspendovány v 1,5 ml pufru (stejné složení jako výše, avšak bez EDTA), znova centrifugovány za stejných podmínek a skladovány při - 80 °C.

2. Buněčné kultury a příprava membrán

Pro sledování vlivu lidského β -amyloidu na jednotlivé podtypy mAChR jsem ve své práci využila buňky CHO trvale transfekované jednotlivými podtypy lidského mAChR (M1 – M5). Experimenty prováděné *in vitro* umožňují nejen odlišit rozdílné působení β -amyloidu na jednotlivé podtypy mAChR, ale také odstranit vliv celé řady proměnných, které v komplexních podmínkách mozkové tkáně či celého organismu nutně působí. Buňky CHO jsou fibroblasty, které se vyznačují velmi jednoduchým fenotypem. Přirozeně exprimují pouze velmi málo různých receptorů a žádné muskarinové receptory, takže případná interakce heterologně exprimovaných mAChR a dalších přirozeně se vyskytujících receptorů v buňce je minimální.

Fibroblasty z ovárií zlatého křečka (CHO cells - Chinese hamster ovary cells) stabilně exprimující jednotlivé podtypy lidských muskarinových receptorů (označované M1-5) byly laskavě poskytnuty profesorem T. I. Bonnerem (National Institute of Mental Health, Bethesda, MD). Byly pěstovány při teplotě 37 °C v přirozené atmosféře saturované vodou obsahující navíc 5% CO₂ v médiu pro tkáňové kultury (Dulbecco's modified Eagle's medium; DMEM) doplněném o 0,005 % geneticin a 10% fetální telecí sérum (Jakubík J. et al., 1995) v Petriho miskách (průměr 10 cm). Konfluentní buňky byly sklízeny po pěti dnech růstu v kultuře. Nejprve byly opláchnuty dvakrát 5 ml fosfátového izotonického roztoku (Phosphate Buffered Saline, PBS; 150 mM NaCl s 10 mM fosfátovým pufrem, pH=7.4) a následně, po přidání 3 ml PBS, jemně sklízeny pomocí škrabky. Poté následovala centrifugace 3 min při 300 xg a po odsátí supernatantu byly uskladněny v -20 °C. Zamražené buňky byly resuspendovány v homogenizačním médiu (100 mM NaCl, 20 mM Hepes, 10 mM EDTA, pH=7.4) a na ledu homogenizovány v homogenizátoru Ultra-Turrax při 22000 otáčkách/min dvakrát po dobu 30 sekund s přestávkou 30 s. Jádra a nerozbité buňky byly odstraněny nízkootáčkovou centrifugací při 300 xg po dobu 3 minut a při 4 °C. Supernatant byl rozdělen do mikrozkumavek a centrifugován 30 min při 30000 xg a 4 °C. Po odsátí supernatantu byl sediment (hrubá membránová frakce) promyt 1 ml reakčního media (stejně složení jako výše, avšak bez EDTA). Následovala druhá centrifugace 30 min při 30000 xg a 4 °C. Po odsátí supernatantu byly membrány zamraženy při -80 °C. Testované látky byly do média přidány druhý den po nasazení a byly přítomny až do okamžiku sklízení buněk. Ke zvýšení exprese muskarinových receptorů pro pokusy sledující bezprostřední účinek Aβ₁₋₄₂ na vazebné vlastnosti [³H]-N-methylskopolaminu ([³H]-NMS) byl do média přidán na posledních 24 hodin 5 mM butyrát sodný.

3. Vazebné saturační a kompetiční studie

Saturační vazebný pokus umožňuje přímo sledovat vazbu radioaktivně značeného ligandu k receptoru. Umožňuje kvantifikovat maximální počet vazebných míst (maximální vazba, B_{max}) a afinitu ligandu k receptoru (rovnovážná disociační konstanta, K_d). Hlavní nevýhodou saturačních pokusů je nutnost mít k dispozici studovaný ligand označený radioaktivním izotopem. Ve své práci jsem saturačními pokusy měřila přímo pouze vazbu muskarinového antagonisty [³H]-NMS.

Vytěsňovací studie obcházejí potřebu radioaktivně značeného ligandu tak, že měří afinitu neznačeného ligandu pomocí jeho interference se značeným ligandem. Neznačený

ligand vytěsňuje z vazebného místa radioaktivně značený ligand a pokles radioaktivního signálu je použit k určení afinity neznačeného ligandu. Z vazebné křivky vytěsňovacího pokusu můžeme odečíst koncentraci neznačeného ligandu, při které je z vazebných míst vytěsněno 50 % značeného kompetujícího ligandu (IC_{50}), a pokud je známa afinita značeného ligandu, můžeme určit také afinitu (K_d) neznačeného ligandu. Pro charakteristiku vazby agonisty jsem používala neznačený karbachol (nehydrolysovatelný analog přirozeného ligandu acetylcholinu) společně s radioaktivně značeným antagonistou [3H]-NMS.

Všechny vazebné studie byly prováděny v 96-jamkových destičkách v triplikátech až kvadruplikátech. Membrány byly resuspendovány v inkubačním médiu tak, aby byla zachována přibližná koncentrace 10 µg proteinu na jamku a poté byly inkubovány při 30 °C v inkubačním médiu (100 mM NaCl, 10 mM MgCl₂, 20 mM Hepes) doplněném o příslušnou koncentraci daného ligandu (v saturačních pokusech [3H]-NMS 62,5 pM až 2 nM, v kompetičních pokusech neznačený karbachol 30 nM až 3 mM a [3H]-NMS 1 nM). Pro určení účinku chronického působení A β ₁₋₄₂ byly k vazbě použity membrány buněk, jež rostly 4 dny v přítomnosti 100 nM A β ₁₋₄₂ (US Peptides, Rancho Cucamonga, CA) a v inkubačním médiu v průběhu vazebného pokusu již A β ₁₋₄₂ nebyl přítomen. Pro určení účinku bezprostředního působení A β ₁₋₄₂ byl do inkubačního média přidán A β ₁₋₄₂ v konečné koncentraci 1 µmol/l. Celkový inkubační objem byl 400 µl a nespecifická vazba byla stanovena pomocí neznačeného atropinu v konečné koncentraci 10 µM. Po stanovené době inkubace byly destičky filtrovány na filtračních zařízeních Tomtec Cell Harvester Mach III (USA) nebo Brandel Cell Harvester (USA) a membrány s navázaným radioaktivně značeným ligandem byly zachyceny na filtroch Whatmann GF/F případně na filtračních destičkách opatřených filtry Whatmann GF/C. Filtry či filtrační destičky byly předem namočeny v polyethyleniminu (snižuje nespecifickou vazbu kladně nabitého [3H]-NMS). Usušené filtry byly zality do scintilačního vosku Meltilex (Perkin Elmer, USA) a radioaktivita zachycená na filtroch v místech jednotlivých jamek změřena scintilačním počítačem Microbeta 1450 (Wallac, Finland). Filtrační destičky byly naplněny scintilačním roztokem Betaplate Scint (Perkin Elmer, USA) a radioaktivita v jednotlivých jamkách rovněž změřena scintilačním počítačem Microbeta. Koncentrace značeného ligandu byla vypočítána ze známé specifické radioaktivity [3H]-NMS a z radioaktivity v médiu stanovené v alikvotech přidávaného média kapalným scintilačním měřením v scintilačním roztoce Rotiszint (Carl Roth, Germany) pomocí scintilačního počítače Microbeta 1450 nebo Tri-Carb 2810 (Perkin Elmer, USA).

4. Vazba ^{35}S -GTP γ S

Zvýšení vazby ^{35}S -GTP γ S vyvolané muskarinovým agonistou karbacholem může být použito jako ukazatel schopnosti mAChR aktivovat G-proteiny. Karbacholem stimulovanou vazbu ^{35}S -GTP γ S jsem měřila na membránách připravených z mozkové kůry pravé hemisféry myší APPswe/PS1dE9 a na membránách připravených z CHO buněk trvale exprimujících jednotlivé podtypy mAChR. Alikvoty membrán obsahující kolem 10 µg proteinů byly nejprve 15 min preinkubovány při teplotě 30 °C ve 150 µl reakčního média obsahujícího 100 mM NaCl, 10 mM MgCl₂, 20 mM Hepes, 1 mM DTT, 50 µM GDP pro membrány z mozkové kůry, 40 µM GDP pro membrány z CHO buněk exprimujících M2 a M4 mAChR a 1 µM GDP pro M1 a M3 mAChR. Muskarinový agonista karbachol byl v médiu obsažen v koncentraci 0,3–100 µM pro membrány z mozkové kůry, 0,15–1000 µM pro M1 a M3 mAChR a 0,02–100 µM pro M2 a M4 mAChR. Po preinkubaci byly do inkubační směsi přidány 50 µl alikvoty ^{35}S -GTP γ S (Biotrend Chemikalien, Germany; SRA 1000 Ci/mmol) tak, aby finální koncentrace ^{35}S -GTP γ S byla 500 pM, a následovala inkubace 20 až 60 min podle typu membrán. Celkový obsah G-proteinů v membráně byl určen pomocí vazby ^{35}S -GTP γ S v nepřítomnosti GDP. Alikvoty membrán obsahující 5 µg proteinů byly inkubovány za stejných podmínek jako při měření stimulované vazby ^{35}S -GTP γ S. Nespecifická vazba byla určena v přítomnosti 10 µM neznačeného GTP γ S. Radioaktivita navázaná na membrány byla oddělena rychlou vakuovou filtrací na přístroji Tomtec Harvester Mach III (USA) s filtry Whatman GF/F (Whatman, USA). Usušené filtry byly zality do scintilačního vosku Meltilex a radioaktivita zachycená na filtroch v místech jednotlivých jamek změřená scintilačním počítačem Microbeta 1450.

5. Měření akumulace inositolfosfátů a inhibice syntézy cAMP

Akumulace inositolfosfátů stimulovaná karbacholem byla měřena v neporušených CHO buňkách, trvale transfekovaných příslušným podtypem muskarinového receptoru, rostoucích v 24-jamkových destičkách. Do média k rostoucím buňkám byl nejprve na 3 hodiny přidán radioaktivně značený ^3H -myo-inositol (ARC, USA). Poté byl volný (neinkorporovaný do buněk) ^3H -myo-inositol odmyt a různými koncentracemi karbacholu (0 – 100 µM) v přítomnosti 10 mM lithia, které inhibuje defosforylací uvolněných inositolfosfátů a tím i inkorporaci značeného myo-inositolu zpět do membrán, bylo

stimulováno štěpení membránového fosfatidylinositolu. Inkubace v přítomnosti karbacholu probíhala 5 min při teplotě 37 °C. Akumulace odštěpených ^3H -inositolfosfátů v buňkách byla stanovena jako radioaktivita extrahovaná do trichloroctové kyseliny v scintilačním roztoku Rotiszint pomocí scintilačního počítače Microbeta 1450.

Inhibice forskolinem stimulované syntézy cAMP byla měřena v suspenzi neporušených buněk exprimujících M2 mAChR, které byly pěstovány na Petriho miskách s průměrem 10 cm. Buňky z jedné 10 cm Petriho misky byly mechanicky uvolněny do PBS (150 mM NaCl, 10 mM fosfátový pufr, pH = 7.4), odděleny od sebe opakovaným opatrným nasáváním do pipety a sedimentovány centrifugací 5 min při 200 xg. Po odsátí supernatantu byly buňky resuspendovány ve 4 ml DMEM s 1 mM isobutylmethylxantinem a saturovaném 5% CO₂/95% O₂. Buňky byly preinkubovány 5 min při pokojové teplotě. Alikvoty buněčné suspenze (100 µl obsahující přibližně 100 µg proteinu) byly přidány do zkumavek se 100 µl alikvoty DMEM s 1 mM IBMX obsahujícím navíc 10 µM forskolin a 0-10 µM karbachol. Inkubace při 37 °C trvající 10 minut byla zastavena zchlazením vzorků na ledu a přidáním HCl v konečné koncentraci 100 mM. Pro stanovení koncentrace cAMP pomocí ELISA kitu (New East Biosciences, USA) podle návodu výrobce byly použity 100 µl alikvoty HCl extraktu.

6. Stanovení kaspázové aktivity a oxidační aktivity

Aktivita kaspázy-3 a kaspázy-8 byla stanovena fluorimetricky v buněčných lyzátech připravených z buněk rostoucích ve 24-jamkových destičkách. Jako substrát byly použity fluorescentní substráty acDVED-AMC pro kaspázu-3 a acIETD-AMC pro kaspázu-8 (oba Sigma Aldrich, Praha). Po odsátí média byla každá jamka promyta 1 ml PBS a buňky byly homogenizovány na ledu ve 200 µl lyzačního pufru (50 mM Hepes, 0.1% CHAPS, 0.1 mM EDTA, 1 mM DTT, pH = 7.4) opakovaným nasáváním do pipety. Poté byly ponechány na ledu 30 minut. Vzniklé homogenáty byly centrifugovány 10 min při 14000 xg a supernatanty byly použity pro stanovení obsahu proteinů a stanovení aktivity kaspáz. K 50 µl alikvotům buněčných lyzátů bylo přidáno 50 µl lyzačního pufru s obsahem příslušné fluorescentní próby (konečná koncentrace 10 µM). Fluorescence vzniklá štěpením substrátu byla měřena v 96-jamkových destičkách na čtečce destiček VictorTM pomocí umbelliferonových filtrů. Výsledná fluorescence byla vztažena na obsah proteinů v buněčném lyzátu. Obsah proteinů

v buněčných lyzátech byl stanoven po vysrážení proteinů kyselinou trichlorocotvou kvůli obsahu DTT, který interferuje se stanovením.

Oxidační aktivita v neporušených buňkách byla stanovena jako oxidace fluorescenční sondy 2',7'-dichlorodihydrofluorescein diacetát (Molecular Probes, USA). Buňky, pěstované v 24-jamkových destičkách, byly inkubovány 1 hodinu při 37 °C v Krebs-Hepes pufru (konečné mM koncentrace NaCl 138, KCl 4, CaCl₂ 1.3, MgCl₂ 1.2, NaH₂PO₄ 1.2, glukosa 11, Hepes 10, pH 7,4) s 10 µM sondou. Fluorescence byla měřena na čtečce destiček Victor™ při excitační/emisní vlnové délce 485/535 nm (fluoresceinové filtry).

7. Určení stupně agregace β-amylóidu 1-42

Rozsah agregace β-amylóidu 1-42 v zásobním roztoku (na počátku inkubace) a v kultivačním médiu po 4-denní inkubaci jsem určovala pomocí vazby thioflavinu T (upraveno podle Betts V. et al., 2008). Alikvoty vzorků o objemu 100 µl byly smíchány se 100 µl 200 mM glycinového pufru (pH 8,5), který obsahoval 12 µM thioflavin T (Sigma Aldrich, Praha, Česká republika). V mikrotitračních destičkách byla měřena fluorescence při 488 nm po excitaci vzorků při 450 nm pomocí čtečky destiček Victor.

8. Stanovení proteinů

Množství proteinů bylo stanovováno spektrofotometricky při 690 nm Lowryho metodou (Lowry OH. et al., 1951) v Petersonově modifikaci (Peterson GL., 1977).

9. Vyhodnocení výsledků

Prokládání křivek a statistické zpracování dat bylo provedeno za použití programů Microsoft Office Excel a GraphPad Prism5 (GraphPad software, Inc., San Diego, USA). Rozdíly mezi jednotlivými skupinami byly hodnoceny podle potřeby ANOVOU a následujícím Tukeyho nebo Dunnettovým testem, t-testem nebo párovým t-testem.

Vaturačních pokusech byly měřeny vlastnosti vazby radioaktivního antagonisty [³H]-NMS. Do grafu se vynáší závislost množství navázaného [³H]-NMS (radioaktivita změřená scintilačním počítáčem, osa y) na jeho známé koncentraci v inkubačním médiu (osa x). Získané body se prokládají rovnicí (1), výsledná funkce má tvar hyperboly. Z křivky

odečítáme B_{max} a K_d . Jednotlivé hodnoty jsou vyjádřeny jako průměr \pm S.E.M. (Standard Error of the Mean; střední chyba průměru).

$$Y = B_{max} \cdot X / (K_d + X) \quad (1)$$

Y – vazba radioligandu při jeho koncentraci X , B_{max} – maximální vazebná kapacita, K_d – rovnovážná disociační konstanta

Ve vytěšňovacích pokusech byly nepřímo měřeny vlastnosti vazby agonisty karbacholu podle poklesu vazby kompetujícího radioligandu $[^3H]$ -NMS. Do grafu se vynáší závislost poklesu vazby (vytěsnování) konstantní koncentrace $[^3H]$ -NMS na zvyšující se koncentraci neznačeného agonisty. Body se prokládají rovnicí pro vytěšňovací křivku o jedné (2) případně dvou (3) vazebných komponentách. Vytěšňovací křivka o jedné vazebné komponentě prokazuje kompetici obou ligandů na ortosterickém vazebném místě s jedinou konformací. V důsledku interakcí s G-proteiny však dochází ke konformační změně receptoru, která se ve vazebných pokusech projevuje jako přítomnost ortosterických vazebných míst s různými afinitami pro agonistu, zatímco $[^3H]$ -NMS (jako i ostatní antagonisté) má stejnou afinitu pro různé konformace receptoru. Z vytěšňovací křivky o dvou vazebných komponentách odečítáme IC_{50}^{high} (koncentrace agonisty, která vytěsní $[^3H]$ -NMS z poloviny vysokoafinitních míst) a IC_{50}^{low} (koncentrace agonisty, která vytěsní $[^3H]$ -NMS z poloviny nízkoafinitních míst) a zároveň poměr zastoupení vysoko a nízkoafinitních míst v populaci receptorů. Jednotlivé hodnoty jsou vyjádřeny jako průměr \pm S.E.M.

$$Y = Bottom + (Top - Bottom) / (1 + 10^{(X - LogIC50)}) \quad (2)$$

$$Y = Bottom + [(Top - Bottom) * Fraction1 / (1 + 10^{(X - LogIC50_1)})] + [(Top - Bottom) * (1 - Fraction1) / (1 + 10^{(X - LogIC50_2)})] \quad (3)$$

Y – vazba $[^3H]$ -NMS při koncentraci agonisty X vyjádřená jako procento vazby v nepřítomnosti agonisty, $Bottom$ – minimální vazba, Top – maximální vazba, $Fraction1$ – frakce nízkoafinitních vazebných míst, $IC50_1$ - koncentrace agonisty vytěsnující 50% radioligandu na nízkoafinitním vazebném místě, $IC50_2$ - koncentrace agonisty vytěsnující 50% radioligandu na vysokoafinitním vazebném místě

Výsledné hodnoty z funkčních pokusů (vazba ^{35}S -GTP γ S, akumulace inositolfosfátů, inhibice syntézy cAMP) byly proloženy sigmoidální křivkou s pevným (4) nebo variabilním sklonem (5) znázorňující závislost účinku na koncentraci agonisty. Jednotlivé hodnoty jsou vyjádřeny jako průměr \pm S.E.M. Výsledky funkčních pokusů odráží alosterickou interakci mezi agonistou (karbacholem), který působí na receptor z extracelulární strany membrány, a G-proteinem, který interaguje s receptorem na intracelulární straně membrány a přenáší signál dál do buňky.

$$Y = Bottom + (Top - Bottom) / (1 + 10^{((X - LogEC50))}) \quad (4)$$

$$Y = Bottom + (Top - Bottom) / (1 + 10^{((LogEC50 - X) * HillSlope)}) \quad (5)$$

Y – funkční odpověď při koncentraci agonisty X, Bottom – bazální odpověď, Top – maximální odpověď, EC50 – koncentrace agonisty, která vyvolá poloviční odpověď mezi bazální a maximální odpovědí, Hill slope – Hillův koeficient („strmost křivky“), který popisuje míru kooperativity děje (Hillův koeficient = 1 v případě, že receptor kooperuje s jedním druhem G-proteinu; je-li koeficient odlišný od jedné, receptor kooperuje s větším počtem různých G-proteinů)

Vhodnější proložení získaných vazebních i funkčních dat bylo určováno pomocí F-testu.

Výsledky

1. Vliv A β ₁₋₄₂ na vazebné vlastnosti jednotlivých podtypů mAChR

1.1. Vliv A β ₁₋₄₂ na vazebné vlastnosti mAChR pro [³H]-NMS

[³H]-NMS je muskarinový antagonist, který se váže ke všem podtypům mAChR a na rozdíl od agonistů nerozeznává nízko- a vysokoafinitní stav receptoru. Vazbu [³H]-NMS jsem měřila na membránách připravených z CHO buněk heterologně exprimujících vždy jeden z pěti podtypů mAChR, které byly vystaveny akutnímu či chronickému působení A β ₁₋₄₂. Z vazby [³H]-NMS jsem určovala expresi jednotlivých podtypů mAChR (B_{max}) a afinitu jednotlivých podtypů k antagonistovi (K_d).

Akutní ani chronické působení A β ₁₋₄₂ signifikantně nezměnilo ani afinitu pro antagonistu [³H]-NMS a ani počet vazebných míst u žádného z podtypů mAChR. Afinita jednotlivých podtypů mAChR pro [³H]-NMS se pohybovala v rozmezí 70 až 600 pM a klesala v pořadí M4 > M1 > M3 > M2 > M5. Změřené afinity a jejich průměrné hodnoty u jednotlivých podtypů bez ohledu na působení A β ₁₋₄₂, které byly použity pro výpočty u vytěšňovacích pokusů, jsou uvedené v Tabulce 1. Hodnoty B_{max} membrán vystavených akutnímu či chronickému působení A β ₁₋₄₂, které se v párovaných pokusech pohybovaly mezi 88 a 124 % kontrolních hodnot, jsou uvedeny v Tabulce 2.

Receptor	M1	M2	M3	M4	M5
Kontrolní membrány	197±16 (9)	411±87 (9)	221±32 (9)	74±94 (7)	625±82 (10)
Akutní působení A β	183±28 (6)	508±126 (4)	204±71 (4)	50±3 (4)	701±16 (7)
Chronické působení A β	217±31 (3)	368±77 (3)	169±19 (3)	76±12 (3)	387±64 (3)
Průměr	195±13 (18)	427±58 (16)	207±24 (16)	67±6 (14)	596±52 (20)

Tabulka 1

Vliv akutního a chronického působení A β_{1-42} na afinitu jednotlivých podtypů mAChR pro antagonistu [3 H]-NMS

Výsledky jsou průměr \pm SEM rovnovážné disociační konstanty (K_d ; pM) naměřené na kontrolních membránách a membránách vystavených akutnímu či chronickému působení A β_{1-42} . Počet pokusů (vždy provedených v kvadruplikátech) je uveden v závorce. V posledním rádku (průměr) jsou hodnoty K_d vypočítané jako průměr ze všech měření, bez ohledu na působení A β_{1-42} .

Receptor	M1	M2	M3	M4	M5
Akutní působení A β (% kontrol)	97 \pm 4 (6)	106 \pm 10 (4)	96 \pm 5 (4)	103 \pm 5 (4)	125 \pm 11 (7)
Chronické působení A β (% kontrol)	110 \pm 5 (3)	89 \pm 12 (3)	105 \pm 12 (3)	114 \pm 24 (3)	91 \pm 17 (3)

Tabulka 2

Vliv akutního a chronického působení A β_{1-42} na expresi jednotlivých podtypů mAChR měřenou jako maximální vazba [3 H]-NMS

Hodnoty B_{max} naměřené na membránách CHO buněk exprimujících jednotlivé podtypy mAChR vystavených akutnímu a chronickému působení A β_{1-42} jsou vyjádřené jako % kontrol \pm SEM v párovaných pokusech. Počet pokusů (vždy provedených v kvadruplikátech) je uveden v závorce. Absolutní hodnoty kontrolní vazby byly pro M1-M5 receptory 10.88 \pm 0.72, 2.54 \pm 0.82, 13.56 \pm 0.86, 2.78 \pm 0.22 a 0.90 \pm 0.13 pmol/mg proteinu u pokusů sledujících bezprostřední účinek A β_{1-42} a 1.83 \pm 0.21, 0.52 \pm 0.11, 0.63 \pm 0.14, 0.42 \pm 0.02 a 0.48 \pm 0.13 pmol/mg u pokusů sledujících chronický účinek. Vyšší exprese receptorů u pokusů s bezprostředním účinkem A β_{1-42} je způsobena přidáním butyrátu do inkubačního média 24 hodin před sklízením u buněk, které byly použity pro přípravu membrán pro tyto pokusy.

1.2. Vliv A β_{1-42} na vazebně vlastnosti mAChR pro karbachol

Na rozdíl od [3 H]-NMS se muskarinový agonista karbachol může k receptoru vázat s vysokou či nízkou afinitou podle aktuálního stavu receptoru. Vazebná vytěšňovací křivka karbacholu a dalších agonistů proto obsahuje dvě vazebné komponenty („dvoumístná“ křivka). Vazbu karbacholu jsem měřila v kompetičních pokusech jako pokles vazby radioaktivně značeného [3 H]-NMS. Stejně jako v případě saturačních pokusů s [3 H]-NMS, také vazbu karbacholu jsem měřila na membránách připravených z CHO buněk heterologně exprimujících vždy jeden z pěti podtypů mAChR, které byly vystaveny akutnímu či

chronickému působení $A\beta_{1-42}$ (Obrázek 1). Na M1 mAChR, u kterého jsem zjistila signifikantní rozdíly ve vazbě karbacholu po chronickém působení 100 nM $A\beta_{1-42}$, jsem rovněž testovala chronické působení $A\beta_{1-42}$ v různých koncentracích a působení scrambled $A\beta_{1-42}$ (peptid se stejným složením aminokyselin jako $A\beta_{1-42}$, avšak v pozmeněném pořadí) a rovněž jsem měřila vazbu karbacholu v přítomnosti nehydrolyzovatelného analogu GTP, GppNHp (Obrázek 2).

Z vazebné křivky pro karbachol obsahující dvě vazebné komponenty je možné určit afinitu receptoru k agonistovi v nízko- a vysokoafinitním stavu a dále poměrné zastoupení receptorů v nízko- a vysokoafinitním stavu v celkové populaci receptorů (běžne označované jako „počet nízko- a vysokoafinitních míst“, přestože se ve skutečnosti nejedná o různá vazebná místa). Průměrné parametry získané z jednotlivých vazebných kompetičních pokusů a počty pokusů jsou uvedené v Tabulce 3. Vazebné křivky z jednotlivých sérií pokusů jsou uvedeny na Obrázku 1, 2 a 3.

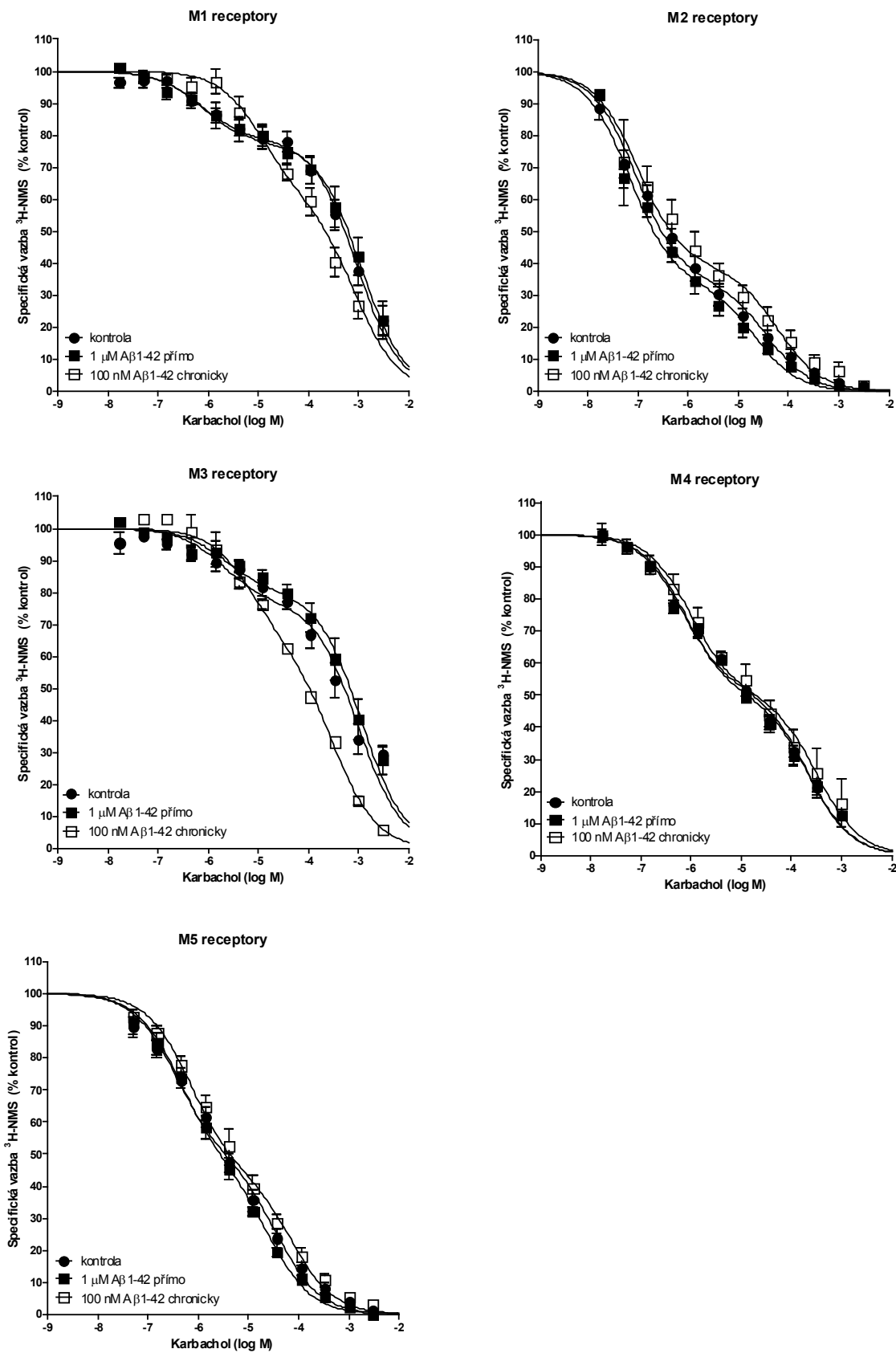
Akutní působení $A\beta_{1-42}$, kdy byl 1 μM $A\beta_{1-42}$ přítomen v médiu pouze 60 min v průběhu inkubace vazebného pokusu, signifikantně nezměnilo žádný parametr vazby agonisty karbacholu u žádného z podtypů mAChR. Na druhou stranu chronické působení, kdy 100 nM $A\beta_{1-42}$ byl přítomen v kultivačním médiu během růstu buněk a naopak do reakčního média v průběhu vazebného pokusu již přidáván nebyl, ovlivnilo vazbu karbacholu na M1 a M3 mAChR. Došlo k signifikantnímu snížení afinity vysokoafinitních vazebných míst pro karbachol a zároveň ke zvýšení jejich poměrného zastoupení u M1 receptoru, u M3 receptoru pak bylo zjištěno pouze signifikantní zvýšení relativního počtu vysokoafinitních vazebných míst. U M1 receptoru byly následně provedeny pokusy s chronickým působením $A\beta_{1-42}$ v dalších koncentracích (10 nM a 1 μM), které rovněž statisticky významně měnily afinitu vysokoafinitního vazebného místa, jejich vliv na počet vysokoafinitních vazebných míst však nebyl signifikantní. Naopak 100 nM scrambled $A\beta_{1-42}$ sloužící jako negativní kontrola signifikantně neměnil žádný z parametrů vazby karbacholu u M1 mAChR. Vazba karbacholu k M1 mAChR i vazba karbacholu k M1 mAChR vystavenému chronickému vlivu $A\beta_{1-42}$ byla provedena také v přítomnosti nehydrolyzovatelného analogu GTP, GppNHp, který působí nevratné rozpřažení receptoru od G-proteinu. Podle očekávání přidání GppNHp do reakčního média vyvolalo přeměnu vazebné křivky o dvou vazebných komponentách na křivku o jedné komponentě, tedy přeměnu vysokoafinitních míst na místa s nízkou afinitou. Afinity vazby karbacholu se v přítomnosti GppNHp (u rozpřažených receptorů) nijak nelišily u kontrolních M1 mAChR a u receptorů připravených z buněk vystavených chronickému vlivu $A\beta_{1-42}$.

		pKi high	pKi low	frakce high
M1	kontrolní (19)	6,73±0,14	3,91±0,08	0,21±0,02
	kontrolní + GppHNp (3)	---	3,88±0,13	---
	akutní Aβ 1 μM (6)	7,08±0,11	3,75±0,18	0,20±0,03
	chronický Aβ 10 nM (5)	5,52±0,15**	3,75±0,05	0,28±0,04
	chronický Aβ 100 nM (8)	5,68±0,27**	4,07±0,16	0,33±0,03**
	chronický Aβ 1 μM (8)	5,65±0,01**	3,77±0,04	0,26±0,04
	chronický scrambled Aβ 100 nM (5)	6,62±0,25	3,90±0,02	0,20±0,03
	chronický Aβ 100 nM + GppHNp (3)	---	3,83±0,12	---
M2	kontrolní (11)	7,56±0,10	4,96±0,08	0,66±0,03
	akutní Aβ 1 μM (4)	7,72±0,09	5,21±0,02	0,66±0,04
	chronický Aβ 100 nM (5)	7,60±0,22	4,84±0,19	0,61±0,03
M3	kontrolní (9)	6,58±0,29	3,93±0,13	0,20±0,02
	akutní Aβ 1 μM (6)	6,74±0,36	3,80±0,13	0,20±0,04
	chronický Aβ 100 nM (3)	6,01±0,36	4,25±0,05	0,38±0,06*
M4	kontrolní (7)	7,39±0,05	4,94±0,09	0,46±0,02
	akutní Aβ 1 μM (4)	7,36±0,09	4,90±0,13	0,48±0,02
	chronický Aβ 100 nM (3)	7,50±0,08	5,10±0,06	0,47±0,01
M5	kontrolní (8)	6,91±0,15	4,93±0,02	0,49±0,03
	akutní Aβ 1 μM (3)	6,81±0,19	5,01±0,08	0,54±0,05
	chronický Aβ 100 nM (4)	6,60±0,11	4,57±0,15	0,55±0,06

Tabulka 3

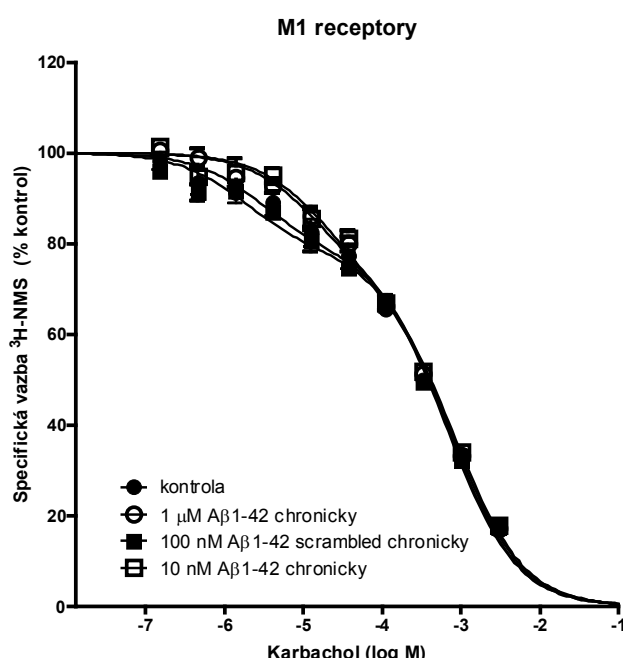
Vliv Aβ₁₋₄₂ na vazebné vlastnosti agonisty karbacholu na membránach CHO buněk exprimujících jednotlivé podtypy mAChR.

Afinita karbacholu byla zjišťována nepřímo podle vytěšňování [³H]-NMS z vazby na receptor. Vytěšňovací pokusy byly provedeny na kontrolních membránách v nepřítomnosti nebo přítomnosti Aβ₁₋₄₂ a na membránách, připravených z buněk pěstovaných v přítomnosti Aβ₁₋₄₂ (v případě M1s různými koncentracemi Aβ₁₋₄₂ a také s Aβ₁₋₄₂ scrambled). U M1 mAChR byla vazba změřena též v přítomnosti GppNHp, který rozpráhuje receptory od G-proteinů. Afinita vysokoafinitních (Ki high) a nízkoafinitních (Ki low) míst jsou vyjádřeny jako záporný dekadický logaritmus koncentrace (pKi) karbacholu ± SEM. Vysokoafinitní frakce (frakce high) je podíl vysokoafinitních míst na celkovém počtu vazebných míst ± SEM. Počet pokusů je uvedený v závorkách. *, p<0.05; **, p<0.01, statisticky významný rozdíl od kontrol (bez působení β-amloidu) pomocí ANOVA a Dunnettova testu.

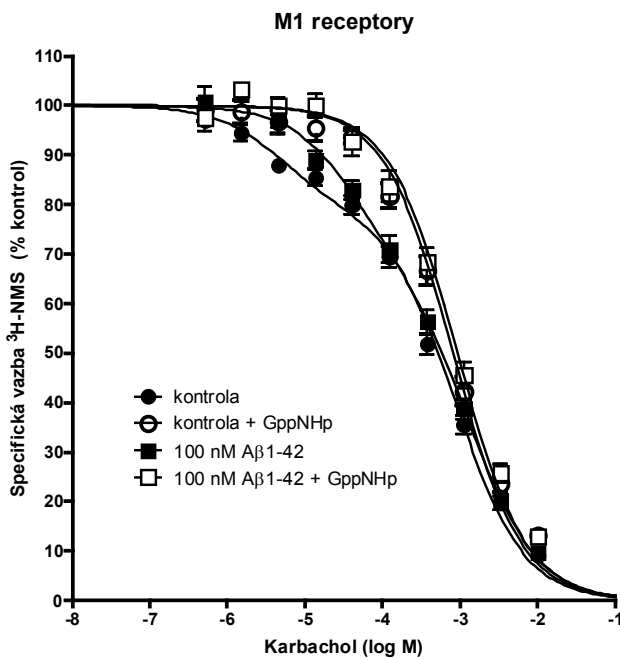


Obrázek 1**Vliv přímého a chronického působení $A\beta_{1-42}$ na vazbu muskarinového agonisty karbacholu k jednotlivým podtypům mAChR**

V grafech pro jednotlivé podtypy mAChR jsou znázorněny vazebné křivky získané u kontrolních membrán v nepřítomnosti (černé body) nebo přítomnosti (černé čtverečky) $A\beta_{1-42}$ a u membrán, připravených z buněk vystavených chronickému působení $A\beta_{1-42}$. Výsledky jsou vyjádřeny jako procento maximální vazby [3 H]-NMS v nepřítomnosti karbacholu. Body jsou průměr \pm SEM. Parametry proložení všech naměřených hodnot vytěšňovací křivkou o dvou vazebných komponentách a počty pokusů jsou uvedeny v Tabulce 3.

**Obrázek 2****Vliv chronického působení různých koncentrací $A\beta_{1-42}$ a scrambled $A\beta_{1-42}$ na vazbu muskarinového agonisty karbacholu k membránám exprimujícím M1 mAChR**

V grafu je znázorněna kontrolní vazebná křivka (černé kroužky) a vazebné křivky membrán vystaveným chronickému působení $A\beta_{1-42}$ v koncentraci 10 nM (bílé čtverečky) nebo 1 μ M (bílé kroužky) a 100 nM $A\beta_{1-42}$ se změněným pořadím aminokyselin (scrambled; černé čtverečky). Výsledky jsou vyjádřeny jako procento maximální vazby [3 H]-NMS v nepřítomnosti karbacholu. Body jsou průměr \pm SEM. Parametry proložení měřených hodnot vytěšňovací křivkou o dvou vazebných komponentách a počty pokusů jsou uvedeny v Tabulce 3.



Obrázek 3

Vliv GppNHp na vazbu karbacholu ke kontrolním membránám exprimujícím M1 mAChR a k membránám připraveným z buněk vystavených chronickému působení A β ₁₋₄₂

V grafu jsou znázorněny vazebné křivky u kontrolních membrán (černé kroužky) a membrán připravených z buněk po chronickém působení A β ₁₋₄₂ (černé čtverečky) v nepřítomnosti GppNHp a křivky pro stejné membrány v přítomnosti GppNHp (bílé kroužky a čtverečky). Původní vytěšňovací křivky o dvou vazebných komponentech se v přítomnosti GppNHp mění na křivku o jedné komponentě s afinitou odpovídající afinitě nízkoafinitních míst. V nepřítomnosti GppNHp se liší průběh vazby u kontrolních membrán a membrán vystavených chronickému vlivu A β ₁₋₄₂, zatímco po přidání GppNHp je průběh vazby u obou typů membrán stejný. Výsledky jsou vyjádřeny jako procento maximální vazby [³H]-NMS v nepřítomnosti karbacholu. Body jsou průměr±SEM. Parametry proložené naměřených hodnot vytěšňovací křivkou o jedné nebo dvou vazebných komponentech a počty pokusů jsou uvedeny v Tabulce 3.

2. Vliv chronického působení A β ₁₋₄₂ na funkční vlastnosti jednotlivých podtypů mAChR

Protože ve vazebných saturačních a kompetičních pokusech byl zjištěn signifikantní účinek pouze u chronického působení A β ₁₋₄₂, provedla jsem funkční pokusy pouze s membránami a celými buňkami, které byly rovněž vystaveny chronickému působení 100 nM A β ₁₋₄₂. Nejprve jsem zjišťovala možný vliv A β ₁₋₄₂ na aktivaci G-proteinů měřenou jako karbacholem stimulovanou vazbu ^{35}S -GTP γ S. Následně jsem zjišťovala vliv A β ₁₋₄₂ na dvě odlišné signalizační dráhy zprostředkovávané lichými a sudými podtypy mAChR – akumulaci inositolfosfátů a inhibici syntézy cAMP stimulované forskolinem.

2.1. Vliv chronického působení A β ₁₋₄₂ na aktivaci G-proteinů

Aktivaci G-proteinů zprostředkovanou jednotlivými podtypy mAChR jsem měřila jako vazbu ^{35}S -GTP γ S stimulovanou karbacholem. Změna konformace receptoru, která následuje po vazbě agonisty, způsobí uvolnění GDP z α -podjednotky spřaženého G-proteinu a jeho výměnu za GTP. V pokusech jsem použila jeho radioaktivně značený analog ^{35}S -GTP γ S, který se váže na α -podjednotku, avšak (podobně jako GppNHp) není hydrolyzován její GTPázovou aktivitou. Z křivek popisujících vztah mezi koncentrací agonisty karbacholu a vazbou ^{35}S -GTP γ S je pak možné odečíst maximální funkční odpověď E_{max} a hodnotu EC₅₀ vyjadřující koncentraci agonisty, která vyvolá 50 % maximální funkční odpovědi.

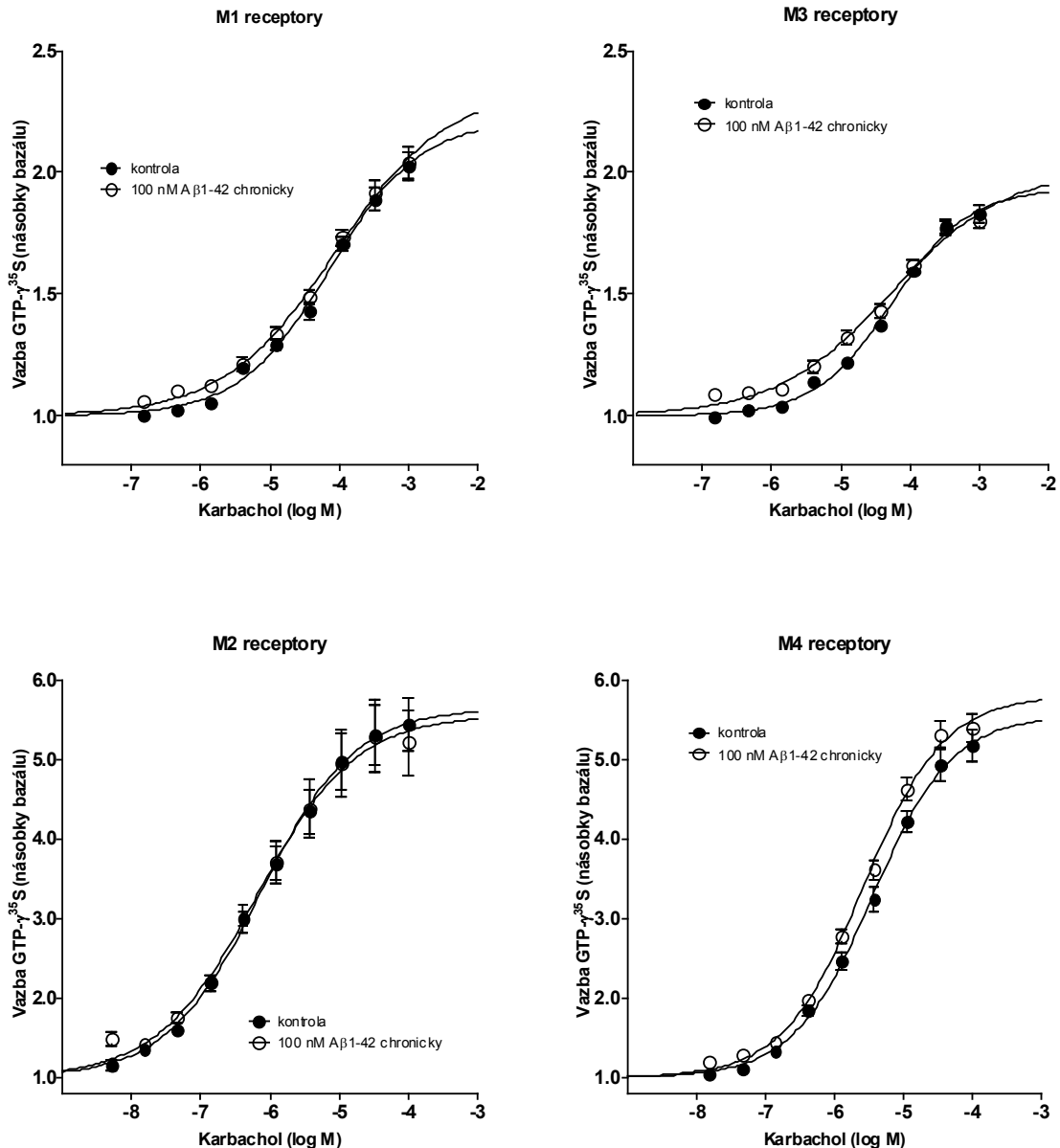
V pokusech s vazbou ^{35}S -GTP γ S jsem nezjistila žádný rozdíl v E_{max} nebo EC₅₀ mezi kontrolními membránami a membránami vystavenými chronickému působení A β ₁₋₄₂ u žádného ze sledovaných podtypů mAChR (M1 – M4; Obrázek 4 a Tabulka 4). Zároveň jsem nezjistila žádný rozdíl ani v bazální vazbě (vazba ^{35}S -GTP γ S bez přidání karbacholu) nebo celkové vazbě (vazba ^{35}S -GTP γ S bez přidání GDP do inkubačního média, při které dojde k obsazení všech vazebných míst α -podjednotek přítomných G-proteinů) u kontrolních membrán a membrán vystavených vlivu A β ₁₋₄₂. U všech sledovaných podtypů mAChR byl Hillův koeficient (sklon křivky) menší než jedna, což znamená, že v daném rozsahu koncentrací karbacholu docházelo nejen k interakci mezi receptorem a preferenčním G-proteinem (G_{i/o} u sudých a G_{q/11} u lichých podtypů), ale také k interakci receptoru s nepreferenčními G-proteiny.

		Emax (násobky bazální vazby)	pEC50	Hillův koeficient	Bazální vazba (dpm/µg)	Celková vazba (dpm/µg)
M1	kontrolní (7)	2,20±0,08	4,21±0,05	0,81±0,07*	1301±193	8433±501
	chronický Aβ 100nM (6)	2,32±0,15	4,23±0,15	0,75±0,08*	1170±162	8019±626
M2	kontrolní (4)	4,67±0,75	6,14±0,04	0,62±0,07*	206±12	6822±219
	chronický Aβ 100nM (4)	4,52±0,94	6,21±0,09	0,61±0,05*	197±45	6225±1027
M3	kontrolní (5)	1,93±0,07	4,27±0,06	0,78±0,06*	1329±201	6963±404
	chronický Aβ 100nM (5)	1,98±0,06	4,23±0,09	0,60±0,05*	1379±166	7611±555
M4	kontrolní (4)	4,59±0,51	5,44±0,09	0,77±0,05*	104±12	6050±595
	chronický Aβ 100nM (4)	4,81±0,37	5,58±0,06	0,75±0,04*	108±16	6536±568

Tabulka 4

Parametry vazby ^{35}S -GTP γ S u kontrolních membrán a membrán připravených z buněk vystavených chronickému vlivu A β_{1-42}

Hodnoty E_{max} jsou vyjádřeny jako násobky bazální vazby v nepřítomnosti karbacholu ± SEM, hodnoty EC₅₀ jako záporný dekadický logaritmus koncentrace (pEC₅₀) karbacholu ± SEM. Bazální vazba a celková vazba ^{35}S -GTP γ S jsou uvedeny v absolutních hodnotách vztažených na proteiny jako průměr ± SEM. Nižší bazální vazba u membrán exprimujících M2 a M4 receptory je způsobena přítomností vyšší koncentrace GDP v inkubačním médiu při měření stimulace vazby (viz metody). Hodnoty Hillova koeficientu jsou ve všech případech signifikantně menší než jedna (*; p<0,05 podle one sample t-testu). V žádném z uvedených parametrů nebyl zjištěn rozdíl mezi kontrolními membránami a membránami vystavenými chronickému působení A β_{1-42} . Počet pokusů je uvedený v závorkách.

**Obrázek 4**

Stimulace vazby 35 S-GTP γ S karbacholem u membrán exprimujících M1-M4 mAChR připravených z kontrolních buněk a buněk pěstovaných v přítomnosti A β ₁₋₄₂

Výsledky měření jsou vyjádřeny jako násobky bazální vazby v nepřítomnosti karbacholu. Průběh vazby se neliší mezi kontrolními membránami a membránami vystavenými chronickému působení A β ₁₋₄₂ u žádného ze sledovaných podtypů mAChR. Hillův koeficient uvedených křivek je ve všech případech menší než jedna. Body jsou průměr \pm SEM. Parametry proložené hodnoty ze všech měření a počty pokusů jsou uvedeny v Tabulce 4.

2.2. Vliv chronického působení A β ₁₋₄₂ na aktivaci nitrobuněčných signalizačních drah M1 a M2 mAChR

Chronické působení A β ₁₋₄₂ ovlivňovalo vazebné vlastnosti pro agonistu u M1 mAChR, avšak nemělo žádný vliv na stimulaci vazby ³⁵S-GTP γ S (viz 2.1.). Hillův koeficient koncentrační závislosti aktivace G-proteinů karbacholem však ukázal, že po vazbě karbacholu dochází k aktivaci nejen preferenčních G-proteinů, a případná změna spřahování receptoru s preferenčním G-proteinem tak může být „překryta“ interakcí s jinou početně silnější třídou nepreferenčních G-proteinů (konkrétně v případě M1 receptoru, který se preferenčně spřahuje s G_{q/11}, může převažovat interakce s G_{i/o}, které jsou výrazně početnější než ostatní třídy G-proteinů).

Abych zjistila, zda změna vazebných vlastností u M1 receptoru ovlivňuje přenos signálu do buňky, studovala jsem možný vliv chronického působení A β ₁₋₄₂ na aktivaci specifických signalizačních drah M1 a M2 mAChR pomocí měření koncentrace takzvaných druhých poslů – akumulaci inositolfosfátů (stimulovanou aktivací lichých podtypů mAChR) a syntézu cAMP (inhibovanou aktivací sudých podtypů mAChR) v neporušených buňkách. Zvyšující se koncentrace muskarinového agonisty karbacholu aktivují nebo inhibují, v závislosti na podtypu mAChR, syntézu druhého posla, jehož koncentraci můžeme měřit. Z křivek popisujících vztah mezi koncentrací karbacholu a tvorbou druhých poslů (inositolfosfátů a cAMP) jsem opět odečítala maximální funkční odpověď E_{max} (I_{max} v případě cAMP, neboť se jedná o inhibici jeho syntézy) a hodnotu EC₅₀ (IC₅₀).

V případě inhibice forskolinem stimulované syntézy cAMP, která je závislá na aktivaci G_{i/o} proteinů skrze sudé podtypy mAChR, nebyl žádný rozdíl v hodnotách I_{max} ani IC₅₀ u buněk exprimujících M2 podtyp mAChR vystavených chronickému působení A β ₁₋₄₂ a kontrolních buněk (Obrázek 5 pravý panel, Tabulka 5). Na druhou stranu, v případě aktivování akumulace inositolfosfátů, které je zprostředkováno lichými podtypy mAChR spřazenými s G_{q/11} proteiny, došlo u buněk vystavených chronickému vlivu A β ₁₋₄₂ a exprimujících M1 podtyp mAChR ke snížení E_{max} přibližně o 14 % (p < 0.01 podle t-testu; Obrázek 5 levý panel, Tabulka 5). Toto snížení nebylo způsobené nižší inkorporací ³H-myoinositolu do membrán ani rozdílem v bazální (klidové) akumulaci značených inositolfosfátů v nepřítomnosti agonisty. Tyto hodnoty se vzájemně nelišily u kontrolních buněk a buněk vystavených chronickému působení A β ₁₋₄₂. Inkorporace ³H-myoinositolu do buněk byla 132±5 dpm/ μ g proteinu u kontrolních buněk a 141±6 dpm/ μ g proteinu u buněk

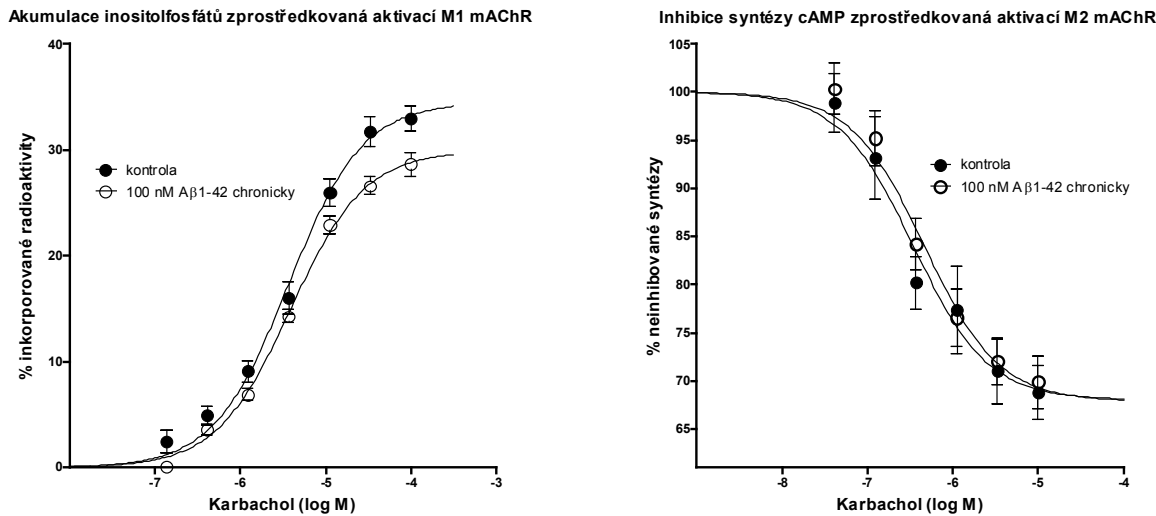
vystavených chronickému působení A β_{1-42} (průměr \pm SEM z pěti pokusů). Bazální akumulace inositolfosfátů byla v těchto pokusech 25,4 \pm 1,8 a 24,4 \pm 1,0 procent z celkové inkorporované radioaktivity (průměr \pm SEM z pěti pokusů). Parametry funkčních pokusů s inhibicí syntézy cAMP skrze aktivaci M2 mAChR a aktivací akumulace inositolfosfátů skrze aktivaci M1 mAChR jsou uvedeny v Tabulce 5, průběh křivek je znázorněn na Obrázku 5.

		E_{max}	pEC₅₀	Hillův koeficient
M1	kontrolní (5)	34,7 \pm 1,8	5,44 \pm 0,11	1,00
Stimulace inositolfosfátů	Chronický Aβ100 nM (5)	30,0 \pm 2,0**	5,40 \pm 0,02	1,00
M2	kontrolní (6)	34,5 \pm 4,0	6,32 \pm 0,28	1,00
Inhibice cAMP	Chronický Aβ 100 nM (6)	33,2 \pm 3,7	6,30 \pm 0,20	1,00

Tabulka 5

Parametry aktivace nitrobuněčných signálních drah u buněk exprimujících M1 a M2 mAChR, které rostly za kontrolních podmínek nebo byly vystaveny chronickému vlivu A β_{1-42}

Hodnoty stimulované akumulace inositolfosfátů (E_{max}) jsou v případě M1 receptoru vyjádřeny jako procenta z radioaktivity inkorporované do membrán (čistý nárůst po odečtení bazální akumulace), v případě M2 receptoru jsou hodnoty inhibice tvorby cAMP vyjádřeny v procentech, o něž se snížila původní (neinhibitovaná) syntéza cAMP. Hodnoty EC₅₀ jsou vyjádřeny jako záporný dekadický logaritmus koncentrace (pEC₅₀) karbacholu \pm SEM. Počet pokusů je uvedený v závorkách. **, p < 0,01, signifikantně odlišné od kontrol pomocí t-testu



Obrázek 5

Vliv chronického působení A β 1-42 na koncentrační závislost akumulace inositolfosfátů v buňkách exprimujících M1 mAChR a inhibice syntézy cAMP stimulované forskolinem v buňkách exprimujících M2 mAChR karbacholem

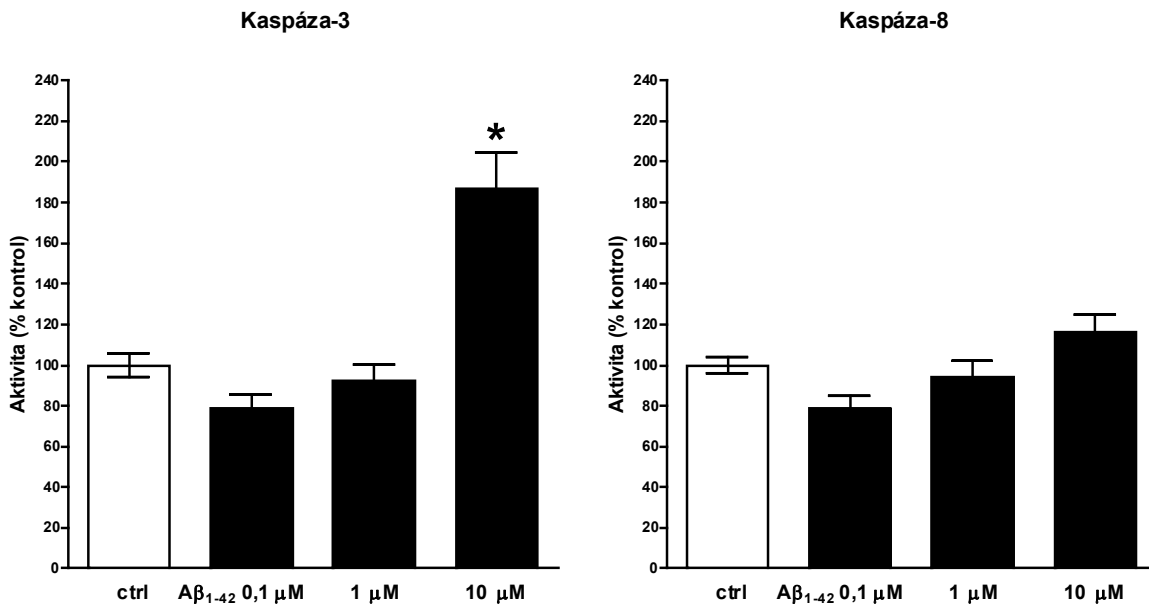
Akumulace inositolfosfátů stimulovaná karbacholem u buněk exprimujících M1 receptor (levý panel) je vyjádřena v procentech celkové inkorporované radioaktivitě. Inhibice forskolinem stimulované syntézy cAMP u buněk exprimujících M2 receptor (pravý panel) je vyjádřena v procentech kontrol v nepřítomnosti karbacholu. Popisy křivek jsou uvedeny v obrázku. V případě M1 mAChR je patrné snížení E_{max} u buněk vystavených chronickému působení A β 1-42. Hillův koeficient uvedených křivek je ve všech případech roven jedné. Body jsou průměr±SEM. Parametry křivek a počet pokusů jsou uvedeny v Tabulce 5.

3. Aktivita kaspáz a tvorba volných kyslíkových radikálů v buňkách vystavených chronickému vlivu A β 1-42

Jedním z možných vysvětlení snížené akumulace inositolfosfátů vyvolané stimulací M1 mAChR karbacholem je obecně toxicí vliv A β 1-42 na buňky. Abych prověřila tuto možnost, měřila jsem aktivitu kaspázy-3 a kaspázy-8 v buňkách rostoucích v přítomnosti různých koncentrací A β 1-42 (100 nM – 10 μ M). V těchto buňkách jsem rovněž určovala hladinu volných kyslíkových radikálů, jejichž tvorba by také mohla být zvýšená vlivem obecné toxicity A β 1-42 a které by posléze mohly negativně ovlivnit funkci signálních drah aktivovaných M1 mAChR.

U buněk exprimujících M1 a M2 mAChR a rostoucích v přítomnosti nižších koncentrací A β 1-42 (až do koncentrace 1 μ M) nebylo patrné žádné signifikantní zvýšení kaspázových aktivit (Obrázek 6). Pouze u buněk rostoucích v přítomnosti 10 μ M A β 1-42 došlo

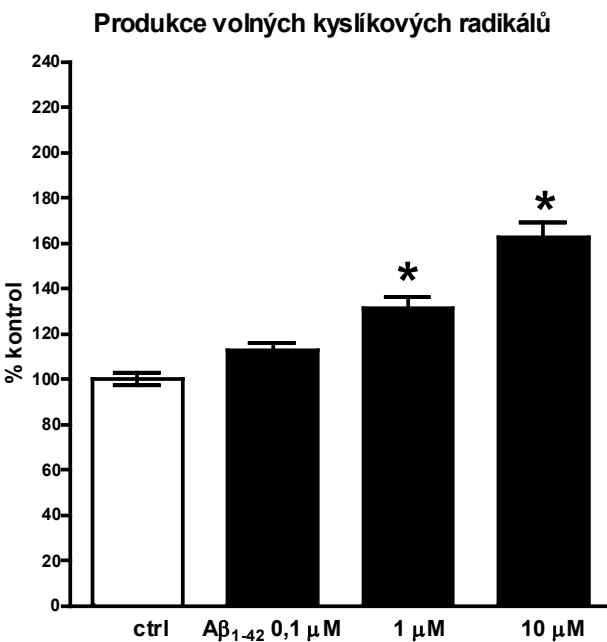
ke statisticky významnému nárůstu aktivity kaspázy-3 (Obrázek 6, levý panel). Také tvorba volných kyslíkových radikálů byla zvýšena pouze u buněk rostoucích v přítomnosti vyšší koncentrace A β_{1-42} (od 1 μM), než byla koncentrace použitá pro testování chronického vlivu A β_{1-42} ve funkčních pokusech (100 nM). Naměřené hodnoty hladiny volných kyslíkových radikálů jsou uvedeny na Obrázku 7.



Obrázek 6

Vliv chronického působení A β_{1-42} na aktivitu kaspáz v CHO buňkách

Buňky exprimující M1 nebo M2 podtyp mAChR byly po dobu růstu vystaveny různým koncentracím A β_{1-42} . Po sklizení buněk byla v buněčných lyzátech stanovena aktivita kaspázy-3 (levý panel) a kaspázy-8 (pravý panel). Uvedené hodnoty jsou průměrem ze dvou nezávislých experimentů s buňkami exprimujícími M1 receptory a dvou nezávislých experimentů s buňkami exprimujícími M2 receptory, vždy provedených v hexaplikátech. Výsledky experimentů s buňkami exprimujícími odlišný podtyp receptoru se navzájem nelišily, proto jsou vyhodnoceny společně. Kontrolní hodnoty aktivity pro kaspázu-3 a kaspázu-8 byly 36.9 ± 5.2 a 30.5 ± 3.8 relativních světelných jednotek (relative light unit, RLU) na μg proteinu a 60 minut. *, p < 0.05, signifikantně odlišné od všech ostatních skupin pomocí ANOVA a Tukeyho testu.

**Obrázek 7****Vliv chronického působení $\text{A}\beta_{1-42}$ na produkci volných kyslíkových radikálů v CHO buňkách**

Buňky exprimující M1 nebo M2 podtyp mAChR byly po dobu růstu vystaveny různým koncentracím $\text{A}\beta_{1-42}$. Uvedené hodnoty oxidativní aktivity vyjádřené jako procenta kontrol v jednotlivých pokusech jsou průměrem ze dvou nezávislých experimentů s buňkami exprimujícími M1 receptory a jednoho experimentu s buňkami exprimujícími M2 receptory, vždy provedených v hexaplikátech. Výsledky u obou typů buněk se nelišily, proto jsou vyhodnoceny společně. Kontrolní hodnoty byly 52.8 ± 5.7 RLU na μg proteinu a 60 minut. *, $p < 0.05$, signifikantně odlišné od všech ostatních skupin pomocí ANOVA a Tukeyho testu

4. Forma $\text{A}\beta_{1-42}$ přítomného v kultivačním médiu

β -amyloid má v médiu tendenci agregovat a snadno vytváří oligomery a polymerní fibrily. V současné době se má za to, že hlavním nositelem (neuro)toxicity jsou právě rozpustné oligomery β -amyloidu, spíše než velké nerozpustné polymery. Proto jsem v další sérii experimentů zjišťovala, v jaké formě je přítomný $\text{A}\beta_{1-42}$ v kultivačním médiu, ve kterém byly pěstovány buňky užívané v předchozích pokusech. Již dříve bylo v naší laboratoři zjištěno pomocí metody Western blotu a následné imunodetekce (kolega Vladimír Rudajev), že $\text{A}\beta_{1-42}$ je jak v kultivačním médiu tak v zásobním roztoku přítomen převážně ve formě oligomerů (obsahujících přibližně 5 - 20 molekul, viz Janickova et al, 2012), a tyto výsledky jsem následně ověřovala také pomocí vazby thioflavinu, který detekuje stupeň agregace β -

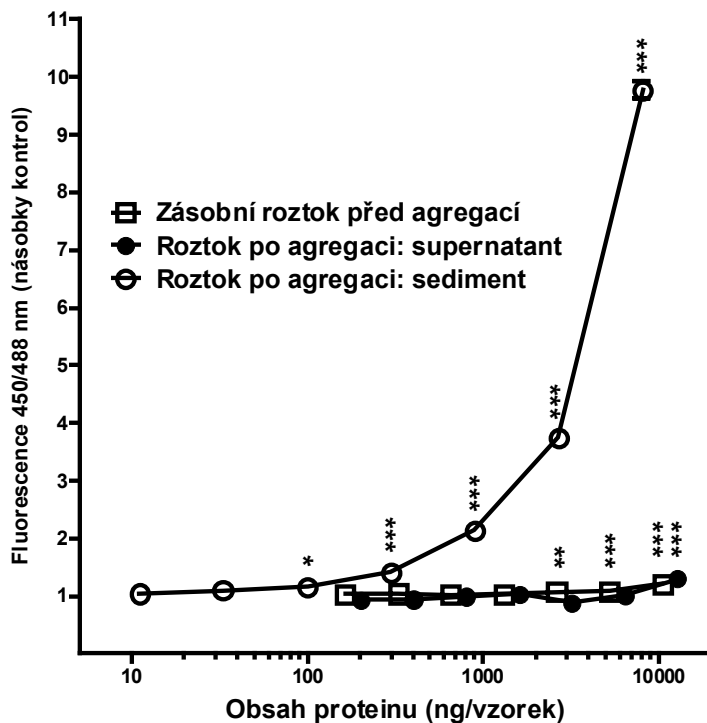
amyloidu. Po navázání thioflavinu na agregovaný amyloid dochází ke spektrálnímu posunu a koncentraci navázaného thioflavinu lze tak měřit jako fluorescenční signál při 450/488 nm.

V následující sérii pokusů jsem nejprve indukovala agregaci A β ₁₋₄₂ v zásobním 100 μ M roztoku. Do něj jsem přidala 10 mM roztok kyseliny chlorovodíkové a nechala proběhnout agregaci při teplotě 37 °C po dobu 24 hodin. Následovala centrifugace (sedimentace aggregovaného amyloidu) při 16 000 xg a sériové ředění výsledných roztoků (supernatant a resuspendovaný sediment) v DMEM. V jednotlivých ředěních jsem měřila fluorescenci navázaného thioflavinu při 488 nm po excitaci při 450 nm. Závislost fluorescenčního signálu na obsahu proteinu aggregovaného amyloidu byla lineární ($r^2 = 0,998$) s detekčním limitem přibližně 33 – 100 ng aggregovaného proteinu (Obrázek 8).

Ve srovnání s roztokem sedimentovaného A β ₁₋₄₂ byla ve vzorcích rozpustného A β ₁₋₄₂ (supernatant po centrifugaci) naměřena jen velmi nízká fluorescence a stejně tak i v původním zásobním roztoku A β ₁₋₄₂ ve vodě, u kterého nebyla indukována agregace pomocí kyseliny chlorovodíkové. Statisticky významné zvýšení signálu vazby thioflavinu v našem zásobním roztoku byl naměřeno při koncentraci zásobního roztoku A β ₁₋₄₂ 128 μ g/ml (211 ng aggregovaného amyloidu v měřeném alikvotu 100 ul což je přibližně 1,6 % z celkového proteinu). U vzorků supernatantu to bylo při koncentraci 104 μ g/ml (138 ng aggregovaného proteinu, což je přibližně 1,2 % z celkového proteinu.

Přítomnost aggregovaného amyloidu jsem pomocí vazby thioflavinu určovala také v médiu po kultivaci buněk v přítomnosti A β ₁₋₄₂. Po čtyřdenní inkubaci buněk v médiu obsahujícím různé koncentrace A β ₁₋₄₂ bylo naměřeno statisticky významné zvýšení fluorescence thioflavinu proti kontrole pouze v médiu s nejvyšší koncentrací (10 μ M A β ₁₋₄₂). V ostatních vzorcích se signál nelišil od kontrolních vzorků bez přidaného A β ₁₋₄₂ (Obrázek 9).

Fluorescenční signál thioflavinu v zásobním roztoku A β 1-42 (100 μ M) před agregací a po aggregaci s centrifugací

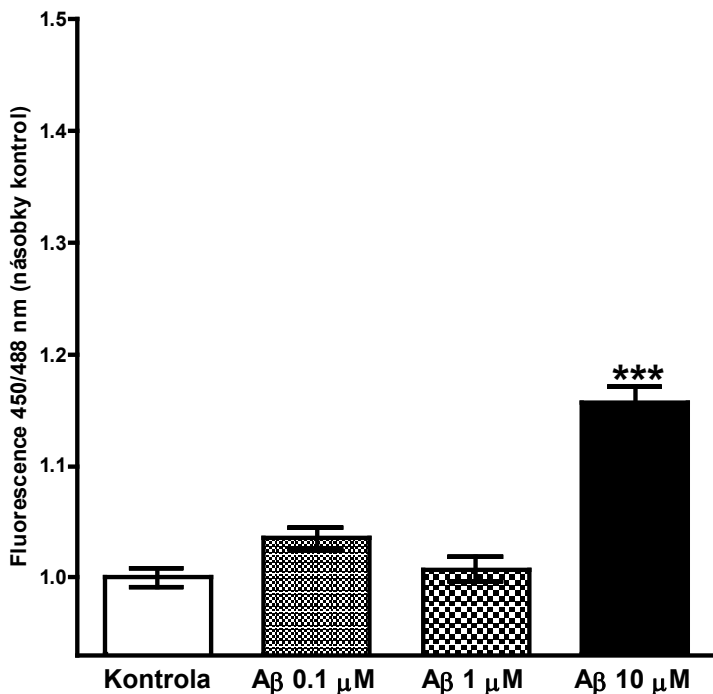


Obrázek 8

Kvantifikace agregovaného β -amyloidu v zásobním roztoku A β 1-42

Fluorescence při 450/488, která je úmerná obsahu agregovaného amyloidu, byla měřena v několika následných ředěních zásobního roztoku 100 μ M A β 1-42 ve vodě (bílé čtverečky). Vodorovná osa (logaritmická) udává koncentraci A β 1-42 v ng proteinu na vzorek. Agregovaný A β 1-42 (bílé kroužky) byl připraven ze zásobního roztoku, který byl inkubován 24 h v přítomnosti 10 mM HCl při 37 °C. Agregovaný amyloid byl z roztoku izolován centrifugací a použit pro měření. Pro stanovení účinnosti separace agregovaného amyloidu by měřen také signál ve vzorcích ze supernatantu (černé kroužky). Vzorky na měření byly ředěny v kultivačním médiu (DMEM). Naměřené hodnoty fluorescence (svislá osa) jsou vyjádřeny jako násobky kontrolních (čisté médium) hodnot fluorescence při 450/488 nm. *, p < 0.05, **, p < 0.01, ***, p < 0.001 signifikantně odlišné od kontrol pomocí ANOVA a Dunnettova testu.

Fluorescenční signál thioflavinu v kultivačním médiu obsahujícím různé koncentrace A_β1-42 po čtyřdenní kultivaci buněk



Obrázek 9

Agregace β-amyloidu v kultivačním médiu s různými koncentracemi A_β1-42 po čtyřech dnech kultivace

Buňky exprimující M1 nebo M2 receptor byly pěstovány po dobu čtyř dní v médiu s 0-10 μM A_β1-42 (vodorovná osa). Alikvoty medií po skončení inkubace byly použity ke změření signálu agregovaného amyloidu v přítomnosti thioflavinu (fluorescence 450/488 nm). Jsou vyjádřeny jako násobek hodnot média bez přidaného A_β1-42 (svislá osa) a představují průměr ze dvou nezávislých experimentů s buňkami exprimujícími M1 nebo M2 receptory. Každý experiment obsahoval osm vzorků. Výsledky u obou typů buněk se navzájem nelišily, a proto jsou vyhodnoceny společně. ***, p < 0.001, signifikantně odlišné od kontrol pomocí ANOVA a Dunnettova testu

5. Vliv rozpustného β -amyloidu na aktivaci G-proteinů *in vivo* v mozkové kůře myší APPswe/PS1dE9

Transgenní myši APPswe/PS1dE9 díky vnesenému konstruktu produkují zvýšené množství β -amyloidu, což vede ve věku kolem šesti měsíců k počínající tvorbě amyloidových plaků. Na membránách připravených z mozkové kůry těchto myší jsem zjišťovala, zda se v naší laboratoři popsané progresivní oslabování muskarinové transmise u dospělých transgenních myší (7-17 měsíců; Machová E. et al., 2008) projevuje během nárůstu koncentrace rozpustného amyloidu nebo zda je způsobeno již samotnou přítomností transgenu. Měřila jsem proto aktivaci G-proteinů muskarinovým agonistou karbacholem jako zvýšení vazby ^{35}S -GTP γ S u mladých zvířat (10 týdnů) a mladých dospělých zvířat (5-6 měsíců), tedy v období, kdy dochází k rychlému zvyšování koncentrace rozpustného amyloidu (zejména fragmentu A β ₁₋₄₂) ještě bez tvorby amyloidových plaků. Výsledky těchto pokusů jsou shrnutý v Tabulce 6.

U mladých dospělých transgenních zvířat jsem zjistila signifikantní snížení EC₅₀ v porovnání s kontrolami, B_{max} však zůstala nezměněná. Naproti tomu u mladých (7–10 týdnů starých) zvířat jsem nezjistila žádný rozdíl u kontrolních a transgenních myší v žádném parametru. Bazální a celková vazba ^{35}S -GTP γ S byly u dospělých myší signifikantně nižší než u mladých myší, nelišily se však mezi kontrolními a transgenními zvířaty stejného věku.

		Emax (fmol/mg)	EC50 (μM)	Bazální vazba (fmol/mg)	Celková vazba (pmol/mg)
Mladé myši (7-10 týdnů)	kontrolní	280,2±11,3 (6)	2,72±0,59 (6)	616,9±67 (6)	5,8±0,5 (4)
	transgenní	286,8±22,2 (7)	4,14±0,88 (7)	805,5±60,3 (7)	5,6±0,2 (5)
Dospělé myši (5-6 měsíců)	kontrolní	95,4±19,3# (4)	1,96±0,44 (4)	187,0±17,0# (5)	3,9±0,1# (3)
	transgenní	119,0±10,4# (5)	7,85±1,53* # (5)	249,9±37,2# (5)	3,9±0,5# (3)

Tabulka 6

Parametry karbacholem stimulované vazby ^{35}S -GTP γ S na membrány z mozkové kůry kontrolních a transgenních myší různého věku

Uvedené hodnoty jsou průměr \pm SEM z hodnot naměřených na membránách z mozkové kůry myší, jejichž počet je uveden v závorkách. *, p<0,05, hodnota signifikantně odlišná od kontrol stejného věku; #, p<0,05, hodnota signifikantně odlišná od geneticky odpovídajících myší různého věku

6. Vliv nutričně obohaceného média na vazbu [³H]-NMS a aktivaci G-proteinů prostřednictvím mAChR

Jedním z možných způsobů, kterým A β_{1-42} může ovlivňovat vazebné a funkční vlastnosti jednotlivých podtypů mAChR, je změna vlastností buněčné membrány, ve které jsou receptory uloženy. V jedné sérii experimentů jsem proto testovala vliv nutričních látek, které podle dřívějších poznatků ovlivňují složení buněčné membrány a syntézu a funkci neurotransmiterů (Cansev M. et Wurtman RJ., 2007; Wang L. et al., 2007; Wurtman RJ. et al., 2006), na vazbu antagonistu [³H]-NMS k jednotlivým podtypům mAChR a na aktivaci G-proteinů těmito receptory.

CHO buňky exprimující M1, M2 nebo M4 podtyp mAChR jsem pěstovala běžným způsobem v kontrolním kultivačním médiu nebo v médiu, které bylo obohaceno o kombinaci těchto nutričních látek (v závorkách je uvedena konečná koncentrace dané látky v kultivačním médiu): dokosahexaenová kyselina (DHA, 20 μ M), eikosapentaenová kyselina (EPA, 20 μ M), uridin (50 μ M), cholin (20 μ M), vitamín B6 (pyridoxin, 10 μ M), vitamín B12 (kobalamin, 0,2 μ M), vitamín B9 (kyselina listová, 15 μ M), fosfatidylcholin (25 μ M), vitamín C (kyselina askorbová, 75 μ M), vitamín E (α -tokoferol, 20 μ M) a selen (0,4 μ M). Na membránách připravených z těchto dvou skupin buněk jsem potom měřila vazbu muskarinového antagonisty [³H]-NMS a vazbu ³⁵S-GTP γ S stimulovanou karbacholem.

V případě M1 receptoru nedošlo k žádné změně parametrů vazby [³H]-NMS u buněk rostoucích v nutričně obohaceném médiu. Na druhou stranu, u membrán připravených z nutričně obohacených buněk exprimujících M1 mAChR byla naměřena významně vyšší aktivace G-proteinů jako zvýšení E_{max} u karbacholem stimulované vazby ³⁵S-GTP γ S, zatímco EC₅₀ zůstala nezměněna. V případě buněk exprimujících M2 mAChR nebyla zjištěna změna v expresi receptoru (B_{max} v obou skupinách bylo stejné), avšak u membrán připravených z buněk rostoucích v obohaceném médiu jsem naměřila signifikantní snížení affinity k [³H]-NMS. Zároveň došlo ke snížení maximální aktivace G-proteinů (snížení E_{max}), zatímco EC₅₀ zůstala beze změny. Nakonec u buněk exprimujících M4 mAChR nebyl zjištěn žádný vliv nutričně obohaceného média na aktivaci G-proteinů (E_{max} i EC₅₀ zůstaly beze změny).

Parametry vazby [³H]-NMS a karbacholem stimulované vazby ³⁵S-GTPγS na membrány z kontrolních a nutričně obohacených buněk exprimujících M1, M2 nebo M4 mAChR jsou uvedeny v Tabulkách 7 a 8.

		B _{max} (% kontrol)	K _d (pM)
M1	kontrolní (4)		289±95
	obohacené médium (4)	95±12	370±92
M2	kontrolní (4)		361±44
	obohacené médium (4)	122±20	428±36*

Tabulka 7

Parametry vazby [³H]-NMS k membránám připraveným z buněk rostoucích v kontrolním nebo obohaceném médiu

Hodnoty B_{max} jsou vyjádřené jako % kontrol ± SEM v párovaných pokusech (kontrolní hodnoty B_{max} jsou 6,4 ± 1,0 a 1,3 ± 0,3 pro M1 a M2 mAChR). Hodnoty K_d jsou průměr ± SEM. Počet pokusů (vždy provedených v kvadruplikátech) je uveden v závorce. *, p<0.05 signifikantně odlišné od kontrol pomocí párového t-testu

		E _{max} (% kontrol)	pEC50 (-logM)	Celková vazba (pmol/mg)
M1	kontrolní (3)		5,60±0,38	1,42±0,45
	obohacené médium (3)	172±5,3**	5,46±0,41	1,63±0,24
M2	kontrolní (3)		6,56±0,28	1,87±0,40
	obohacené médium (3)	85±6*	6,43±0,12	1,76±0,29
M4	kontrolní (7)		5,65±0,09	---
	obohacené médium (7)	111±11	5,73±0,12	---

Tabulka 8

Parametry karbacholem stimulované vazby ³⁵S-GTPγS na membrány připravené z buněk rostoucích v kontrolním nebo obohaceném médiu

Hodnoty E_{max} jsou vyjádřené jako % kontrol ± SEM v párovaných pokusech (kontrolní hodnoty E_{max} jsou 410 ± 177, 445 ± 76 a 69 ± 6 dpm/μg proteinu pro M1, M2 a M4 mAChR). Hodnoty pEC50 a celkové vazby jsou průměr±SEM. Počet pokusů (provedených v kvadruplikátech) je uvedený v závorkách. *, p<0.05; **, p<0.01 signifikantně odlišné od kontrol pomocí párového t-testu.

Diskuze

Tato dizertační práce je založena na výsledcích průběžně uveřejněných v několika publikacích, jejichž jednotícím tématem je úloha mAChR při rozvoji Alzheimerovy nemoci, působení β -amyloidu na funkci mAChR a pokus o identifikaci mechanismů, které se podílejí na poškození mAChR působením β -amyloidu.

I když výzkumu změn různých částí cholinergního systému v průběhu Alzheimerovy choroby se již více než třicet let věnovala celá řada autorů, k dispozici je z pochopitelných důvodů jen poměrně málo prací, které by zkoumaly vliv β -amyloidu na jednotlivé podtypy mAChR v počátečních stádiích onemocnění *in vivo*. Počáteční působení β -amyloidu lze však do jisté míry napodobit v pokusech *in vitro*. Až dosud publikované práce, které se zabývaly vlivem β -amyloidu na různé primární buněčné kultury a buněčné linie *in vitro*, zpravidla používaly velmi vysokou koncentraci syntetického β -amyloidu, která naprosto neodpovídá „přirozeným“ poměrům v mozkové tkáni. V první části této práce (publikováno v Janickova H. et al., 2012) jsem zjistila, že chronické působení již relativně nízkých koncentrací β -amyloidu (100 nM) vyvolává změny vazebních a funkčních vlastností u M1 případně M3 podtypu mAChR. Nositelem toxicity je přitom s největší pravděpodobností $A\beta_{1-42}$ v rozpustné oligomerní formě, což je ve shodě s hypotézou, která je v současné době všeobecně uznávána. Poškození funkce mAChR jsem přitom ve své práci zjistila nejen u CHO buněk heterologně exprimujících jednotlivé podtypy mAChR, ale také v mozkové kůře transgenních myší APPswe/PS1dE9, a to již v době, kdy se v jejich mozku teprve začínají objevovat první amyloidové plaky (Machová E. et al., 2010) a kognitivní deficit u těchto myší není dosud patrný.

Mechanismus vzniku poruch vazby a funkce určitých podtypů mAChR (zejména M1 podtypu), které vznikají jako důsledek dlouhodobého působení $A\beta_{1-42}$, není zcela jasný. Některé výsledky však naznačují, že se na jejich vzniku podílí změny ve struktuře buněčné membrány (Savelkoul PJ. et al., 2012), které mohou například ovlivnit spřahování jednotlivých podtypů mAChR s G-proteiny. Výsledky publikované v práci Jakubík et al., 2011a přitom ukazují, že způsob spřahování lichých a sudých podtypů mAChR s preferenčními a nepreferenčními G-proteiny je do značné míry odlišný (viz také Abdulaev NG. et al., 2006).

Na rozdíl od antagonistů mAChR, které se k receptoru váží vždy se stejnou afinitou, je vazba muskarinových agonistů (například karbacholu) ovlivněna konformací receptoru, která se mění vlivem spřažení receptoru s G-proteinem a na něj navázaným guaninovým nukleotidem. Receptor především významně snižuje svou afinitu pro agonistu v případě, kdy díky navázání GTP k α -podjednotce G-proteinu dojde k odpřažení G-proteinu od receptoru a jeho disociaci na signalizační molekuly (α -podjednotka a dimer podjednotek $\beta\gamma$). Naopak pokud je na α -podjednotce G-proteinu navázáno GDP (G-protein existuje jako trimer podjednotek $\alpha\beta\gamma$), receptor se spřaženým G-proteinem se nachází v konformaci s relativně vyšší afinitou k agonistovi. K tomu dochází v celistvých buňkách, které vždy obsahují GTP a GDP. Při pokusech prováděných na izolovaných membránách je situace jiná. V inkubačním médiu během pokusu na membránách není přítomné GTP (pokud ho záměrně nepřidáme) a jen velmi nízká koncentrace zbytkového GDP. Některé receptory jsou tak spřažené i s G-proteiny bez navázaného nukleotidu, k čemuž za normálních podmínek v buňce nedochází. Právě tyto receptory s navázaným G-proteinem bez nukleotidu, které nejsou ovlivněny alosterickým působením GDP, se nacházejí v konformaci s relativně nejvyšší afinitou k agonistovi a ve své práci je označují jako „vysokoafinitní vazebná místa“. Receptory spřažené s G-proteinem s navázaným GDP (které je v izolovaných membránách na rozdíl od GTP stále přítomné) jsou pak receptory označované jako „nízkoafinitní vazebná místa“.

Při studiu toxického působení $A\beta_{1-42}$ na mAChR jsem nejdříve sledovala vliv $A\beta_{1-42}$ na vazbu antagonisty [3H]-NMS k jednotlivým podtypům mAChR. Akutní působení $A\beta_{1-42}$ ($A\beta_{1-42}$ přítomen v inkubačním médiu v průběhu vazebného pokusu) ani chronické ($A\beta_{1-42}$ přítomen v kultivačním médiu v průběhu růstu buněk, do inkubačního média během vazebného pokusu se již nepřidává) nevyvolalo změnu v afinitě pro [3H]-NMS u žádného podtypu mAChR. Vazba antagonistů mAChR není ovlivněna změnou konformace receptoru, která nastává v závislosti na spřahování mAChR s G-proteinem a na něj navázanými guaninovými nukleotidy. [3H]-NMS na receptoru nerozeznává takzvané nízko- a vysokoafinitní místo, a proto by případná změna spřahování mAChR s G-proteinami vyvolaná $A\beta_{1-42}$ neměla jeho vazbu ovlivnit. Ke změně vazby v rovnovážných pokusech (zvýšení disociační konstanty K_d) by naopak došlo v případě, že by se $A\beta_{1-42}$ vázel do stejného místa receptoru jako [3H]-NMS nebo jinak snižoval vazbu [3H]-NMS. Nic takového však nenastalo v případně akutního ani chronického působení $A\beta_{1-42}$. Stejně tak přidání $A\beta_{1-42}$ do kultivačního média k rostoucím buňkám nezměnilo ani maximální vazbu (B_{max}) [3H]-NMS k receptoru, nemělo tedy žádný vliv na expresi receptorů v buněčné membráně.

Na rozdíl od vazby antagonisty, která zůstala beze změny, jsem ve vazebných pokusech s agonistou karbacholem zjistila signifikantní zvýšení relativního zastoupení vysokoafinitních vazebných míst u M1 mAChR a zároveň signifikantní snížení afinity těchto míst pro karbachol u těch membrán, které byly připraveny z buněk vystavených dlouhodobému působení A β_{1-42} . U M3 mAChR došlo pouze ke zvýšení relativního zastoupení vysokoafinitních vazebných míst, zatímco snížení jejich afinity nebylo signifikantní. U ostatních podtypů mAChR se chronické působení A β_{1-42} na vazebných vlastnostech karbacholu nijak neprojevilo.

Protože u buněk exprimujících M1 a M3 mAChR a vystavených chronickému vlivu A β_{1-42} došlo ke zvýšení frakce vysokoafinitních vazebných míst, bylo by možné uvažovat o tom, že působení A β_{1-42} na buněčnou membránu či zabudování A β_{1-42} do membrány snížilo koncentraci „zbytkového“ GDP přítomného v membránové frakci připravené z těchto buněk (analogicky jak je tomu u M2 mAChR; Jakubík J. et al., 2011b a Janíčková, bakalářská práce). Tato hypotéza však nevysvětluje snížení afinity vysokoafinitního vazebného místa a už vůbec nebere v úvahu skutečnost, že ke změnám v relativním zastoupení vysokoafinitních vazebných míst případně jejich afinity došlo specificky u dvou lichých podtypů mAChR (M1 a M3). Je proto pravděpodobnější, že působení A β_{1-42} nějakým způsobem ovlivnilo konformaci receptoru, která může být závislá také na konkrétním aminokyselinovém složení jednotlivých podtypů (vždy liché a sudé podtypy mAChR jsou si navzájem strukturně více podobné). Tato změna konformace může být způsobena i změnou alosterické inerakce mezi receptorem a GDP, která by mohla být vyvolána chronickým působením A β_{1-42} na buněčnou membránu. Svou roli zde může hrát i skutečnost, že preferenční G-proteiny se u lichých a sudých podtypů mAChR navzájem liší (sudé podtypy se preferenčně spřahují s G_{i/o}, liché podtypy s G_{q/11} proteiny) a spřahování G-proteinů s lichými a sudými podtypy mAChR je odlišné. Podtypy M1 a M3, na rozdíl od sudých podtypů, vykazují například i v nepřítomnosti agonisty spřahování receptoru (precoupling) s nepreferenčními G-proteinami (Jakubík J. et al., 2011a).

V pokusech s akutním působením A β_{1-42} nebyla zjištěna žádná změna vazebných vlastností jednotlivých podtypů mAChR pro karbachol, což také potvrzuje hypotézu vyslovenou na základě výsledků pokusů s vazbou antagonisty [³H]-NMS, že totiž A β_{1-42} se neváže přímo k mAChR a nijak nebrání vazbě ligandu na receptor.

Poté, co jsem zjistila změnu vazebných vlastností u M1 a M3 mAChR vystavených chronickému působení A β_{1-42} , jsem se zaměřila na funkční vlastnosti receptorů a zjišťovala,

zda působení A β ₁₋₄₂ má vliv také na signalizační dráhy aktivované lichými a sudými podtypy mAChR. Z literatury je známo, že v mozcích pacientů s Alzheimerovou chorobou dochází k poškození spřahování mezi mAChR a G-proteiny a toto poškození je přímo úměrné rozsahu kognitivního deficitu (Flynn DD. et al., 1991; Flynn DD. et al., 1995; Tsang SW. et al., 2006). Tato pozorování se však vztahují k terminálnímu stadiu onemocnění a nelze tak odlišit, zda se jedná o následek pokročilé neurodegenerace nebo o specifické poškození, které se uplatňuje při rozvoji onemocnění. Poškození spřahování mAChR s G-proteiny, které je klíčové pro zahájení signálních drah aktivovaných mAChR, jsem rovněž zaznamenala ve svých pokusech provedených na mozkové kůře transgenních myší APPswe/PS1dE9. Ve věku 5–6 měsíců se u těchto myší začínají objevovat první amyloidové plaky v mozkové kůře a hipokampu, v té době však ještě nejsou patrné žádné známky kognitivního deficitu. Z výsledků mých pokusů vyplynulo, že u myší tohoto věku je také již přítomná porucha funkce mAChR měřená jako snížení vazby ^{35}S -GTP γ S. Porucha spřahování mAChR s G-proteiny a porucha aktivace navazujících signálních drah se tedy objevuje v době vzniku prvních amyloidních plaků, na druhou stranu však ještě před tím, než se patologické změny projeví znatelným narušením kognitivních funkcí. U myší mladých (7–10 týdnů), u kterých ještě nejsou přítomné amyloidové plaky, jsem žádné snížení aktivace G-proteinů skrze mAChR nezaznamenala. Oslabení muskarinové transmise se tedy rozvíjí během postupného zvyšování hladiny rozpustného amyloidu v mozku. To podporuje myšlenku, že poruchy cholinergní transmise jsou patrné již v časných fázích onemocnění Alzheimerovou chorobou snad roky až desítky let před prvními projevy deficitu kognitivních funkcí (Selkoe DJ., 2011, 2012), i když je podle všeho nelze obecně považovat za primární příčinu vzniku samotného onemocnění.

Výsledky pokusů na mozkové kůře myší APPswe/PS1dE9 dále ukázaly, že ke snížení aktivace G-proteinů skrze mAChR dochází také u kontrolních (netransgenních ze stejného vrchu) myší v průběhu stárnutí. Maximální hodnoty vazby ^{35}S -GTP γ S (E_{\max}) vyvolané karbacholem byly u kontrolních mladých dospělých (5–6 měsíčních) myší statisticky významně nižší než u kontrolních myší mladých (7–10 týdnů). Tento pokles byl však u 7 měsíčních myší významně nižší než u transgenních APPswe/PS1dE9 myší. U ještě starších 17 měsíčních myší se tyto hodnoty u transgenních a kontrolních myší nelišily (Machová E. et al., 2008). Výraznější poškození muskarinové transmise se u transgenních zvířat od věku 5–6 měsíců projevovalo snížením účinnosti (zvýšením EC₅₀) karbacholu při aktivaci G-proteinů, která se s věkem stávala výraznější (Machová E. et al., 2008). Poruchy cholinergní transmise u pacientů s Alzheimerovou chorobou nelze proto považovat jen za přirozený projev stárnutí.

Na rozdíl od pokusů na mozkové kůře transgenních myší APPswe/PS1dE9 experimenty s vazbou ^{35}S -GTP γ S na membrány připravené z CHO buněk heterologně exprimujících jednotlivé podtypy mAChR a vystavených chronickému působení A β_{1-42} žádnou poruchu aktivace G-proteinů nepotvrdily. Možným vysvětlením, proč se v pokusech s vazbou ^{35}S -GTP γ S nepodařilo zachytit poruchu spřahování mAChR a G-proteinu, může být fakt, že aktivace M1 mAChR agonistou vede ke spřahování receptoru s více typy G-proteinů, nejen s preferenčním G $_{q/11}$, jak ukázal Hillův sklon výsledné křivky, který byl nižší než jedna.

Pro odlišení aktivace jednotlivých tříd G-proteinů jsem měřila aktivaci proteinů G $_{q/11}$ M1 podtypem mAChR jako akumulaci inositolfosfátů v buňce vyvolanou karabacholem a aktivaci proteinů G $_{i/o}$ M2 podtypem mAChR jako inhibici syntézy cAMP rovněž vyvolanou karbacholem. V těchto pokusech jsem, ve shodě s výsledky získanými ve vytěšňovacích vazebných pokusech, zaznamenala snížení aktivace (statisticky významné snížení E $_{max}$) pouze u proteinů G $_{q/11}$ aktivovaných M1 podtypem mAChR. Všechny tyto výsledky podporují myšlenku, že chronické působení A β_{1-42} *in vitro* i *in vivo* selektivně poškozuje funkci lichých podtypů mAChR preferenčně se spřahujících s G $_{q/11}$ třídou G-proteinů.

Selektivní poškození M1 podtypu mAChR a jím aktivované signalizační dráhy chronickým působením A β_{1-42} naznačuje, že toto poškození, není vyvolané celkovým toxickým působením A β_{1-42} na CHO buňky heterologně exprimující mAChR. Přesto jsem tuto možnost ještě ověřila ve zvláštní sérii pokusů, ve které jsem CHO buňky exprimující M1 nebo M2 mAChR vystavila chronickému působení A β_{1-42} ve vznětovajících koncentracích a projevy toxicity jsem sledovala jako nárůst aktivity kaspázy-3 a kaspázy-8 případně jako zvýšení produkce volných kyslíkových radikálů. V těchto pokusech bylo potvrzeno, že A β_{1-42} v relativně nízké koncentraci 100 nM, kterou jsem běžně používala ve svých pokusech, nemá viditelné toxicické účinky na CHO buňky. A β_{1-42} přítomný v kultivačním médiu zvyšoval aktivitu kaspáz případně produkci volných kyslíkových radikálů až od koncentrací 1 – 10 μM a tento účinek se nijak nelišil u CHO buněk exprimujících M1 nebo M2 podtyp mAChR. V literatuře je sice popsána řada toxicických účinků A β_{1-42} na buňky nervového i nenervového původu *in vitro* (např. Kim HS. et al., 2009; Cenini G. et al., 2010; Perálvarez-Marín A. et al., 2009), tyto účinky jsou však většinou pozorované až při řádově vyšších koncentracích než 100 nM.

V současnosti je všeobecně přijímána myšlenka, že kromě koncentrace má pro toxicitu A β_{1-42} velký význam také stupeň jeho agregace v médiu a především to, zda je A β_{1-42}

přítomen ve formě rozpustných oligomerů nebo ve formě polymerů tvořících nerozpustné fibrily. Oligomery A β_{1-42} jsou strukturně odlišné od polymerů. Oligomery na rozdíl od polymerů například neobsahují pravidelnou β -sheet strukturu (Ahmed M. et al., 2010). Také konkrétní velikost oligomerů A β_{1-42} pravděpodobně ovlivňuje jeho (neuro)toxicitu, schopnost vstupovat do lipidové dvojvrstvy buněčné membrány, případně schopnost internalizace dovnitř buňky (Ono K. et al., 2009; Ahmed M. et al., 2010; Perálvarez-Marín A. et al., 2009; Ladiwala AR. et al., 2012). Znalost konkrétní formy A β_{1-42} přítomného v průběhu experimentu je proto velmi důležitá pro správnou interpretaci výsledků.

Podle některých údajů tvoří A β_{1-42} polymerní fibrily spontánně (bez indukce agregace např. v roztoku HCl) pouze při relativně vysokých koncentracích řádově kolem 10 μM (Ladiwala AR. et al., 2012). Při nižších koncentracích dochází naopak spontánně ke vzniku toxických oligomerů. Protože jsem ve svých pokusech používala většinou nízké koncentrace A β_{1-42} (100 nM), očekávala jsem, že v kultivačním médiu bude A β_{1-42} přítomen především ve formě oligomerů. Tuto hypotézu jsme také následně ověřili jak s pomocí Western blotu a následné imunodetekce (pokusy provedl kolega Vladimír Rudajev), tak také pomocí vazby thioflavinu, u kterého dochází ke spektrálnímu posunu po vazbě na polymerní fibrily β -amyloidu.

Otázkou zůstává, jakým způsobem oligomery A β_{1-42} interagují s buněčnou membránou nebo zda případně dochází k jejich internalizaci dovnitř buňky. Výsledky prezentované v této práci (A β_{1-42} působí změnu vazebních vlastností a poruchu spřahování mezi M1 receptorem a G-proteinem, látky ovlivňující charakteristiku buněčných membrán mají příznivý účinek na funkci M1 receptor) podporují hypotézu, že škodlivý účinek A β_{1-42} je alespoň zpočátku zprostředkován především vlivem A β_{1-42} na buněčnou membránu. Tento závěr je ve shodě také s údaji z literatury (například Jang H. et al., 2013; Milanesi L. et al., 2012; Evangelisti E. et al., 2012).

Z myšlenky, že pro buňky toxický β -amyloid primárně poškozuje buněčné membrány, vychází některé snahy o snížení toxicity β -amyloidu pomocí látek, které podle starších poznatků příznivě ovlivňují lipidové složení a strukturu membrán. Ve starších pracích bylo zjištěno, že konkrétně obohacení média kyselinou docosahexaenovou (DHA), uridinem a cholinem podporuje tvorbu cholinergních synapsí a uvolňování acetylcholinu (Wurtman RJ. et al., 2006; Wang L. et al., 2007). Přídavek DHA do definovaného média (bez séra) buněčných kultur NG108-15 podporoval růst buněk a zvyšoval expresi muskarinových receptorů a také aktivitu ChAT (Machová E. et al., 2006). Zvýšený obsah fosfolipidových

prekurzorů v potravě zlepšoval kognitivní funkce u laboratorních zvířat (Teather LA. et Wurtman RJ., 2006). Také u muskarinových receptorů uložených v membráně ovlivňovalo jejich bezprostřední lipidové prostředí vazebné vlastnosti a schopnost spřahování s G-proteiny, a to i tehdy, když nebyl patrný žádný vliv na permeabilitu membrány, oxidační aktivitu nebo expresi proteinů (Michal P. et al., 2009). V další sérii pokusů uvedených v této práci jsem proto zkoumala schopnost několika různých nutrientů (fosfatidylcholinu, polynenasycených mastných kyselin, vitamínů) podpořit funkci muskarinových receptorů, konkrétně aktivaci G-proteinů měřenou jako vazbu ^{35}S -GTP γ S.

Používaná kombinace jedenácti nutričních látek překvapivě zvýšila maximální vazbu (E_{\max}) ^{35}S -GTP γ S vyvolanou karbacholem pouze na M1 mAChR, zatímco u M4 neměla vliv a u M2 podtypu dokonce došlo k mírnému snížení maximální vazby ^{35}S -GTP γ S. Kombinace těchto nutričních látek neměla vliv na expresi M1 a M2 mAChR v membránách. U M2 podtypu způsobila mírné snížení afinity pro [^3H]-NMS. Je tedy možné, že změny ve složení buněčné membrány způsobené některými nutričními látkami ovlivňují specificky jednotlivé podtypy mAChR snad na základě jejich rozdílné struktury nebo díky preferenčnímu spřahování s jinými třídami G-proteinů nebo také díky membránové lokalizaci ve specifických membránových doménách.

Je pravděpodobné, že spíše než jednotlivé nutriční látky samy o sobě mají příznivý vliv na vlastnosti buněčných membrán a funkci v nich obsažených receptorů kombinace několika nutričních látek. Vliv některých vybraných nutričních látek (například DHA) byl totiž zkoumán také jednotlivě, jejich přidání do kultivačního média však nevyvolalo ve vazbě ^{35}S -GTP γ S žádnou změnu (nepublikované výsledky). Rovněž z literatury je znám například příznivý účinek směsi několika nenasycených mastných kyselin na štěpení APP (zvýšení poměru A β ₁₋₄₀/A β ₁₋₄₂), které se také odehrává v membráně. V buněčných kulturách transfekovaných genem pro lidský APP obsahujícím švédskou mutaci zvyšovala směs několika mastných kyselin poměr uvolňovaných fragmentů A β ₁₋₄₀/A β ₁₋₄₂, přičemž tento účinek nebylo možné připsat žádné individuální mastné kyselině (Amtul Z. et al., 2011). Jiné práce však ukazují, že i samotná DHA snižuje aktivitu γ -sekretázy (Grimm MO. et al., 2011) kdežto trans-mastné kyseliny zvyšují amyloidogenní štěpení APP (Grimm MO. et al., 2012). Výsledky těchto pokusů potvrzují vzájemný vztah mezi metabolismem lipidů a štěpením APP, které se rovněž odehrává v membránách (Grimm MO. et al., 2006).

Přestože lipidové prostředí membrány má nepochybně velký vliv na funkci (nejen) muskarinových receptorů, je dosud k dispozici jen málo informací o konkrétních

mechanismech, kterými je receptorová signalizace (jež se z velké části odehrává v membráně nebo v těsném styku s ní) modulována. Složení membrány a bezprostřední okolí transmembránového receptoru ovlivňuje spřahování receptoru s G-proteiny (Mitchell DC. et al., 1990; Klein U. et al., 1995; Michal P. et al., 2009). Z výsledků publikovaných v práci Jakubík J. et al., 2011a a rovněž částečně obsažených již v mé diplomové práci vyplývá, že způsob spřahování muskarinových receptorů s G-proteiny je odlišný u sudých a lichých podtypů mAChR. Všechny podtypy mAChR vykazují takzvaný precoupling se svými preferenčními G-proteiny, na rozdíl od sudých podtypů však liché podtypy vykazují precoupling i s nepreferenčními $G_{i/o}$ G-proteiny. U M1 i M2 mAChR jsem tento rozdíl zjistila nejen u karbacholu (což je blízký analog přirozeného ligandu acetylcholinu), ale potvrdila také u dalších tří agonistů (methylfurmethid, oxotremorin a částečný agonista pilokarpin). Odlišnost ve spřahování sudých a lichých podtypů mAChR může podle všeho přispívat k selektivnímu poškození M1 a M3 mAChR působením $A\beta_{1-42}$.

Závěr

Hlavním cílem této práce bylo zjistit, zda a případně jakým způsobem ovlivňuje rozpustný β -amyloid přenos signálu muskarinovými receptory. Z výsledků práce vyplývá, že $A\beta_{1-42}$ ve formě rozpustných oligomerů mění vazebné vlastnosti na dvou lichých podtypech mAChR (především M1) a to pouze tehdy, pokud jsou CHO buňky heterologně exprimující jednotlivé podtypy mAChR vystaveny působení $A\beta_{1-42}$ dlouhodobě. Kromě účinku na vazebné vlastnosti má chronické působení $A\beta_{1-42}$ negativní vliv také na funkci M1 mAChR, neboť snižuje maximální funkční odpověď (akumulaci inositolfosfátů) vyvolanou vazbou agonisty na receptor. V pokusech s transgenními myšmi APPswe/PS1dE9 ^{35}S -GTP γ S jsem prokázala, že oslabení muskarinové transmise (podle snížení karbacholem stimulované vazby ^{35}S -GTP γ S) není způsobeno přítomností transgenu, ale vyvíjí se v průběhu zvyšování koncentrace β -amyloidu a je patrné již v době vzniku prvních amyloidových plaků.

Mechanismus, jakým dlouhodobé působení $A\beta_{1-42}$ vyvolává vazebné a funkční změny u mAChR, zůstává nejasný. Je však pravděpodobné, že působením $A\beta_{1-42}$ dochází ke změnám ve struktuře buněčné membrány, které ovlivňují interakci mezi jednotlivými podtypy mAChR a preferenčními G-proteiny. Tuto hypotézu podporuje také skutečnost, že nutriční látky mající vliv na složení buněčné membrány mohou specificky ovlivnit také spřahování mezi mAChR a G-proteiny.

Jednotlivé hypotézy uvedené v úvodu této práce se podařilo z velké části potvrdit či upřesnit a vyvodit následující závěry:

1. $A\beta_{1-42}$ negativně ovlivňuje vazebné a funkční vlastnosti pouze u M1 a M3 podtypů mAChR a to pouze tehdy, pokud je v kultivačním médiu přítomen dlouhodobě. $A\beta_{1-42}$ přitom působí i v relativně nízké koncentraci (100 nM).
2. V uvedené koncentraci a za mnou používaných podmínek je $A\beta_{1-42}$ v roztoku přítomen téměř výlučně ve formě rozpustných oligomerů.
3. Oslabení muskarinové transmise *in vivo* se u transgenního myšího modelu Alzheimerovy nemoci rozvíjí až v době zvyšování koncentrace rozpustného $A\beta_{1-42}$, avšak zároveň dříve, než je patrná zjevná amyloidová patologie a behaviorální poruchy.
4. $A\beta_{1-42}$ neinteraguje přímo s receptorem; naopak se zdá, že vliv $A\beta_{1-42}$ na receptor je zprostředkován účinkem $A\beta_{1-42}$ na strukturu a složení buněčné membrány.

5. Struktura a složení buněčné membrány, které lze ovlivnit například přidáním některých nutričních látek do kultivačního média, má vliv na funkci přinejmenším některých podtypů mAChR. Je možné, že ovlivňuje také spřahování receptoru s G-proteinem, které má prokazatelný vliv na vazebné vlastnosti receptoru (viz výsledky uvedené v diplomové práci a Jakubik J. et al., 2011)

Souhrn

Poškození cholinergního neurotransmiterového systému se pravidelně objevuje u zvířecích modelů Alzheimerovy choroby stejně tak jako v mozku pacientů s tímto onemocněním. Kromě toho některé výsledky ukazují, že aktivace jednotlivých podtypů mAChR specificky ovlivňuje štěpení APP, které může probíhat amyloidogenním či neamyloidogenním způsobem a určuje tak množství vytvořeného neurotoxického β -amyloidu. Ve své práci jsem studovala vliv akutního a dlouhodobého působení $A\beta_{1-42}$ na mAChR, které tvoří významnou součást cholinergního systému. Z výsledků mé práce vyplývá, že $A\beta_{1-42}$ dlouhodobě přítomný v kultivačním médiu s rostoucími buňkami exprimujícími jednotlivé podtypy mAChR negativně ovlivňuje vazebné i funkční vlastnosti některých lichých podtypů mAChR (především M1, méně M3). Podobné poškození funkce mAChR jsem zaznamenala také v mozkové kůře transgenních myší APPswe/PS1dE9, které jsou jedním z běžně používaných zvířecích modelů Alzheimerovy choroby. Postižení muskarinové transmise se u myšího modelu Alzheimerovy choroby objevuje během postupného zvyšování koncentrace rozpustného β -amyloidu (zejména fragmentu $A\beta_{1-42}$), tj. dříve než typická patologie nebo behaviorální poruchy, a lze ho napodobit *in vitro* působením nízké koncentrace $A\beta_{1-42}$. Tato pozorování podporují představu časného postižení muskarinové transmise u Alzheimerovy choroby. Mechanismus chronického účinku $A\beta_{1-42}$, který vede k poškození uvedených lichých podtypů mAChR, není zcela jasný. Je však možné, že se na něm podílejí změny buněčné membrány, které mají vliv na spřahování jednotlivých typů mAChR s příslušnými G-proteiny.

Summary

Impairment of the cholinergic neurotransmission system is regularly detected in animal models of Alzheimer's disease as well as in human patients suffering from this serious disease. Moreover, there is increasing amount of evidence suggesting that activation of individual mAChR subtypes specifically influences the cleavage of APP, the precursor for β -amyloid. APP can be processed in an amyloidogenic or non-amyloidogenic pathway and a relative abundance of these pathways contributes to establishing the final concentration of neurotoxic β -amyloid in the brain. In this work, I have studied the acute and chronic effects of $A\beta_{1-42}$ on binding and functional characteristics of mAChR. I have demonstrated that $A\beta_{1-42}$ present in cell culture expressing the individual subtypes of mAChR negatively and specifically influences the function of the M1 mAChR subtype. I have also detected a decline in muscarinic receptor-mediated signal transduction in brain tissue of young adult APPswe/PS1dE9 mice, a commonly used animal model of Alzheimer's disease. Demonstration of the impairment of muscarinic transmission in transgenic mice by soluble β -amyloid that occurs earlier than amyloid pathology and behavioral deficit, and its imitation by soluble $A\beta_{1-42}$ *in vitro* lend strong support to the notion of the early involvement of muscarinic transmission in pathogenesis of Alzheimer's disease. Mechanisms underlying the negative effects of $A\beta_{1-42}$ on mAChR are not yet clear. Some results suggest that structural changes of cell membrane and successive changes in receptor/G-protein interaction may be involved.

Seznam použité literatury

1. AbdAlla S, Lothe R, el Missiry A, Langer A, Sergeev P, el Faramawy Y, Quittner U.: Angiotensin II AT2 receptor oligomers mediate G-protein dysfunction in an animal model of Alzheimer disease. *J Biol Chem.* 2009, 284(10):6554-65.
2. Abdulaev NG, Ngo T, Ramon E, Brabazon DM, Marino JP, Ridge KD.: The receptor-bound "empty pocket" state of the heterotrimeric G-protein alpha-subunit is conformationally dynamic. *Biochemistry.* 2006, 45(43):12986-97.
3. Adams JP, Sweatt JD.: Molecular psychology: roles for the ERK MAP kinase cascade in memory. *Annu Rev Pharmacol Toxicol.* 2002, 42:135-63.
4. Ahmed M, Davis J, Aucoin D, Sato T, Ahuja S, Aimoto S, Elliott JI, Van Nostrand WE, Smith SO.: Structural conversion of neurotoxic amyloid-beta(1-42) oligomers to fibrils. *Nat Struct Mol Biol.* 2010, 17(5):561-7.
5. Aisen PS, Gauthier S, Ferris SH, Saumier D, Haine D, Garceau D, Duong A, Suhy J, Oh J, Lau WC, Sampalis J.: Tramiprosate in mild-to-moderate Alzheimer's disease - a randomized, double-blind, placebo-controlled, multi-centre study (the Alphase Study). *Arch Med Sci.* 2011, 7(1):102-11.
6. Aisen PS, Cummings J, Schneider LS.: Symptomatic and nonamyloid/tau based pharmacologic treatment for Alzheimer disease. *Cold Spring Harb Perspect Med.* 2012, 2(3):a006395.
7. Amtul Z, Uhrig M, Beyreuther K.: Additive effects of fatty acid mixtures on the levels and ratio of amyloid β 40/42 peptides differ from the effects of individual fatty acids. *J Neurosci Res.* 2011, 89(11):1795-801.
8. Apelt J, Lessig J, Schliebs R.: Beta-amyloid-associated expression of intercellular adhesion molecule-1 in brain cortical tissue of transgenic Tg2576 mice. *Neurosci Lett.* 2002, 329(1):111-5.
9. Arrasate M, Mitra S, Schweitzer ES, Segal MR, Finkbeiner S.: Inclusion body formation reduces levels of mutant huntingtin and the risk of neuronal death. *Nature.* 2004, 431(7010):805-10.
10. Arvanitakis Z, Schneider JA, Wilson RS, Bienias JL, Kelly JF, Evans DA, Bennett DA.: Statins, incident Alzheimer disease, change in cognitive function, and neuropathology. *Neurology.* 2008, 70(19 Pt 2):1795-802.
11. Bartus RT, Dean RL 3rd, Beer B, Lippa AS.: The cholinergic hypothesis of geriatric memory dysfunction. *Science.* 1982, 217(4558):408-14.
12. Bartus RT.: On neurodegenerative diseases, models, and treatment strategies: lessons learned and lessons forgotten a generation following the cholinergic hypothesis. *Exp Neurol.* 2000, 163(2):495-529.
13. Benilova I, Karran E, De Strooper B.: The toxic A β oligomer and Alzheimer's disease: an emperor in need of clothes. *Nat Neurosci.* 2012, 15(3):349-57.
14. Berkeley JL, Gomeza J, Wess J, Hamilton SE, Nathanson NM, Levey AI.: M1 muscarinic acetylcholine receptors activate extracellular signal-regulated kinase in CA1 pyramidal neurons in mouse hippocampal slices. *Mol Cell Neurosci.* 2001, 18(5):512-24.
15. Betts V, Leissring MA, Dolios G, Wang R, Selkoe DJ, Walsh DM.: Aggregation and catabolism of disease-associated intra-Abeta mutations: reduced proteolysis of AbetaA21G by neprilysin. *Neurobiol Dis.* 2008, 31(3):442-50.

16. Bodick NC, Offen WW, Levey AI, Cutler NR, Gauthier SG, Satlin A, Shannon HE, Tollefson GD, Rasmussen K, Bymaster FP, Hurley DJ, Potter WZ, Paul SM.: Effects of xanomeline, a selective muscarinic receptor agonist, on cognitive function and behavioral symptoms in Alzheimer disease. *Arch Neurol.* 1997, 54(4):465-73.
17. Bonner TI, Buckley NJ, Young AC, Brann MR.: Identification of a family of muscarinic acetylcholine receptor genes. *Science.* 1987, 237(4814):527-32.
18. Bonner TI, Young AC, Brann MR, Buckley NJ.: Cloning and expression of the human and rat m5 muscarinic acetylcholine receptor genes. *Neuron.* 1988, 1(5):403-10.
19. Bowen DM, Sims NR, Benton JS, Curzon G, Davison AN, Neary D, Thomas DJ.: Treatment of Alzheimer's disease: a cautionary note. *N Engl J Med.* 1981, 305(17):1016.
20. Brann MR, Ellis J, Jørgensen H, Hill-Eubanks D, Jones SV.: Muscarinic acetylcholine receptor subtypes: localization and structure/function. *Prog Brain Res.* 1993, 98:121-7.
21. Buckley NJ, Bonner TI, Brann MR.: Localization of a family of muscarinic receptor mRNAs in rat brain. *J Neurosci.* 1988, 8(12):4646-52.
22. Buxbaum JD, Oishi M, Chen HI, Pinkas-Kramarski R, Jaffe EA, Gandy SE, Greengard P.: Cholinergic agonists and interleukin 1 regulate processing and secretion of the Alzheimer beta/A4 amyloid protein precursor. *Proc Natl Acad Sci USA.* 1992, 89(21):10075-8.
23. Cansev M, Wurtman RJ.: Chronic administration of docosahexaenoic acid or eicosapentaenoic acid, but not arachidonic acid, alone or in combination with uridine, increases brain phosphatide and synaptic protein levels in gerbils. *Neuroscience.* 2007, 148(2):421-31.
24. Caulfield MP.: Muscarinic receptors--characterization, coupling and function. *Pharmacol Ther.* 1993, 58(3):319-79.
25. Cenini G, Cecchi C, Pensalfini A, Bonini SA, Ferrari-Toninelli G, Liguri G, Memo M, Uberti D.: Generation of reactive oxygen species by beta amyloid fibrils and oligomers involves different intra/extracellular pathways. *Amino Acids.* 2010, 38(4):1101-6.
26. Citron M, Oltersdorf T, Haass C, McConlogue L, Hung AY, Seubert P, Vigo-Pelfrey C, Lieberburg I, Selkoe DJ.: Mutation of the beta-amyloid precursor protein in familial Alzheimer's disease increases beta-protein production. *Nature.* 1992, 360(6405):672-4.
27. Cleary JP, Walsh DM, Hofmeister JJ, Shankar GM, Kuskowski MA, Selkoe DJ, Ashe KH.: Natural oligomers of the amyloid-beta protein specifically disrupt cognitive function. *Nat Neurosci.* 2005, 8(1):79-84.
28. Cole AR, Astell A, Green C, Sutherland C.: Molecular connexions between dementia and diabetes. *Neurosci Biobehav Res.* 2007, 31(7):1046-63.
29. Contestabile A.: The history of the cholinergic hypothesis. *Behav Brain Res.* 2011, 221(2):334-40.
30. Cramer PE, Cirrito JR, Wesson DW, Lee CY, Karlo JC, Zinn AE, Casali BT, Restivo JL, Goebel WD, James MJ, Brunden KR, Wilson DA, Landreth GE.: ApoE-directed therapeutics rapidly clear β -amyloid and reverse deficits in AD mouse models. *Science.* 2012, 335(6075):1503-6.
31. Cummings CJ, Reinstein E, Sun Y, Antalffy B, Jiang Y, Ciechanover A, Orr HT, Beaudet AL, Zoghbi HY.: Mutation of the E6-AP ubiquitin ligase reduces nuclear inclusion frequency while accelerating polyglutamine-induced pathology in SCA1 mice. *Neuron.* 1999, 24(4):879-92.

32. Davies P, Maloney AJ.: Selective loss of central cholinergic neurons in Alzheimer's disease. *Lancet.* 1976, 2(8000):1403.
33. Davis KL, Mohs RC, Marin D, Purohit DP, Perl DP, Lantz M, Austin G, Haroutunian V.: Cholinergic markers in elderly patients with early signs of Alzheimer disease. *JAMA.* 1999, 281(15):1401-6.
34. Davis AA, Fritz JJ, Wess J, Lah JJ, Levey AI.: Deletion of M1 muscarinic acetylcholine receptors increases amyloid pathology in vitro and in vivo. *J Neurosci.* 2010, 30(12):4190-6.
35. DeKosky ST, Ikonomovic MD, Styren SD, Beckett L, Wisniewski S, Bennett DA, Cochran EJ, Kordower JH, Mufson EJ.: Upregulation of choline acetyltransferase activity in hippocampus and frontal cortex of elderly subjects with mild cognitive impairment. *Ann Neurol.* 2002, 51(2):145-55.
36. Dickson DW.: The pathogenesis of senile plaques. *J Neuropathol Exp Neurol.* 1997, 56(4):321-39.
37. Dörje F, Levey AI, Brann MR.: Immunological detection of muscarinic receptor subtype proteins (m1-m5) in rabbit peripheral tissues. *Mol Pharmacol.* 1991, 40(4):459-62.
38. Drachman DA, Leavitt J.: Human memory and the cholinergic system. A relationship to aging? *Arch Neurol.* 1974, 30(2):113-21.
39. Evangelisti E, Wright D, Zampagni M, Cascella R, Bagnoli S, Relini A, Nichino D, Scartabelli T, Nacmias B, Sorbi S, Cecchi C.: Lipid Rafts Mediate Amyloid-induced Calcium Dyshomeostasis and Oxidative Stress in Alzheimer's Disease. *Curr Alzheimer Res.* 2012, Aug 30. [Epub ahead of print]
40. Evans RM, Hui S, Perkins A, Lahiri DK, Poirier J, Farlow MR.: Cholesterol and APOE genotype interact to influence Alzheimer disease progression. *Neurology.* 2004, 62(10):1869-71.
41. Fisher A.: Cholinergic modulation of amyloid precursor protein processing with emphasis on M1 muscarinic receptor: perspectives and challenges in treatment of Alzheimer's disease. *J Neurochem.* 2012, 120 Suppl 1:22-33.
42. Flynn DD, Weinstein DA, Mash DC.: Loss of high-affinity agonist binding to M1 muscarinic receptors in Alzheimer's disease: implications for the failure of cholinergic replacement therapies. *Ann Neurol.* 1991, 29(3):256-62.
43. Flynn DD, Ferrari-DiLeo G, Levey AI, Mash DC.: Differential alterations in muscarinic receptor subtypes in Alzheimer's disease: implications for cholinergic-based therapies. *Life Sci.* 1995, 56(11-12):869-76.
44. Francis PT, Sims NR, Procter AW, Bowen DM.: Cortical pyramidal neurone loss may cause glutamatergic hypoactivity and cognitive impairment in Alzheimer's disease: investigative and therapeutic perspectives. *J Neurochem.* 1993, 60(5):1589-604.
45. Francis PT, Palmer AM, Snape M, Wilcock GK.: The cholinergic hypothesis of Alzheimer's disease: a review of progress. *J Neurol Neurosurg Psychiatry.* 1999, 66(2):137-47.
46. Gibson GE, Sheu KF, Blass JP, Baker A, Carlson KC, Harding B, Perrino P.: Reduced activities of thiamine-dependent enzymes in the brains and peripheral tissues of patients with Alzheimer's disease. *Arch Neurol.* 1988, 45(8):836-40.
47. Gilman S, Koller M, Black RS, Jenkins L, Griffith SG, Fox NC, Eisner L, Kirby L, Rovira MB, Forette F, Orgogozo JM; AN1792(QS-21)-201 Study Team.: Clinical effects of Abeta immunization (AN1792) in patients with AD in an interrupted trial. *Neurology.* 2005, 64(9):1553-62.

48. Glabe CG.: Common mechanisms of amyloid oligomer pathogenesis in degenerative disease. *Neurobiol. Aging.* 2006, 27(4):570-5.
49. Glenner GG, Wong CW.: Alzheimer's disease: initial report of the purification and characterization of a novel cerebrovascular amyloid protein. *Biochem Biophys Res Commun.* 1984, 120(3):885-90.
50. Goto Y, Niidome T, Hongo H, Akaike A, Kihara T, Sugimoto H.: Impaired muscarinic regulation of excitatory synaptic transmission in the APPswe/PS1dE9 mouse model of Alzheimer's disease. *Eur J Pharmacol.* 2008, 583(1):84-91.
51. Götz J, Chen F, van Dorpe J, Nitsch RM.: Formation of neurofibrillary tangles in P301L tau transgenic mice induced by A β 42 fibrils. *Science.* 2001, 293(5534):1491-1495.
52. Grimm MO, Tschäpe JA, Grimm HS, Zinser EG, Hartmann T.: Altered membrane fluidity and lipid raft composition in presenilin-deficient cells. *Acta Neurol Scand Suppl.* 2006, 185:27-32.
53. Grimm MO, Kuchenbecker J, Grösgen S, Burg VK, Hundsdörfer B, Rothhaar TL, Friess P, de Wilde MC, Broersen LM, Penke B, Péter M, Vigh L, Grimm HS, Hartmann T.: Docosahexaenoic acid reduces amyloid beta production via multiple pleiotropic mechanisms. *J Biol Chem.* 2011, 286(16):14028-39.
54. Grimm MO, Rothhaar TL, Grösgen S, Burg VK, Hundsdörfer B, Haupenthal VJ, Friess P, Kins S, Grimm HS, Hartmann T.: Trans fatty acids enhance amyloidogenic processing of the Alzheimer amyloid precursor protein (APP). *J Nutr Biochem.* 2012, 23(10):1214-23.
55. Haass C, Selkoe DJ.: Soluble protein oligomers in neurodegeneration: lessons from the Alzheimer's amyloid beta-peptide. *Nat Rev Mol Cell Biol.* 2007, 8(2):101-12.
56. Hamilton SE, Loose MD, Qi M, Levey AI, Hille B, McKnight GS, Idzerda RL, Nathanson NM.: Disruption of the m1 receptor gene ablates muscarinic receptor-dependent M current regulation and seizure activity in mice. *Proc Natl Acad Sci USA.* 1997, 94(24):13311-6.
57. Hamilton SE, Nathanson NM.: The M1 receptor is required for muscarinic activation of mitogen-activated protein (MAP) kinase in murine cerebral cortical neurons. *J Biol Chem.* 2001, 276(19):15850-3.
58. Hardy JA, Higgins GA.: Alzheimer's disease: the amyloid cascade hypothesis. *Science.* 1992, 256(5054):184-5.
59. Huang HM, Ou HC, Hsieh SJ.: Amyloid beta peptide impaired carbachol but not glutamate-mediated phosphoinositide pathways in cultured rat cortical neurons. *Neurochem Res.* 2000, 25(2):303-12.
60. Huang Y, Mucke L.: Alzheimer mechanisms and therapeutic strategies. *Cell.* 2012, 148(6):1204-22.
61. Hulme EC, Curtis CA, Page KM, Jones PG.: Agonist activation of muscarinic acetylcholine receptors. *Cell Signal.* 1993, 5(6):687-94.
62. Jakubík J, Bacáková L, el-Fakahany EE, Tucek S.: Subtype selectivity of the positive allosteric action of alcuronium at cloned M1-M5 muscarinic acetylcholine receptors. *J Pharmacol Exp Ther.* 1995, 274(3):1077-83.
63. Jakubík J, Janíčková H, Randáková A, El-Fakahany EE, Doležal V.: Subtype differences in pre-coupling of muscarinic acetylcholine receptors. *PLoS One.* 2011a, 6(11):e27732.
64. Jakubík J, Janíčková H, El-Fakahany EE, Doležal V.: Negative cooperativity in binding of muscarinic receptor agonists and GDP as a measure of agonist efficacy. *Br J Pharmacol.* 2011b, 162(5):1029-44.

65. Jang H, Connelly L, Arce FT, Ramachandran S, Kagan BL, Lal R, Nussinov R.: Mechanisms for the Insertion of Toxic, Fibril-like β -Amyloid Oligomers into the Membrane. *J Chem Theory Comput.* 2013, 9(1):822-833.
66. Janíčková H, Rudajev V, Zimčík P, Jakubík J, Tanila H, El-Fakahany EE, Doležal V.: Uncoupling of M1 muscarinic receptor/G-protein interaction by amyloid β (1-42). *Neuropharmacology.* 2012, 67C:272-283. doi: 10.1016/j.neuropharm.2012.11.014.
67. Jankowsky JL, Fadale DJ, Anderson J, Xu GM, Gonzales V, Jenkins NA, Copeland NG, Lee MK, Younkin LH, Wagner SL, Younkin SG, Borchelt DR.: Mutant presenilins specifically elevate the levels of the 42 residue beta-amyloid peptide in vivo: evidence for augmentation of a 42-specific gamma secretase. *Hum Mol Genet.* 2004, 13(2):159-70.
68. Jelic V, Kivipelto M, Winblad B: Clinical trials in mild cognitive impairment: lessons for the future. *J Neurol Neurosurg Psychiatry.* 2006, 77(4):429-38.
69. Jicha GA, Parisi JE, Dickson DW, Johnson K, Cha R, Ivnik RJ, Tangalos EG, Boeve BF, Knopman DS, Braak H, Petersen RC.: Neuropathologic outcome of mild cognitive impairment following progression to clinical dementia. *Arch Neurol.* 2006, 63(5):674-81.
70. Joseph JA, Fisher DR.: Muscarinic receptor subtype determines vulnerability to amyloid beta toxicity in transfected cos-7 cells. *J Alzheimers Dis.* 2003, 5(3):197-208.
71. Kandiah N, Feldman HH: Therapeutic potential of statins in Alzheimer's disease. *J Neurol Sci.* 2009, 283(1-2):230-4.
72. Kang J, Lemaire HG, Unterbeck A, Salbaum JM, Masters CL, Grzeschik KH, Multhaup G, Beyreuther K, Müller-Hill B.: The precursor of Alzheimer's disease amyloid A4 protein resembles a cell-surface receptor. *Nature.* 1987, 325(6106):733-6.
73. Kelly JF, Furukawa K, Barger SW, Rengen MR, Mark RJ, Blanc EM, Roth GS, Mattson MP.: Amyloid beta-peptide disrupts carbachol-induced muscarinic cholinergic signal transduction in cortical neurons. *Proc Natl Acad Sci USA.* 1996, 93(13):6753-8.
74. Kim HS, Sul D, Lim JY, Lee D, Joo SS, Hwang KW, Park SY.: Delphinidin ameliorates beta-amyloid-induced neurotoxicity by inhibiting calcium influx and tau hyperphosphorylation. *Biosci Biotechnol Biochem.* 2009, 73(7):1685-9.
75. Kimura M, Akasofu S, Ogura H, Sawada K.: Protective effect of donepezil against Abeta(1-40) neurotoxicity in rat septal neurons. *Brain Res.* 2005, 1047(1):72-84.
76. Kitamura Y, Shibagaki K, Takata K, Tsuchiya D, Taniguchi T, Gebicke-Haerter PJ, Miki H, Takenawa T, Shimohama S.: Involvement of Wiskott-Aldrich syndrome protein family verprolin-homologous protein (WAVE) and Rac1 in the phagocytosis of amyloid-beta(1-42) in rat microglia. *J Pharmacol Sci.* 2003, 92(2):115-23.
77. Kish SJ, Robitaille Y, el-Awar M, Deck JH, Simmons J, Schut L, Chang LJ, DiStefano L, Freedman M.: Non-Alzheimer-type pattern of brain cholineacetyltransferase reduction in dominantly inherited olivopontocerebellar atrophy. *Ann Neurol.* 1989, 26(3):362-7.
78. Klein U, Gimpl G, Fahrenholz F.: Alteration of the myometrial plasma membrane cholesterol content with beta-cyclodextrin modulates the binding affinity of the oxytocin receptor. *Biochemistry.* 1995, 34(42):13784-93.

79. Klyubin I, Walsh DM, Lemere CA, Cullen WK, Shankar GM, Betts V, Spooner ET, Jiang L, Anwyl R, Selkoe DJ, Rowan MJ.: Amyloid beta protein immunotherapy neutralizes Abeta oligomers that disrupt synaptic plasticity in vivo. *Nat Med.* 2005, 11(5):556-61.
80. Krejci A, Tucek S.: Quantitation of mRNAs for M(1) to M(5) subtypes of muscarinic receptors in rat heart and brain cortex. *Mol Pharmacol.* 2002, 61(6):1267-72.
81. Ladiwala AR, Litt J, Kane RS, Aucoin DS, Smith SO, Ranjan S, Davis J, Van Nostrand WE, Tessier PM.: Conformational differences between two amyloid β oligomers of similar size and dissimilar toxicity. *J Biol Chem.* 2012, 287(29):24765-73.
82. Lambert MP, Barlow AK, Chromy BA, Edwards C, Freed R, Liosatos M, Morgan TE, Rozovsky I, Trommer B, Viola KL, Wals P, Zhang C, Finch CE, Krafft GA, Klein WL.: Diffusible, nonfibrillar ligands derived from Abeta1-42 are potent central nervous system neurotoxins. *Proc Natl Acad Sci USA.* 1998, 95(11):6448-53.
83. Levey AI, Kitt CA, Simonds WF, Price DL, Brann MR.: Identification and localization of muscarinic acetylcholine receptor proteins in brain with subtype-specific antibodies. *J Neurosci.* 1991, 11(10):3218-26.
84. Levey AI.: Immunological localization of m1-m5 muscarinic acetylcholine receptors in peripheral tissues and brain. *Life Sci.* 1993, 52(5-6):441-8.
85. Lichtenhaler SF.: Alpha-secretase in Alzheimer's disease: molecular identity, regulation and therapeutic potential. *J Neurochem.* 2011, 116(1):10-21.
86. Longo VG.: Behavioral and electroencephalographic effects of atropine and related compounds. *Pharmacol Rev.* 1966, 18(2):965-96.
87. Lopez OL, Becker JT, Wahed AS, Saxton J, Sweet RA, Wolk DA, Klunk W, Dekosky ST.: Long-term effects of the concomitant use of memantine with cholinesterase inhibition in Alzheimer disease. *J Neurol Neurosurg Psychiatry.* 2009, 80(6):600-7.
88. Lowry, O.H., Rosebrough, N.J., Farr, A.L., Randall, R.J.: Protein measurement with the Folin phenol reagent. *J Biol Chem.* 1951, 193(1):265-75.
89. Machová E, Nováková J, Lisá V, Dolezal V.: Docosahexaenoic acid supports cell growth and expression of choline acetyltransferase and muscarinic receptors in NG108-15 cell line. *J Mol Neurosci.* 2006, 30(1-2):25-6.
90. Machová E, Jakubík J, Michal P, Oksman M, Iivonen H, Tanila H, Dolezal V.: Impairment of muscarinic transmission in transgenic APPswe/PS1dE9 mice. *Neurobiol Aging.* 2008, 29(3):368-78.
91. Machová E, Rudajev V, Smycková H, Koivisto H, Tanila H, Dolezal V.: Functional cholinergic damage develops with amyloid accumulation in young adult APPswe/PS1dE9 transgenic mice. *Neurobiol Dis.* 2010, 38(1):27-35.
92. Maggio R, Vogel Z, Wess J.: Reconstitution of functional muscarinic receptors by co-expression of amino- and carboxyl-terminal receptor fragments. *FEBS Lett.* 1993, 319(1-2):195-200.
93. Mann DM.: Cerebral amyloidosis, ageing and Alzheimer's disease; a contribution from studies on Down's syndrome. *Neurobiol Aging.* 1989, 10(5):397-9
94. Martins IJ, Berger T, Sharman MJ, Verdile G, Fuller SJ, Martins RN.: Cholesterol metabolism and transport in the pathogenesis of Alzheimer's disease. *J Neurochem.* 2009, 111(6):1275-308.

95. Masters CL, Simms G, Weinman NA, Multhaup G, McDonald BL, Beyreuther K.: Amyloid plaque core protein in Alzheimer disease and Down syndrome. *Proc Natl Acad Sci USA.* 1985, 82(12):4245-9.
96. McLean CA, Cherny RA, Fraser FW, Fuller SJ, Smith MJ, Beyreuther K, Bush AI, Masters CL.: Soluble pool of Abeta amyloid as a determinant of severity of neurodegeneration in Alzheimer's disease. *Ann Neurol.* 1999, 46(6):860-6.
97. Medeiros R, Kitazawa M, Caccamo A, Baglietto-Vargas D, Estrada-Hernandez T, Cribbs DH, Fisher A, LaFerla FM.: Loss of muscarinic M1 receptor exacerbates Alzheimer's disease-like pathology and cognitive decline. *Am J Pathol.* 2011, 179(2):980-91.
98. Michal P, Lysíková M, Tucek S.: Dual effects of muscarinic M(2) acetylcholine receptors on the synthesis of cyclic AMP in CHO cells: dependence on time, receptor density and receptor agonists. *Br J Pharmacol.* 2001, 132(6):1217-28.
99. Michal P, El-Fakahany EE, Dolezal V.: Muscarinic M2 receptors directly activate Gq/11 and Gs G-proteins. *J Pharmacol Exp Ther.* 2007, 320(2):607-14.
100. Michal P, Rudajev V, El-Fakahany EE, Dolezal V.: Membrane cholesterol content influences binding properties of muscarinic M2 receptors and differentially impacts activation of second messenger pathways. *Eur J Pharmacol.* 2009, 606(1-3):50-60.
101. Mitchell DC, Straume M, Miller JL, Litman BJ.: Modulation of metarhodopsin formation by cholesterol-induced ordering of bilayer lipids. *Biochemistry.* 1990, 29(39):9143-9.
102. Milanesi L, Sheynis T, Xue WF, Orlova EV, Hellewell AL, Jelinek R, Hewitt EW, Radford SE, Saibil HR.: Direct three-dimensional visualization of membrane disruption by amyloid fibrils. *Proc Natl Acad Sci USA.* 2012, 109(50):20455-60.
103. Müller DM, Mendla K, Farber SA, Nitsch RM.: Muscarinic M1 receptor agonists increase the secretion of the amyloid precursor protein ectodomain. *Life Sci.* 1997, 60(13-14):985-91.
104. Murdoch I, Perry EK, Court JA, Graham DI, Dewar D.: Cortical cholinergic dysfunction after human head injury. *J Neurotrauma.* 1998, 15(5):295-305.
105. Nagy Z, Esiri MM, Jobst KA, Morris JH, King EM, McDonald B, Litchfield S, Smith A, Barnetson L, Smith AD.: Relative roles of plaques and tangles in the dementia of Alzheimer's disease: correlations using three sets of neuropathological criteria. *Dementia.* 1995, 6(1):21-31.
106. Näslund J, Haroutunian V, Mohs R, Davis KL, Davies P, Greengard P, Buxbaum JD.: Correlation between elevated levels of amyloid beta-peptide in the brain and cognitive decline. *JAMA.* 2000, 283(12):1571-7.
107. Nestler EJ, Duman RS.: G proteins, v knize Basic neurochemistry, Molecular, cellular and medical aspects, (Siegel, J. ed.) Lippincott-Raven Publishers, New York str. 401 - 414 (1999)
108. Nikolajsen GN, Jensen MS, West MJ.: Cholinergic axon length reduced by 300 meters in the brain of an Alzheimer mouse model. *Neurobiol Aging.* 2011, 32(11):1927-31.
109. Nilsson L, Nordberg A, Hardy J, Wester P, Winblad B.: Physostigmine restores 3H-acetylcholine efflux from Alzheimer brain slices to normal level. *J Neural Transm.* 1986, 67(3-4):275-85.
110. Nitsch RM, Slack BE, Wurtman RJ, Growdon JH.: Release of Alzheimer amyloid precursor derivatives stimulated by activation of muscarinic acetylcholine receptors. *Science.* 1992, 258(5080):304-7.

111. Nitsch RM.: From acetylcholine to amyloid: neurotransmitters and the pathology of Alzheimer's disease. *Neurodegeneration*. 1996, 5(4):477-82.
112. Noble W, Olm V, Takata K, Casey E, Mary O, Meyerson J, Gaynor K, LaFrancois J, Wang L, Kondo T, Davies P, Burns M, Veeranna, Nixon R, Dickson D, Matsuoka Y, Ahljanian M, Lau LF, Duff K.: Cdk5 is a key factor in tau aggregation and tangle formation in vivo. *Neuron*. 2003, 38(4):555-65.
113. Oddo S, Billings L, Kesslak JP, Cribbs DH, LaFerla FM.: A β immunotherapy leads to clearance of early, but not late, hyperphosphorylated tau aggregates via the proteasome. *Neuron*. 2004, 43(3):321-332.
114. Ono K, Condron MM, Teplow DB.: Structure-neurotoxicity relationships of amyloid beta-protein oligomers. *Proc Natl Acad Sci USA*. 2009, 106(35):14745-50.
115. Pákski M, Kálman J.: Interactions between the amyloid and cholinergic mechanisms in Alzheimer's disease. *Neurochem Int*. 2008, 53(5):103-11.
116. Peralta EG, Winslow JW, Peterson GL, Smith DH, Ashkenazi A, Ramachandran J, Schimerlik MI, Capon DJ.: Primary structure and biochemical properties of an M2 muscarinic receptor. *Science*. 1987, 236(4801):600-5.
117. Perálvarez-Marín A, Mateos L, Zhang C, Singh S, Cedazo-Mínguez A, Visa N, Morozova-Roche L, Gräslund A, Barth A.: Influence of residue 22 on the folding, aggregation profile, and toxicity of the Alzheimer's amyloid beta peptide. *Biophys J*. 2009, 97(1):277-85.
118. Perez SE, He B, Muhammad N, Oh KJ, Fahnestock M, Ikonomovic MD, Mufson EJ.: Cholinotrophic basal forebrain system alterations in 3xTg-AD transgenic mice. *Neurobiol Dis*. 2011, 41(2):338-52.
119. Perry EK, Gibson PH, Blessed G, Perry RH, Tomlinson BE.: Neurotransmitter enzyme abnormalities in senile dementia. Choline acetyltransferase and glutamic acid decarboxylase activities in necropsy brain tissue. *J Neurol Sci*. 1977a, 34(2):247-65.
120. Perry EK, Perry RH, Blessed G, Tomlinson BE.: Necropsy evidence of central cholinergic deficits in senile dementia. *Lancet*. 1977b, 1(8004):189.
121. Perry EK, Tomlinson BE, Blessed G, Bergmann K, Gibson PH, Perry RH.: Correlation of cholinergic abnormalities with senile plaques and mental test scores in senile dementia. *Br Med J*. 1978, 2(6150):1457-9.
122. Perry EK, Curtis M, Dick DJ, Candy JM, Atack JR, Bloxham CA, Blessed G, Fairbairn A, Tomlinson BE, Perry RH.: Cholinergic correlates of cognitive impairment in Parkinson's disease: comparisons with Alzheimer's disease. *J Neurol Neurosurg Psychiatry*. 1985, 48(5):413-21.
123. Perry EK, Kilford L, Lees AJ, Burn DJ, Perry RH.: Increased Alzheimer pathology in Parkinson's disease related to antimuscarinic drugs. *Ann Neurol*. 2003, 54(2):235-8.
124. Peterson GL.: A simplification of the protein assay method of Lowry et al. which is more generally applicable. *Anal Biochem*. 1977, 83(2):346-56.
125. Roberson MR, Harrell LE.: Cholinergic activity and amyloid precursor protein metabolism. *Brain Res Brain Res Rev*. 1997, 25(1):50-69.
126. Rodbell M.: The complex regulation of receptor-coupled G-proteins. *Adv Enzyme Regul*. 1997, 37:427-35.

127. Rountree SD, Chan W, Pavlik VN, Darby EJ, Siddiqui S, Doody RS.: Persistent treatment with cholinesterase inhibitors and/or memantine slows clinical progression of Alzheimer disease. *Alzheimers Res Ther.* 2009, 1(2):7.
128. Russ TC, Morling JR.: Cholinesterase inhibitors for mild cognitive impairment. *Cochrane Database Syst Rev.* 2012, 9:CD009132.
129. Rylett RJ, Ball MJ, Colhoun EH.: Evidence for high affinity choline transport in synaptosomes prepared from hippocampus and neocortex of patients with Alzheimer's disease. *Brain Res.* 1983, 289(1-2):169-75.
130. Sardi F, Fassina L, Venturini L, Inguscio M, Guerriero F, Rolfo E, Ricevuti G.: Alzheimer's disease, autoimmunity and inflammation. The good, the bad and the ugly. *Autoimmun Rev.* 2011, 11(2):149-53.
131. Sarter M, Bruno JP.: Mild cognitive impairment and the cholinergic hypothesis: a very different take on recent data. *Ann Neurol.* 2002, 52(3):384-5.
132. Savelkoul PJ, Janickova H, Kuipers AA, Hageman RJ, Kamphuis PJ, Dolezal V, Broersen LM.: A specific multi-nutrient formulation enhances M1 muscarinic acetylcholine receptor responses in vitro. *J Neurochem.* 2012, 120(4):631-40.
133. Savonenko A, Xu GM, Melnikova T, Morton JL, Gonzales V, Wong MP, Price DL, Tang F, Markowska AL, Borchelt DR.: Episodic-like memory deficits in the APPswe/PS1dE9 mouse model of Alzheimer's disease: relationships to beta-amyloid deposition and neurotransmitter abnormalities. *Neurobiol. Dis.* 2005, 18(3):602-17.
134. Schor NF.: What the halted phase III γ -secretase inhibitor trial may (or may not) be telling us. *Ann Neurol.* 2011, 69(2):237-9.
135. Selkoe DJ.: Alzheimer's disease is a synaptic failure. *Science.* 2002, 298(5594):789-91.
136. Selkoe DJ.: Resolving controversies on the path to Alzheimer's therapeutics. *Nat Med.* 2011, 17(9):1060-5.
137. Selkoe DJ.: Preventing Alzheimer's disease. *Science.* 2012, 337(6101):1488-92.
138. Sims NR, Bowen DM, Smith CC, Flack RH, Davison AN, Snowden JS, Neary D.: Glucose metabolism and acetylcholine synthesis in relation to neuronal activity in Alzheimer's disease. *Lancet.* 1980, 1(8164):333-6.
139. Sims NR, Bowen DM, Davison AN.: [14C]acetylcholine synthesis and [14C]carbon dioxide production from [U-14C]glucose by tissue prisms from human neocortex. *Biochem J.* 1981, 196(3):867-76.
140. Smith DE, Roberts J, Gage FH, Tuszyński MH.: Age-associated neuronal atrophy occurs in the primate brain and is reversible by growth factor gene therapy. *Proc Natl Acad Sci USA.* 1999, 96(19):10893-8.
141. Sparks DL, Hunsaker JC 3rd, Slevin JT, DeKosky ST, Kryscio RJ, Markesberry WR.: Monoaminergic and cholinergic synaptic markers in the nucleus basalis of Meynert (nbM): normal age-related changes and the effect of heart disease and Alzheimer's disease. *Ann Neurol.* 1992, 31(6):611-20.
142. Teather LA, Wurtman RJ.: Chronic administration of UMP ameliorates the impairment of hippocampal-dependent memory in impoverished rats. *J Nutr.* 2006, 136(11):2834-7.
143. Terry AV Jr, Buccafusco JJ.: The cholinergic hypothesis of age and Alzheimer's disease-related cognitive deficits: recent challenges and their implications for novel drug development. *J Pharmacol Exp Ther.* 2003, 306(3):821-7

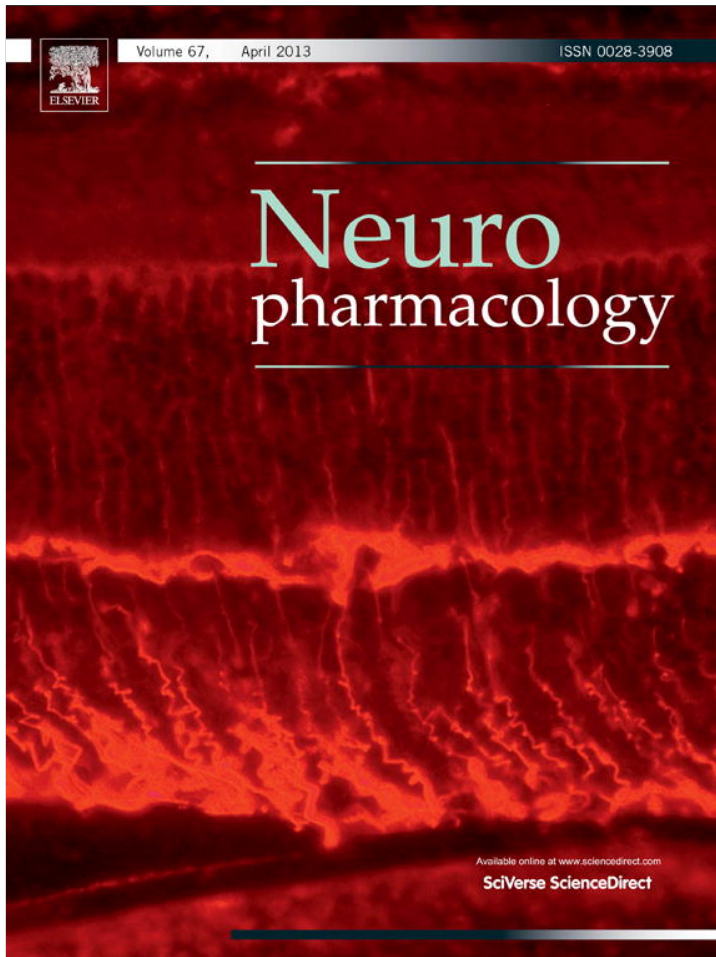
144. Terwel D, Muyllaert D, Dewachter I, Borghgraef P, Croes S, Devijver H, Van Leuven F.: Amyloid activates GSK-3beta to aggravate neuronal tauopathy in bigenic mice. *Am J Pathol.* 2008, 172(3):786-98.
145. Tiraboschi P, Hansen LA, Alford M, Masliah E, Thal LJ, Corey-Bloom J.: The decline in synapses and cholinergic activity is asynchronous in Alzheimer's disease. *Neurology.* 2000, 55(9):1278-83.
146. Tsang SW, Lai MK, Kirvell S, Francis PT, Esiri MM, Hope T, Chen CP, Wong PT.: Impaired coupling of muscarinic M1 receptors to G-proteins in the neocortex is associated with severity of dementia in Alzheimer's disease. *Neurobiol Aging.* 2006, 27(9):1216-23.
147. Wall SJ, Yasuda RP, Li M, Wolfe BB.: Development of an antiserum against m3 muscarinic receptors: distribution of m3 receptors in rat tissues and clonal cell lines. *Mol Pharmacol.* 1991, 40(5):783-9.
148. Walsh DM, Klyubin I, Fadeeva JV, Cullen WK, Anwyl R, Wolfe MS, Rowan MJ, Selkoe DJ.: Naturally secreted oligomers of amyloid beta protein potently inhibit hippocampal long-term potentiation in vivo. *Nature.* 2002, 416(6880):535-9.
149. Wang L, Albrecht MA, Wurtman RJ.: Dietary supplementation with uridine-5'-monophosphate (UMP), a membrane phosphatide precursor, increases acetylcholine level and release in striatum of aged rat. *Brain Res.* 2007, 1133(1):42-8.
150. Wess J, Duttaroy A, Zhang W, Gomeza J, Cui Y, Miyakawa T, Bymaster FP, McKinzie L, Felder CC, Lampert KG, Faraci FM, Deng C, Yamada M.: M1-M5 muscarinic receptor knockout mice as novel tools to study the physiological roles of the muscarinic cholinergic system. *Receptors Channels.* 2003, 9(4):279-90.
151. Wess J.: Muscarinic acetylcholine receptor knockout mice: novel phenotypes and clinical implications. *Annu Rev Pharmacol Toxicol.* 2004, 44:423-50.
152. Wess J, Eglen RM, Gautam D.: Muscarinic acetylcholine receptors: mutant mice provide new insights for drug development. *Nat Rev Drug Discov.* 2007, 6(9):721-33.
153. Whitehouse PJ, Price DL, Clark AW, Coyle JT, DeLong MR.: Alzheimer disease: evidence for selective loss of cholinergic neurons in the nucleus basalis. *Ann Neurol.* 1981, 10(2):122-6.
154. Whitehouse PJ, Price DL, Struble RG, Clark AW, Coyle JT, Delon MR.: Alzheimer's disease and senile dementia: loss of neurons in the basal forebrain. *Science* 1982, 215(4537):1237-9.
155. Wilcock GK, Esiri MM, Bowen DM, Smith CC.: Alzheimer's disease. Correlation of cortical choline acetyltransferase activity with the severity of dementia and histological abnormalities. *J Neurol Sci.* 1982, 57(2-3):407-17.
156. Williamson R, McNeilly A, Sutherland C.: Insulin resistance in the brain: an old-age or new-age problem? *Biochem Pharmacol.* 2012, 84(6):737-45.
157. Wurtman RJ, Ulus IH, Cansev M, Watkins CJ, Wang L, Marzloff G.: Synaptic proteins and phospholipids are increased in gerbil brain by administering uridine plus docosahexaenoic acid orally. *Brain Res.* 2006, 1088(1):83-92.
158. Xia W, Wong ST, Hanlon E, Morin P.: γ -secretase modulator in Alzheimer's disease: shifting the end. *J Alzheimers Dis.* 2012, 31(4):685-96.

159. Yasuda RP, Ciesla W, Flores LR, Wall SJ, Li M, Satkus SA, Weissstein JS, Spagnola BV, Wolfe BB.: Development of antisera selective for m₄ and m₅ muscarinic cholinergic receptors: distribution of m₄ and m₅ receptors in rat brain. *Mol Pharmacol.* 1993, 43(2):149-57.
160. Zhang Y, Hamilton SE, Nathanson NM, Yan J.: Decreased input-specific plasticity of the auditory cortex in mice lacking M₁ muscarinic acetylcholine receptors. *Cereb Cortex.* 2006, 16(9):1258-65.
161. Zhang W, Bai M, Xi Y, Hao J, Liu L, Mao N, Su C, Miao J, Li Z.: Early memory deficits precede plaque deposition in APPswe/PS1dE9 mice: involvement of oxidative stress and cholinergic dysfunction. *Free Radic Biol Med.* 2012, 52(8):1443-52.

Seznam příloh:

1. Janickova H, Rudajev V, Zimcik P, Jakubik J, Tanila H, El-Fakahany EE, Dolezal V: Uncoupling of M1 muscarinic receptor/G-protein interaction by amyloid β 1-42. *Neuropharmacology*. 2012; pii: S0028-3908(12)00561-8. doi: 10.1016/j.neuropharm.2012.11.014.
2. Savelkoul PJ, Janickova H, Kuipers AA, Hageman RJ, Kamphuis PJ, Dolezal V, Broersen LM.: A specific multi-nutrient formulation enhances M1 muscarinic acetylcholine receptor responses in vitro. *J Neurochem*. 2012; 120(4):631-40.
3. Jakubik J, Janickova H, Randakova A, El-Fakahany EE, Dolezal V: Subtype differences in precoupling of muscarinic acetylcholine receptors. *PLoS One*. 2011; 6(11):e27732.
4. Lyukmanova EN, Shenkarev ZO, Shulepko MA, Mineev KS, D'Hoedt D, Kasheverov IE, Filkin SY, Krivolapova AP, Janickova H, Dolezal V, Dolgikh DA, Arseniev AS, Bertrand D, Tsetlin VI, Kirpichnikov MP: NMR structure and action on nicotinic acetylcholine receptors of water-soluble domain of human LYNX1. *J Biol Chem*. 2011;286:10618-27
5. Jakubik J, Janickova H, El-Fakahany E, Dolezal V.: Negative cooperativity in binding of muscarinic receptor agonists and GDP as a measure of agonist efficacy. *Br J Pharmacol*. 2011;162:1029-44
6. Machova E, Rudajev V, Smyckova H, Koivisto H, Tanila H, Dolezal V.: Functional cholinergic damage develops with amyloid accumulation in young adult APPswe/PS1dE9 transgenic mice. *Neurobiol Dis*. 2010;38:27-35

Provided for non-commercial research and education use.
Not for reproduction, distribution or commercial use.



This article appeared in a journal published by Elsevier. The attached copy is furnished to the author for internal non-commercial research and education use, including for instruction at the authors institution and sharing with colleagues.

Other uses, including reproduction and distribution, or selling or licensing copies, or posting to personal, institutional or third party websites are prohibited.

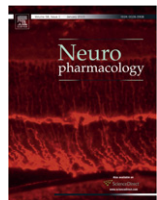
In most cases authors are permitted to post their version of the article (e.g. in Word or Tex form) to their personal website or institutional repository. Authors requiring further information regarding Elsevier's archiving and manuscript policies are encouraged to visit:

<http://www.elsevier.com/copyright>



Contents lists available at SciVerse ScienceDirect

Neuropharmacology

journal homepage: www.elsevier.com/locate/neuropharmUncoupling of M1 muscarinic receptor/G-protein interaction by amyloid β_{1-42} Helena Janíčková^a, Vladimír Rudajev^a, Pavel Zimčík^a, Jan Jakubík^a, Heikki Tanila^{b,c}, Esam E. El-Fakahany^d, Vladimír Doležal^{a,*}^a Institute of Physiology CAS, Vídeňská 1083, 14220 Prague 4, Czech Republic^b A. I. Virtanen Institute, University of Eastern Finland, P.O. Box 1627, 70211 Kuopio, Finland^c Department of Neurology, Kuopio University Hospital, P.O. Box 1777, 70211 Kuopio, Finland^d Department of Experimental and Clinical Pharmacology, University of Minnesota College of Pharmacy, Minneapolis, Minnesota, United States

ARTICLE INFO

Article history:

Received 28 September 2012

Received in revised form

19 November 2012

Accepted 21 November 2012

Keywords:

Amyloid β_{1-42}

Muscarinic receptors

G-proteins

Agonist binding

Phosphatidylinositol breakdown

ABSTRACT

The overproduction of β -amyloid ($A\beta$) fragments in transgenic APPswe/PS1dE9 mice results in formation of amyloid deposits in the cerebral cortex and hippocampus starting around four months of age and leading to cognitive impairment much later. We have previously found an age and transgene-dependent weakening of muscarinic receptor-mediated transmission that was not present in young (6–10-week-old) animals but preceded both amyloid deposits and cognitive deficits. Now we investigated immediate and prolonged *in vitro* effects of non-aggregated $A\beta_{1-42}$ on coupling of individual muscarinic receptor subtypes expressed in CHO (Chinese hamster ovary) cells and their underlying mechanisms. Immediate application of 1 μ M $A\beta_{1-42}$ had no effect on the binding of the muscarinic antagonist *N*-methylscopolamine or the agonist carbachol. In contrast, 4-day treatment of CHO cells expressing the M1 muscarinic receptor with 100 nM $A\beta_{1-42}$ significantly changed the binding characteristics of the muscarinic agonist carbachol and reduced the extent of the M1 receptor-stimulated breakdown of phosphatidylinositol while it did not demonstrate overt toxic effects. The treatment had no influence on the expression of either G-proteins or muscarinic receptors. In concert, we found no change in the gene expression of muscarinic receptor subtypes and gene or protein expression of the G_s , $G_{q/11}$, and $G_{i/o}$ G-proteins in the cerebral cortex of young adult APPswe/PS1dE9 mice that demonstrate high concentrations of soluble $A\beta_{1-42}$ and impaired muscarinic receptor-mediated G-protein activation. Our results provide strong evidence that the initial injurious effects of $A\beta_{1-42}$ on M1 muscarinic receptor-mediated transmission is due to compromised coupling of the receptor with $G_{q/11}$ G-protein.

© 2012 Elsevier Ltd. All rights reserved.

1. Introduction

Alzheimer's disease (AD) is presently the most widespread dementing neurodegenerative disease. A major hallmark of the disease is the presence of amyloid plaques and neurofibrillary tangles in the cerebral cortex and hippocampus. Studies of familial cases detected three genes directly linked to the disease and persuasively pointed to a crucial role of amyloid- β ($A\beta$) fragments

in the pathogenesis of the disease (Masters et al., 1985a,b; Hardy and Higgins, 1992; Selkoe, 2001). A general consensus now exists that an increase in soluble $A\beta$ oligomers concentration initiates and drives the pathology of AD (McLean et al., 1999; Selkoe, 2002; Glabe, 2006). However, the initial harmful functional effects that precede clinical manifestation, characteristic amyloid pathology, and neurodegeneration remain largely unknown. Consistent damage of cholinergic neurons in the basal forebrain in the terminal state of AD led to the formulation of the cholinergic hypothesis of AD (Bartus et al., 1982). Despite doubts about the general applicability of this hypothesis (Davis et al., 1999; Bartus, 2000; DeKosky et al., 2002), the responsiveness of the disease to cholinesterase inhibitor therapy supports its viability. It has been demonstrated that immunolesion of basal forebrain cholinergic neurons in rats resulting in presynaptic cholinergic deficit alters APP metabolism in cerebral cortex (Rossner et al., 1997). In addition, treatment of Parkinson's patients with antimuscarinic drugs

Abbreviations: AD, Alzheimer's disease; CHO cells, Chinese hamster ovary cells; CHO-M1 through CHO-M5, Chinese hamster ovary cells expressing individual subtypes (M1 through M5) of human muscarinic receptors.

* Corresponding author. Tel.: +420 296442287; fax: +420 296442488.

E-mail addresses: smyckova@biomed.cas.cz (H. Janíčková), rudajev@biomed.cas.cz (V. Rudajev), zimcik@biomed.cas.cz (P. Zimčík), jakubik@biomed.cas.cz (J. Jakubík), heikki.tanila@uef.fi (H. Tanila), elfak001@umn.edu (E.E. El-Fakahany), doleza@biomed.cas.cz (V. Doležal).

increases amyloid pathology (Perry et al., 2003) and M1 receptor gene knockout in mice increases amyloidogenic metabolism of APP (Davis et al., 2010).

The development of transgenic mouse models of AD has enabled studies on deviations of neuronal functioning in the course of gradual *in vivo* increase in the concentration of soluble human A β fragments and development of amyloid pathology. The APPswe/PS1dE9 transgenic mouse model of AD demonstrates a robust overproduction of A β _{1–42} fragments that finally leads to the appearance of amyloid pathology, cognitive decline, and neurodegeneration (Jankowsky et al., 2004; Savonenko et al., 2005; Liu et al., 2008). In this model we have previously demonstrated age and transgene-dependent weakening of muscarinic receptor-mediated G-protein activation. This reduction was not present in young (6–10-week-old) mice but was already present at the time when amyloid plaques formation just started (Machova et al., 2008, 2010).

In the present *in vitro* experiments we show that prolonged, but not immediate, treatment of Chinese hamster ovary (CHO) cells expressing individual muscarinic receptor subtypes with the A β _{1–42} fragment specifically affects muscarinic M1 receptor/G-protein interaction. This damage manifests itself as a change in agonist binding characteristics and reduced efficacy in activating G_{q/11} G-protein signaling. We next tested the hypothesis that reduction in muscarinic receptor-mediated signal transduction is due to changes in the expression of receptor/G-protein complex components. However, we found no changes in either gene expression of individual subtypes of muscarinic receptor or gene and protein expression of major subclasses of their preferential G-proteins in APPswe/PS1dE9 mice. In accordance, prolonged A β _{1–42} treatment of CHO cells expressing muscarinic receptor subtypes did not change membrane concentration of either G-proteins or muscarinic receptors. These findings support the notion that the early functional impairment of muscarinic transmission is likely due to a change that primarily occurs within the cell membrane and selectively impacts the M1 receptor/G-protein interaction.

2. Methods

2.1. Experimental animals

The APPswe/PS1dE9 founder mice were obtained from the Johns Hopkins University, Baltimore, MD, USA (D. Borchelt and J. Jankowsky, Dept. Pathology) and a colony was established at the University of Eastern Finland at Kuopio Finland as described previously (Machova et al., 2008). The housing conditions (Laboratory Animal Center, Kuopio, Finland and Animal Facility of the Institute of Physiology, v.v.i. in Prague, Czech Republic) were controlled (temperature 22 °C, light from 07:00 to 19:00; humidity 50–60%), and fresh food and water were freely available. Female transgenic mice and littermate controls were transported to Prague by air and left to adapt for at least two weeks before experiments. Two age groups of mice were used, young (7–10 weeks) and adult (5–7 months). The experiments were conducted according to the Council of Europe (Directive 86/609) in accordance with the Declaration of Helsinki.

2.2. Cell cultures and preparation of membranes

Cell culturing and membrane preparation were done essentially as described earlier (Jakubik et al., 2006). Briefly, Chinese hamster ovary cells stably transfected with the human M1 through M5 muscarinic receptor genes (kindly supplied by Prof. T.I. Bonner) were grown to confluence in 75 cm² flasks in Dulbecco's modified Eagle's medium supplemented with 10% fetal bovine serum and 0.01% genetecine to confluence. Then they were subcultured to sixteen 100-mm Petri dishes. For experiments on prolonged effects, 100 nM human amyloid β _{1–42} (A β _{1–42}; US Peptides, Rancho Cucamonga, CA) was added to medium next day after subculturing. Stock solution of A β _{1–42} was prepared in redistilled water and stored in aliquots at –20 °C. Cells were grown in a CO₂ incubator for 5 days without change of medium (four days in the presence of A β _{1–42}) and then harvested. For experiments on immediate effects of A β _{1–42} during binding assay, 5 mM sodium butyrate was added to the culture medium one day before harvesting to increase receptor expression (levels of receptor expression are shown in Supplementary material Table S2). Incubation medium was removed; cells were washed with 10 ml of phosphate-buffered saline (PBS), mechanically released into 5 ml of fresh PBS, and collected

by 3-min centrifugation at 1000 × g. Washed cells were diluted in ice-cold homogenization medium (100 mM NaCl, 20 mM Na-HEPES buffer, and 10 mM EDTA, pH 7.4) and homogenized on ice by two 30-s strokes in Ultra-Turrax homogenizer (Janke and Kunkel, Germany) with a 30 s pause between strokes. Cell homogenate was first centrifuged for 3 min at 300 g to remove coarse cell debris and nuclei. The crude membrane fraction was sedimented for 30 min at 30 000 g at 4 °C. The pellet was resuspended in incubation medium (100 mM NaCl, and 20 mM Na-HEPES buffer, pH 7.4), and centrifuged again under the same conditions. Pellets were kept at –75 °C until assayed for no more than 12 weeks. Membrane protein content was determined using Peterson's modification of Lowry's method (Lowry et al., 1951; Peterson, 1977) with human serum albumin as a standard.

2.3. mRNA expression of muscarinic receptor subtypes and G-proteins α -subunits

Total RNA from about 20 mg of cerebral cortices of 6–10 weeks and 5–6 months old APPswe/PS1dE9 female mice was isolated using RNAwiz (Ambion, UK) and further processed using DNA-free kit (Ambion, UK). The purity was checked spectrophotometrically at 260 nm and 280 nm. Reverse transcription of isolated RNA was performed using M-MLV RT (Promega, USA) in accordance with the manufacturer's instructions in a final volume of 10 μ l with 1 μ g of isolated RNA and 1 μ g of anchored oligo(dT)23 primers (Sigma, Prague). Primers are listed in Supplementary material (Table S1). Quantification of mRNA was done essentially as described (Machova et al., 2009) using Light Cycler (Roche, USA) and Light Cycler software. Denaturation analysis was performed to verify the identity of the product. Glyceraldehyde-3-phosphate dehydrogenase (GAPDH) was used as an internal standard.

2.4. Western blot and immunodetection of G-protein α -subunits

Separation and detection of membrane proteins was done essentially as described (Rudajev et al., 2005). Briefly, membranes (40 μ g of proteins) were dissolved in sodium dodecylsulphate and separated on 13% polyacrylamide gels. Separated proteins were transferred to nitrocellulose membrane and visualized using primary antibodies (from Santa Cruz Biotechnology, USA) and secondary HRP-labeled antibodies and ECL kit (from Pierce, USA).

2.5. Saturation and displacement binding studies

Density and affinity of muscarinic receptors incorporated in CHO cell membranes (5 μ g of membrane proteins for M1 and M3 receptors, and 20 μ g of membrane proteins for M2, M4, and M5 receptors) were determined in saturation binding experiments with the subtype non-selective muscarinic antagonist [³H]-N-methyl scopolamine (³H-NMS; GE Healthcare, UK) as described previously (Michal et al., 2009). Affinity of the agonist carbachol was estimated in displacement experiments using 1 nM ³H-NMS as a tracer. Non-specific binding was determined in the presence of 10 μ M atropine. Fast filtration to separate bound and free ligand was carried out using Unifilter plates (Whatman, USA) and Brandel Harvester (Brandel, USA). Plates were dried in vacuum and radioactivity retained on filters was determined in Rotisint (Carl Roth, Germany) using Microbeta scintillation counter (PerkinElmer Wallac, Finland).

2.6. GTP- γ ³⁵S binding

Muscarinic receptor-induced activation of G-proteins was determined as an increase of GTP- γ ³⁵S binding to membranes induced by the muscarinic receptor agonist carbachol, essentially as described earlier (Jakubik et al., 2006; Machova et al., 2008). Briefly, 50 μ l aliquots of membranes containing 5–20 μ g protein were first incubated for 15 min at 30 °C in 150 μ l of reaction buffer containing 100 mM NaCl, 10 mM MgCl₂, 20 mM HEPES, 1 mM DTT, 40 μ M GDP for M2 and M4 receptors or 1 μ M GDP for M1 and M3 receptors, and the non-hydrolyzable acetylcholine analog carbachol at a concentration range 0.15–1000 μ M for M1 and M3 receptors or 0.02–100 μ M for M2 and M4 receptors. Afterward 50 μ l aliquots of GTP- γ ³⁵S (Biotrend Chemikalien, Germany; SRA 1000 Ci/mmol) were added to give a final concentration of 500 pM and incubation continued for another 20 min. Total content of G-proteins in membranes was determined as GTP- γ ³⁵S binding in the absence of GDP. Non-specific binding was assessed in the presence of 10 μ M unlabeled GTP. Incubation was terminated by rapid vacuum filtration through Whatman GF/F filters using Tomtec Harvester Mach III (USA). Radioactivity retained on filters was measured with Wallac Microbeta counter.

2.7. Functional assays in intact cells

Inositol phosphates accumulation induced by carbachol was assayed in attached cells expressing M1 receptor grown in 24-well-plates essentially as described previously (Michal et al., 2009). Cells were loaded with ³H-myoinositol (ARC, USA) for 3 h, free ³H-myoinositol was washed off, and the carbachol-induced ³H-inositol phosphates accumulation was measured in medium containing 10 mM lithium and respective concentrations of carbachol (0–100 μ M) after 5 min lasting incubation at 37 °C. Inhibition of forskolin-stimulated cAMP synthesis was measured in M2 receptor expressing cell suspension in DMEM saturated with 5% CO₂/95% O₂.

Cells from one 10 cm diameter Petri dish were mechanically released to phosphate-buffered saline, separated by careful repeated aspiration to a pipette, sedimented at 200 × g for 5 min, and supernatant was discarded. The cell pellet was resuspended in 4 ml DMEM containing 1 mM isobutylmethylxanthine (IBMX) and preincubated for 5 min at room temperature. One hundred μ l aliquots of cell suspension (approximately 100 μ g of proteins) were transferred to prewarmed 100 μ l aliquots of DMEM containing forskolin and relevant concentrations of carbachol (final concentrations during incubation were 100 μ M for IBMX, 10 μ M for forskolin and 0–10 μ M for carbachol). Incubation for 10 min at 37 °C was stopped by transferring samples on ice and adding HCl to a final 100 mM concentration. Aliquots (100 μ l) of HCl extracts were taken for cAMP determination using Elisa kit (New East Biosciences, USA) according to instructions of the manufacturer. Influence of prolonged A β _{1–42} treatment on the formation of reactive oxygen intermediates in cells grown in 24-well-plates was determined using the fluorescence probe 6-carboxy-2',7'-dichlorodihydrofluorescein diacetate (Molecular Probes, USA) as described earlier (Novakova et al., 2005).

2.8. Activities of caspase-3 and caspase-8

Activities of caspase-3 and caspase-8 were determined in cell lysates prepared from cells grown in 24-well-plates fluorometrically using acDVED-AMC and acIETD-AMC substrates (Sigma, Prague) as described earlier (Novakova et al., 2005).

2.9. Determination of A β _{1–42} aggregation

The extent of A β _{1–42} aggregation in stock solution (at the beginning of cultivation) and in cultivation medium after 4-day incubations was determined using thioflavineT binding and Western blot. Thioflavine binding was estimated in

microtitration plates as described by Betts et al. (2008). One hundred microlitre aliquots of samples were mixed with 100 μ l of 200 mM glycine buffer (pH 8.5) containing 12 μ M thioflavine T (Sigma Aldrich, Czech Republic). The fluorescence at 485 nm after excitation at 435 nm was determined by plate reader Victor™ (Perkin Elmer). Western blot and immunodetection was done after separation on 4–20% gradient polyacrylamide gel. Separated samples were transferred to nitrocellulose membrane and assemblies of A β _{1–42} were visualized using primary antibodies 4G8 and 6E10 (from Covance, USA) and secondary HRP-labeled antibodies and ECL kit (from Pierce, USA). For electron microscopy, five μ l drops of A β _{1–42} stock solution (100 μ M in water) were applied onto glow-discharge activated carbon-coated grids (Benada and Pokorný, 1990) and let adsorb for 30 s. The grids were then washed with 1% ammonium molybdate and immediately negatively stained with 2% uranyl acetate in double distilled water for 30 s. The excess of water was blotted with filter paper and the grids were air-dried. The samples were examined in a Philips CM100 electron microscope at 80 kV. The images were digitally recorded using MegaViewII slow scan camera at 64 000 times magnification, which gives pixel size of about 1 nm.

2.10. Data treatment and statistical evaluation

Curve fitting and statistical evaluation of data was done using Prism 5 (GraphPad Software Inc., CA, USA). Rectangular hyperbolae were fitted to data obtained in saturation analysis experiments. A sigmoidal concentration-response curve equation with constant or variable slope as appropriate was fitted to data obtained in GTP- γ ³⁵S binding, inositolphosphates accumulation, and cAMP inhibition experiments. A two-sites displacement curve equation was fitted to data obtained in displacement experiments. Better fits were determined using F-test. The significance of differences among groups was tested by Anova and indicated post-hoc tests, t-test, or paired t-test as appropriate. Results are shown as means ± S.E.M.

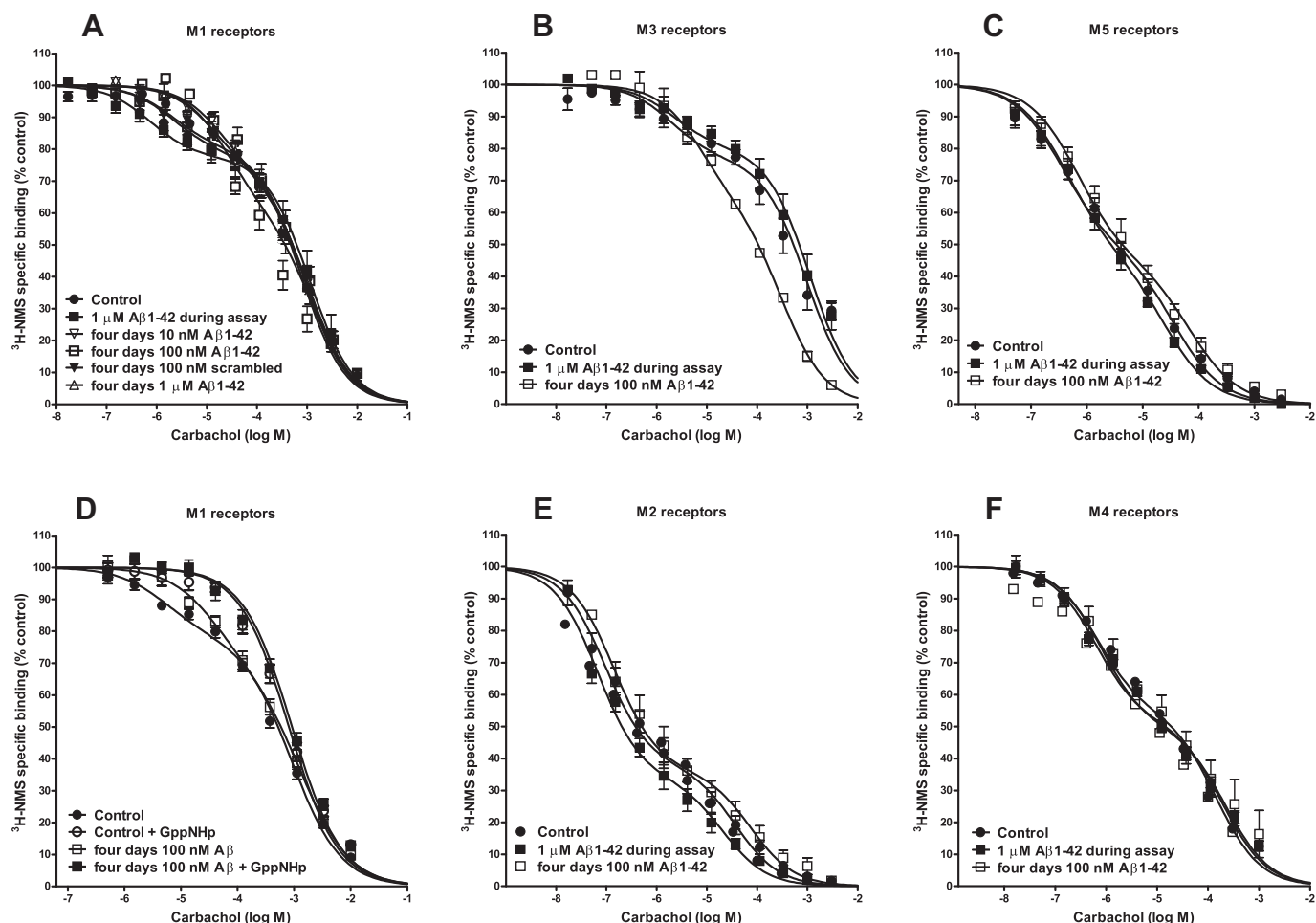


Fig. 1. Immediate and prolonged influence of A β _{1–42} on carbachol binding to individual subtypes of muscarinic receptors. Competition of carbachol (abscissa, log M) with 1 nM 3 H-N-methylscopolamine (3 H-NMS) binding in the absence (closed circles) or presence (closed squares) of 1 μ M A β _{1–42} during binding assay in membranes prepared from control cells, and in membranes prepared from cells grown for four days in the presence of 100 nM A β _{1–42} (open squares) is expressed as percentage of control binding (ordinate) in the absence of carbachol. A–F: Receptor subtypes are indicated in each graph. D: Displacement of 3 H-NMS binding in M1 receptor expressing membranes prepared from control cells (circles) or cells grown in the presence of 100 nM A β _{1–42} (squares) performed in the absence (closed symbols) or presence of GppNHP (open symbols). Parameters of displacement curves and number of observations are shown in Table 1.

3. Results

3.1. Effects of $A\beta_{1-42}$ on agonist binding to different muscarinic receptor subtypes

Binding characteristics of the muscarinic agonist carbachol were determined in displacement experiments using the labeled muscarinic antagonist $^3\text{H-N-methylscopolamine}$ ($^3\text{H-NMS}$) as a tracer. Neither direct addition of 1 $\mu\text{M } A\beta_{1-42}$ to the binding assay buffer in membranes prepared from CHO cells grown in control medium nor prolonged treatment of cells with 100 nM $A\beta_{1-42}$ for four days before preparation of membranes influenced the binding characteristics of $^3\text{H-NMS}$ (see Supplementary material Table S2).

As expected, the displacement of $^3\text{H-NMS}$ binding by the muscarinic agonist carbachol, a non-hydrolyzable analog of acetylcholine, demonstrated high- and low-affinity binding sites (Fig. 1, closed circles; Table 1) at all receptor subtypes. Similar to $^3\text{H-NMS}$ binding, the direct addition of 1 $\mu\text{M } A\beta_{1-42}$ to the binding assay buffer in displacement experiments had no influence on binding parameters of carbachol (Fig. 1 and Table 1) at any receptor subtype. In contrast, prolonged treatment with 100 nM $A\beta_{1-42}$ for four days changed carbachol binding in membranes prepared from cells expressing the M1, and to a lesser extent also the M3 receptors but not the M5 receptors (Fig. 1 and Table 1). Specifically, prolonged treatment with $A\beta_{1-42}$ resulted in an increase in the proportion of agonist high-affinity binding sites at the M1 and the M3 subtypes (from 0.21 to 0.33, $p < 0.01$, and 0.20 to 0.38, $p < 0.05$, respectively) and a decrease in the affinity of the agonist at the high-affinity binding site, specifically at the M1 subtype (K_i -high from 0.15 μM to 2.1 μM , $p < 0.01$). Prolonged treatment of M1 receptor expressing cells with 10 or 1000 nM concentration of $A\beta_{1-42}$ also induced a decrease in affinity of the agonist at the high-affinity binding site (to 3.0 and 2.2 μM , respectively; $p < 0.01$) while an increase in the proportion of the high-affinity binding sites (to 0.28 and 0.26, respectively) was not statistically significant (Table 1). As expected, prolonged treatment with 100 nM of the $A\beta_{42}$ scrambled peptide

was without effect (Fig. 1A; Table 1). Uncoupling of M1 receptors by 200 μM of the non-hydrolyzable GTP analog guanosine-5'-($\beta\gamma$ -imino)triphosphate (GppNHp) shifted the two-site carbachol displacement curves to a single-site curve with a similar low-affinity in membranes prepared from both control and 100 nM $A\beta_{1-42}$ treated cells (pK_i 3.88 \pm 0.13 and 3.83 \pm 0.12, respectively; $n = 3$) (Fig. 1D; Table 1).

3.2. Functional consequences of prolonged $A\beta_{1-42}$ treatment

In subsequent experiments we probed muscarinic receptor-mediated G-protein activation as carbachol-induced $\text{GTP-}\gamma^{35}\text{S}$ binding in membranes prepared from cells subjected to prolonged treatment with 100 nM $A\beta_{1-42}$. This treatment did not change either basal (in the absence of agonist) or total (in the absence of GDP in the reaction mixture) binding of $\text{GTP-}\gamma^{35}\text{S}$ at any receptor subtype (see Supplementary material; Table S3). Similarly, prolonged $A\beta_{1-42}$ treatment had no effect on the concentration-response curves of receptor activation at any of the M1 through M4 receptor subtypes (Fig. 2, Table 2A). However, all curves displayed Hill slopes significantly smaller than unity, indicating interactions of muscarinic receptor subtypes with more than one G-protein over the applied concentration range of carbachol.

To test more closely for a possible influence of the treatment on M1 receptor signaling pathways, we determined M1 receptor-stimulated inositolphosphates accumulation that is mediated by M1 preferential $G_{q/11}$ G-proteins in intact CHO cells. M2 receptor-mediated inhibition of forskolin-stimulated cAMP synthesis that is mediated by $G_{i/o}$ G-proteins served as a negative control. As shown in Fig. 3 and Table 2B, prolonged treatment with 100 nM $A\beta_{1-42}$ reduced the efficacy of M1 receptor-mediated inositolphosphates accumulation by about 14% ($p < 0.01$ by paired t -test, five independent experiments in triplicates) while M2 receptor-mediated inhibition of forskolin-stimulated cAMP synthesis remained intact (six independent experiments in triplicates).

Attenuation of phosphatidylinositol hydrolysis was not due to changes in membrane concentrations of labeled phosphatidylinositol (see text to Fig. 3). Similarly, the density of muscarinic receptor subtypes (see Supplementary material Table S2) or their preferential G-proteins (Fig. 4) was not changed by the treatment. Another possible explanation for the observed effects of prolonged treatment with 100 nM $A\beta_{1-42}$ on attenuation of M1 receptor signaling is potential general noxious effects of $A\beta_{1-42}$ (Yankner, 1996; Yankner and Lu, 2009). This is unlikely, however, because four-day treatment of CHO cells with $A\beta_{1-42}$ up to 1 μM concentration had no effect on either caspase-3 or caspase-8 activity (Fig. 5A and B, respectively), while 10 $\mu\text{M } A\beta_{1-42}$ significantly induced caspase-3 activity. Similarly, an increase in formation of reactive oxygen intermediates in intact cells became apparent only at $A\beta_{1-42}$ concentration of 1 μM and above (Fig. 5C).

3.3. Determination of $A\beta_{1-42}$ species in cultivation medium

In the next experiments we determined which molecular forms of $A\beta_{1-42}$ are present in cultivation media after four days of treatment. As is shown in Fig. 6, using Western blot and immunodetection, two different antibodies detected low molecular mass oligomers both in stock solution of $A\beta_{1-42}$ and in media after 4-day incubation of $A\beta_{1-42}$ treated CHO cells in culture. We further verified this finding with the help of thioflavine binding (Fig. 7). The aggregation of 100 μM stock solution of $A\beta_{1-42}$ in 10 mM HCl for 24 h at 37 °C followed by centrifugation at 16 000 g (Stine et al., 2003) yielded aggregated amyloid that contained 44% of original peptide in stock solution. Measurements of serial dilutions of aggregated amyloid dispersed in supplemented DMEM displayed a linear

Table 1
Effects of $A\beta_{1-42}$ on parameters of carbachol binding.

Receptor subtype treatment	Parameter			
	p K_i -high	p K_i -low	fH	(n)
M1 control	6.73 \pm 0.14	3.91 \pm 0.08	0.21 \pm 0.02	19
M1 control + GppNHp	—	3.88 \pm 0.13	n.a.	3
M1 acute 1 $\mu\text{M } A\beta$	7.08 \pm 0.11	3.75 \pm 0.18	0.20 \pm 0.03	6
M1 four days 10 nM $A\beta$	5.52 \pm 0.15 ^b	3.75 \pm 0.05	0.28 \pm 0.04	5
100 nM $A\beta$	5.68 \pm 0.27 ^b	4.07 \pm 0.16	0.33 \pm 0.03 ^b	8
100 nM scrambled	6.62 \pm 0.25	3.90 \pm 0.02	0.20 \pm 0.03	5
100 nM $A\beta$ + GppNHp	—	3.83 \pm 0.12	n.a.	3
1 $\mu\text{M } A\beta$	5.65 \pm 0.01 ^b	3.77 \pm 0.04	0.26 \pm 0.04	5
M2 control	7.56 \pm 0.10	4.96 \pm 0.08	0.66 \pm 0.03	11
M2 acute 1 $\mu\text{M } A\beta$	7.72 \pm 0.09	5.21 \pm 0.02	0.66 \pm 0.04	4
M2 four days 100 nM $A\beta$	7.60 \pm 0.22	4.84 \pm 0.19	0.61 \pm 0.03	5
M3 control	6.58 \pm 0.29	3.93 \pm 0.13	0.20 \pm 0.02	9
M3 acute 1 $\mu\text{M } A\beta$	6.74 \pm 0.36	3.80 \pm 0.13	0.20 \pm 0.04	6
M3 four days 100 nM $A\beta$	6.01 \pm 0.36	4.25 \pm 0.05	0.38 \pm 0.06 ^a	3
M4 control	7.39 \pm 0.05	4.94 \pm 0.09	0.46 \pm 0.02	7
M4 acute 1 $\mu\text{M } A\beta$	7.36 \pm 0.09	4.90 \pm 0.13	0.48 \pm 0.02	4
M4 four days 100 nM $A\beta$	7.50 \pm 0.08	5.10 \pm 0.06	0.47 \pm 0.01	3
M5 control	6.91 \pm 0.15	4.93 \pm 0.016	0.49 \pm 0.03	8
M5 acute 1 $\mu\text{M } A\beta$	6.81 \pm 0.19	5.01 \pm 0.08	0.54 \pm 0.05	3
M5 four days 100 nM $A\beta$	6.60 \pm 0.11	4.57 \pm 0.15	0.55 \pm 0.06	4

^a $p < 0.05$; significantly different from control by one-way Anova followed by Dunnett's multiple comparison test.

^b $p < 0.01$; significantly different from control by one-way Anova followed by Dunnett's multiple comparison test.

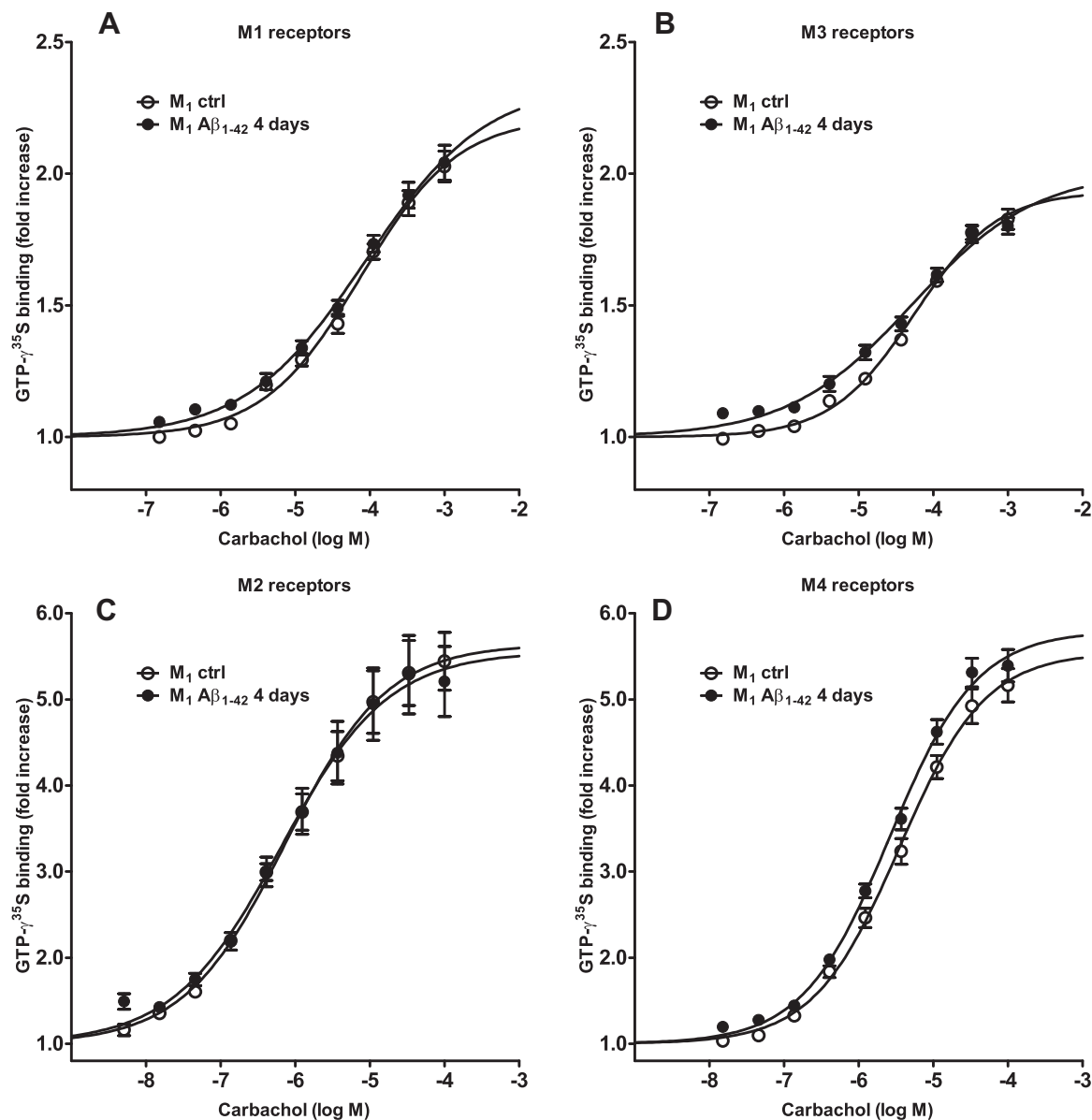


Fig. 2. Prolonged A β ₁₋₄₂ treatment and G-protein activation in CHO cell membranes. Prolonged treatment of CHO-M1 through CHO-M4 cells with 100 nM A β ₁₋₄₂ has no effect on carbachol-stimulated GTP- γ^{35} S binding. Membranes prepared from control cells (open circles) and cells grown for four days in the presence of 100 nM A β ₁₋₄₂ (closed circles) were stimulated by carbachol (abscissa, log M) as described in Methods. A–D: Receptor subtypes are indicated in each graph. The increase in GTP- γ^{35} S binding (ordinate) is expressed as fold increase over resting binding. Parameters of the concentration–response relationship are summarized in Table 2. Basal binding of GTP- γ^{35} S is shown in Supplementary material Table S3.

relationship between peptide concentration and fluorescence signal, and a detection limit between 33 and 100 ng (Fig. 7B). The soluble (16 000 g supernatant) amyloid as well as the original stock solution in water showed only small aggregation signal that became significant at concentrations ranging from 128 µg/ml (211 ng of thioflavine-positive species, i.e. 1.6%) and 26 µg/ml (138 ng of thioflavine-positive species at a concentration of 104 µg/ml, i.e. 1.2%), respectively. In concert with thioflavine binding, electron microscopy analysis of 100 µM A β ₁₋₄₂ stock solution showed no amyloid aggregates and only sporadic fibrils (Fig. 7C). After 4-day incubation of CHO cells in the presence of increasing concentrations of A β ₁₋₄₂ we found significant fluorescence signal only in medium containing 10 µM A β ₁₋₄₂ (98 ng of thioflavine-positive species, i.e. 2.2%). We did not detect any signal in media with 0.1–1 µM A β ₁₋₄₂ after four days in culture (Fig. 7A).

3.4. Muscarinic receptors and G-proteins expression in transgenic animals

Finally we investigated if gradual *in vivo* accumulation of soluble A β ₁₋₄₂ influences muscarinic receptor and G-proteins expression. The mRNA concentration of M1 through M4 muscarinic receptor subtypes did not differ between wild-type littermate control and transgenic APPswe/PS1dE9 female mice in the cerebral cortex of both 6–10-week-old (young) and 5–7-month-old (young adult) mice. The expression of the M5 subtype mRNA was under the detection limit in both age groups. Expression of the M1 muscarinic receptor, the most abundant subtype, represented similar proportions of all subtypes in young and young adult animals (51% and 62%, respectively). However, the rank order of abundance of muscarinic receptor subtypes changed from M1 > M4 > M2 > M3

Table 2

Effects of prolonged treatment with 100 nM A β _{1–42} on G-protein activation in membranes and functional response of M1 and M2 receptor expressing cells.

Receptor subtype treatment	Parameter	E_{max}	pEC ₅₀	Hill slope	(n)
<i>A: membranes</i>					
GTP-γ ³⁵ S binding (fold of resting)					
M1 ctrl	2.20 ± 0.08	4.21 ± 0.05	0.81 ± 0.07 ^a	7	
M1 A β _{1–42}	2.32 ± 0.15	4.23 ± 0.15	0.75 ± 0.08 ^a	6	
M2 ctrl	4.67 ± 0.75	6.14 ± 0.04	0.62 ± 0.07 ^a	4	
M2 A β _{1–42}	4.52 ± 0.94	6.21 ± 0.09	0.61 ± 0.05 ^a	4	
M3 ctrl	1.93 ± 0.07	4.27 ± 0.06	0.78 ± 0.06 ^a	5	
M3 A β _{1–42}	1.98 ± 0.06	4.23 ± 0.09	0.60 ± 0.05 ^a	5	
M4 ctrl	4.59 ± 0.51	5.44 ± 0.09	0.77 ± 0.05 ^a	4	
M4 A β _{1–42}	4.81 ± 0.37	5.58 ± 0.06	0.75 ± 0.04 ^a	4	
<i>B: Intact cells</i>					
IP accumulation (net increase)					
M1 ctrl	34.7 ± 1.8	5.44 ± 0.11	1.00	5	
M1 A β _{1–42}	30.0 ± 2.0 ^b	5.40 ± 0.02	1.00	5	
cAMP synthesis (% inhibition)					
M2 ctrl	34.5 ± 4.0	6.32 ± 0.28	1.00	6	
M2 A β _{1–42}	33.2 ± 3.7	6.30 ± 0.20	1.00	6	

^a p < 0.05, significantly different from unity by one sample t-test.

^b p < 0.01, significantly different from control by t-test.

in young to M1 > M2 > M4 > M3 in young adult animals (Fig. 8A and B).

Similar to muscarinic receptor subtypes, the mRNA expression of the α -subunits of both inhibitory (Fig. 8C and D) and stimulatory (Fig. 8E and F) G-proteins was the same in wild-type and transgenic animals in both age groups. The rank order of abundance of stimulatory G-protein α -subunits was G₁₁ > G_q > G_s in both young and young adult animals, whereas that of inhibitory G-protein α -subunits changed from Gi2 > Go > Gi1 > Gi3 in young mice to

Gi1 > Gi3 > Go > Gi2 in young adult mice. Because we have earlier observed a decrease in the potency of muscarinic receptor-mediated G-protein activation in transgenic mice starting at the age of 5–6 months (Machova et al., 2008, 2010), we also determined protein expression of α -subunits of major G-protein classes in cortical membranes. None of the major G-protein classes or the protein levels of the house-keeping gene Na/K-ATPase differed between wild-type and transgenic animals at the age of 5–6 months (see Supplementary material Fig. S1).

4. Discussion

Despite decades of intensive research, the exact role of cholinergic neurotransmission in the pathogenesis of Alzheimer's disease (AD; Bartus et al., 1982) is still unclear. General malfunction of postsynaptic cholinergic mechanisms in *post mortem* AD brain samples (Roth et al., 1995; Greenwood et al., 1995; Jope et al., 1994, 1997; Shiozaki and Iseki, 2004), as well as correlation of impaired muscarinic M1 receptor/G-protein coupling with disease severity (Tsang et al., 2005) are in favor of an involvement of impairment of muscarinic signaling. However, all these findings relate to the advanced or end-state of the disease, which makes it difficult to discern whether deficits in cholinergic transmission also play a significant role in the early pathogenesis. Since such studies are difficult to carry out in humans, we employed a transgenic mouse model of AD to probe integrity of cholinergic transmission during aging and amyloid accumulation. We found an early reduction of muscarinic receptor-mediated activation of G-proteins that was not present in young transgenic animals and developed parallel to a gradual increase in the concentration of soluble human A β fragments (Machova et al., 2008, 2010).

The present experiments investigated whether *in vitro* application of non-mutated human A β _{1–42} influence signal transduction

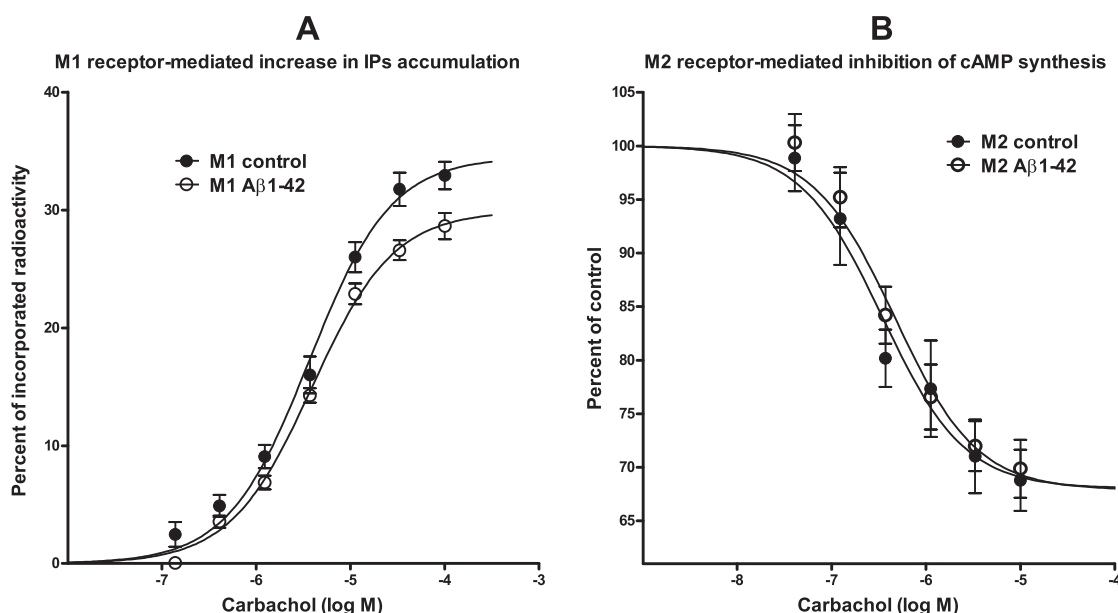


Fig. 3. Effect of prolonged treatment with A β _{1–42} on inositolphosphates (IP's) accumulation in intact CHO-M1 cells and inhibition of cAMP synthesis in intact CHO-M2 cells. The cells were grown in control medium (open circles) or in medium containing 100 nM A β _{1–42} (closed circles) for four days and then used for experiments. A: Cells were labeled with ³H-myoinositol, and concentration-response curves for stimulation by carbachol (abscissa, log M) were determined. The carbachol-induced increase in IP's accumulation is expressed as net increase in percent of loaded radioactivity (ordinate). The treatment with A β _{1–42} had no effect either on inositol loading (132 ± 5 and 141 ± 6 dpm/ μ g of protein) or basal accumulation of inositolphosphates (25.4 ± 1.8 and 24.4 ± 1.0 percent of loaded radioactivity in control and treated cells, respectively; mean ± S.E.M. from five independent experiments). B: Cells were incubated in medium containing phosphodiesterase inhibitor and forskolin to stimulate cAMP synthesis, and the concentration-response curves of cAMP synthesis inhibition by carbachol (abscissa, log M) were determined as described in Methods. The inhibition of forskolin-stimulated cAMP synthesis during incubations is expressed in percent of control (ordinate). Treatment with A β _{1–42} had no effect on forskolin-stimulated synthesis of cAMP in the absence of carbachol (478 ± 50 and 488 ± 61 pmol/mg protein/10 min in control and A β _{1–42} treated cells, respectively). The sigmoidal three parameter concentration-response equation was fitted to data in both graphs. Parameters of fits are shown in Table 2.

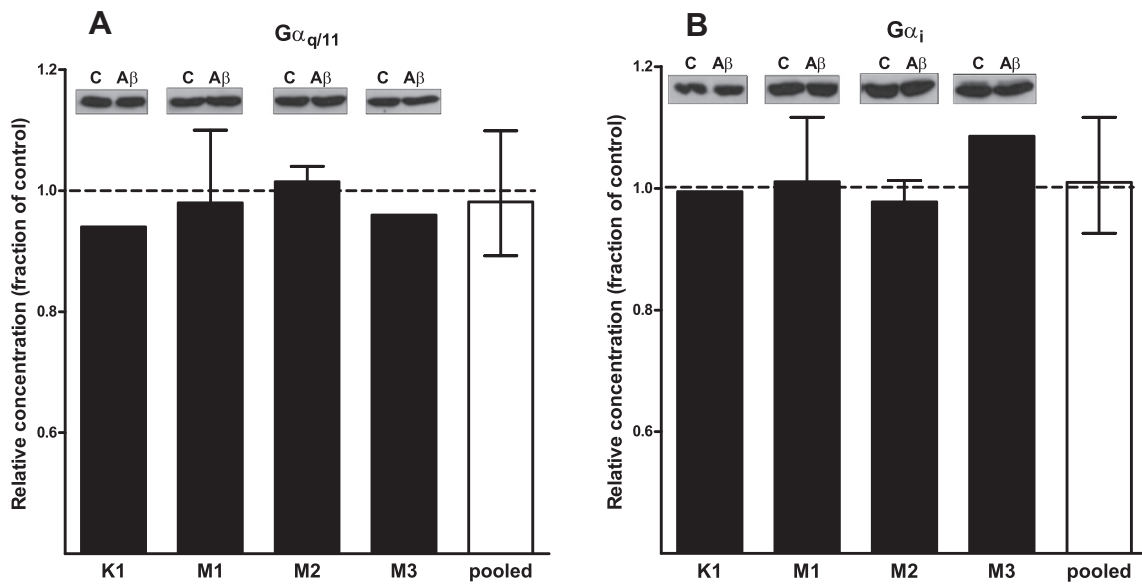


Fig. 4. Prolonged $A\beta_{1-42}$ treatment and G-protein concentrations in CHO cell membranes. Prolonged treatment with 100 nM $A\beta_{1-42}$ has no effect on the concentration of $G_{q/11}$ and $G_{i/o}$ G-protein in membranes prepared from K1 and CHO-M1 through CHO-M3 cells. Inserts above columns show representative blots. Membranes prepared from control (C) and $A\beta_{1-42}$ ($A\beta$) treated cells were used for western blot and immunodetection analysis as described in Methods. Relative density of $G_{q/11}$ and $G_{i/o}$ α -subunits (ordinate; density of bands of treated membranes is expressed as a fraction of density in control membranes from paired experiments) is shown in A and B graph as indicated. Columns K1 (CHO-K1 cells that do not express any muscarinic receptor) M1, M2, and M3 represent one, three, two, and one independent experiments, respectively. Open column denoted "pooled" shows average value of all seven experiments. Error bars where appropriate indicate range of individual values.

across plasma membrane in CHO cells expressing muscarinic receptor subtypes in isolation. The muscarinic receptor family comprises five subtypes (Bonner, 1989; Buckley et al., 1989) of which M2 and M4 receptors preferentially signal through $G_{i/o}$ G-proteins, while M1, M3, and M5 subtypes preferentially employ $G_{q/11}$ G-proteins (Jones et al., 1988; Jones, 1993). We found a selective impairment of M1 receptor/ $G_{q/11}$ G-protein coupling after 4-day treatment of cells with relatively low (100 nM) concentration of $A\beta_{1-42}$. This detrimental effect was not due to a general $A\beta_{1-42}$ toxicity, because consistent with results in neuronal cell lines (Huang et al., 1998; Novakova et al., 2005) and primary neurons (Huang et al., 2000), we observed commonly described toxic effects

like increased reactive oxygen species or caspase-3 activity only at concentrations 10–100 times higher. In concert, we did not observe morphological abnormalities in either living cells using phase contrast microscopy or nuclear staining of fixed cells (see Supplementary material Fig. 2S). We found only a small proportion of amyloid aggregates in stock solution we used, and detectable thioflavine binding only after 4-day incubation of cells in 10 μ M $A\beta_{1-42}$. Our results thus support the view that overt cellular toxicity requires higher concentrations of $A\beta_{1-42}$ to allow formation of amyloid aggregates.

The abnormal M1 receptor agonist binding after $A\beta_{1-42}$ treatment at 100 nM manifested itself as increased proportion of high-

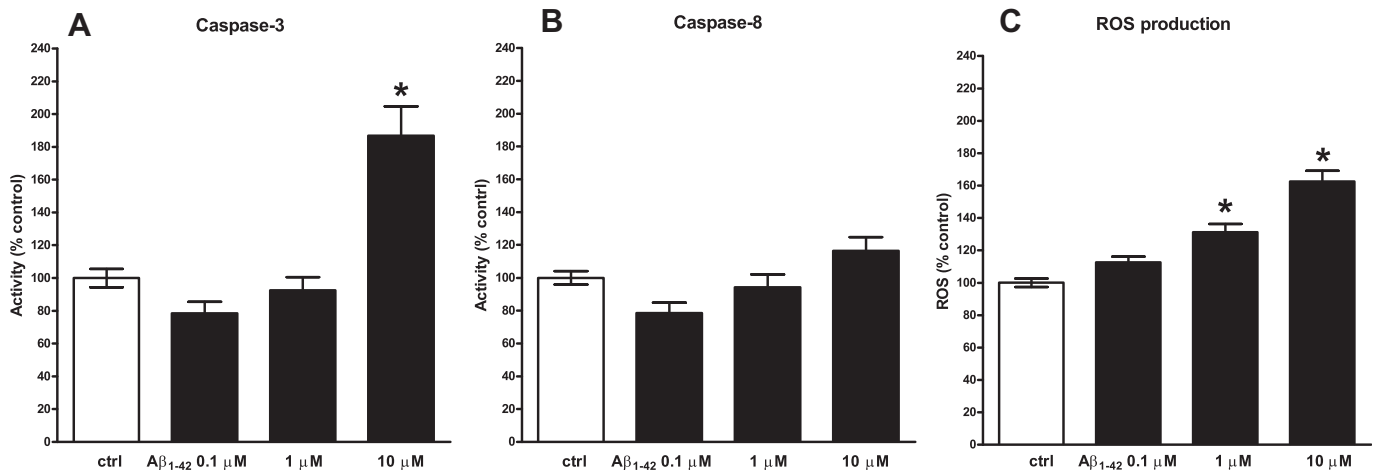


Fig. 5. Toxic effects of prolonged $A\beta_{1-42}$ treatment. Cells were exposed to the indicated concentration of $A\beta_{1-42}$ (abscissa) for four days and then used for assay. A and B graph: Caspase-3 and caspase-8 activities were determined in cell lysates. Data represent pooled values derived from two independent experiments on CHO-M1 cells and two independent experiments on CHO-M2 cells run in hexaplicates that yielded the same results. Control values were 36.9 ± 5.2 and 30.5 ± 3.8 of relative light units/ μ g protein*60 min for caspase-3 and caspase-8, respectively. C: Production of reactive oxygen species (ROS) in intact cells represents pooled values derived from two independent experiments on CHO-M1 cells and one experiment on CHO-M2 cells run in hexaplicates that yielded the same results. Control values were 52.8 ± 5.7 of relative light units/ μ g protein*60 min. Shown are pooled values expressed in percent of control (open column) in individual experiments. *: $p < 0.05$; significantly different from all other groups by Anova followed by Tukey's multiple comparison test.

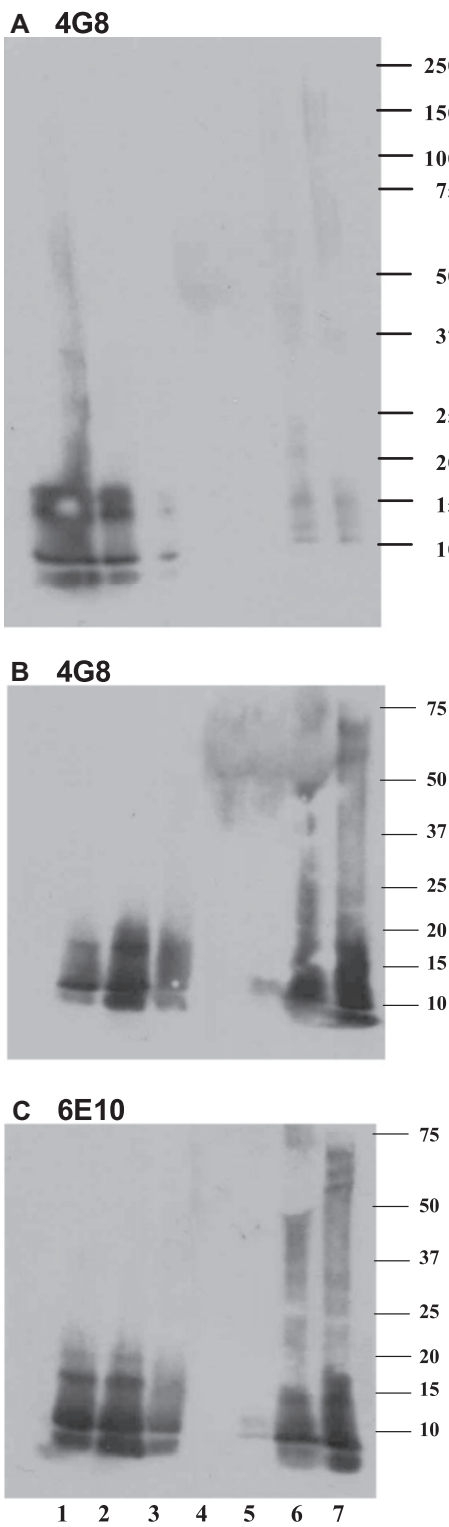


Fig. 6. Western blot determination of $\text{A}\beta_{1-42}$ species in stock solutions and incubation media after four days of incubation. A: Samples of $\text{A}\beta_{1-42}$ in water stock solution (lines 1–3: 2000 ng, 400 ng, and 80 ng in 15 μl of water, respectively) and in incubation media after four days in culture (lines 4–7: 0 ng/15 μl , 6.75 ng/15 μl , 67.5 ng/15 μl , 67.5 ng/15 μl of incubation medium, respectively) were separated on gradient 4–20% polyacrylamide gel, transferred to nitrocellulose membrane, and visualized using 4G8 antibody. Shown immunoblot includes bottom of wells to check for presence of amyloid that did not enter the gel. B and C: Samples of $\text{A}\beta_{1-42}$ in stock solution (lines 1–3: 50 ng, 100 ng, and 50 ng from another stock solution in 15 μl of water, respectively) and in incubation media after four days in culture (lines 4–7: 0 ng/15 μl , 6.75 ng/15 μl , 67.5 ng/15 μl , and 90 ng/2 μl of incubation medium, respectively) were separated as above and visualized using 4G8 (B) or 6E10 (C) antibody.

affinity binding sites, accompanied by decreased binding affinity. In contrast, ten times higher concentrations of $\text{A}\beta_{1-42}$ had no direct effect on the binding characteristics of either the muscarinic antagonist *N*-methylscopolamine or the agonist carbachol. Increased proportion of high-affinity binding sites were found to a lesser extent also at M3 receptors but not at the remaining muscarinic receptor subtypes, including the $\text{G}_{q/11}$ G-protein preferring M5 subtype. Low-affinity agonist binding was not changed at any subtype. Uncoupling of M1 receptors using a non-hydrolyzable analog of GTP shifted the two-site carbachol binding curves to the same affinity single-site low-affinity binding curve irrespective of $\text{A}\beta_{1-42}$ treatment. Agonists bind with low-affinity to free receptors, uncoupled from G-proteins. The lack of $\text{A}\beta_{1-42}$ treatment effect on low-affinity binding further indicates the absence of a direct interaction of $\text{A}\beta_{1-42}$ with the M1 receptor. The high-affinity agonist binding conformation is due to allosteric interactions of carbachol and the complex of receptor with free or GDP-ligated G-protein (Abdullaev et al., 2006; Jakubik et al., 2011). The decrease in affinity and increase in proportion of high-affinity binding sites evidence that prolonged treatment with $\text{A}\beta_{1-42}$ impacts interactions between the receptor and G-protein within the plasma membrane, downstream of agonist binding.

Despite influencing agonist binding at M1 receptor, the treatment had no influence on muscarinic receptor-mediated stimulation of GTP- γS binding. However, carbachol-stimulated GTP- γS binding displayed a flat concentration–response curve (Hill slope significantly less than unity), indicating activation of more than one class of G-proteins (Tucek et al., 2002; Michal et al., 2007; Jakubik et al., 2006, 2011). This complicates accurate detection of the presumed impairment of M1 receptor-mediated $\text{G}_{q/11}$ G-protein activation deduced from increased GTP- γS binding in membranes. Nonetheless, the observed decrease in carbachol-stimulated inositolphosphates accumulation supports the view of impaired M1 receptor coupling with $\text{G}_{q/11}$ G-proteins. The selectivity of prolonged $\text{A}\beta_{1-42}$ treatment in impairing $\text{G}_{q/11}$ G-protein signaling was also supported by the observation of unimpaired M2 receptor/ $\text{G}_{i/o}$ G-protein-mediated inhibition of cAMP accumulation in intact cells, in agreement with intact $\text{G}_{i/o}$ G-protein-mediated auto-inhibition of acetylcholine release in cortical slices from transgenic mice (Machova et al., 2010). The specific effect of $\text{A}\beta$ on M1 receptor coupling is further evidenced by the differential influence on the binding characteristics at other receptor subtypes and the lack of effect of the scrambled peptide on the M1 receptor.

A conceivable explanation for the compromised muscarinic receptor signaling would be a reduced membrane concentration of G-proteins that are an integral part of the signal transduction apparatus. However, a prolonged $\text{A}\beta_{1-42}$ treatment of CHO cells did not change membrane concentration of G-proteins. Similarly, in line with current literature on human brain (McLaughlin et al., 1991; Jope et al., 1994; Wang and Friedman, 1994; Greenwood et al., 1995; Muma et al., 2003; Hashimoto et al., 2004), we found no changes in membrane G-protein concentrations or gene expression of major G-protein classes in the cerebral cortex of 5–6-month-old transgenic APPswe/PS1dE9 mice that at this age already demonstrate a significant attenuation of muscarinic receptor-mediated G-protein activation (Machova et al., 2008).

Disorders of many G-protein coupled receptors are habitually found at autopsy in verified AD, which points to their contribution to AD pathogenesis (for review see Thathiah and De Strooper, 2011). An interesting explanation of impaired receptor/G-protein-mediated signaling in transgenic mouse models of AD is $\text{G}_{q/11}$ G-protein buffering by oligomerized angiotensin AT2 receptors (AbdAlla et al., 2009a,b). This potential mechanism, however, does not seem to explain our findings, because the prolonged treatment with 100 nM $\text{A}\beta_{1-42}$ did not induce oxidative stress that triggers

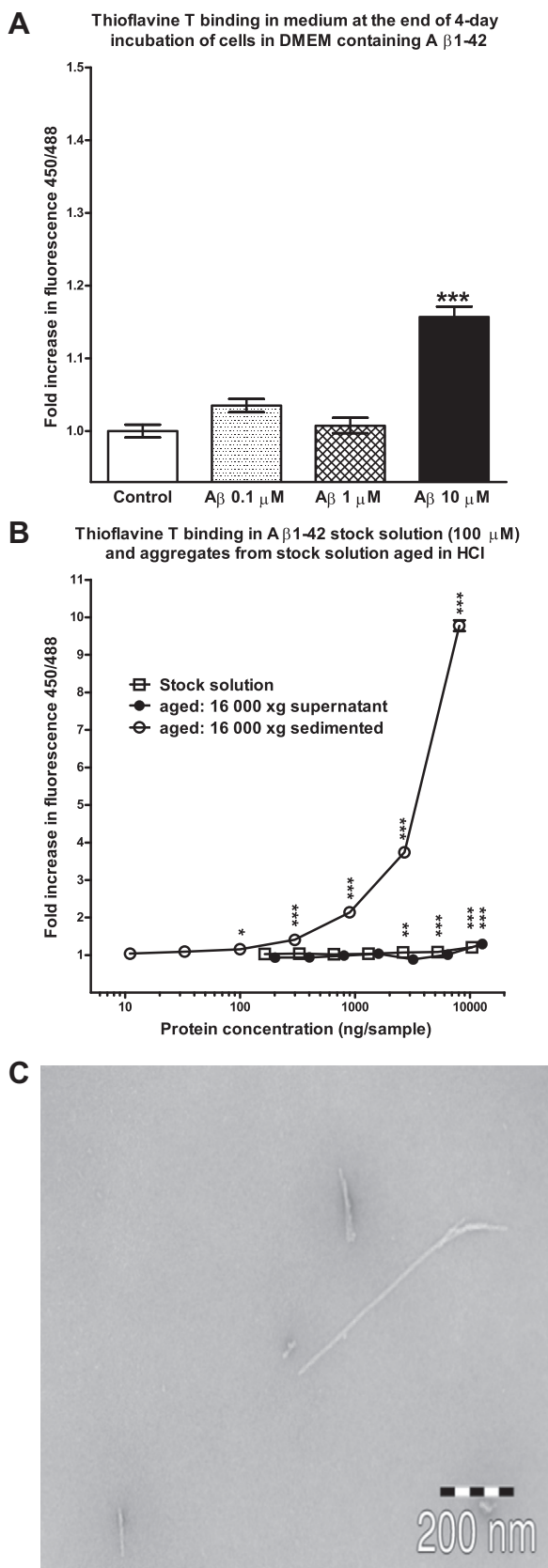


Fig. 7. Determination of A_β1-42 aggregation using thioflavine T binding and electron microscopy. Thioflavine T binding in media after four days in culture. A: Thioflavine binding in 100 μl aliquots of cultivation medium without or with 0.1, 1, and 10 μM A_β1-42 after 4-day incubation of CHO-M1 and CHO-M2 is shown as fold increase over control (ordinate) in fluorescence (450 nm excitation, 488 nm emission). Values are

receptor oligomerization, and in addition, CHO cells do not express AT2-receptors (Feng et al., 2005). Dysregulation of the signaling pathway activated by G_{q/11} G-proteins have been suggested to play a role in AD (for review see Bothmer and Jolles, 1994; Fowler et al., 1996). Non-toxic concentrations of A_β fragments *in vitro* have been shown to affect distant targets like inositolphosphate receptors (Cowburn et al., 1995; Kurumatani et al., 1998), intracellular calcium levels (Huang et al., 1998), inositol(1,4,5)-trisphosphate-5-phosphatase activity (Ronnback and Fowler, 2000) or choline transport via protein kinase C pathway (Novakova et al., 2005). A direct effect of A_β fragments on tachykinine receptor and synergy of its activation with glutamate signaling has also been demonstrated (Kimura and Schubert, 1993). In binding and functional experiments we investigated the interaction of muscarinic receptors with G-protein and the formation of second messengers by enzymes incorporated in the cell membrane. The observed reduction of phosphatidylinositol hydrolysis could have derived from decreased availability of the labeled substrate. This seems unlikely, however, because A_β1-42 had no effect on the labeling of cells with myo-inositol. A direct inhibition of phospholipase C activity is also an unlikely explanation, since we found no difference in the basal inositolphosphates accumulation between control and treated cells as we would expect in case of phospholipase C inhibition. The lack of prolonged treatment with A_β1-42 on phospholipase C activity also supports the observation on primary cortical neurons demonstrating inhibition of intracellular calcium mobilization by carbachol but not by stimulation of metabotropic glutamate receptor (Huang et al., 2000).

Numerous studies have failed to find a correlation between the degree of cognitive decline and the number of amyloid plaques in *post mortem* samples (e.g. Nagy et al., 1995). However, the cognitive decline in AD has been demonstrated to correlate with *post mortem* levels of soluble A_β x-40 and x-42 fragments in the cerebral cortex preceding clear tau pathology (Naslund et al., 2000). On the other hand, a decline in the presynaptic cholinergic marker choline acetyltransferase that correlates with both neuritic plaques and neurofibrillary tangles densities are observed only in advanced stages of the disease (Davis et al., 1999). This observation speaks for a rather late damage of cholinergic transmission in the course of the disease. In contrast, another recent study reported impaired M1 muscarinic receptor/G-protein coupling that correlates with severity of dementia, thus favoring the contention of an early postsynaptic malfunction of cholinergic transmission (Tsang et al., 2005). Our results support the view that the increase in soluble A_β fragments results in the attenuation of M1 receptor-mediated signaling that may underlie the early functional deficits and further drive A_β production (Buxbaum et al., 1992; Nitsch et al., 1992, 2000; Rossner et al., 1997; Caccamo et al., 2006; Medeiros et al., 2011). Indeed, pharmacological reduction of A_β level reverses behavioral deficits and disorders of piriform cortex field potentials in APPswe/PS1dE9 mice (Cramer et al., 2012).

In summary, we demonstrate that prolonged *in vitro* A_β1-42 treatment of CHO cells expressing M1 muscarinic receptors changes characteristics of agonist binding and attenuates agonist-

means of eight samples from two independent seedings. B: Concentration-response relationship of thioflavine fluorescence in stock solution of A_β1-42 (open squares), and pellet (open circles) or supernatant (closed circles) prepared from 100 μM A_β1-42 stock solution incubated for one day in 10 mM HCl at 37 °C by centrifugation at 16 000 g for 15 min. All samples were diluted in supplemented DMEM. The increase in thioflavine fluorescence shown as fold increase (ordinate) over control (DMEM alone) is plotted against A_β1-42 concentration in ng per sample (abscissa, logarithmic scale). Points are means from quadruplicates. *, p < 0.05, ***, p < 0.001; significantly different from control by one-way Anova followed by Dunnett's multiple comparison test. C: Electron microscopy analysis of 100 μM A_β1-42 stock solution shows only sporadic fibrils and no amyloid aggregates. Scale bar 200 nm.

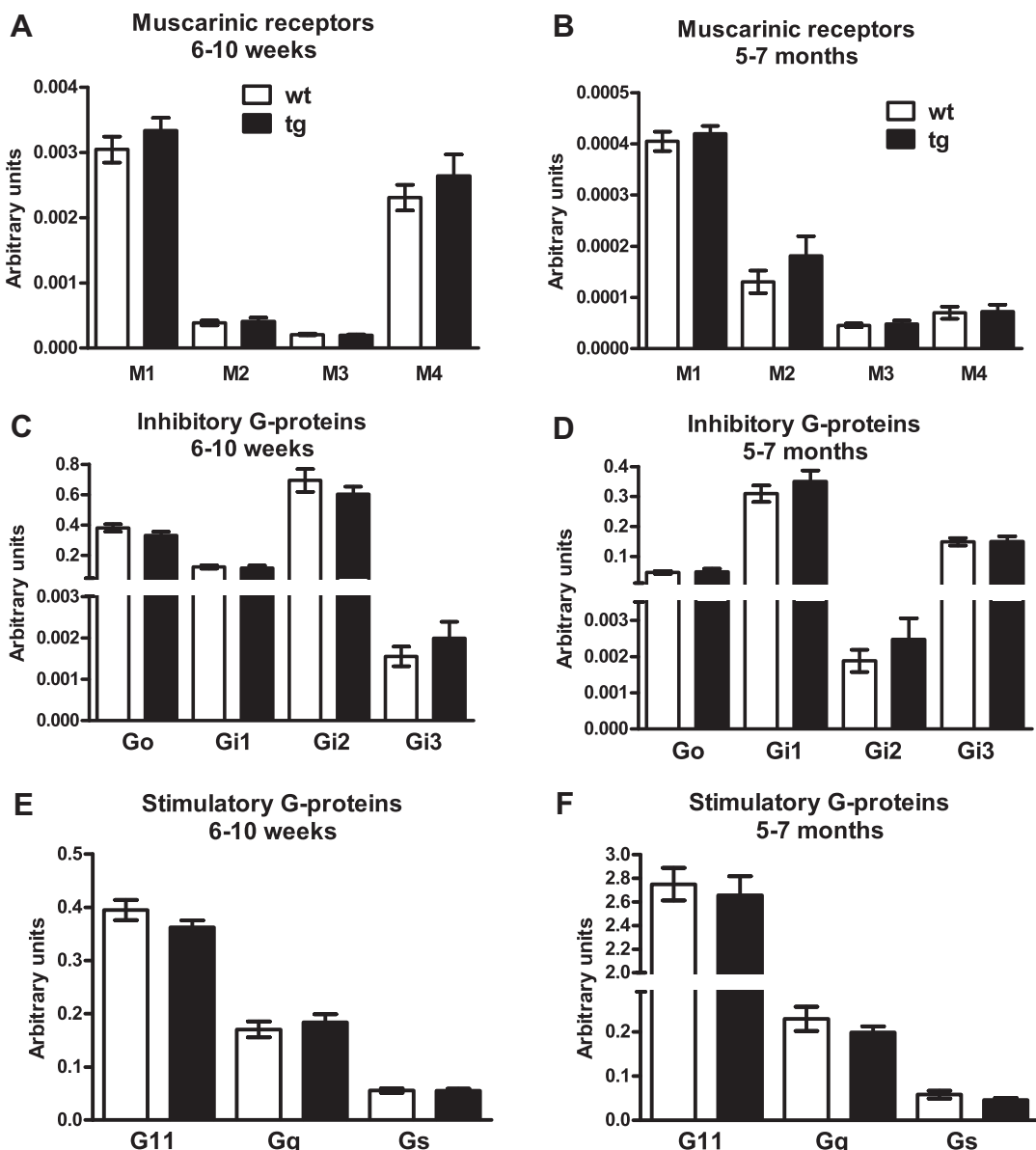


Fig. 8. Gene expression of muscarinic receptors subtypes and G-protein α -subunits in temporal cortex of control and APPswe/PS1dE9 transgenic mice. The concentration of mRNA in transgenic mice (black columns) and control littermate mice (open columns) was determined in young (6–10-week-old; A, C, E) and young adult (5–6-month-old; B, D, F) animals as described in Methods. The expression of any of the tested genes (ordinate, arbitrary units corrected for expression of house-keeping gene GAPDH) differs between age-matched control and transgenic animals. Abbreviations: wt, wild-type; tg, transgenic; A–B: M1 through M4, subtypes of muscarinic receptors; C–D: Go, Gi1, Gi2, Gi3, α -subunits of inhibitory G_{i/o} G-proteins; E–F: G₁₁, G_q, G_s, α -subunits of stimulatory G_{q/11}- and G_s G-proteins. Results are mean \pm SEM of values obtained from 5 (muscarinic receptors and G-proteins in young animals and muscarinic receptors in young adult animals) or 7 (G-proteins in young adult animals) animals.

induced activation of phosphatidylinositol signaling. This effect, in line with the notion of the early involvement in pathogenesis of AD, is apparently mediated by low molecular mass A β_{1-42} species. In concert with *in vivo* results, the treatment does not induce either changes in the expression of major G-proteins, and does not induce oxidative stress or cytotoxicity. These results implicate that the noxious effects of A β_{1-42} on M1 receptor-mediated transmission involve a mechanism that develops within the plasma membrane and impacts receptor/G-protein/phospholipase C interaction. However, detection of specific responsible molecular mechanisms will need further investigation. The attenuation of muscarinic receptor signaling previously reported in a rather early stage of amyloid overproduction in a transgenic mouse model of AD (Machova et al., 2008, 2010) and the demonstration of M1 receptor-mediated signaling attenuation induced by generally non-toxic

concentrations of A β_{1-42} *in vitro* evidence the important role of the M1 muscarinic transmission in early pathogenesis of AD.

Acknowledgments

We are grateful to Dr. O. Benada for electron microscopy images and Dr. L. Bacakova for help with light microscopy. This research was supported by projects EU FP7 project LipiDiDiet (Grant Agreement No 211696), AV0Z50110509, RVO: 67985823, and grants GACR 305/09/0681 and P304/12/G069.

Appendix A. Supplementary material

Supplementary material related to this article can be found at <http://dx.doi.org/10.1016/j.neuropharm.2012.11.014>.

References

- AbdAlla, S., Loether, H., el Missiry, A., Langer, A., Sergeev, P., el Faramawy, Y., Quitterer, U., 2009a. Angiotensin II AT2 receptor oligomers mediate G-protein dysfunction in an animal model of Alzheimer disease. *J. Biol. Chem.* 284, 6554–6565.
- AbdAlla, S., Loether, H., el Missiry, A., Sergeev, P., Langer, A., el Faramawy, Y., Quitterer, U., 2009b. Dominant negative AT2 receptor oligomers induce G-protein arrest and symptoms of neurodegeneration. *J. Biol. Chem.* 284, 6566–6574.
- Abdulaev, N.G., Ngo, T., Ramon, E., Brabazon, D.M., Marino, J.P., Ridge, K.D., 2006. The receptor-bound “empty pocket” state of the heterotrimeric G-protein alpha-subunit is conformationally dynamic. *Biochemistry* 45, 12986–12997.
- Bartus, R.T., 2000. On neurodegenerative diseases, models, and treatment strategies: lessons learned and lessons forgotten a generation following the cholinergic hypothesis. *Exp. Neurol.* 163, 495–529.
- Bartus, R.T., Dean, R.L., Beer, B., Lippa, A.S., 1982. The cholinergic hypothesis of geriatric memory dysfunction. *Science* 217, 408–414.
- Beneda, O., Pokorný, V., 1990. Modification of the Polaron sputter-coater unit for glow-discharge activation of carbon support films. *J. Electron Microsc. Tech.* 16, 235–239.
- Betts, V., Leissing, M.A., Dolios, G., Wang, R., Selkoe, D.J., Walsh, D.M., 2008. Aggregation and catabolism of disease-associated intra-Abeta mutations: reduced proteolysis of AbetaA21G by neprilysin. *Neurobiol. Dis.* 31, 442–450.
- Bonner, T.I., 1989. The molecular basis of muscarinic receptor diversity. *Trends Neurosci.* 12, 148–151.
- Bothmer, J., Jolles, J., 1994. Phosphoinositide metabolism, aging and Alzheimer's disease. *Biochim. Biophys. Acta* 1225, 111–124.
- Buckley, N.J., Bonner, T.I., Buckley, C.M., Brann, M.R., 1989. Antagonist binding properties of five cloned muscarinic receptors expressed in CHO-K1 cells. *Mol. Pharmacol.* 35, 469–476.
- Buxbaum, J.D., Oishi, M., Chen, H.J., Pinkas-Kramarski, R., Jaffe, E.A., Gandy, S.E., Greengard, P., 1992. Cholinergic agonists and interleukin 1 regulate processing and secretion of the Alzheimer beta/A4 amyloid protein precursor. *Proc. Natl. Acad. Sci. U.S.A.* 89, 10075–10078.
- Caccamo, A., Oddo, S., Billings, L.M., Green, K.N., Martinez-Coria, H., Fisher, A., LaFerla, F.M., 2006. M1 receptors play a central role in modulating AD-like pathology in transgenic mice. *Neuron* 49, 671–682.
- Cowburn, R.F., Wiegager, B., Sundstrom, E., 1995. beta-Amyloid peptides enhance binding of the calcium mobilising second messengers, inositol(1,4,5)trisphosphate and inositol-(1,3,4,5)tetrakisphosphate to their receptor sites in rat cortical membranes. *Neurosci. Lett.* 191, 31–34.
- Cramer, P.E., Cirrito, J.R., Wesson, D.W., Lee, C.Y., Karlo, J.C., Zinn, A.E., Casali, B.T., Restivo, J.L., Goebel, W.D., James, M.J., Brunden, K.R., Wilson, D.A., Landreth, G.E., 2012. ApoE-directed therapeutics rapidly clear beta-amyloid and reverse deficits in AD mouse models. *Science* 335, 1503–1506.
- Davis, A.A., Fritz, J.J., Wess, J., Lah, J.J., Levey, A.I., 2010. Deletion of M1 muscarinic acetylcholine receptors increases amyloid pathology in vitro and in vivo. *J. Neurosci.* 30, 4190–4196.
- Davis, K.L., Mohs, R.C., Marin, D., Purohit, D.P., Perl, D.P., Lantz, M., Austin, G., Haroutunian, V., 1999. Cholinergic markers in elderly patients with early signs of Alzheimer disease. *JAMA* 281, 1401–1406.
- DeKosky, S.T., Ikonomovic, M.D., Styren, S.D., Beckett, L., Wisniewski, S., Bennett, D.A., Cochran, E.J., Kordower, J.H., Mufson, E.J., 2002. Upregulation of choline acetyltransferase activity in hippocampus and frontal cortex of elderly subjects with mild cognitive impairment. *Ann. Neurol.* 51, 145–155.
- Feng, Y.H., Zhou, L., Sun, Y., Douglas, J.G., 2005. Functional diversity of AT2 receptor orthologues in closely related species. *Kidney Int.* 67, 1731–1738.
- Fowler, C.J., Garlind, A., O'Neill, C., Cowburn, R.F., 1996. Receptor-effector coupling dysfunctions in Alzheimer's disease. *Ann. N.Y. Acad. Sci.* 786, 294–304.
- Globe, C.G., 2006. Common mechanisms of amyloid oligomer pathogenesis in degenerative disease. *Neurobiol. Aging* 27, 570–575.
- Greenwood, A.F., Powers, R.E., Jope, R.S., 1995. Phosphoinositide hydrolysis, G alpha q, phospholipase C, and protein kinase C in post mortem human brain: effects of post mortem interval, subject age, and Alzheimer's disease. *Neuroscience* 69, 125–138.
- Hardy, J.A., Higgins, G.A., 1992. Alzheimer's disease: the amyloid cascade hypothesis. *Science* 256, 184–185.
- Hashimoto, E., Ozawa, H., Saito, T., Gsell, W., Takahata, N., Riederer, P., Frolich, L., 2004. Impairment of G(salpha) function in human brain cortex of Alzheimer's disease: comparison with normal aging. *J. Neural Transm.* 111, 311–322.
- Huang, H.M., Ou, H.C., Hsueh, S.J., 1998. Amyloid beta peptide enhanced bradykinin-mediated inositol (1,4,5)trisphosphate formation and cytosolic free calcium. *Life Sci.* 63, 195–203.
- Huang, H.M., Ou, H.C., Hsieh, S.J., 2000. Amyloid beta peptide impaired carbachol but not glutamate-mediated phosphoinositide pathways in cultured rat cortical neurons. *Neurochem. Res.* 25, 303–312.
- Jakubik, J., El-Fakahany, E.E., Dolezal, V., 2006. Differences in kinetics of xanomeline binding and selectivity of activation of G proteins at M(1) and M(2) muscarinic acetylcholine receptors. *Mol. Pharmacol.* 70, 656–666.
- Jakubik, J., Janíková, H., El-Fakahany, E.E., Dolezal, V., 2011. Negative cooperativity in binding of muscarinic receptor agonists and GDP as a measure of agonist efficacy. *Br. J. Pharmacol.* 162, 1029–1044.
- Jankowsky, J.L., Fadale, D.J., Anderson, J., Xu, G.M., Gonzales, V., Jenkins, N.A., Copeland, N.G., Lee, M.K., Younkin, L.H., Wagner, S.L., Younkin, S.G., Borchelt, D.R., 2004. Mutant presenilins specifically elevate the levels of the 42-residue beta-amyloid peptide in vivo: evidence for augmentation of a 42-specific gamma secretase. *Hum. Mol. Genet.* 13, 159–170.
- Jones, S.V., Barker, J.L., Buckley, N.J., Bonner, T.I., Collins, R.M., Brann, M.R., 1988. Cloned muscarinic receptor subtypes expressed in A9 L cells differ in their coupling to electrical responses. *Mol. Pharmacol.* 34, 421–426.
- Jones, S.V., 1993. Muscarinic receptor subtypes: modulation of ion channels. *Life Sci.* 52, 457–464.
- Jope, R.S., Song, L., Li, X., Powers, R., 1994. Impaired phosphoinositide hydrolysis in Alzheimer's disease brain. *Neurobiol. Aging* 15, 221–226.
- Jope, R.S., Song, L., Powers, R.E., 1997. Cholinergic activation of phosphoinositide signaling is impaired in Alzheimer's disease brain. *Neurobiol. Aging* 18, 111–120.
- Kimura, H., Schubert, D., 1993. Amyloid beta-protein activates tachykinin receptors and inositol trisphosphate accumulation by synergy with glutamate. *Proc. Natl. Acad. Sci. U.S.A.* 90, 7508–7512.
- Kurumatani, T., Fastbom, J., Bonkale, W.L., Bogdanovic, N., Winblad, B., Ohm, T.G., Cowburn, R.F., 1998. Loss of inositol 1,4,5-trisphosphate receptor sites and decreased PKC levels correlate with staging of Alzheimer's disease neurofibrillary pathology. *Brain Res.* 796, 209–221.
- Liu, Y., Yoo, M.J., Savonenko, A., Stirling, W., Price, D.L., Borchelt, D.R., Mamounas, L., Lyons, W.E., Blue, M.E., Lee, M.K., 2008. Amyloid pathology is associated with progressive monoaminergic neurodegeneration in a transgenic mouse model of Alzheimer's disease. *J. Neurosci.* 28, 13805–13814.
- Lowry, O.H., Rosebrough, N.J., Farr, A.L., Randall, R.J., 1951. Protein measurement with the Folin phenol reagent. *J. Biol. Chem.* 193, 265–275.
- Machova, E., Jakubik, J., Michal, P., Oksman, M., Iivonen, H., Tanila, H., Dolezal, V., 2008. Impairment of muscarinic transmission in transgenic APPswe/PS1dE9 mice. *Neurobiol. Aging* 29, 368–378.
- Machova, E., O'Regan, S., Newcombe, J., Meunier, F.M., Prentice, J., Dove, R., Lisa, V., Dolezal, V., 2009. Detection of choline transporter-like 1 protein CTL1 in neuroblastoma x glioma cells and in the CNS, and its role in choline uptake. *J. Neurochem.* 110, 1297–1309.
- Machova, E., Rudajev, V., Smyckova, H., Koivisto, H., Tanila, H., Dolezal, V., 2010. Functional cholinergic damage develops with amyloid accumulation in young adult APPswe/PS1dE9 transgenic mice. *Neurobiol. Dis.* 38, 27–35.
- Masters, C.L., Multhaup, G., Simms, G., Pottgiesser, J., Martins, R.N., Beyreuther, K., 1985a. Neuronal origin of a cerebral amyloid: neurofibrillary tangles of Alzheimer's disease contain the same protein as the amyloid of plaque cores and blood vessels. *EMBO J.* 4, 2757–2763.
- Masters, C.L., Simms, G., Weinman, N.A., Multhaup, G., McDonald, B.L., Beyreuther, K., 1985b. Amyloid plaque core protein in Alzheimer disease and Down syndrome. *Proc. Natl. Acad. Sci. U.S.A.* 82, 4245–4249.
- McLaughlin, M., Ross, B.M., Milligan, G., McCulloch, J., Knowler, J.T., 1991. Robustness of G proteins in Alzheimer's disease: an immunoblot study. *J. Neurochem.* 57, 9–14.
- McLean, C.A., Cherny, R.A., Fraser, F.W., Fuller, S.J., Smith, M.J., Beyreuther, K., Bush, A.I., Masters, C.L., 1999. Soluble pool of Abeta amyloid as a determinant of severity of neurodegeneration in Alzheimer's disease. *Ann. Neurol.* 46, 860–866.
- Medeiros, R., Kitazawa, M., Caccamo, A., Baglietto-Vargas, D., Estrada-Hernandez, T., Cribbs, D.H., Fisher, A., LaFerla, F.M., 2011. Loss of muscarinic M1 receptor exacerbates Alzheimer's disease-like pathology and cognitive decline. *Am. J. Pathol.* 179, 980–991.
- Michal, P., El-Fakahany, E.E., Dolezal, V., 2007. Muscarinic M2 receptors directly activate Gq/11 and Gs G-proteins. *J. Pharmacol. Exp. Ther.* 320, 607–614.
- Michal, P., Rudajev, V., El-Fakahany, E.E., Dolezal, V., 2009. Membrane cholesterol content influences binding properties of muscarinic M2 receptors and differentially impacts activation of second messenger pathways. *Eur. J. Pharmacol.* 606, 50–60.
- Muma, N.A., Mariyappa, R., Williams, K., Lee, J.M., 2003. Differences in regional and subcellular localization of G(q/11) and RGS4 protein levels in Alzheimer's disease: correlation with muscarinic M1 receptor binding parameters. *Synapse* 47, 58–65.
- Nagy, Z., Esiri, M.M., Jobst, K.A., Morris, J.H., King, E.M., McDonald, B., Litchfield, S., Smith, A., Barnetson, L., Smith, A.D., 1995. Relative roles of plaques and tangles in the dementia of Alzheimer's disease: correlations using three sets of neuropathological criteria. *Dementia* 6, 21–31.
- Naslund, J., Haroutunian, V., Mohs, R., Davis, K.L., Davies, P., Greengard, P., Buxbaum, J.D., 2000. Correlation between elevated levels of amyloid beta-peptide in the brain and cognitive decline. *JAMA* 283, 1571–1577.
- Nitsch, R.M., Slack, B.E., Wurtman, R.J., Growdon, J.H., 1992. Release of Alzheimer amyloid precursor derivatives stimulated by activation of muscarinic acetylcholine receptors. *Science* 258, 304–307.
- Nitsch, R.M., Deng, M., Tennis, M., Schoenfeld, D., Growdon, J.H., 2000. The selective muscarinic M1 agonist AF102B decreases levels of total Abeta in cerebrospinal fluid of patients with Alzheimer's disease. *Ann. Neurol.* 48, 913–918.
- Novakova, J., Mikasova, L., Machova, E., Lisa, V., Dolezal, V., 2005. Chronic treatment with amyloid beta(1–42) inhibits non-cholinergic high-affinity choline transport in NC108–15 cells through protein kinase C signaling. *Brain Res.* 1062, 101–110.
- Perry, E.K., Kilford, L., Lees, A.J., Burn, D.J., Perry, R.H., 2003. Increased Alzheimer pathology in Parkinson's disease related to antimuscarinic drugs. *Ann. Neurol.* 54, 235–238.
- Peterson, G.L., 1977. A simplification of the protein assay method of Lowry et al. which is more generally applicable. *Anal. Biochem.* 83, 346–356.

- Ronnback, A., Fowler, C.J., 2000. beta-Amyloid(25–35) inhibits the activity of inositol(1,4,5)-trisphosphate-5-phosphatase. *Amyloid* 7, 90–94.
- Rossner, S., Ueberham, U., Yu, J., Kirazov, L., Schliebs, R., Perez-Polo, J.R., Bigl, V., 1997. In vivo regulation of amyloid precursor protein secretion in rat neocortex by cholinergic activity. *Eur. J. Neurosci.* 9, 2125–2134.
- Roth, G.S., Joseph, J.A., Mason, R.P., 1995. Membrane alterations as causes of impaired signal transduction in Alzheimer's disease and aging. *Trends Neurosci.* 18, 203–206.
- Rudajev, V., Novotny, J., Hejnova, L., Milligan, G., Svoboda, P., 2005. Dominant portion of thyrotropin-releasing hormone receptor is excluded from lipid domains. Detergent-resistant and detergent-sensitive pools of TRH receptor and G_qalpha/G11alpha protein. *J. Biochem.* 138, 111–125.
- Savonenko, A., Xu, G.M., Melnikova, T., Morton, J.L., Gonzales, V., Wong, M.P., Price, D.L., Tang, F., Markowska, A.L., Borchelt, D.R., 2005. Episodic-like memory deficits in the APPswe/PS1dE9 mouse model of Alzheimer's disease: relationships to beta-amyloid deposition and neurotransmitter abnormalities. *Neurobiol. Dis.* 18, 602–617.
- Selkoe, D.J., 2001. Alzheimer's disease: genes, proteins, and therapy. *Physiol. Rev.* 81, 741–766.
- Selkoe, D.J., 2002. Alzheimer's disease is a synaptic failure. *Science* 298, 789–791.
- Shiozaki, K., Iseki, E., 2004. Decrease in GTP-sensitive high affinity agonist binding of muscarinic acetylcholine receptors in autopsied brains of dementia with Lewy bodies and Alzheimer's disease. *J. Neurol. Sci.* 223, 145–148.
- Stine Jr., W.B., Dahlgren, K.N., Krafft, G.A., LaDu, M.J., 2003. In vitro characterization of conditions for amyloid-beta peptide oligomerization and fibrillogenesis. *J. Biol. Chem.* 278, 11612–11622.
- Thathiah, A., De Strooper, B., 2011. The role of G protein-coupled receptors in the pathology of Alzheimer's disease. *Nat. Rev. Neurosci.* 12, 73–87.
- Tsang, S.W., Lai, M.K., Kirvell, S., Francis, P.T., Esiri, M.M., Hope, T., Chen, C.P., Wong, P.T., 2005. Impaired coupling of muscarinic M(1) receptors to G-proteins in the neocortex is associated with severity of dementia in Alzheimer's disease. *Neurobiol. Aging* 27, 1216–1223.
- Tucek, S., Michal, P., Vlachova, V., 2002. Modelling the consequences of receptor-G protein promiscuity. *Trends Pharmacol. Sci.* 23, 171–176.
- Wang, H.Y., Friedman, E., 1994. Receptor-mediated activation of G proteins is reduced in postmortem brains from Alzheimer's disease patients. *Neurosci. Lett.* 173, 37–39.
- Yankner, B.A., 1996. Mechanisms of neuronal degeneration in Alzheimer's disease. *Neuron* 16, 921–932.
- Yankner, B.A., Lu, T., 2009. Amyloid beta-protein toxicity and the pathogenesis of Alzheimer disease. *J. Biol. Chem.* 284, 4755–4759.

ORIGINAL
ARTICLE

A specific multi-nutrient formulation enhances M1 muscarinic acetylcholine receptor responses *in vitro*

Paul J. M. Savelkoul,* Helena Janickova,† Almar A. M. Kuipers,* Robert J. J. Hageman,* Patrick J. Kamphuis,*‡ Vladimir Dolezal† and Laus M. Broersen*

*Nutricia Advanced Medical Nutrition, Danone Research, Centre for Specialised Nutrition, Wageningen, The Netherlands

†Institute of Physiology, Academy of Sciences of the Czech Republic, Prague, Czech Republic

‡Utrecht Institute for Pharmaceutical Sciences (UIPS), University Utrecht, The Netherlands

Abstract

Recent evidence indicates that supplementation with a specific combination of nutrients may affect cell membrane synthesis and composition. To investigate whether such nutrients may also modify the physical properties of membranes, and affect membrane-bound processes involved in signal transduction pathways, we studied the effects of nutrient supplementation on G protein-coupled receptor activation *in vitro*. In particular, we investigated muscarinic receptors, which are important for the progression of memory deterioration and pathology of Alzheimer's disease. Nerve growth factor differentiated pheochromocytoma cells that were supplemented with specific combinations of nutrients showed enhanced responses to muscarinic receptor agonists in a membrane potential assay. The largest effects were obtained with a combination of nutrients known as Fortasyn™ Connect, comprising docosahexaenoic acid, eicosapentaenoic acid, uridine monophosphate as a uridine source, choline, vitamin B6, vitamin B12, folic acid, phospholipids, vitamin C, vitamin E, and selenium. In subsequent experiments, it was shown that the effects of supplementation could not be attributed to single

nutrients. In addition, it was shown that the agonist-induced response and the supplement-induced enhancement of the response were blocked with the muscarinic receptor antagonists atropine, telenzepine, and AF-DX 384. In order to determine whether the effects of Fortasyn™ Connect supplementation were receptor subtype specific, we investigated binding properties and activation of human muscarinic M1, M2 and M4 receptors in stably transfected Chinese hamster ovary cells after supplementation. Multi-nutrient supplementation did not change M1 receptor density in plasma membranes. However, M1 receptor-mediated G protein activation was significantly enhanced. In contrast, supplementation of M2- or M4-expressing cells did not affect receptor signaling. Taken together, these results indicate that a specific combination of nutrients acts synergistically in enhancing muscarinic M1 receptor responses, probably by facilitating receptor-mediated G protein activation.

Keywords: Alzheimer's disease, docosahexaenoic acid, G protein-coupled receptors, muscarinic receptor, PC12, uridine.

J. Neurochem. (2012) **120**, 631–640.

Cell membranes consist of a double layer of lipids, mostly phospholipids, in which membrane proteins are embedded (van Meer *et al.* 2008). In the brain, the major phospholipid in membranes is phosphatidylcholine (PC), which can be synthesized by the CDP-choline or Kennedy cycle from its precursors, polyunsaturated fatty acids (PUFAs, e.g. docosahexaenoic acid, DHA), uridine and choline (Kennedy and Weiss 1956; Wurtman *et al.* 2009). It has been demonstrated that oral supplementation of these nutrients increases brain phospholipid levels (Cansev and Wurtman 2007), and

Received October 5, 2011; revised manuscript received November 24, 2011; accepted December 5, 2011.

Address correspondence and reprint requests to Paul J. M. Savelkoul, Danone Research, Centre for Specialised Nutrition, PO Box 7005, 6700 CA Wageningen, The Netherlands. E-mail: paul.savelkoul@danone.com

Abbreviations used: AD, Alzheimer's disease; CHO, Chinese Hamster Ovary; DHA, docosahexaenoic acid; DUC, DHA, uridine and choline; EPA, eicosapentaenoic acid; [³H]NMS, [³H]*N*-methyl scopolamine; FC, Fortasyn™ Connect; FLIPR®, fluorometric imaging plate reader; GPCR, G protein-coupled receptor; MPA, membrane potential assay; NGF, nerve growth factor; PC, phosphatidylcholine; PUFA, polyunsaturated fatty acid.

promotes synthesis of new synaptic membranes (Cansev *et al.* 2008). In addition, it has been shown that administration of phosphatide precursors increases neurotransmitter release (Wang *et al.* 2007) and promotes synaptic protein expression in brain (Wurtman *et al.* 2006). Moreover, feeding animals with these dietary membrane precursors improved their cognitive behaviors (Teather and Wurtman 2006; Holguin *et al.* 2008a,b). Together, these data suggest that specific nutrient intake may potentially alter membranes and their properties, which might influence membrane-related processes like, for example, receptor signaling via G protein-coupled receptors (GPCRs). These receptors are encoded by the largest gene family known in the mammalian genome and comprise the main family of receptors for neurotransmitters, hormones, and neuromodulators (Fredriksson and Schioth 2005; Rajagopal *et al.* 2010). When neurotransmitters bind to these receptors, they cause a conformational change that results in activation of heterotrimeric G proteins, which in turn modulate the activity of effector proteins (Wetschureck and Offermanns 2005; Rosenbaum *et al.* 2009). As a consequence, cytosolic levels of second messengers are altered and downstream processes initiated. As GPCRs, as well as their G proteins, are associated with the plasma membrane, lipid–protein interactions are essential to their function, which therefore is sensitive to changes in their lipid environment. Consequently, modification of the membrane structure by dietary intervention may influence GPCR signaling. Indeed, it has been shown that alteration of membrane lipids can influence GPCR-mediated signaling. For example, n-3 fatty acid deficiency leads to reduced rhodopsin G protein-coupled signaling efficiency in retinal rod outer segments (Niu *et al.* 2004), while others have shown that DHA has significant effects on rhodopsin's stability, leading to enhanced kinetics of the photocycle (Grossfield *et al.* 2006). In addition, it has been shown that G protein coupling of the serotonin(1A) receptor is enhanced in membranes from cholesterol-depleted cells (Prasad *et al.* 2009). Upon aging, modifications in membrane composition occur that have been associated with alterations in GPCR signaling (reviewed in Yeo and Park 2002; Alemany *et al.* 2007).

As DHA, uridine and choline can potentially modify membrane properties we addressed their single and combined effects on GPCR signaling. In addition, we compared the effects of these nutrients to a multi-nutrient composition that was designed to enhance synaptic membrane formation, containing nutritional co-factors in addition to DHA, uridine and choline. This composition, called Fortasyn™ Connect (FC), comprises DHA, eicosapentaenoic acid (EPA), uridine monophosphate, choline, vitamin B6, vitamin B12, folic acid, phospholipids, vitamin C, vitamin E, and selenium. As we recently showed that this nutrient composition also modified membrane composition by increasing membrane n-3 PUFA and PC content (de Wilde *et al.* 2011), we also

tested the effects of all individual nutrients in this formulation on GPCR function. To detect changes in GPCR signaling we used neuron-like pheochromocytoma (PC12) cells, as these cells endogenously express various GPCRs, including several of the metabotropic muscarinic acetylcholine receptors (mAChRs). mAChRs have been implicated in higher brain functions such as learning and memory, and lose their sensitivity to acetylcholine both during aging and more markedly in Alzheimer's disease (Joseph *et al.* 1993). Here, we tested the effects of nutrient supplementation on muscarinic receptor agonist-induced changes in membrane potential as measured by a fluorometric imaging plate reader (FLIPR®) membrane potential assay (Whiteaker *et al.* 2001; Baxter *et al.* 2002). In addition, we measured the influence of nutrient administration on G protein activation in human M1/M2/M4 mAChR-transfected Chinese Hamster Ovary cells (CHO-M1/M2/M4) by measuring agonist induced GTP γ^{35} S binding.

Materials and methods

Cell culture

Pheochromocytoma cells (PC12, kindly provided by Prof. R.J. Wurtman) were maintained in Dulbecco's modified Eagle's medium (Fischer Scientific, Landsmeer, The Netherlands), supplemented with 10% fetal bovine serum, penicillin (100 units/mL), and streptomycin (100 μ g/mL; Gibco), under a humidified atmosphere with 95% air and 5% CO₂ at 37°C. Cells were subcultured twice a week and used for analysis up to passage 30.

Chinese Hamster Ovary (CHO) cells were stably transfected with the human genes of the muscarinic M1, M2, or M4 receptor subtypes (CHO-M1, CHO-M2, and CHO-M4, kindly supplied by Prof. T. Bonner). Cells were grown in Dulbecco's modified Eagle's medium with 10% fetal calf serum and 0.005% geneticin under a humidified atmosphere with 95% air and 5% CO₂ at 37°C. Cells were subcultured once a week. They were seeded for experiments on 10 cm diameter Petri dishes (Coming). Supplements were added the day after seeding and cells were left to grow for another 2–4 days before measurements as indicated.

Nutritional supplementation

In the supplementation experiments the following nutritional components were used (final concentration used in FC supplementation of cell cultures): docosahexaenoic acid (DHA, 20 μ M), EPA (20 μ M), uridine (50 μ M), choline chloride (20 μ M), vitamin B6 (pyridoxine, 10 μ M), vitamin B12 (0.2 μ M), vitamin B9 (folic acid, 15 μ M), phospholipids (phosphatidylcholine, 25 μ M), vitamin C (ascorbic acid, 75 μ M), vitamin E (alpha-tocopherol, 20 μ M), and selenium (sodium selenite, 0.4 μ M). EPA and DHA were resuspended in absolute ethanol and diluted 5 times in fetal bovine serum. Solutions were aliquoted and stored at -80°C. All compounds were purchased from Sigma (Zwijndrecht, The Netherlands). Length of supplementation of PC12 cells and the concomitant concentrations of DHA and uridine monophosphate were based on literature reports on phospholipid synthesis *in vitro* (Richardson and Wurtman 2007; Pooler *et al.* 2005). Doses of additional components were based on

pilot studies searching for concentrations that did not affect cell viability.

As a combination of DHA, uridine and choline (DUC) has been shown previously to have an effect on membrane related processes (see Introduction), we chose this combination as a reference. We compared this reference to supplementation with single nutrients, several nutrient combinations or the complete FC composition.

Membrane potential assay

To examine the effect of nutritional compounds on muscarinic receptor activation in PC12 cells, we used the FLIPR® membrane potential explorer kit (Molecular Devices, Berkshire, UK) according to the manufacturer's protocol. The membrane potential assay (MPA) is based on the uptake of fluorescent dye that depends on membrane potential. Membrane depolarization increases the uptake and thus the fluorescence of cells (Whiteaker *et al.* 2001; Baxter *et al.* 2002). In brief, PC12 cells (7×10^3 cells per well) were seeded on type IV human collagen (Sigma, Zwijndrecht, the Netherlands) coated black colored 96-well plates with a clear bottom (Corning Costar, Amsterdam, the Netherlands). After 24 h culture medium containing 50 ng/mL nerve growth factor (NGF; Promega Benelux BV, Leiden, the Netherlands) without or with indicated supplements was added. Cells were grown for another 72 h and subsequently used for assay. Culture medium was then removed and 75 μ L of the FLIPR® dye solution was added per well. Next, the cells were incubated for 30 min at 20°C and then measured in a FlexStation II³⁸⁴ (Molecular Devices) at 20°C. The baseline signal was read for 16 s at an excitation wavelength of 530 nm and an emission wavelength of 565 nm. At 17 s, cells were stimulated by the muscarinic receptor agonists carbachol (Sigma) or oxotremorine-M (Tocris Bioscience, Bristol, UK), with or without the non-selective muscarinic receptor antagonists atropine (Sigma), M1-selective antagonist telenzepine (Tocris Bioscience), or M2-selective antagonist AF-DX 384 (Tocris Bioscience). Changes in fluorescence were measured for 3 min and data were analyzed using SoftMax Pro 4.8. Data were calculated as percentage of baseline to correct for differences in cell density, and subsequently presented as receptor activation as percentage of control (PC12 cells grown without supplementation of nutritional compounds). Experiments were performed at least three times in sextuplicate.

Binding studies

Membranes from CHO cells were prepared essentially as described in Jakubik *et al.* (2006). Briefly, control and supplemented cells grown on Petri dishes were twice washed with phosphate-buffered saline, mechanically detached in phosphate-buffered saline, pelleted by 3 min centrifugation at 250 g, and supernatants were discarded. Washed cells were diluted in ice-cold homogenization medium (100 mM NaCl, 20 mM Na-HEPES, and 10 mM EDTA, pH 7.4) and homogenized on ice by two 30-s strokes using a homogenizer (Ultra-Turrax; Janke and Kunkel GmbH and Co. KG, IKA-Labortechnik, Staufen, Germany) with a 30-s pause between strokes. Cell homogenates were centrifuged for 30 min at 30 000 g. The supernatants were discarded; the pellets were resuspended in incubation medium (100 mM NaCl, 10 mM MgCl₂, and 20 mM HEPES, pH 7.4), centrifuged for 30 min at 30 000 g, and supernatants were again discarded. Pellets were either used for experiments immediately or kept at -20°C until assayed, for

10 weeks at maximum. Chemicals were purchased from Sigma (Prague, Czech Republic) unless indicated otherwise.

Saturation analysis of membrane receptor density

Densities and affinities of muscarinic receptors incorporated in CHO cell membranes were determined in saturation binding experiments with the muscarinic antagonist [³H]N-methyl scopolamine ([³H]NMS) (GE Healthcare, Little Chalfont, Buckinghamshire, UK) as described previously (Michal *et al.* 2009). Non-specific binding was determined in the presence of 10 μ M atropine. Fast filtration to separate bound and free ligand was carried out using Unifilter plates (Whatman, Clifton, NJ, USA) and a Brandel Harvester (Brandel, Gaithersburg, MD, USA). Plates were dried in vacuum and radioactivity retained on filters was determined in Rotiszint (Carl Roth, Karlsruhe, Germany) using a Microbeta scintillation counter (PerkinElmer Wallac, Turku, Finland).

Determination of GTP γ ³⁵S binding

Experiments were carried out in 96-well plates at 30°C in the incubation medium described above supplemented with freshly prepared dithiothreitol at a final concentration of 1 mM as described (Jakubik *et al.* 2006, 2009). Briefly, aliquots of 5–20 μ g of membrane protein were pre-incubated for 5 min in incubation medium containing 5 μ M GDP for M1 or 50 μ M GDP for M2 and M4 receptor-expressing membranes, and indicated concentrations of carbachol in a final incubation volume of 200 μ L. Incubation was initiated by adding 500 pM [³⁵S]GTP γ S. Non-specific binding was determined in the presence of 1 μ M GTP γ S. Incubation lasted 20 min, and free ligand was removed by fast filtration through GF/F glass fiber filters (Whatman) using a Mach III cell harvester (Tomtec, Hamden, CT, USA). Filters were dried in a vacuum and then solid scintillator Meltilex A was melted on filters (105°C; 90 s) using a hot plate. After cooling, radioactivity on the filters was determined using a Microbeta scintillation counter.

Statistical analysis

All data obtained in the FLIPR assay were analysed with SPSS, using ANOVA and *post hoc* analyses when appropriate. Curve fitting of the binding studies was done using Prism5 (GraphPad Software Inc., San Diego, CA, USA). Effects of supplementation on binding parameters were analyzed using paired *t*-tests. For all analyses, the significance level was set at $p < 0.05$.

Results

After 3 days of NGF (50 ng/mL) treatment, either with or without nutrient supplementation, PC12 cells were stimulated with increasing amounts of the muscarinic receptor agonist carbachol (Fig. 1a). Carbachol induced a concentration-dependent increase of signal in the MPA (used as a measure for receptor activation) with concentrations ranging from 0.01 mM up to 10 mM, as evidenced by a main effect of concentration [carbachol: $F(3,18) = 375.16$, $p < 0.001$]. *Post hoc* tests indicated that a maximum response was achieved at a concentration of 1 mM. Supplementation of the cells with nutrients resulted in an increased response to carbachol [$F(2,6) = 228.53$, $p < 0.001$]. *Post hoc*

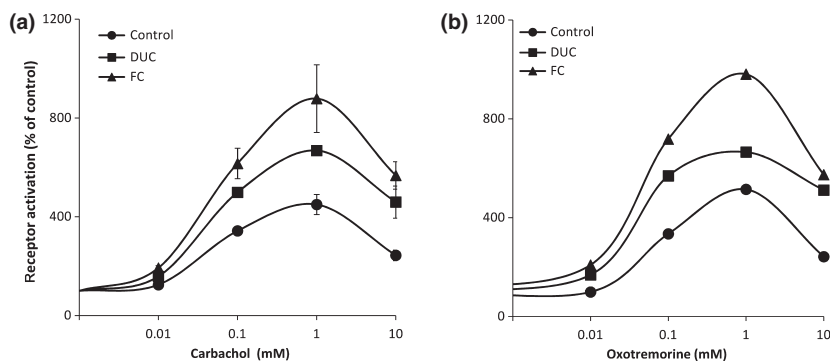


Fig. 1 Concentration-response curve of muscarinic receptor agonist induced changes in membrane potential in PC12 cells expressed as the percentage of baseline of control without agonist. (a) Concentration–response curve of carbachol and (b) concentration–response curve of oxotremorine. During 3 days prior to measurement, cells received NGF (50 ng/mL) with either no supplementation (Control) or

nutrient supplementation with DUC (DHA, uridine and choline) or FC (DHA, EPA, uridine, choline, vitamin B6, vitamin B12, folic acid, phosphatidylcholine, vitamin C, vitamin E, and selenium). Results for carbachol are shown as the means \pm SD of three independent experiments run in sextuplicates. Results for oxotremorine are displayed as single data points, $n = 1$.

comparisons indicated that responses with DUC (DHA, uridine and choline) were larger than Control, and those with FC were again larger than with DUC supplementation (all $p < 0.01$). In addition, significant Concentration \times Supplementation interactions were obtained [$F(6,18) = 3.19$, $p < 0.05$]. *Post hoc* tests indicated that FC supplementation resulted in a larger increase in membrane depolarization than DUC supplementation at the 0.1 mM and 1 mM concentrations of the agonists, but not at the 10 mM concentrations. Based on these results, 1 mM carbachol was selected for subsequent experiments. In addition to the concentration–effect experiments summarized in Fig. 1a, we performed a single concentration–effect experiment with the muscarinic agonist oxotremorine. As can be seen in Fig. 1b, similar results were observed for this compound, indicating that the effects were not agonist-specific.

Next, we performed a concentration–response experiment for FC supplementation, in which PC12 cells were incubated with increasing concentrations of the FC composition, and recorded the carbachol-induced changes in membrane potential. As shown in Fig. 2, FC supplementation induced a concentration-dependent enhancement of the carbachol-induced response [$F(4,10) = 9.28$, $p < 0.005$]. The maximal response was observed at the arbitrarily chosen 100% concentration, which was used in subsequent experiments.

To confirm that the observed changes in membrane potential were indeed mediated by muscarinic receptors, we examined the effect of co-administration of the non-selective muscarinic receptor antagonist atropine. As shown in Fig. 3, atropine induced a concentration-dependent reduction of carbachol-induced depolarization [$F(4,16) = 138.41$; $p < 0.001$]. Every concentration of atropine reduced the carbachol-induced response more strongly than the preceding concentration (all $p < 0.001$). Antagonism by atropine was equally effective in PC12 cells with and without FC

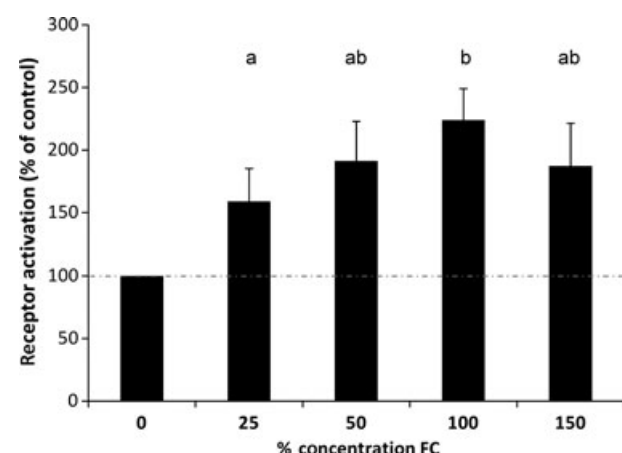


Fig. 2 Concentration-dependent increase of carbachol (1 mM)-induced changes in membrane potential compared with control after supplementation of PC12 cells grown with NGF (50 ng/mL) and increasing concentrations of FC (in % compared with concentration used in Fig. 1) for 3 days. Values represent means \pm SD, $n = 3$. Bars that do not share the same letters significantly differ, $p < 0.05$.

supplementation, as evidenced by the absence of both a main effect of nutrient supplementation ($p = 0.525$) and an atropine \times supplementation interaction ($p = 0.833$).

To determine which nutrients in the FC formulation were responsible for the enhancement of muscarinic receptor activation, we supplemented NGF-differentiated PC12 cells for 3 days with single nutrients from the formulation and recorded their responses to stimulation with carbachol in the MPA. Figure 4a shows the carbachol-induced changes in membrane potential after supplementation with the different single nutrients as compared with both the control without supplementation and the full combination of FC nutrients. As some of the nutrients were dissolved in ethanol, which is

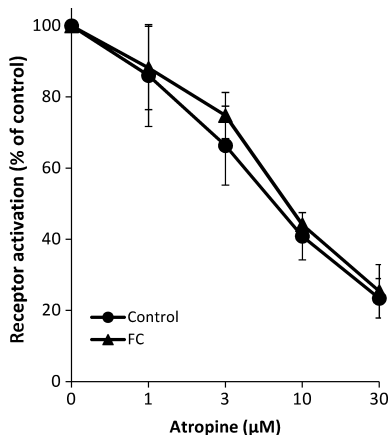


Fig. 3 Concentration-dependent inhibition of carbachol (1 mM)-induced changes in membrane potential by the non-selective muscarinic receptor antagonist atropine. PC12 cells were supplemented with NGF (50 ng/mL), with or without multi-nutrient supplementation (FC) for 3 days. Values represent means \pm SD, $n = 3$.

known to evoke potassium currents, we also tested a combination of all solvents. A main effect of supplementation [$F(13,43) = 16.60$; $p < 0.001$] together with subsequent analyses indicated that single nutrients had little or no effect, except for the PUFAs EPA and DHA, which both induced an increased response that was smaller than the effect of the FC combination (all $p < 0.005$). Supplementation of the solvents alone did not induce any changes.

Subsequently, we pooled single nutrients into several nutrient groups to explore their combined effects (Fig. 4b). Again, a main effect of supplementation was found [$F(4,14) = 27.414$; $p < 0.001$]. Post hoc comparisons indicated that combined PUFAs (DHA and EPA) increased the response to carbachol to a lesser extent than the FC formulation (all $p < 0.001$), while combined B-vitamins (B6, B12, folic acid) and combined antioxidants (vitamins C and E, and selenium) did not have an effect on response to carbachol.

Next, we combined different nutrient groups to examine their potential additive or synergistic effects. As shown in Fig. 4c, different supplementations resulted in an increased response to carbachol [$F(4,14) = 17.30$; $p < 0.001$]. Combining DHA, uridine and choline resulted in an increase compared with control ($p < 0.05$) and the subsequent additions of B-vitamins, antioxidants, and PUFAs further increased the response to carbachol stimulation ($p < 0.05$). Final addition of phospholipids to complete the FC formula yielded the maximum receptor response observed.

To determine which muscarinic receptors are implicated in the response to carbachol and nutritional supplementation in PC12 cells, we used different receptor-selective antagonists. Concentration-dependent decreases in responses were observed with increasing concentrations (1–30 μM) of the M1 antagonist telenzepine (Eltze *et al.* 1985), which resulted in a

near complete block of the carbachol-induced signal with and without prior FC supplementation [$F(4,16) = 190.08$; $p < 0.001$; see Fig. 5a]. Antagonism by telenzepine was equally effective in PC12 cells supplemented or not with FC, as indicated by the absence of both a main effect of nutrient supplementation ($p = 0.308$) and a telenzepine \times supplementation interaction ($p = 0.469$). However, increasing concentrations (1–30 μM) of the M2/M4 antagonist AF-DX 384 (Alexander *et al.* 2009) also induced a significant decrease in carbachol-induced responses [$F(4,8) = 127.78$, $p < 0.001$; see Fig. 5b]. The antagonistic effect of AF-DX 384 was similar in PC12 cells with and without FC supplementation, as shown by the absence of a main effect of nutrient supplementation ($p = 0.978$) and a AF-DX 384 \times supplementation interaction ($p = 0.077$). Consequently, we were not able to distinguish between the involvement of different endogenous muscarinic receptors in the observed effects, using these antagonists in PC12 cells.

Next, to explore nutrient-mediated effects on muscarinic receptors we used CHO cells stably transfected with the human genes of the muscarinic M1, M2 or M4 receptor subtype (Buckley *et al.* 1989). Treatment of CHO cells expressing the M1 subtype of muscarinic receptors with the FC nutrient formula did not change either M1 receptor density in plasma membranes (B_{max} in treated cells $95 \pm 12\%$ of controls, $p = 0.448$) or affinity of [3 H]NMS binding (K_d 289 ± 95 and 370 ± 92 pM in control and FC-supplemented cells, respectively, $p = 0.258$). However, FC supplementation significantly enhanced receptor activation determined as the increase of GTP- γ^{35} S binding induced by carbachol [Fig. 6, M1; $E_{max} 172 \pm 5.3\%$ of controls, $t(2) = 23.5$, $p < 0.01$] with no change in potency (pEC50 5.60 ± 0.38 and 5.46 ± 0.41 in control and supplemented cells, respectively). The same supplementation of cells expressing M2 receptors did not result in major changes in [3 H]NMS-binding properties [B_{max} in treated cells was $122 \pm 20\%$ of controls; $t(2) = 1.876$; $p = 0.2015$], but the affinity for M2 was decreased K_d [428 ± 36 and 361 ± 44 pM in control and FC-supplemented cells, respectively, $t(4) = 3.366$, $p < 0.05$]. In addition, receptor activation by carbachol was decreased [Fig. 6, M2; $E_{max} 85 \pm 6\%$ of controls, $t(2) = 4.457$, $p < 0.05$, and pEC50 was not significantly different (6.56 ± 0.28 and 6.43 ± 0.12 in control and FC supplemented cells, respectively, $n = 3$)]. Growth of M4 receptor expressing CHO cells in medium supplemented with FC mixture had no effect on carbachol-induced stimulation of GTP- γ^{35} S binding (Fig. 6, M4; $E_{max} 111 \pm 11\%$ of controls in FC-treated cells, and pEC50 5.65 ± 0.09 and 5.73 ± 0.12 in control and FC treated cells, respectively; $n = 7$).

Discussion

The present data indicate that the muscarinic receptor agonists carbachol and oxotremorine both induced concen-

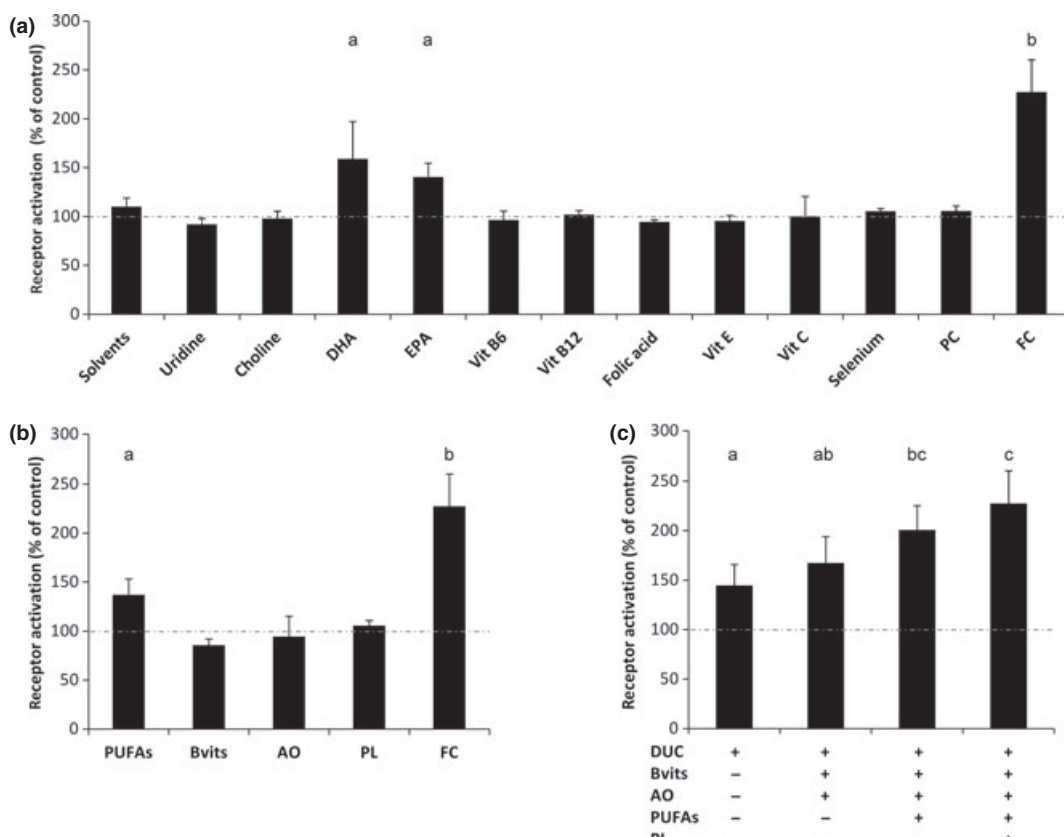


Fig. 4 Changes in carbachol (1 mM)-induced membrane potential compared with control after supplementation of NGF (50 ng/mL)-treated PC12 cells for 3 days with (a) single nutrients (letters a and b significantly different from each other and from control, $p < 0.05$), and (b) compounds pooled into different nutrient categories (letters a and b significantly different from each other and from control, $p < 0.05$; PUFAs: DHA and EPA; Bvits: VitB6, VitB12 and folic acid; AO: Vit E, Vit C and selenium; PL: phosphatidylcholine); (c) synergistic increase

in carbachol (1 mM)-induced membrane potential change compared with control after administration of different nutrient groups [different letters (a–c) are significantly different from each other and from control, $p < 0.05$; DUC: DHA, uridine and choline; PUFAs: EPA; Bvits: VitB6, VitB12 and folic acid; AO: Vit E, Vit C and selenium; PL: Vit C and selenium; PL: phosphatidylcholine]. Data are expressed as means \pm SD, $n = 3$. Dotted line represents control level.

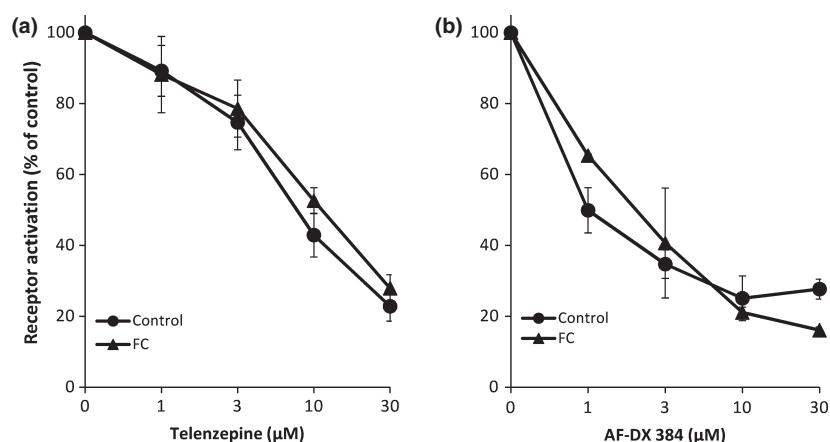


Fig. 5 Concentration-dependent inhibition of carbachol (1 mM)-induced changes in membrane potential after administration of (a) the M1-selective muscarinic antagonist telenzepine, and (b) the M2/M4-selective muscarinic antagonist AF-DX 384. PC12 cells were supplemented with NGF (50 ng/mL), with or without the FC nutrient composition, for 3 days. Data are expressed as means \pm SD, $n = 3$.

selective muscarinic antagonist AF-DX 384. PC12 cells were supplemented with NGF (50 ng/mL), with or without the FC nutrient composition, for 3 days. Data are expressed as means \pm SD, $n = 3$.

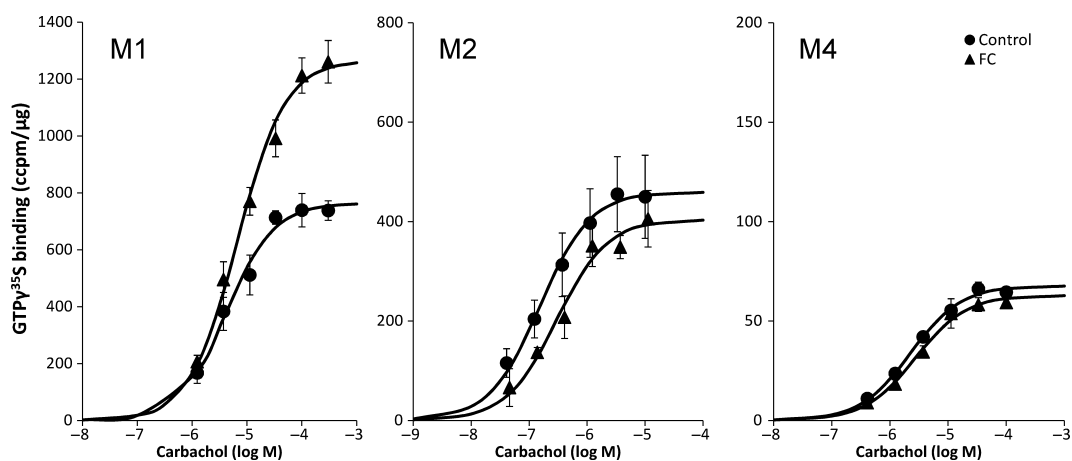


Fig. 6 Carbachol-induced $\text{GTP}\gamma^{35}\text{S}$ binding in CHO cells stably transfected with human M1, M2 or M4 muscarinic receptor genes. Membranes prepared from control and multi-nutrient (FC) supplemented CHO cells were prepared as described in Methods. Carbachol

(abscissa, log M) stimulated $\text{GTP}\gamma^{35}\text{S}$ binding mediated by M1, M2, or M4 receptors is expressed in $\text{ccpm}/\mu\text{g}$ protein. Shown are representative experiments. Data are expressed as means \pm SEM. A summary of parameters of fits is given in Results.

tration-dependent changes in membrane potential in PC12 cells as measured by the FLIPR assay. Supplementation with DHA, uridine and choline that was shown to support formation of synapses (Wurtman *et al.* 2006; Cansev and Wurtman 2007; Cansev *et al.* 2008) and acetylcholine release (Wang *et al.* 2007) yielded an increased depolarization of the cell membrane, although the specific combination of nutrients in FC induced an even larger increase in the response. Furthermore, the carbachol-induced changes observed either with or without FC supplementation, could be blocked by the non-selective muscarinic receptor antagonist atropine, evidencing that the observed effects were actually mediated by muscarinic receptors.

Subsequently, we investigated the effects of the nutrients in FC on agonist-induced changes in membrane potential. Supplementation with individual compounds did not lead to an agonist-induced increase in membrane potential except for DHA and EPA. However, the combined action of all nutrients in the specific blend of FC led to agonist-induced increase in membrane potential signal that is higher than what could be achieved with single nutrient supplementation. Furthermore, combined supplementation of DHA plus EPA (Fig. 4b) did not induce an effect size similar to FC. Only addition of the other nutrient groups yielded the maximum effect as observed with FC (Fig. 4c). These data indicate that the concerted action of the nutrients in FC could have larger effects than fish oil alone or a combination of DHA, uridine and choline on membrane related processes, possibly by enhancing phospholipid synthesis and changing membrane composition.

It has been shown that dietary supplementation with a combination of DHA, uridine and choline enhanced learning and memory more than supplementing these nutrients alone

(Holguin *et al.* 2008a,b), probably by synergistic improvement of synaptic membrane synthesis. In this study, we demonstrate that these nutrients, which affect membrane synthesis may also affect membrane-related processes, like GPCR functioning. Furthermore, the addition of co-factors present in FC significantly enhanced the carbachol-induced change in membrane potential compared with a combination of DHA, uridine and choline in our cell model. As the FC formulation yielded the largest effects, we used this nutrient combination to investigate muscarinic receptor activation.

The muscarinic receptor agonists carbachol and oxotremorine both induced concentration-dependent depolarization of PC12 cells as measured by the FLIPR assay. Agonist-induced depolarization was inhibited by muscarinic antagonists, demonstrating involvement of muscarinic receptors. It has been shown that M1, M2, M4, and M5 muscarinic receptors are endogenously expressed in PC12 cells (Lee and Malek 1998; Berkeley and Levey 2000; Clancy *et al.* 2007) and that M2 and M4 receptors are up-regulated by NGF treatment (Lee and Malek 1998; Clancy *et al.* 2007). The most abundant subtype in PC12 cells is the M4 receptor, which accounts for more than 95% of all muscarinic receptors (Berkeley and Levey 2000). Nonetheless, the response (depolarization) that we measured was most likely mediated by the M1 subtype (Brown *et al.* 2007; Brown and Passmore 2009) because activation of the M4 (or M2) receptor subtype would lead to a hyperpolarization (Jones 1993; Clancy *et al.* 2007). In addition, M4 and M2 receptors appear to be predominantly localized in the cytoplasm whereas M1 receptors appear to be more expressed at the plasma membrane (Clancy *et al.* 2007). However, we could not discriminate between the various endogenously expressed muscarinic receptors using muscarinic antagonists

that display certain specificity for M1/M3 or M2/M4 (Fig. 5). This may be due to a fairly low expression of muscarinic receptors (data not shown). Considering minute relative amounts of M1 receptors, any marginal occupancy by the selective M2/M4 antagonist may abolish M1 receptor-mediated effects. Similarly, in line with muscarinic M1 receptor-stimulated activation of mitogen-activated protein kinase (Berkeley and Levey 2000), comparable rather high concentrations of agonists (> 1 mM) were needed to evoke the maximal effect, again demonstrating the necessity of full receptor occupancy (and a lack of receptor reserve).

To further investigate the effects of multi-nutrient supplementation on muscarinic receptor activation, we used human M1/M2/M4 transfected CHO cells. We have shown in CHO-M1 cells that supplementation with multi-nutrient formulation (FC) leads to an enhanced M1 receptor-mediated G protein activation, whereas supplementation of either CHO-M2 or CHO-M4 cells did not show any increased receptor activation as measured by the [35 S]GTP γ S-binding assay. Together, these data suggest that multi-nutrient supplementation can potentially enhance GPCR signaling in general and M1 muscarinic receptor signaling in particular.

As the muscarinic acetylcholine receptors lose their sensitivity to acetylcholine during aging and more substantially in Alzheimer's disease (AD) (Joseph *et al.* 1993; Kelly *et al.* 1996; Jope *et al.* 1997; Tsang *et al.* 2006; Machova *et al.* 2008, 2010; Thatthiah and De Strooper 2009), interventions are aimed to target these receptors to restore cholinergic functioning. Of the five mACh receptor subtypes (M1–M5) that have been identified in humans (Bonner *et al.* 1987, 1988; Peralta *et al.* 1987, 1988; Bonner 1989a,b), the M1 subtype is the most abundant subtype in the cortex and hippocampus (Levey *et al.* 1991), which are also the main brain regions that develop plaques and tangles. In AD pathology M1 receptors are important, as deletion of these receptors increases amyloid pathology *in vitro* as well as *in vivo* (Davis *et al.* 2010). In addition, it has been shown that activation of M1 receptors positively influences the processing of the amyloid precursor protein towards the non-amyloidogenic pathway (Buxbaum *et al.* 1992; Nitsch *et al.* 1992; Caccamo *et al.* 2006; Jones *et al.* 2008).

Taken together, our results indicate that the specific combination of nutrients in FC acts synergistically in sustaining muscarinic M1 receptor responses, probably by facilitating receptor-mediated G protein activation. As muscarinic M1 receptors are important for the progression of memory deterioration and pathology of Alzheimer's disease, it would be of interest to confirm the observed increase in M1 receptor responses as a result of nutrient supplementation *in vivo*. In addition, these results suggest that the detected effects on M1 activation might have contributed to the improved memory performance in mild AD patients that was observed after a 12-week multi-nutrient intervention (Scheltens *et al.* 2010) using FortasynTM Connect.

Acknowledgements

Part of the research leading to these results was funded by Nutricia Advanced Medical Nutrition, Danone Research, Centre for Specialised Nutrition and the EU FP7 project LipiDiDiet, Grant Agreement No 211696.

Disclosure statement

PJMS, AAMK, RJH, PJK and LMB are all employees of Danone Research, Centre for Specialised Nutrition.

References

- Alemany R., Perona J. S., Sanchez-Dominguez J. M., Montero E., Canizares J., Bressani R., Escriba P. V. and Ruiz-Gutierrez V. (2007) G protein-coupled receptor systems and their lipid environment in health disorders during aging. *Biochim. Biophys. Acta-biomembr.* **1768**, 964–975.
- Alexander S. P. H., Mathie A. and Peters J. A. (2009) Guide to Receptors and Channels (GRAC), 4th edition (2009). *Br. J. Pharmacol.* **158**, S1–S254.
- Baxter D. F., Kirk M., Garcia A. F. *et al.* (2002) A novel membrane potential-sensitive fluorescent dye improves cell-based assays for ion channels. *J. Biomol. Screen.* **7**, 79–85.
- Berkeley J. L. and Levey A. I. (2000) Muscarinic activation of mitogen-activated protein kinase in PC12 cells. *J. Neurochem.* **75**, 487–493.
- Bonner T. I. (1989a) The molecular basis of muscarinic receptor diversity. *Trends Neurosci.* **12**, 148–151.
- Bonner T. I. (1989b) New subtypes of muscarinic acetylcholine receptors. *Trends Pharmacol. Sci. Dec (Suppl.)*, 11–15.
- Bonner T. I., Buckley N. J., Young A. C. and Brann M. R. (1987) Identification of a family of muscarinic acetylcholine receptor genes. *Science* **237**, 527–532.
- Bonner T. I., Young A. C., Brann M. R. and Buckley N. J. (1988) Cloning and expression of the human and rat m5 muscarinic acetylcholine receptor genes. *Neuron* **1**, 403–410.
- Brown D. A. and Passmore G. M. (2009) Neural KCNQ (Kv7) channels. *Br. J. Pharmacol.* **156**, 1185–1195.
- Brown D. A., Hughes S. A., Marsh S. J. and Tinker A. (2007) Regulation of M(Kv7.2/7.3) channels in neurons by PIP2 and products of PIP2 hydrolysis: significance for receptor-mediated inhibition. *J. Physiol.* **582**, 917–925.
- Buckley N. J., Bonner T. I., Buckley C. M. and Brann M. R. (1989) Antagonist binding properties of five cloned muscarinic receptors expressed in CHO-K1 cells. *Mol. Pharmacol.* **35**, 469–476.
- Buxbaum J. D., Oishi M., Chen H. I., Pinkas-Kramarski R., Jaffe E. A., Gandy S. E. and Greengard P. (1992) Cholinergic agonists and interleukin 1 regulate processing and secretion of the Alzheimer beta/A4 amyloid protein precursor. *Proc. Natl Acad. Sci. USA* **89**, 10075–10078.
- Caccamo A., Oddo S., Billings L. M., Green K. N., Martinez-Coria H., Fisher A. and LaFerla F. M. (2006) M1 receptors play a central role in modulating AD-like pathology in transgenic mice. *Neuron* **49**, 671–682.
- Cansev M. and Wurtman R. J. (2007) Chronic administration of docosahexaenoic acid or eicosapentaenoic acid, but not arachidonic acid, alone or in combination with uridine, increases brain phosphatide and synaptic protein levels in gerbils. *Neuroscience* **148**, 421–431.
- Cansev M., Wurtman R. J., Sakamoto T. and Ulus I. H. (2008) Oral administration of circulating precursors for membrane phosphat-

- ides can promote the synthesis of new brain synapses. *Alzheimer's Dementia* **4**, S153–S168.
- Clancy S. M., Boyer S. B. and Slesinger P. A. (2007) Coregulation of natively expressed pertussis toxin-sensitive muscarinic receptors with G-protein-activated potassium channels. *J. Neurosci.* **27**, 6388–6399.
- Davis A. A., Fritz J. J., Wess J., Lah J. J. and Levey A. I. (2010) Deletion of m1 muscarinic acetylcholine receptors increases amyloid pathology in vitro and in vivo. *J. Neurosci.* **30**, 4190–4196.
- Eltze M., Gönné S., Riedel R., Schlotke B., Schudt C. and Simon W. A. (1985) Pharmacological evidence for selective inhibition of gastric acid secretion by telenzepine, a new antimuscarinic drug. *Eur. J. Pharmacol.* **112**, 211–224.
- Fredriksson R. and Schioth H. B. (2005) The repertoire of G-protein-coupled receptors in fully sequenced genomes. *Mol. Pharmacol.* **67**, 1414–1425.
- Grossfield A., Feller S. E. and Pitman M. C. (2006) A role for direct interactions in the modulation of rhodopsin by ω-3 polyunsaturated lipids. *Proc. Natl Acad. Sci. USA* **103**, 4888–4893.
- Holguin S., Huang Y., Liu J. and Wurtman R. (2008a) Chronic administration of DHA and UMP improves the impaired memory of environmentally impoverished rats. *Behav. Brain Res.* **191**, 11–16.
- Holguin S., Martinez J., Chow C. and Wurtman R. (2008b) Dietary uridine enhances the improvement in learning and memory produced by administering DHA to gerbils. *FASEB J.* **22**, 3938–3946.
- Jakubik J., El-Fakahany E. E. and Dolezal V. (2006) Differences in kinetics of xanomeline binding and selectivity of activation of g proteins at M1 and M2 muscarinic acetylcholine receptors. *Mol. Pharmacol.* **70**, 656–666.
- Jakubik J., Randakova A., El-Fakahany E. and Dolezal V. (2009) Divergence of allosteric effects of rapacuronium on binding and function of muscarinic receptors. *BMC Pharmacol.* **9**, 15.
- Jones S. V. (1993) Muscarinic receptor subtypes: modulation of ion channels. *Life Sci.* **52**, 457–464.
- Jones C. K., Brady A. E., Davis A. A. et al. (2008) Novel selective allosteric activator of the M1 muscarinic acetylcholine receptor regulates amyloid processing and produces antipsychotic-like activity in rats. *J. Neurosci.* **28**, 10422–10433.
- Jope R. S., Song L. and Powers R. E. (1997) Cholinergic activation of phosphoinositide signaling is impaired in Alzheimer's disease brain. *Neurobiol. Aging*, **18** 111–120.
- Joseph J. A., Cutler R. and Roth G. S. (1993) Changes in G Protein-mediated Signal Transduction in Aging and Alzheimer's Disease. *Ann. N Y Acad. Sci.* **695**, 42–45.
- Kelly J. F., Furukawa K., Barger S. W., Rengen M. R., Mark R. J., Blanc E. M., Roth G. S. and Mattson M. P. (1996) Amyloid beta-peptide disrupts carbachol-induced muscarinic cholinergic signal transduction in cortical neurons. *Proc. Natl Acad. Sci. USA* **93**, 6753–6758.
- Kennedy E. P. and Weiss S. B. (1956) The function of cytidine coenzymes in the biosynthesis of phospholipides. *J. Biol. Chem.* **222**, 193–214.
- Lee N. H. and Malek R. L. (1998) Nerve growth factor regulation of m4 muscarinic receptor mRNA stability but not gene transcription requires mitogen-activated protein kinase activity. *J. Biol. Chem.* **273**, 22317–22325.
- Levey A., Kitt C., Simonds W., Price D. and Brann M. (1991) Identification and localization of muscarinic acetylcholine receptor proteins in brain with subtype-specific antibodies. *J. Neurosci.* **11**, 3218–3226.
- Machova E., Jakubik J., Michal P., Oksman M., Iivonen H., Tanila H. and Dolezal V. (2008) Impairment of muscarinic transmission in transgenic APPswe/PS1dE9 mice. *Neurobiol. Aging* **29**, 368–378.
- Machova E., Rudajev V., Smycka H., Koivisto H., Tanila H. and Dolezal V. (2010) Functional cholinergic damage develops with amyloid accumulation in young adult APPswe/PS1dE9 transgenic mice. *Neurobiol. Dis.* **38**, 27–35.
- van Meer G., Voelker D. R. and Feigenson G. W. (2008) Membrane lipids: where they are and how they behave. *Nat. Rev. Mol. Cell Biol.* **9**, 112–124.
- Michal P., Rudajev V., El-Fakahany E. E. and Dolezal V. (2009) Membrane cholesterol content influences binding properties of muscarinic M2 receptors and differentially impacts activation of second messenger pathways. *Eur. J. Pharmacol.* **606**, 50–60.
- Nitsch R. M., Slack B. E., Wurtman R. J. and Growdon J. H. (1992) Release of Alzheimer amyloid precursor derivatives stimulated by activation of muscarinic acetylcholine receptors. *Science* **258**, 304–307.
- Niu S.-L., Mitchell D. C., Lim S.-Y., Wen Z.-M., Kim H.-Y., Salem N. and Litman B. J. (2004) Reduced G protein-coupled signaling efficiency in retinal rod outer segments in response to n-3 fatty acid deficiency. *J. Biol. Chem.* **279**, 31098–31104.
- Peralta E. G., Ashkenazi A., Winslow J. W., Smith D. H., Ramachandran J. and Capon D. J. (1987) Distinct primary structures, ligand-binding properties and tissue-specific expression of four human muscarinic acetylcholine receptors. *EMBO J.* **6**, 3923–3929.
- Peralta E. G., Winslow J. W., Ashkenazi A., Smith D. H., Ramachandran J. and Capon D. J. (1988) Structural basis of muscarinic acetylcholine receptor subtype diversity. *Trends Pharmacol. Sci.* Feb (Suppl.), 6–11.
- Pooler A. M., Guez D. H., Benedictus R. and Wurtman R. J. (2005) Uridine enhances neurite outgrowth in nerve growth factor-differentiated pheochromocytoma cells. *Neuroscience* **134**, 207–214.
- Prasad R., Paila Y. D., Jafurulla M. and Chattopadhyay A. (2009) Membrane cholesterol depletion from live cells enhances the function of human serotonin(1A) receptors. *Biochem. Biophys. Res. Commun.* **389**, 333–337.
- Rajagopal S., Rajagopal K. and Lefkowitz R. J. (2010) Teaching old receptors new tricks: biasing seven-transmembrane receptors. *Nat. Rev. Drug Discov.* **9**, 373–386.
- Richardson U. I. and Wurtman R. J. (2007) Polyunsaturated fatty acids stimulate phosphatidylcholine synthesis in PC12 cells. *Biochim. Biophys. Acta (BBA), Mol. Cell Biol. Lipids* **1771**, 558–563.
- Rosenbaum D. M., Rasmussen S. G. F. and Kobilka B. K. (2009) The structure and function of G-protein-coupled receptors. *Nature* **459**, 356–363.
- Scheltens P., Kamphuis P. J., Verhey F. R., Olde Rikkert M. G., Wurtman R. J., Wilkinson D., Twisk J. W. and Kurz A. (2010) Efficacy of a medical food in mild Alzheimer's disease: a randomized, controlled trial. *Alzheimers Dement.* **6**, 1–10; e11.
- Teather L. A. and Wurtman R. J. (2006) Chronic administration of UMP ameliorates the impairment of hippocampal-dependent memory in impoverished rats. *J. Nutr.* **136**, 2834–2837.
- Thatthiah A. and De Strooper B. (2009) G protein-coupled receptors, cholinergic dysfunction, and Abeta toxicity in Alzheimer's disease. *Sci. Signal.* **2**, re8.
- Tsang S. W., Lai M. K., Kirvell S., Francis P. T., Esiri M. M., Hope T., Chen C. P. and Wong P. T. (2006) Impaired coupling of muscarinic M1 receptors to G-proteins in the neocortex is associated with severity of dementia in Alzheimer's disease. *Neurobiol. Aging* **27**, 1216–1223.
- Wang L., Albrecht M. A. and Wurtman R. J. (2007) Dietary supplementation with uridine-5'-monophosphate (UMP), a membrane

- phosphatide precursor, increases acetylcholine level and release in striatum of aged rat. *Brain Res.* **1133**, 42–48.
- Wettschureck N. and Offermanns S. (2005) Mammalian G proteins and their cell type specific functions. *Physiol. Rev.* **85**, 1159–1204.
- Whiteaker K. L., Gopalakrishnan S. M., Groebe D., Shieh C. C., Warrior U., Burns D. J., Coghan M. J., Scott V. E. and Gopalakrishnan M. (2001) Validation of FLIPR membrane potential dye for high throughput screening of potassium channel modulators. *J. Biomol. Screen.* **6**, 305–312.
- de Wilde M. C., Penke B., van der Beek E. M., Kuipers A. A., Kamphuis P. J. and Broersen L. M. (2011) Neuroprotective effects of a specific multi-nutrient intervention against abeta42-induced toxicity in rats. *J. Alzheimers Dis.* **27**, 327–339.
- Wurtman R. J., Ulus I. H., Cansev M., Watkins C. J., Wang L. and Marzloff G. (2006) Synaptic proteins and phospholipids are increased in gerbil brain by administering uridine plus docosahexaenoic acid orally. *Brain Res.* **1088**, 83–92.
- Wurtman R. J., Cansev M., Sakamoto T. and Ulus I. H. (2009) Use of phosphatide precursors to promote synaptogenesis. *Annu. Rev. Nutr.* **29**, 6.1–6.29.
- Yeo E.-J. and Park S. C. (2002) Age-dependent agonist-specific dysregulation of membrane-mediated signal transduction: emergence of the gate theory of aging. *Mech. Ageing Dev.* **123**, 1563–1578.

Subtype Differences in Pre-Coupling of Muscarinic Acetylcholine Receptors

Jan Jakubík^{1*}, Helena Janíčková¹, Alena Randáková¹, Esam E. El-Fakahany², Vladimír Doležal¹

1 Department of Neurochemistry, Institute of Physiology Academy of Sciences of the Czech Republic v.v.i., Prague, Czech Republic, **2** Department of Experimental and Clinical Pharmacology, University of Minnesota College of Pharmacy, Minneapolis, Minnesota, United States of America

Abstract

Based on the kinetics of interaction between a receptor and G-protein, a myriad of possibilities may result. Two extreme cases are represented by: 1/Collision coupling, where an agonist binds to the free receptor and then the agonist-receptor complex “collides” with the free G-protein. 2/Pre-coupling, where stable receptor/G-protein complexes exist in the absence of agonist. Pre-coupling plays an important role in the kinetics of signal transduction. Odd-numbered muscarinic acetylcholine receptors preferentially couple to $G_{q/11}$, while even-numbered receptors prefer coupling to $G_{i/o}$. We analyzed the coupling status of the various subtypes of muscarinic receptors with preferential and non-preferential G-proteins. The magnitude of receptor-G-protein coupling was determined by the proportion of receptors existing in the agonist high-affinity binding conformation. Antibodies directed against the C-terminus of the α -subunits of the individual G-proteins were used to interfere with receptor-G-protein coupling. Effects of mutations and expression level on receptor-G-protein coupling were also investigated. Tested agonists displayed biphasic competition curves with the antagonist [³H]-N-methylscopolamine. Antibodies directed against the C-terminus of the α -subunits of the preferential G-protein decreased the proportion of high-affinity sites, and mutations at the receptor-G-protein interface abolished agonist high-affinity binding. In contrast, mutations that prevent receptor activation had no effect. Expression level of preferential G-proteins had no effect on pre-coupling to non-preferential G-proteins. Our data show that all subtypes of muscarinic receptors pre-couple with their preferential classes of G-proteins, but only M₁ and M₃ receptors also pre-couple with non-preferential G_{i/o} G-proteins. Pre-coupling is not dependent on agonist efficacy nor on receptor activation. The ultimate mode of coupling is therefore dictated by a combination of the receptor subtype and the class of G-protein.

Citation: Jakubík J, Janíčková H, Randáková A, El-Fakahany EE, Doležal V (2011) Subtype Differences in Pre-Coupling of Muscarinic Acetylcholine Receptors. PLoS ONE 6(11): e27732. doi:10.1371/journal.pone.0027732

Editor: Karl-Wilhelm Koch, University of Oldenburg, Germany

Received September 7, 2011; **Accepted** October 24, 2011; **Published** November 16, 2011

Copyright: © 2011 Jakubík et al. This is an open-access article distributed under the terms of the Creative Commons Attribution License, which permits unrestricted use, distribution, and reproduction in any medium, provided the original author and source are credited.

Funding: This work was supported by the Academy of Sciences of the Czech Republic [Project AV0Z 50110509], the Grant Agency of the Czech Republic [Grant 305/09/0681], the Grant Agency of the Czech Academy of Sciences [Grant IAA500110703], the Ministry of Education, Youth and Sports of the Czech Republic [Grant LC554], and National Institutes of Health [Grant NS25743]. The funders had no role in study design, data collection and analysis, decision to publish, or preparation of the manuscript.

Competing Interests: The authors have declared that no competing interests exist.

* E-mail: jakubik@biomed.cas.cz

Introduction

G-protein coupled receptors (GPCR) represent the largest family of receptors, with more than 900 encoding genes [1]. They process and transduce a multitude of signals elicited by hormones, neurotransmitter and odorants and are thus involved in a very wide array of physiological and pathological processes. This makes this class of receptors a major pharmacological target for drug development [2].

Agonist-stimulated GPCRs in turn activate heterotrimeric GTP-binding proteins (G-proteins) that activate various signaling pathways. Two distinctive types of interaction between a receptor and G-protein exist: collision coupling and pre-coupling. In the former case, an agonist binds to the free receptor, activates it and then the receptor with bound agonist “collides” with free G-protein and activates it. In the latter case, stable receptor-G-protein complexes exist in the absence of agonist, agonist binds to this complex, induces change in the receptor conformation that leads to G-protein activation and dissociation of the complex [3]. It should, however, be noted that the distinction between collision coupling and pre-coupling is rather a matter of kinetics of

receptor-G-protein interaction, activation state and receptor to G-protein stoichiometry [4]. Additional modes of interaction intermediate between pure collision coupling and pre-coupling, like transient receptor to G-protein complexing (“dynamic scaffolding”), have been observed [5].

There is accumulating evidence for both collision coupling and pre-coupling of GPCRs. Interestingly, coimmunoprecipitation studies showed pre-coupling of α_{2A} -adrenergic receptors [6] with $G_{i/o}$ G-proteins and β_2 -adrenergic receptors with $G_{s/\text{olf}}$ G-proteins [7]. In contrast, rapid collision coupling of G-proteins with α_{2A} -adrenergic receptors has been demonstrated in resonance energy transfer studies [8] and with β_2 -adrenergic receptors in living cell imaging studies [9]. Overall, current data on GPCR coupling suggest that the mode of receptor to G-protein coupling may differ depending on the receptor type, cell type and membrane composition [3,10]. Thus, understanding the dynamic behavior of GPCR systems including receptor-G-protein coupling is important in discovery and development of more organ-specific drugs.

Muscarinic acetylcholine receptors are GPCRs present at synapses of the central and peripheral nervous systems but also exist in non-innervated cells and tissues. There are five subtypes of

muscarinic receptors encoded by distinct genes without splicing variants [11]. Development of selective ligands for muscarinic receptors thus represents an enormous challenge due to their omnipresence, with only a few types of tissues being endowed by a single or predominant subtype of these receptors. So far very little is known about the nature of coupling of muscarinic receptors to G-proteins [12]. We have demonstrated that the M₂ receptor can directly activate all three classes of G-proteins [13], and that it probably pre-couple to G_{i/o} but not to G_{s/olf} G-proteins [14]. To further clarify the mechanisms of muscarinic receptor subtypes signaling we analyzed the mode of coupling of M₁ through M₄ muscarinic receptors with G_{i/o}, G_{s/olf} and G_{q/11} G-proteins in membranes from Chinese hamster ovary cells expressing individual receptor subtypes. We show that while M₁ and M₃ receptors pre-couple both with their preferential G_{q/11} and non-preferential G_{i/o} G-proteins, M₂ and M₄ receptors pre-couple only to preferential G_{i/o} G-proteins.

Results

Stimulation of [³⁵S]GTPγS binding to G_{i/o}, G_{s/olf} and G_{q/11} G-proteins

Membranes from CHO cells containing from 1.4 to 2.5 fmol of M₁ through M₄ muscarinic receptors per mg of protein were exposed to carbachol in concentrations ranging from 0.1 μM to 1 mM and binding of [³⁵S]GTPγS to G-protein classes was determined using a scintillation proximity assay (SPA) (Fig. 1). Carbachol stimulated [³⁵S]GTPγS binding to all three major classes of G-proteins via all four receptors, with highest potency (EC₅₀ about 1 μM) and efficacy (more than 3-fold increase over basal) for

preferential G-proteins (G_{q/11} for M₁ and M₃ and G_{i/o} for M₂ and M₄ receptors) (Table 1). The potency of carbachol in stimulating [³⁵S]GTPγS binding to non-preferential G-proteins was 2- (M₃ G_{s/olf}) to 10-fold (M₂ G_{s/olf}) lower than to preferential G-proteins.

Competition of carbachol with [³H]NMS binding at M₁ through M₄ receptors

Binding of the tritiated antagonist N-methylscopolamine ([³H]NMS) in the presence of agonist carbachol concentrations ranging from 10 nM to 10 mM (Fig. 2) was best described by competition for two sites (Eq. 3) at all four receptor subtypes. The equilibrium inhibition constant (K_I) of carbachol was similar among receptor subtypes, both for high and low affinity sites (Table 2). At M₁ and M₃ receptors that preferentially couple to G_{q/11} G-proteins carbachol displayed more low affinity binding sites than at M₂ and M₄ receptors that preferentially couple to G_{i/o} G-proteins. In some cases preincubation of membranes with antibodies directed against the C-termini of α-subunits of individual classes of G-proteins led to an increase in the proportion of low affinity sites. The proportion of low affinity sites was increased by anti-G_{i/o} and anti-G_{q/11} antibodies at M₁ and M₃ receptors but only by anti-G_{i/o} antibodies at M₂ and M₄ receptors. The anti-G_{s/olf} antibody did not change the proportion of low affinity sites at any receptor subtype. None of the antibodies affected K_I of either the low or high affinity sites.

Competition of agonists with [³H]NMS binding at M₁ and M₂ receptors

All tested agonists at M₁ receptors (carbachol, fumethide, oxotremorine, and pilocarpine) bound to two binding sites (Fig. 3,

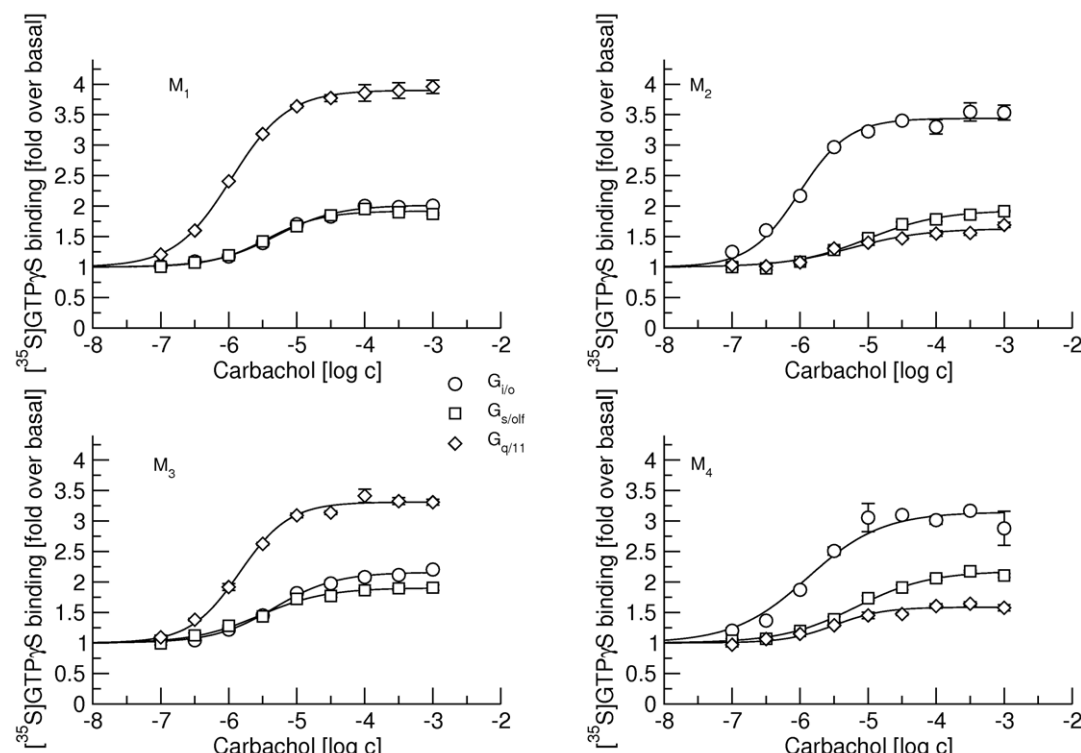


Figure 1. Stimulation of [³⁵S]GTPγS binding by carbachol. [³⁵S]GTPγS binding to G_{i/o} (circles), G_{s/olf} (squares) and G_{q/11} G-proteins (diamonds) via M₁ (upper left), M₂ (upper right), M₃ (lower left) and M₄ (lower right) receptors by increasing concentrations (abscissa, log M) of carbachol is expressed as fold over basal (ordinate). Data are means ± S.E.M of values from 3 experiments performed in quadruplicate. Curves were fitted using equation 2 and results of fits are shown in Table 1.

doi:10.1371/journal.pone.0027732.g001

Table 1. Stimulation of [35 S]GTP γ S binding by carbachol to G_{i/o} or G_{s/olf} and G_{q/11} subtypes of G-proteins via M₁ through M₄ receptors.

	G _{i/o}		G _{s/olf}		G _{q/11}	
	pEC ₅₀	E _{MAX}	pEC ₅₀	E _{MAX}	pEC ₅₀	E _{MAX}
M ₁	5.31 ± 0.05	2.01 ± 0.05	5.44 ± 0.05	1.92 ± 0.05	5.96 ± 0.05	3.90 ± 0.08
M ₂	6.01 ± 0.06	3.44 ± 0.07	5.01 ± 0.06	1.93 ± 0.05	5.24 ± 0.02	1.63 ± 0.02
M ₃	5.32 ± 0.05	2.16 ± 0.06	5.54 ± 0.05	2.16 ± 0.05	5.83 ± 0.04	3.31 ± 0.06
M ₄	5.89 ± 0.05	3.15 ± 0.08	5.18 ± 0.06	2.18 ± 0.06	5.49 ± 0.05	1.59 ± 0.04

Data are means ± S.E.M. From 3 experiments performed in quadruplicate. E_{MAX} is expressed as fold increase of basal binding.

doi:10.1371/journal.pone.0027732.t001

full circles). Although they bound with different affinities they recognized the same proportion of low-affinity sites (Table 3). Anti-G_{i/o} and anti-G_{q/11} antibodies increased the proportion of low affinity sites to a comparable extent for all tested agonists (Fig. 3, open circles and open diamonds). The anti-G_{s/olf} antibody did not change the proportion of the low-affinity binding sites for any of the agonists tested (Fig. 3, open squares). None of the antibodies affected K_t values.

Similarly, all tested agonists bound to two binding sites at M₂ receptors (Fig. 4, full circles). As in the case of the M₁ receptor they bound with different affinities but they recognized the same

proportion of low-affinity sites (Table 4). Similar to carbachol, the proportion of low-affinity sites was lower at M₂ than at M₁ receptors for all tested agonists (Table 4 vs. Table 3) and only the anti-G_{i/o} antibody increased the proportion of low affinity sites (Fig. 4, open circles). The anti-G_{s/olf} and anti G_{q/11} antibodies did not change either the proportion of low-affinity binding sites or K_ts for any of the agonists tested (Fig. 4, open squares and open diamonds).

Effects of mutations of M₁ receptors that affect receptor activation

To further investigate the role of receptor activation in receptor-G-protein pre-coupling we prepared cell lines expressing mutant M₁ receptor with mutations known to interfere with receptor signaling. Mutation of aspartate 71 in the middle of the second transmembrane domain to asparagine (D71N) has been shown to abolish receptor activation [15]. Mutation of aspartate 122 in the conserved E/DRY-motif at the intracellular edge of the third transmembrane domain to asparagine (D122N) has been shown to reduce the potency of muscarinic agonists [16]. Opsin arginine in the conserved E/DRY-motif at the intracellular edge of the third transmembrane domain has been shown to directly interact with the C-terminal cysteine of the α -subunit of G-protein [16]. At M₁ muscarinic receptors mutation of corresponding arginine 123 asparagine (R123N) blocks activation of G-proteins [17]. The appropriate control CHO cell line expressing the wild-type receptor was also generated using the same expression vector. Expression levels of receptor mutants

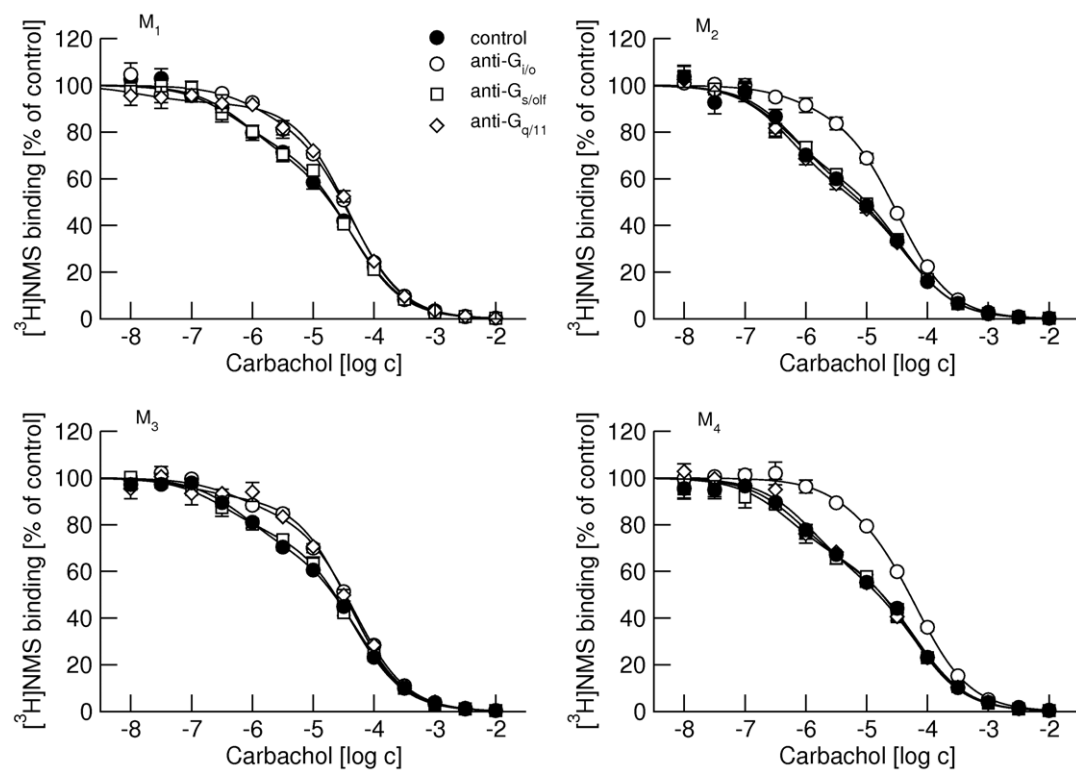


Figure 2. Effects of anti-G-protein antibodies on competition between carbachol and [^{3}H]NMS binding at M₁ to M₄ receptors. Binding of 1 nM [^{3}H]NMS to membranes from CHO cells expressing M₁ (upper left), M₂ (upper right), M₃ (lower left) and M₄ (lower right) receptors in the presence of increasing concentrations (abscissa, log M) of carbachol is expressed as per cent of control binding in the absence of carbachol. Filled circles, control binding in the absence of antibodies. Open symbols, binding in the presence of anti-G_{i/o} (circles), anti-G_{s/olf} (squares), and anti-G_{q/11} (diamonds) antibodies. Data are means ± S.E.M. of values from 3 experiments performed in quadruplicate. Curves were fitted using equation 3 and results of fits are shown in the Table 2.
doi:10.1371/journal.pone.0027732.g002

Table 2. Effects of IgG antibodies directed against the α -subunits of individual subtypes of G-proteins on binding parameters of carbachol in membranes of CHO cells expressing individual subtypes of muscarinic receptors.

		control	anti- $G_{i/o}$	anti- $G_{s/olf}$	anti- $G_{q/11}$
M_1	p K_i high	7.01 ± 0.08	6.93 ± 0.09	7.09 ± 0.08	7.14 ± 0.08
	p K_i low	5.21 ± 0.07	5.25 ± 0.06	5.27 ± 0.07	5.30 ± 0.07
	f low	69 ± 7	84 ± 8*	74 ± 7	92 ± 8*
M_2	p K_i high	6.81 ± 0.08	6.70 ± 0.07	6.93 ± 0.08	6.88 ± 0.07
	p K_i low	5.01 ± 0.07	5.13 ± 0.07	5.06 ± 0.07	5.01 ± 0.08
	f low	56 ± 8	89 ± 8*	61 ± 9	54 ± 9
M_3	p K_i high	7.03 ± 0.08	7.15 ± 0.09	7.23 ± 0.08	7.14 ± 0.09
	p K_i low	5.15 ± 0.09	5.20 ± 0.09	5.23 ± 0.08	5.27 ± 0.09
	f low	72 ± 7	89 ± 9*	76 ± 7	92 ± 8*
M_4	p K_i high	6.91 ± 0.09	7.03 ± 0.08	7.09 ± 0.09	6.94 ± 0.08
	p K_i low	5.01 ± 0.09	4.95 ± 0.08	5.08 ± 0.09	5.00 ± 0.08
	f low	62 ± 7	82 ± 8*	66 ± 7	58 ± 7

Data are means ± S.E.M. From 3 experiments performed in quadruplicates. f_{low}: fraction of low-affinity sites in percent;

*, significantly different from control by t-test ($P < 0.05$).

doi:10.1371/journal.pone.0027732.t002

(0.42 to 0.87 pmol per mg of protein) were the same as expression level of the wild-type receptor (0.63 to 0.71 pmol per mg of protein).

Association of 0.5 nM [³⁵S]GTP γ S with membranes from the newly prepared CHO cell line expressing M₁ receptors occurred with observed association rate k_{obs} = 0.036 min⁻¹ (Fig. 5 upper left, full circles, and Table 5). One hundred μ M carbachol (Fig. 5, open circles) accelerated association of [³⁵S]GTP γ S two-times and increased equilibrium binding (B_{eq}) by one third. Mutations D71N (Fig. 5 upper right) and R123N (Fig. 5 lower right) did not change basal (in the absence of carbachol) association of [³⁵S]GTP γ S but they both abolished acceleration induced by carbachol. Mutation D122N accelerated basal association of [³⁵S]GTP γ S by 50%. One hundred μ M carbachol further accelerated association of [³⁵S]GTP γ S. The rate of association as well as B_{eq} in the presence of carbachol at R123N receptors was the same as at control (M₁ wt) (Fig. 5 and Table 5).

On the newly prepared cell line expressing M₁ wt receptors carbachol displayed binding to two binding sites in competition with [³H]NMS with the same proportion of low affinity sites and similar affinities (Fig. 6, full circles) as in Fig. 2. While mutation D71N did not change the binding parameters of carbachol, mutation D122N brought about an increase in low affinity sites and mutation R123N completely abolished high-affinity binding (Fig. 6 and Table 6).

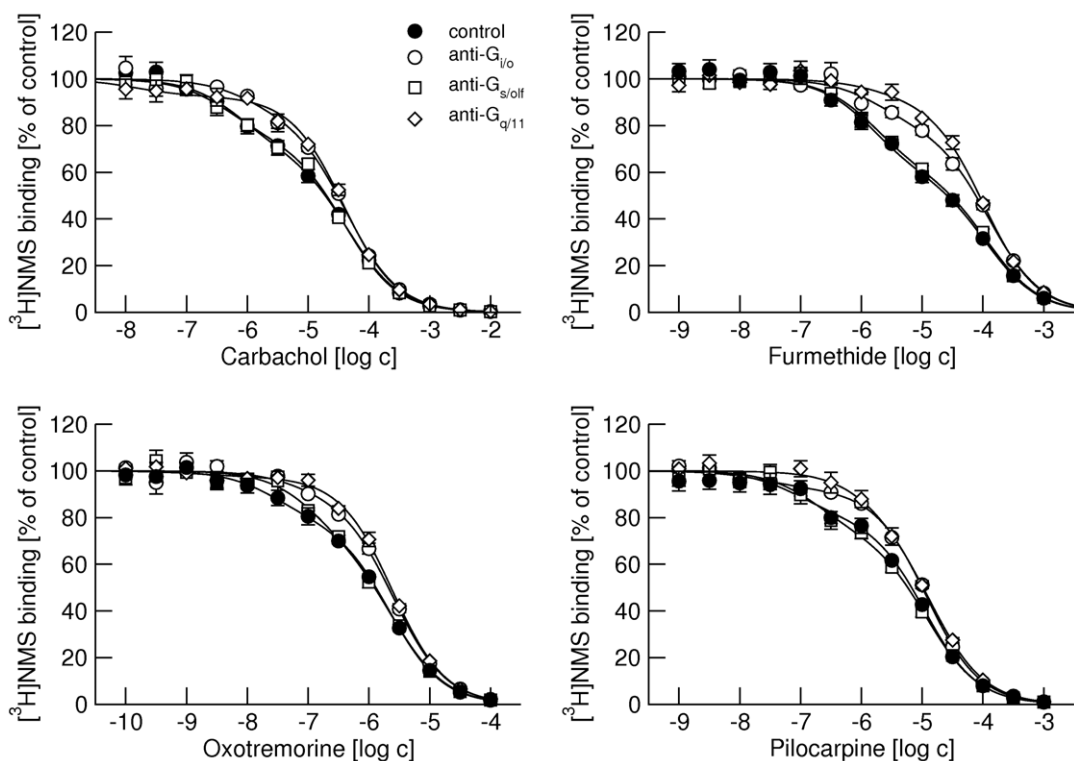


Figure 3. Effects of anti-G-protein antibodies on competition between different agonists and [³H]NMS binding at M₁ receptors. Binding of 1 nM [³H]NMS to membranes from CHO cells expressing M₁ receptors in the presence of increasing concentrations (abscissa, log M) of the agonists carbachol (upper left), furmethide (upper right), oxotremorine (lower left) and pilocarpine (lower right) is expressed as per cent of control binding in the absence of agonist. Filled circles, control binding in the absence of antibodies. Open symbols, binding in the presence of anti-G_{i/o} (circles), anti-G_{s/olf} (squares) and anti-G_{q/11} (diamonds) antibodies. Data are means ± S.E.M. of values from 3 experiments performed in quadruples. Curves were fitted using equation 3 and results of fits are shown in Table 3.

doi:10.1371/journal.pone.0027732.g003

Table 3. Effects of IgG antibodies directed against α -subunits of individual subtypes of G-proteins on binding parameters of different muscarinic agonists in membranes of M₁ CHO cells.

	Control	anti-G _{i/o}	anti-G _{s/olf}	anti-G _{q/11}	
carbachol	pK _i high	7.01±0.08	6.93±0.09	7.09±0.08	7.14±0.08
	pK _i low	5.21±0.07	5.25±0.06	5.27±0.07	5.30±0.07
	f _{low}	69±7	86±8*	74±7	92±8*
furmethide	pK _i high	6.70±0.07	6.59±0.08	6.66±0.07	6.63±0.08
	pK _i low	4.82±0.07	4.78±0.07	4.81±0.07	4.87±0.07
	f _{low}	62±7	84±8*	62±6	92±8*
oxotremorine	pK _i high	8.12±0.08	8.04±0.8	7.96±0.06	8.14±0.08
	pK _i low	6.53±0.06	6.47±0.07	6.46±0.06	6.49±0.06
	f _{low}	69±6	90±8*	69±6	95±5*
pilocarpine	pK _i high	7.72±0.07	7.64±0.07	7.61±0.07	7.66±0.07
	pK _i low	5.84±0.06	5.81±0.06	5.80±0.06	5.71±0.06
	f _{low}	75±7	92±8*	73±7	90±8*

Data are means ± S.E.M. From 3 experiments performed in quadruplicates. f_{low}, fraction of low-affinity sites in percent;

*, significantly different from control by t-test (P<0.05).

doi:10.1371/journal.pone.0027732.t003

Effects of attenuation of expression of G_{i/o} G-proteins in M₂-CHO cells

Total binding capacity of (saturating) 500 nM [³⁵S]GTPγS in control M₂-CHO membranes (in the absence of GDP) showed prevalence of G_{i/o} G-proteins over G_{s/olf} and G_{q/11} (37.5±3.9, 22.0±2.3 and 25.4±2.8 pmol/mg prot., respectively; mean ± S.E.M., n = 3). Treatment of M₂-CHO cells with siRNA directed to G_{i/o} G-proteins resulted in more than a 70% decrease in the [³⁵S]GTPγS binding capacity of G_{i/o} (10.1±1.8 pmol/mg prot.; mean ± S.E.M., n = 3) without a change in the binding capacity of G_{s/olf} and G_{q/11} G-proteins (24.1±2.2, 23.8±2.5 pmol/mg prot., respectively; mean ± S.E.M., n = 3). This treatment resulted in a 10-fold decrease in the potency of carbachol in stimulation of [³⁵S]GTPγS binding to G_{i/o} G-proteins (Fig. 7 vs. Fig. 1 upper right, open circles; Table 7 vs. Table 1) and decreased its efficacy more than 5-times. The efficacy of carbachol in stimulation of [³⁵S]GTPγS binding to G_{s/olf} or G_{q/11} G-proteins was unchanged while its potency increased about 3-times in both cases.

Based on competition binding of agonists and [³H]NMS (Fig. 8; Table 8), attenuation of G_{i/o} expression led to an increase in the proportion of low-affinity sites for all tested agonists (see controls in Table 4 and Table 8) without change in K_I values. The anti-G_{i/o} antibody further increased the proportion of low-affinity sites in G_{i/o} G-proteins-depleted membranes only for the full agonists carbachol and furmethide. In contrast to control M₂-CHO cells, the proportion of low-affinity sites of the partial agonists oxotremorine and pilocarpine in G_{i/o} G-proteins-depleted mem-

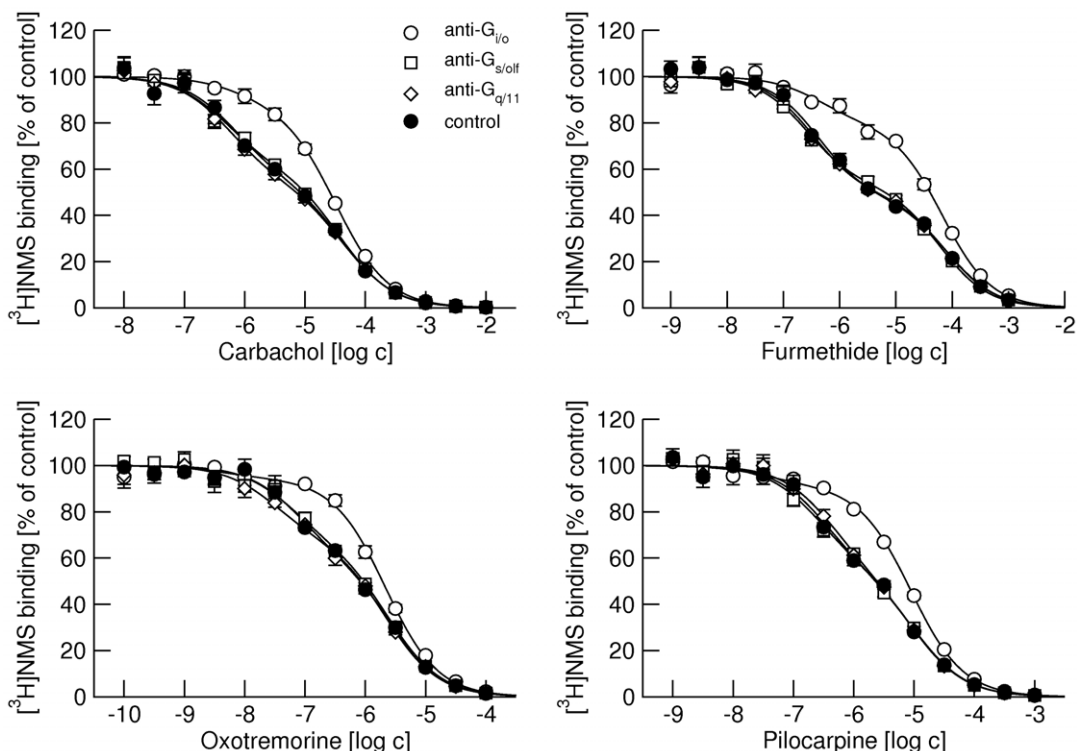


Figure 4. Effects of anti-G-protein antibodies on competition between different agonists and [³H]NMS binding at M₂ receptors. Binding of 1 nM [³H]NMS to membranes from CHO cells expressing M₂ receptors in the presence of increasing concentrations (abscissa, log M) of the agonists carbachol (upper left), furmethide (upper right), oxotremorine (lower left) and pilocarpine (lower right) is expressed as per cent of control binding in the absence of agonist. Filled circles, control binding in the absence of antibodies. Open symbols, binding in the presence of anti-G_{i/o} (circles), anti-G_{s/olf} (squares) and anti-G_{q/11} (diamonds) antibodies. Data are means ± S.E.M. of values from 3 experiments performed in quadruplicates. Curves were fitted using equation 3 and results of fits are shown in Table 4.

doi:10.1371/journal.pone.0027732.g004



Table 4. Effects of IgG antibodies directed against α -subunits of individual subtypes of G-proteins on binding parameters of different muscarinic agonists in membranes of M₂ CHO cells.

	Control	anti-G _{i/o}	anti-G _{s/olf}	anti-G _{q/11}
carbachol	pK _i high	6.81±0.08	6.70±0.07	6.93±0.08
	pK _i low	5.01±0.07	5.13±0.07	5.06±0.07
	f _{low}	56±8	89±8*	61±9
furmethide	pK _i high	6.99±0.08	6.98±0.07	7.19±0.07
	pK _i low	4.70±0.08	4.79±0.07	4.84±0.08
	f _{low}	48±8	80±7*	49±8
oxotremorine	pK _i high	7.74±0.09	7.76±0.08	7.83±0.08
	pK _i low	6.17±0.08	5.78±0.08	6.22±0.09
	f _{low}	60±8	84±7*	65±8
pilocarpine	pK _i high	7.10±0.09	7.05±0.11	7.22±0.09
	pK _i low	5.58±0.09	5.67±0.09	5.62±0.09
	f _{low}	53±10	76±11*	53±10

Data are means ± S.E.M. From 3 experiments performed in quadruplicates. f_{low}, fraction of low-affinity sites in percent;

*, significantly different from control by t-test (P<0.05).

doi:10.1371/journal.pone.0027732.t004

brates was not changed by the anti-G_{i/o} antibody. Similar to untreated M₂-CHO cells, the anti-G_{s/olf} and anti-G_{q/11} antibodies had no effect on either the proportion of low affinity sites or K_i values in membranes with attenuated expression of G_{i/o} G-proteins.

Discussion

Binding of an agonist to a G-protein-coupled receptor (GPCR) results in transforming the receptor to an active state that facilitates guanosine diphosphate (GDP) dissociation from the α -subunit of interacting heterotrimeric G-proteins and its exchange for guanosine triphosphate (GTP) [18]. In principle there are many possible ways for receptor-G-protein interactions to take effect, with two extreme possibilities. In one scenario receptors and G-proteins diffuse freely within the plasma membrane, agonist binds to the free receptor that then randomly “collides” with G-proteins and activates them. Alternatively, receptors and G-proteins form stable complexes regardless of the receptor activation state and agonist binding, the agonist binds to this complex and induces conformational changes in the receptor protein that leads to G-protein activation and dissipation of the receptor-G-protein complex. We will refer to the former situation as “collision coupling” and the latter one as “pre-coupling” [3]. It should, however, be noted that even if receptors are partially pre-coupled to G-proteins, an agonist can also bind to free receptors and then “collide” with G-protein. Also the distinction between collision coupling and pre-coupling is rather a matter of kinetics of

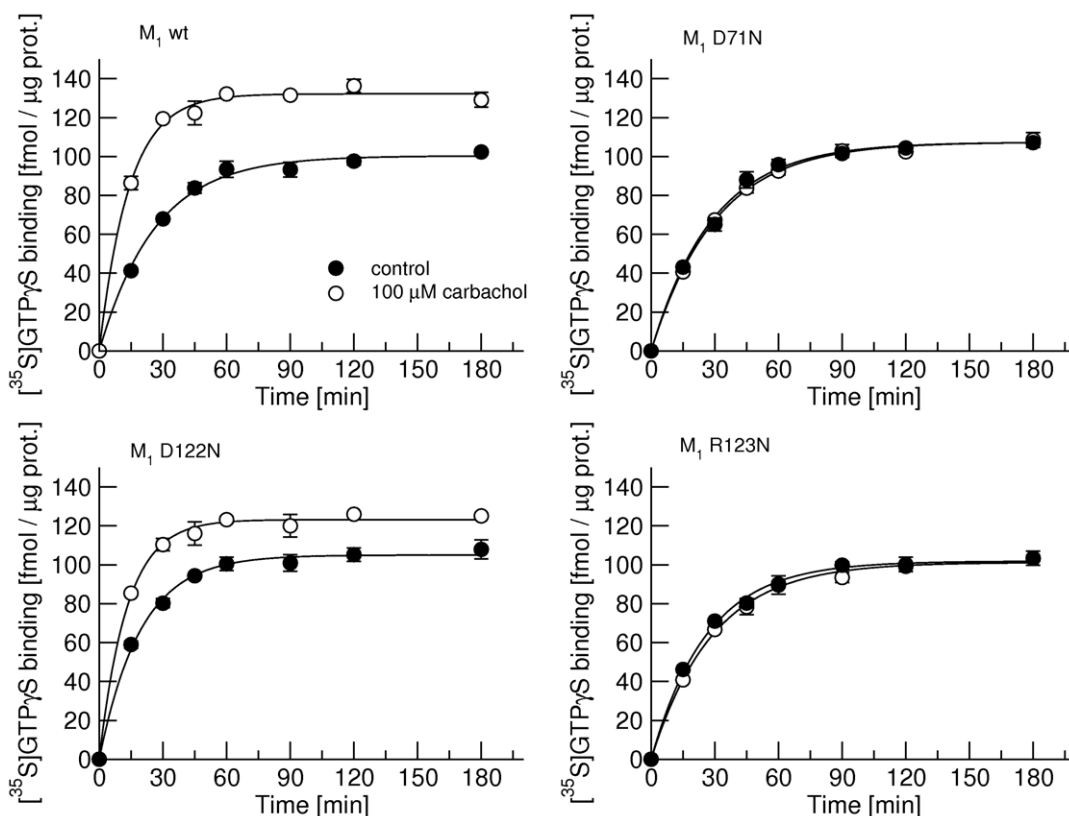


Figure 5. Effects of point mutations of the M₁ receptor on carbachol-induced stimulation of [³⁵S]GTP γ S. Binding of 0.5 nM [³⁵S]GTP γ S to all G-proteins in the presence of 50 μ M GDP was measured in membranes from newly prepared CHO cell lines expressing either wild-type (M₁ wt) or mutant (D71N, D122N, R123N) M₁ receptors in the absence (full circles) or in the presence (open circles) of 100 μ M carbachol. Data are means ± S.E.M. of values from 3 experiments performed in quadruples. Curves were fitted using equation 4 and results of fits are shown in Table 5. doi:10.1371/journal.pone.0027732.g005

Table 5. Rates of basal and carbachol-stimulated association of [³⁵S]GTP γ S in CHO membranes expressing wild type and mutant M₁ receptors.

		M ₁ wt	D71N	D122N	R123N
control	k _{obs} [min ⁻¹]	0.036±0.007	0.034±0.007	0.054±0.005#	0.038±0.007
	B _{eq} [fmol/:g prot.]	101±6	107±12	103±8	105±6
+100 μ M carbachol	k _{obs} [min ⁻¹]	0.075±0.006*	0.033±0.006#	0.077±0.005*	0.036±0.007#
	B _{eq} [fmol/ μ g prot.]	133±8*	105±9#	126±6*	100±5#

Data are means ± S.E.M. From 3 experiments performed in quadruplicates.

*, Significantly different from control;

#, significantly different from wild type (M₁ wt), t-test (P<0.05).

doi:10.1371/journal.pone.0027732.t005

receptor-G-protein interaction and activation and receptor to G-protein stoichiometry [4]. Thus a myriad of possible ways for interaction among receptor, G-protein and agonist exist, e.g., transient receptor to G-protein complexing (“dynamic scaffolding”) [5]. Receptor G-protein pre-coupling plays an important role in signaling. It may accelerate kinetics of signal transduction. If receptor G-protein complexes pre-exist, instantaneous activation of G-protein takes place upon agonist binding to the receptor [4].

As shown repeatedly [10,13,19,20] and also in Fig. 1, muscarinic acetylcholine receptors couple with all 3 major classes of G-proteins (G_{i/o}, G_{s/olf} and G_{q/11}). Our recent data show that at M₂ receptors the agonist carbachol slows down the association of GDP with G_{i/o} but not G_{s/olf} G-proteins [14]. This finding may evidence the pre-existence of a receptor/G-protein complex prior to carbachol binding. Data thus suggest that muscarinic M₂ receptors pre-couple to G_{i/o} but not to G_{s/olf} G-proteins. Alternatively, M₂ receptors may precouple with G_{s/olf} but carbachol has no effect on GDP association. To exclude this possibility we analyzed in detail pre-coupling of all 3 major classes of G-proteins with M₂ receptors and compared it with pre-coupling at other G_{i/o} preferring (M₄) and G_{q/11} preferring (M₁ and M₃) muscarinic receptors.

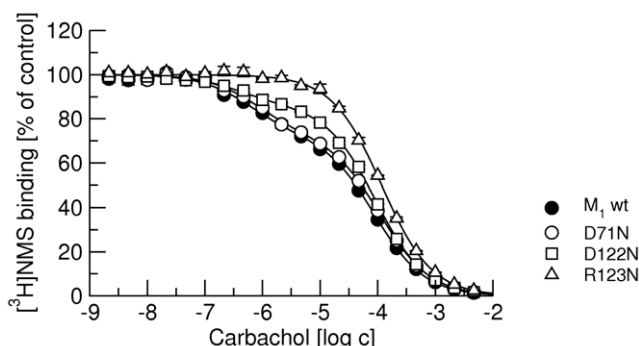


Figure 6. Effects of point mutations of the M₁ receptor on competition between carbachol and [³H]NMS binding. Binding of 1 nM [³H]NMS to membranes from newly prepared CHO cell lines expressing wild type and mutant M₁ receptors in the presence of increasing concentrations carbachol is expressed as per cent of control binding in the absence of agonist. Filled circles, binding to wild-type M₁ receptors. Open symbols, binding to D71N (circles), D122N (squares) and R123N (triangles) mutant M₁ receptors. Data are means ± S.E.M. of values from 3 experiments performed in quadruplicates. Curves were fitted using equation 3 and results of fits are shown in Table 6.

doi:10.1371/journal.pone.0027732.g006

At all receptor subtypes carbachol displays a “two site” binding curve with high affinity binding in the nanomolar range and low affinity binding in the micromolar range (Fig. 2, Table 2). According to the ternary complex model of GPCRs [21] agonists bind with high affinity to the receptor-G-protein complex and with low-affinity to receptors uncoupled from G-proteins. The interface of interaction between the receptor and G-protein consists of the intracellular edge of the third, fifth and sixth transmembrane domains and adjacent parts of the third and fourth intracellular loops of the receptor and the C-terminus of the G-protein α -subunit [16,22]. Antibodies directed against the C-terminus of G-protein should prevent receptor-G-protein interaction (or break existing receptor G-protein complex) and lower the affinity of the receptor for agonists. Indeed, IgG antibodies directed against the C-terminus of the G_{i/o} class of G-proteins increased the fraction of low-affinity sites at all receptor subtypes including the G_{i/o} non-prefering M₁ and M₃ receptors. Similarly, IgG antibodies directed against the C-terminus of G_{q/11} class of G-proteins increased the fraction of low-affinity sites only at their preferring M₁ and M₃ receptors, but IgG antibodies directed against the C-terminus of G_{s/olf} class of G-proteins had no effect. Antibodies only changed the proportion of low-affinity sites without an effect on receptor affinity. Our data also show that all receptors pre-couple with their preferential G-proteins (M₁ and M₃ with G_{q/11} and M₂ and M₄ with G_{i/o}) and that M₁ and M₃ receptors also pre-couple with non-preferential G_{i/o} G-proteins. In contrast, pre-coupling of G_{s/olf} G-proteins was not detected at any subtype of muscarinic receptors. In other words, the interaction between receptor and G_{s/olf} is so short-lived that cannot be detected by antibodies. This is in agreement with our kinetic measurements at G_{s/olf} and M₂ receptors [14].

Table 6. Effects of single amino acid mutations of M₁ receptor on the binding parameters of carbachol.

	M ₁ control	D71N	D122N	R123N
pK _i high	7.13±0.08	7.01±0.08	7.07±0.09	
pK _i low	4.91±0.06	4.85±0.05	4.92±0.05	4.80±0.07
f _{low}	72±6	74±7	86±7*	99±1*

Data are means ± S.E.M. From 3 experiments performed in quadruplicates. f_{low}, fraction of low-affinity sites in percent;

*, significantly different from control by t-test (P<0.05).

doi:10.1371/journal.pone.0027732.t006

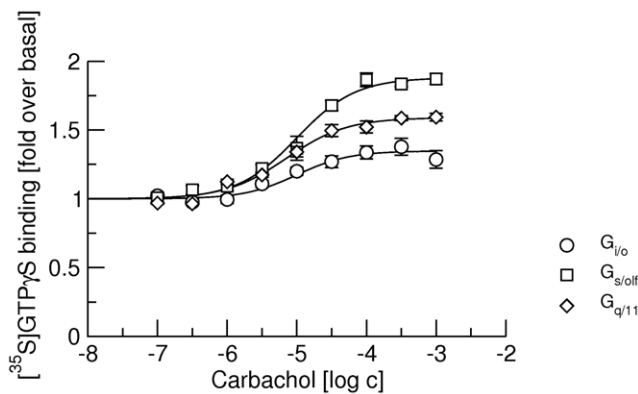


Figure 7. Stimulation of $[^{35}\text{S}]GTP\gamma\text{S}$ binding by carbachol at the M_2 receptor after suppression of expression of $\text{G}_{i/o}$ G-proteins. M_2 receptor-mediated stimulation of $[^{35}\text{S}]GTP\gamma\text{S}$ binding to $\text{G}_{i/o}$ (circles), $\text{G}_{s/olf}$ (squares) and $\text{G}_{q/11}$ G-proteins (diamonds) after suppression of expression of $\text{G}_{i/o}$ G-proteins by siRNA was stimulated by increasing concentrations of carbachol (abscissa, log M). Response is expressed as fold over basal (ordinate). Data are means \pm S.E.M. of values from 3 experiments performed in quadruplicates. Curves were fitted using equation 2 and results of fits are shown in Table 5.

doi:10.1371/journal.pone.0027732.g007

We tested binding of four structurally different agonists (carbachol, fumethide, oxotremorine and pilocarpine) that also differ in potency and efficacy in activating muscarinic receptors [14] and binding kinetics [23]. Importantly, all tested agonists recognize the same proportion of low-affinity binding sites (Figs 3 and 4; Tables 3 and 4). It is very unlikely that these agonists induce the same proportion of transient high-affinity states (in collision coupling, dynamic scaffolding or a similar scenario). Rather receptor G-protein complexes preexist prior to agonists binding and their proportion is given by stoichiometry of receptors and G-proteins. Moreover, the antibodies have the same effect on binding of all agonists, further excluding the role of agonists in the formation of receptor-G-protein complexes.

To further investigate the role of receptor activation in receptor-G-protein pre-coupling we prepared cell lines expressing mutant M_1 receptor with mutations known to interfere with receptor signaling. Mutation of aspartate 71 in the middle of the second transmembrane domain to asparagine ($D71N$) has been shown to prevent activation of the M_1 receptor [15]. This residue is neither part of the agonist binding site nor the receptor-G-protein interface. It is supposed that the $D71N$ mutation disrupts intramolecular hydrogen bond network and prevents the receptor from gaining an active conformation. Its effect on suppressing

receptor activation is confirmed in Fig. 5 (upper right). Although $D71N$ receptors cannot be activated by carbachol they still display both high- and low-affinity sites for carbachol with the same proportion as control wild-type M_1 receptors (Fig. 6, full and open circles). Thus, an active conformation of the receptor is not a prerequisite for receptor-G protein pre-coupling. These data are in perfect fit with a report by Quin et al. [24] published during completion of this manuscript that M_3 receptors form inactive complexes with G_q G-proteins.

In contrast, mutations that interfere with receptor signaling by being directed against the receptor G-protein interface do affect pre-coupling. Mutation of aspartate 122 in the conserved E/DRY-motif at the intracellular edge of the third transmembrane domain to asparagine ($D122N$) has been shown to reduce the potency of muscarinic agonists [13]. Measurements of the association rate of $GTP\gamma\text{S}$ shows that at $D122N$ receptors $GTP\gamma\text{S}$ binding under basal conditions (in the absence of agonist) is accelerated and that carbachol has smaller effect on $GTP\gamma\text{S}$ association rate than at wild-type M_1 receptors (Fig. 5, lower left). Meanwhile, the proportion of low-affinity sites for carbachol is increased in $D122N$ receptors in comparison with control (Fig. 6). Most likely, increased basal activity of $D122N$ results in more activated G-proteins and thus more uncoupled receptors in membrane preparations. Crystal structure of complex of opsin and C-terminus of G-protein α -subunit revealed that arginine in the conserved E/DRY-motif at the intracellular edge of the third transmembrane domain interacts directly with the α -subunit C-terminal cysteine [16]. At M_1 muscarinic receptors mutation of arginine 123 to asparagine ($R123N$) blocks activation of G-proteins (Fig. 5, lower right). In accordance with the ternary complex model of GPCRs [21], $R123N$ receptors (uncoupled from G-proteins) display only low-affinity for carbachol (Fig. 6, triangles).

It is worth noting that carbachol can activate all three classes of G-proteins at both M_1 and M_2 receptors (Fig. 1) and M_1 receptors pre-couple both to preferential $\text{G}_{q/11}$ and non-preferential $\text{G}_{i/o}$ G-proteins. In contrast, M_2 receptors pre-couple only to preferential $\text{G}_{i/o}$ G-proteins. $\text{G}_{i/o}$ are the major class of G-proteins in membranes from CHO cells, representing almost half of all G-proteins. To exclude the possibility that M_2 receptors do not pre-couple with $\text{G}_{q/11}$ G-proteins due to competition with preferential $\text{G}_{i/o}$ G-proteins, we attenuated the expression of $\text{G}_{i/o}$ α -subunits by siRNA to one quarter, making $\text{G}_{i/o}$ G-proteins the least abundant class in CHO membranes. Such reduction in expression of $\text{G}_{i/o}$ G-proteins diminishes the efficacy of carbachol in activating these preferential G-proteins to a level lower than at any of non-preferential G-proteins (Fig. 7). It also reduced its potency (Table 7 vs. Table 1). On the other hand, the potency of carbachol to stimulate $GTP\gamma\text{S}$ binding increases at non-preferential $\text{G}_{s/olf}$ and $\text{G}_{q/11}$ G-proteins, demonstrating competition among G-proteins for M_2 receptors [25]. In concert, the proportion of low-affinity sites increases and the effect of the anti- $\text{G}_{i/o}$ antibody is reduced (Fig. 8, cf. Table 4 and Table 8). Again, these findings indicate the presence of a lower proportion of high-affinity receptor/G-protein complexes. However, the anti- $\text{G}_{q/11}$ antibody has no effect on the proportion of low-affinity sites even after such reduction in the expression of $\text{G}_{i/o}$ G-proteins. This suggests that the lack of pre-coupling of $\text{G}_{q/11}$ G-proteins with M_2 receptors is not due to competition with $\text{G}_{i/o}$ G-proteins.

In summary, we show that muscarinic receptors pre-couple with their preferential class of G-proteins in the absence of an agonist. In contrast to the M_1 and M_3 receptors that pre-couple both with preferential $\text{G}_{q/11}$ and non-preferential $\text{G}_{i/o}$ G-proteins, the M_2 and M_4 receptors pre-couple only with their preferential $\text{G}_{i/o}$ G-

Table 7. Stimulation of $[^{35}\text{S}]GTP\gamma\text{S}$ binding by carbachol via M_2 receptors to $\text{G}_{i/o}$, $\text{G}_{s/olf}$ and $\text{G}_{q/11}$ subtypes of G-proteins in membranes with reduced expression of the $\text{G}_{i/o}$ subclass of G-proteins.

	pEC_{50}	E_{MAX}
$\text{G}_{i/o}$	5.01 ± 0.06	1.43 ± 0.08
$\text{G}_{s/olf}$	5.54 ± 0.05	1.82 ± 0.06
$\text{G}_{q/11}$	5.65 ± 0.05	1.63 ± 0.04

Data are means \pm S.E.M. From 3 experiments performed in quadruples. E_{MAX} is expressed as fold increase of basal binding.
doi:10.1371/journal.pone.0027732.t007

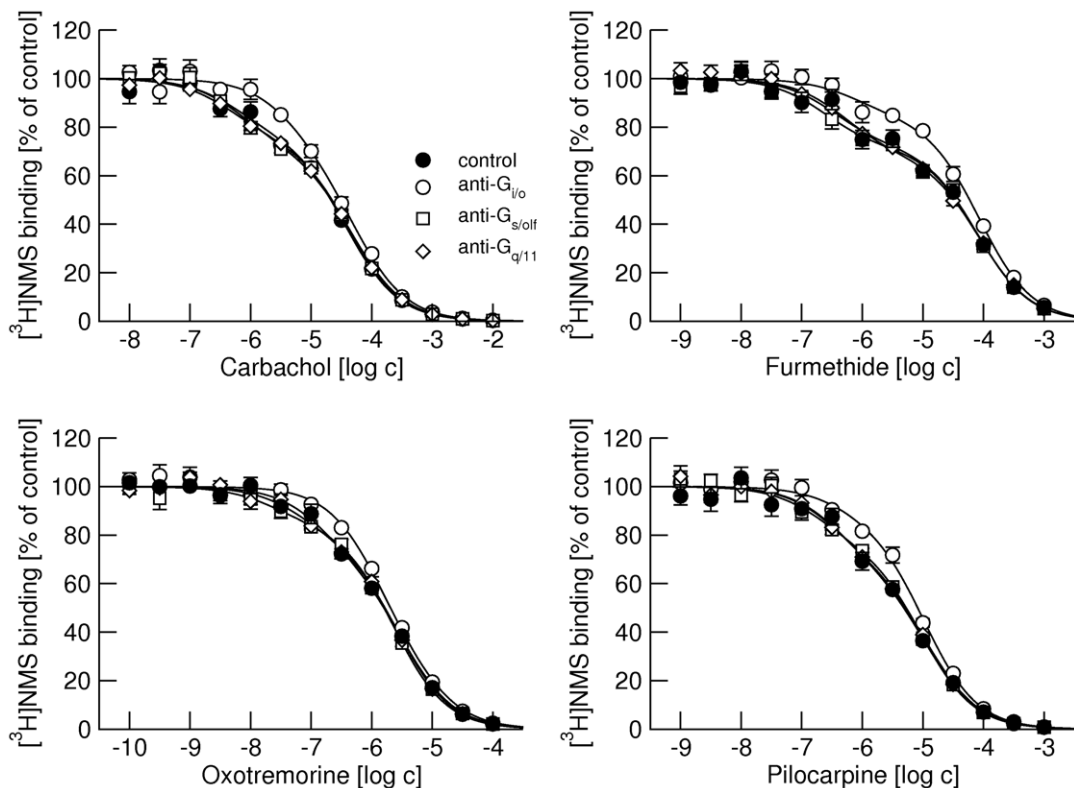


Figure 8. Effects of anti-G-protein antibodies on competition between agonists and $[^3\text{H}]$ NMS binding at M_2 receptors after suppression of $\text{G}_{i/o}$ G-proteins expression. Binding of 1 nM $[^3\text{H}]$ NMS to membranes from CHO cells expressing M_2 receptors after suppression of expression of $\text{G}_{i/o}$ G-proteins by siRNA was determined in the presence of increasing concentrations (abscissa, log M) of the agonists carbachol (upper left), furmethide (upper right), oxotremorine (lower left), and pilocarpine (lower right). Binding is expressed as per cent of control binding in the absence of agonist. Filled circles, control binding in the absence of antibodies. Open symbols, binding in the presence of anti- $\text{G}_{i/o}$ (circles), anti- $\text{G}_{s/olf}$ (squares) and anti- $\text{G}_{q/11}$ (diamonds) antibodies. Data are means \pm S.E.M. of values from 3 experiments performed in quadruplicate. Curves were fitted using equation 3 and results of fits are shown in Table 6.

doi:10.1371/journal.pone.0027732.g008

Table 8. Effects of IgG antibodies directed against α -subunits of individual subtypes of G-proteins on binding parameters of muscarinic agonists in membranes of M_2 CHO cells with reduced expression of $\text{G}_{i/o}$ G-proteins by siRNA.

		control	anti- $\text{G}_{i/o}$	anti- $\text{G}_{s/olf}$	anti- $\text{G}_{q/11}$
carbachol	pK _i high	6.85 \pm 0.08	6.89 \pm 0.07	6.94 \pm 0.08	6.77 \pm 0.07
	pK _i low	5.03 \pm 0.07	4.88 \pm 0.07	4.98 \pm 0.07	4.95 \pm 0.08
	f _{low}	73 \pm 8	90 \pm 8*	75 \pm 9	72 \pm 9
furmethide	pK _i high	7.07 \pm 0.08	6.72 \pm 0.07	7.91 \pm 0.07	6.97 \pm 0.08
	pK _i low	4.72 \pm 0.08	4.68 \pm 0.07	4.69 \pm 0.08	4.71 \pm 0.07
	f _{low}	72 \pm 7	86 \pm 7*	69 \pm 8	72 \pm 9
oxotremorine	pK _i high	7.55 \pm 0.09	7.54 \pm 0.08	7.76 \pm 0.08	7.63 \pm 0.08
	pK _i low	6.09 \pm 0.08	6.15 \pm 0.08	6.17 \pm 0.09	6.25 \pm 0.08
	f _{low}	78 \pm 8	89 \pm 7	84 \pm 8	79 \pm 7
pilocarpine	pK _i high	7.00 \pm 0.09	6.91 \pm 0.11	7.06 \pm 0.09	7.31 \pm 0.10
	pK _i low	5.55 \pm 0.09	5.58 \pm 0.09	5.54 \pm 0.09	5.62 \pm 0.09
	f _{low}	72 \pm 11	87 \pm 12	76 \pm 10	73 \pm 11

Data are means \pm S.E.M. From 3 experiments performed in quadruplicate. f_{low}, fraction of low-affinity sites in percent;

*, significantly different from control by t-test ($P < 0.05$).

doi:10.1371/journal.pone.0027732.t008

proteins. Lack of pre-coupling of the M_2 and M_4 receptors to $\text{G}_{q/11}$ G-proteins is not due to competition with preferential $\text{G}_{i/o}$ G-proteins. None of the four subtypes of muscarinic receptors pre-couples to $\text{G}_{s/olf}$ G-proteins. Thus, the mode of coupling of a given subtype of muscarinic receptors is governed by a combination of the receptor subtype and the class of G-protein. Advanced instrumental methods like fluorescence resonance energy transfer (FRET) between receptor and G-protein [7] and plasmon surface resonance [5] were developed to monitor kinetics of receptor G-protein interactions. Although these methods give better picture of receptor G-protein interaction, our simple method, that can only detect pre-coupling, does not require recombinant systems like FRET-based methods nor reconstituted systems like plasmon surface resonance methods and can be easily applied *ex vivo*, e.g. to tissues of experimental animals.

Materials and Methods

Materials

The radioligands $[^3\text{H}]$ -N-methylscopolamine chloride ($[^3\text{H}]$ NMS), guanosine-5'- γ [^{35}S]thiophosphate ($[^3\text{S}]$ GTP γ S), and anti-rabbit IgG-coated scintillation proximity beads were from Amersham (UK). Rabbit polyclonal antibodies against C-terminus of G-protein ($\text{G}_{i/o}$, C-10, and $\text{G}_{s/olf}$, C-18) were from Santa Cruz Biotechnology (Santa Cruz, CA). Carbamoylcholine chloride (carbachol), dithiotreitol, ethylenediaminetetraacetic acid (EDTA), guanosine-5'-biphosphate

sodium salt (GDP), guanosine-5'-[γ -thio]triphosphate tetralithium salt (GTP γ S), N-methylscopolamine bromide (NMS), and pilocarpine hydrochloride were from Sigma (St. Louis, MO). Oxotremorine sesquifumarate was from RBI (Natick, MA) and Nonidet P-40 was from USB Corporation (Cleveland, OH). Furfuryltrimethylammonium bromide (furmethide) was kindly donated by Dr. Shelkovnikov (University of St. Petersburg). Small interfering RNA (siRNA) was designed and synthesized by Ambion/Applied Biosystems, Czech Republic.

Cell culture and membrane preparation

Chinese hamster ovary cells stably transfected with the human M₁ to M₄ muscarinic receptor genes (CHO cells) were kindly donated by Prof. T.I.Bonner (National Institutes of Health, Bethesda, MD). Cell cultures and crude membranes were prepared as described previously [18]. Briefly, cells were grown to confluence in 75 cm² flasks in Dulbecco's modified Eagle's medium supplemented with 10% fetal bovine serum. Two million of cells were subcultured to 100 mm Petri dishes. Medium was supplemented with 5 mM butyrate for the last 24 hours of cultivation to increase receptor expression. Cells were detached by mild trypsinization on day 5 after subculture. Detached cells were washed twice in 50 ml of phosphate-buffered saline and 3 min centrifugation at 250 x g. Washed cells were suspended in 20 ml of ice-cold incubation medium (100 mM NaCl, 20 mM Na-HEPES, 10 mM MgCl₂; pH = 7.4) supplemented with 10 mM EDTA and homogenized on ice by two 30 sec strokes using Polytron homogenizer (Ultra-Turrax; Janke & Kunkel GmbH & Co. KG, IKA-Labortechnik, Staufen, Germany) with a 30-sec pause between strokes. Cell homogenates were centrifuged for 30 min at 30,000 x g. Supernatants were discarded, pellets resuspended in fresh incubation medium and centrifuged again. Resulting membrane pellets were kept at -20°C until assayed within 10 weeks at a maximum.

Attenuation of expression of G_{i/o} G-proteins

Expression of G_{i/o} G-proteins α -subunits was attenuated by siRNAs of following sequences (5'->3' sense): G_o, GGC UCC AAC ACC UAU GAA Gtt; G_{j1}, CCU CAA CAA AAG AAA GGA Ctt; G_{j2}, CCU CCA UCA UCC UCU UCC Utt; G_{j3}, GGG AGU GAC AGC AAU UAU Ctt. Cells were treated with complexes of all 4 siRNAs and lipofectamine 48 hours prior to experiment. Final concentrations were 50 nM for each siRNA and 0.5 vol. % for lipofectamine.

Preparation of new stable cell lines

New stable CHO cell lines expressing wild-type M₁ and mutant M₁ receptors have been prepared. Coding sequence of wild-type human M₁ muscarinic receptor (in expression vector pcDNA ver. 3.2, cDNA resource center, University of Missouri-Rolla, MO, USA) was mutated by PCR and mismatch primers using Qiagene QuickChange kit. Mutations were verified by sequencing of complete receptor coding sequence. Then CHO-K1 cells were transfected with either original M₁-pcDNA or mutated plasmid using Lipofectamine 2000 (Lipofectamine 10 μ l/ml, DNA 0.5 μ g/ml). After 48 hours geneticine was added to cultivation medium to final concentration of 800 μ g/ml. After selection, the concentration of geneticine was lowered to 50 μ g/ml and maintained during cultivation.

Equilibrium radioligand binding experiments

All radioligand binding experiments were optimized and carried out as described earlier [20]. Briefly, membranes were incubated in 96-well plates at 30 °C in the incubation medium described above that was supplemented with freshly prepared dithiothreitol

at a final concentration of 1 mM. Incubation volume was 200 μ l or 800 μ l for [³H]NMS saturation experiments. Approximately 30 and 10 μ g of membrane proteins per sample were used for [³H]NMS and [³⁵S]GTP γ S binding, respectively. N-methylscopolamine binding was measured directly in saturation experiments using six concentrations (30 pM to 1000 pM) of [³H]NMS for 1 hour. Depletion of radioligand was smaller than 20% for the lowest concentration. For calculations, radioligand concentrations were corrected for depletion. Agonist binding was determined in competition experiments with 1 nM [³H]NMS. Membranes were first preincubated 60 min with agonists and IgG antibodies against C-terminus of α -subunits of G-proteins, if applicable, and then incubated with [³H]NMS for additional 180 min. Final dilution of antibodies was 1:200 for G_{i/o} and G_{s/olf} and 1:500 for G_{q/11}. Nonspecific binding was determined in the presence of 10 μ M NMS. Agonist stimulated [³⁵S]GTP γ S binding was measured in a final volume of 200 μ l of incubation medium with 200 pM (M₁ or M₃ receptors) or 500 pM (M₂ or M₄ receptors) of [³⁵S]GTP γ S and 5 μ M (M₁ or M₃ receptors) or 50 μ M (M₂ or M₄ receptors) GDP for 20 min at 30°C after 60 min preincubation with GDP and agonist. Nonspecific binding was determined in the presence of 1 μ M unlabeled GTP γ S. Incubations were terminated by filtration through Whatman GF/F glass fiber filters (Whatman) using a Tomtech Mach III cell harvester (Perkin Elmer, USA). Filters were dried in vacuum for 1 h while heated at 60°C and then solid scintillator Meltilex A was melted on filters (105°C, 90 s) using a hot plate. The filters were cooled and counted in Wallac Microbeta scintillation counter.

Scintillation proximity assay

In case of scintillation proximity assay, incubation with [³⁵S]GTP γ S as described above was terminated by membrane solubilization by the addition of 20 μ l of 10% Nonidet P-40. After 20 min 10 μ l of individual primary antibodies against C-termini of G-protein α -subunits were added and incubation was continued for 1 h. The final dilution was 1:500 in case of anti-G_{i/o}- α and anti-G_{s/olf}- α antibodies and 1:1000 in case of the anti-G_{q/11}- α antibody. One batch of anti-rabbit IgG-coated scintillation beads was diluted in 20 ml of incubation medium and 50 μ l of the suspension was added to each well for 3 h. Then plates were spun for 15 min at 1,000 x g and counted using the scintillation proximity assay protocol in a Wallac Microbeta scintillation counter.

Data analysis

In general binding data were analyzed as described previously [20]. Data were preprocessed by Open Office version 3.2 (www.openoffice.org) and subsequently analyzed by Grace version 5.1 (plazma-gate.weizmann.ac.il) and statistic package R version 2.13 (www.r-project.org) on Scientific Linux version 6 distribution of GNU/Linux.

The following equations were fitted to data:

Saturation of radioligand binding

$$y = B_{MAX} * x / (x + K_D) \quad (1)$$

y, binding of radioligand at free concentration of radioligand x; B_{MAX}, maximum binding capacity; K_D, equilibrium dissociation constant.

Concentration-response

$$y = 1 + (E_{MAX}-1) / (1 + (EC_{50}/x)^{nH}) \quad (2)$$

y, radioactivity in the presence of agonist at concentration x normalized to radioactivity in the absence of agonist; E_{MAX}, maximal increase by agonist; EC₅₀, concentration of agonist producing 50% of maximal effect; nH, Hill coefficient.

Interference of agonist with [³H]NMS

$$y = (100 - f_{\text{low}}) * (1 - x / (IC_{50\text{high}} + x)) + f_{\text{low}} * (1 - x / (IC_{50\text{low}} + x)) \quad (3)$$

y, binding of radioligand at a concentration of displacer x normalized to binding in the absence of displacer; f_{low}, percentage of low affinity sites; IC_{50high}, concentration causing 50% decrease in binding to high affinity sites; IC_{50low}, concentration causing 50% decrease in binding to low affinity sites. Equilibrium

dissociation constant of displacer (K_I) was calculated according to Cheng and Prusoff [26].

Rate of association

$$y = B_{\text{eq}} * (1 - e^{-k_{\text{obs}} * x}) \quad (4)$$

y, binding of radioligand at a time x; B_{eq}, equilibrium binding; k_{obs}, observed rate of association.

Author Contributions

Conceived and designed the experiments: JJ AR HJ EEE VD. Performed the experiments: JJ AR HJ. Analyzed the data: JJ AR HJ EEE VD. Wrote the paper: JJ AR HJ EEE VD.

References

- Kroese WK, Sheffler DJ, Roth BL (2003) G-protein-coupled receptors at a glance. *J Cell Sci* 116: 4867–4869.
- Overington JP, Al-Lazikani B, Hopkins AL (2006) How many drug targets are there? *Nat Rev Drug Discov* 5: 993–996.
- Hein P, Bünnemann M (2009) Coupling mode of receptors and G proteins. *Naunyn Schmiedebergs Arch Pharmacol* 379: 435–443.
- Shea LD, Neubig RR, Linderman JJ (2000) Timing is everything—the role of kinetics in G protein activation. *Life Sci* 68: 647–658.
- Dell'orco D, Koch K (2011) A dynamic scaffolding mechanism for rhodopsin and transducin interaction in vertebrate vision. *Biochem J* in press; (doi:10.1042/BJ20110871).
- Okuma Y, Reisine T (1992) Immunoprecipitation of alpha 2a-adrenergic receptor-GTP-binding protein complexes using GTP-binding protein selective antisera. Changes in receptor/GTP-binding protein interaction following agonist binding. *J Biol Chem* 267: 14826–14831.
- Lachance M, Ether N, Wolbring G, Schnetkamp PP, Hébert TE (1999) Stable association of G proteins with beta 2AR is independent of the state of receptor activation. *Cell Signal* 11: 523–533.
- Hynes TR, Mervine SM, Yost EA, Sabo JL, Berlot CH (2004) Live cell imaging of Gs and the beta2-adrenergic receptor demonstrates that both alphas and beta1gamma7 internalize upon stimulation and exhibit similar trafficking patterns that differ from that of the beta2-adrenergic receptor. *J Biol Chem* 279: 44101–44112.
- Hein P, Frank M, Hoffmann C, Lohse MJ, Bünnemann M (2005) Dynamics of receptor/G protein coupling in living cells. *EMBO J* 24: 4106–4114.
- Michal P, Rudajev V, El-Fakahany EE, Dolezal V (2009) Membrane cholesterol content influences binding properties of muscarinic M2 receptors and differentially impacts activation of second messenger pathways. *Eur J Pharmacol* 606: 50–60.
- Bonner TI (1989) The molecular basis of muscarinic receptor diversity. *Trends Neurosci* 12: 148–151.
- Nobles M, Benians A, Tinker A (2005) Heterotrimeric G proteins precouple with G protein-coupled receptors in living cells. *Proc Natl Acad Sci U S A* 102: 18706–18711.
- Michal P, El-Fakahany EE, Dolezal V (2007) Muscarinic M2 receptors directly activate Gq/11 and Gs G-proteins. *J Pharmacol Exp Ther* 320: 607–614.
- Jakubík J, Janíčková H, El-Fakahany EE, Doležal V (2011) Negative cooperativity in binding of muscarinic receptor agonists and GDP as a measure of agonist efficacy. *Br J Pharmacol* 162: 1029–1044.
- Fraser CM, Wang CD, Robinson DA, Gocayne JD, Venter JC (1989) Site-directed mutagenesis of m1 muscarinic acetylcholine receptors: conserved aspartic acids play important roles in receptor function. *Mol Pharmacol* 36: 840–847.
- Scheerer P, Park JH, Hildebrand PW, Kim YJ, Krauss N, et al. (2008) Crystal structure of opsin in its G-protein-interacting conformation. *Nature* 455: 497–502.
- Zhu SZ, Wang SZ, Hu J, El-Fakahany EE (1994) An arginine residue conserved in most G protein-coupled receptors is essential for the function of the m1 muscarinic receptor. *Mol Pharmacol* 45: 517–523.
- Oldham WM, Hamm HE (2008) Heterotrimeric G protein activation by G-protein-coupled receptors. *Nat Rev Mol Cell Biol* 9: 60–71.
- Jakubík J, Bačáková L, Lisá V, El-Fakahany EE, Tuček S (1996) Activation of muscarinic acetylcholine receptors via their allosteric binding sites. *Proc Natl Acad Sci U S A* 93: 8705–8709.
- Jakubík J, El-Fakahany EE, Doležal V (2006) Differences in kinetics of xanomeline binding and selectivity of activation of G proteins at M(1) and M(2) muscarinic acetylcholine receptors. *Mol Pharmacol* 70: 656–666.
- De Lean A, Stadel JM, Lefkowitz RJ (1980) A ternary complex model explains the agonist-specific binding properties of the adenylyl cyclase-coupled beta-adrenergic receptor. *J Biol Chem* 255: 7108–7117.
- Gilchrist A, Mazzoni MR, Dineen B, Dice A, Linden J, et al. (1998) Antagonists of the receptor-G protein interface block Gi-coupled signal transduction. *J Biol Chem* 273: 14912–14919.
- Sykes DA, Dowling MR, Charlton SJ (2009) Exploring the mechanism of agonist efficacy: a relationship between efficacy and agonist dissociation rate at the muscarinic M3 receptor. *Mol Pharmacol* 76: 543–551.
- Qin K, Dong C, Wu G, Lambert NA (2011) Inactive-state preassembly of G(q)-coupled receptors and G(q) heterotrimers. *Nat Chem Biol* 7: 740–747.
- Kukkonen JP, Näslund J, Akerman KE (2001) Modelling of promiscuous receptor-Gi/Gs-protein coupling and effector response. *Trends Pharmacol Sci* 22: 616–622.
- Cheng Y, Prusoff WH (1973) Relationship between the inhibition constant (K_I) and the concentration of inhibitor which causes 50 per cent inhibition (I₅₀) of an enzymatic reaction. *Biochem Pharmacol* 22: 3099–3108.

NMR Structure and Action on Nicotinic Acetylcholine Receptors of Water-soluble Domain of Human LYNX1^{*§}

Received for publication, September 27, 2010, and in revised form, December 20, 2010 Published, JBC Papers in Press, January 20, 2011, DOI 10.1074/jbc.M110.189100

Ekaterina N. Lyukmanova[†], Zakhar O. Shenkarev[‡], Mikhail A. Shulepko[‡], Konstantin S. Mineev[‡], Dieter D'Hoedt[§], Igor E. Kasheverov[‡], Sergey Yu. Filkin[‡], Alexandra P. Krivolapova[‡], Helena Janickova^{¶¶}, Vladimir Dolezal^{¶¶}, Dmitry A. Dolgikh^{¶¶}, Alexander S. Arseniev[‡], Daniel Bertrand[§], Victor I. Tsetlin^{‡‡}, and Mikhail P. Kirpichnikov^{¶¶}

From the [‡]Shemyakin-Ovchinnikov Institute of Bioorganic Chemistry, Russian Academy of Sciences, 16/10 Miklukho-Maklaya Street, 117997 Moscow, Russia, the [§]Department of Neuroscience, Centre Medical Universitaire, 1 Rue Michel Servet, 1211 Geneva 4, Switzerland, the ^{¶¶}Institute of Physiology, Academy of Sciences of the Czech Republic, 14220 Prague, Czech Republic, and ^{¶¶}Lomonosov Moscow State University, 119991 Moscow, Russia

Discovery of proteins expressed in the central nervous system sharing the three-finger structure with snake α -neurotoxins provoked much interest to their role in brain functions. Proto-toxin LYNX1, having homology both to Ly6 proteins and three-finger neurotoxins, is the first identified member of this family membrane-tethered by a GPI anchor, which considerably complicates *in vitro* studies. We report for the first time the NMR spatial structure for the water-soluble domain of human LYNX1 lacking a GPI anchor (ws-LYNX1) and its concentration-dependent activity on nicotinic acetylcholine receptors (nAChRs). At 5–30 μ M, ws-LYNX1 competed with 125 I- α -bungarotoxin for binding to the acetylcholine-binding proteins (AChBPs) and to *Torpedo* nAChR. Exposure of *Xenopus* oocytes expressing α 7 nAChRs to 1 μ M ws-LYNX1 enhanced the response to acetylcholine, but no effect was detected on α 4 β 2 and α 3 β 2 nAChRs. Increasing ws-LYNX1 concentration to 10 μ M caused a modest inhibition of these three nAChR subtypes. A common feature for ws-LYNX1 and LYNX1 is a decrease of nAChR sensitivity to high concentrations of acetylcholine. NMR and functional analysis both demonstrate that ws-LYNX1 is an appropriate model to shed light on the mechanism of LYNX1 action. Computer modeling, based on ws-LYNX1 NMR structure and AChBP x-ray structure, revealed a possible mode of ws-LYNX1 binding.

Endogenous “prototoxins” like LYNX1, LYNX2, SLURP-1, and SLURP-2, belonging to the Ly6 protein family, modulate

nicotinic acetylcholine receptors (nAChRs)³ (1–8). In the central nervous system, LYNX1 and LYNX2 regulate nAChR activity, preventing excessive excitation (3, 4). Gene deletion of LYNX1 or LYNX2 indicates that these modulators are critical for nAChR function in the brain. LYNX1 knock-out mice demonstrated enhanced performance in specific tests of learning ability and memory, whereas loss of LYNX2 results in increased anxiety-related behaviors (3, 4). Prototoxins have also been shown to affect cell growth in lung carcinoma (9), are involved in skin diseases (6, 7), and are related to prostate stem cell antigen (10).

LYNX1 and LYNX2 are tethered to the membrane by a GPI anchor, which considerably complicates *in vitro* studies. LYNX1 is co-localized in the brain with α 4 β 2 and α 7 nAChRs (1–3), and its modulatory activity on α 4 β 2 nAChR was shown in experiments on *Xenopus* oocytes (1, 3). It was reported that soluble form of LYNX1 (not containing a GPI anchor) potentiates α 4 β 2 receptor (1), but the concentration at which it acts remains unknown. A secreted water-soluble protein SLURP-1 expressed in palmoplantar skin acts on α 7 nAChR and regulates keratinocyte proliferation (5).

It was predicted that the prototoxins should have a spatial structure similar to that of snake venom α -neurotoxins, effective competitive inhibitors of nAChR (1). α -Neurotoxins are characterized by a three-finger fold formed by three adjacent loops arising from a small globular hydrophobic core, cross-linked by four conserved disulfide bonds (11–13). Nicotinic acetylcholine receptors are targeted by short-chain α -neurotoxins, by long-chain α -neurotoxins with additional fifth disulfide in the central loop II and an extended C-terminal tail, and by structurally similar κ -bungarotoxins, as well as by some so-called nonconventional (or weak) neurotoxins. The latter, similarly to Ly6 proteins, have the additional fifth disulfide bond in the N-terminal loop I (see Fig. 1).

Elucidating molecular mechanisms of the prototoxins interaction with nAChRs requires the knowledge of their three-dimensional structures. Because the production of GPI-linked

* This work was supported by grants from the Russian Academy of Sciences “Molecular and Cellular Biology,” Russian Foundation for Basic Research (RFBR) Grants 08-04-01603 and 09-04-01567, RFBR-NWO (Netherlands Organization for Scientific Research) Grant 06-04-89400, and FP7 Grant “Neurocypres.”

§ The on-line version of this article (available at <http://www.jbc.org>) contains supplemental “Experimental Procedures,” Tables S1 and S2, Figs. S1–S3, and additional references.

The atomic coordinates and structure factors (code 2L03) have been deposited in the Protein Data Bank, Research Collaboratory for Structural Bioinformatics, Rutgers University, New Brunswick, NJ (<http://www.rcsb.org/>).

¹ Supported by Project AV0Z50110509 of the Institute of Physiology and Agency of the Czech Republic Grant 305/09/0681.

² To whom correspondence should be addressed: Shemyakin-Ovchinnikov Institute of Bioorganic Chemistry, Russian Academy of Sciences, 16/10 Miklukho-Maklaya str., 117997 Moscow, Russia. Tel.: 7-495-3355733; E-mail: vits@mx.ibch.ru.

³ The abbreviations used are: nAChR, nicotinic acetylcholine receptor; ws-LYNX1, water-soluble LYNX1; ACh, acetylcholine; AChBP, acetylcholine-binding protein; GPI, glycosylphosphatidylinositol; Ac-AChBP, *Aplysia californica* AChBP; Ls-AChBP, *Lymnaea stagnalis* AChBP; mAChR, muscarinic acetylcholine receptor; α -Cbtx, α -cobra toxin; WTX, weak toxin; α -Bgtx, α -bungarotoxin; NMS, N-methylscopolamine; Epi, epibatidine.

LYNX1 as an individual protein represents an unfeasible task, a water-soluble LYNX1 appears to be a good substitute for structural analysis and may provide an adequate model for functional studies. Here, we present the expression in *Escherichia coli* of a water-soluble LYNX1 lacking a GPI anchor (ws-LYNX1) and its high resolution NMR structure. It was found that the protein has classical a three-finger fold formed by two β -sheets composed of six antiparallel strands. A high degree of structural homology between ws-LYNX1 and other members of the Ly6/neurotoxin family was observed. Furthermore, we demonstrated the interaction of ws-LYNX1 with acetylcholine-binding proteins (AChBPs) and several nAChR subtypes. The observed competition with ^{125}I - α -bungarotoxin (α -Bgtx) for binding to AChBPs and *Torpedo* nAChR revealed partial overlap in binding sites for ws-LYNX1 and α -neurotoxins on the receptor surface. The concentration-dependent activation/deactivation effects of ws-LYNX1 on $\alpha 7$ nAChR were observed in electrophysiological experiments. This is of special interest because for LYNX1 itself, no concentration dependences were analyzed earlier.

EXPERIMENTAL PROCEDURES

Cloning and Bacterial Expression of ws-LYNX1—The *ws-lynx1* gene encoding 73 amino acids of water-soluble fragment of a human LYNX1 (UniProt database accession no. Q9BZG9) was constructed from six overlapping synthetic oligonucleotides (supplemental Table S1) using a three-stage PCR. The *ws-lynx1* gene was cloned into the expression vector pET-22b(+) (Novagen) on the NdeI and BamHI restriction sites. *E. coli* BL21(DE3) cells transformed with pET-22b(+)/*ws-lynx1* vector were grown at 37 °C on Terrific Broth medium using a fermenter (Bioflow 3000, New Brunswick Scientific) under automatic maintenance of oxygen content in the system at a level of 30%. Gene expression was induced by addition of isopropyl 1-thio- β -D-galactopyranoside to a final concentration of 0.025 mM at A_{600} 0.6, and cells were grown additionally for 18 h. Ws-LYNX1 was purified and refolded as was described for nonconventional neurotoxin WTX from *Naja kaouthia* venom (17). Briefly, ws-LYNX1 was extracted from inclusion bodies after incubation with 50 mM NaPi, 8 M urea, 1 mM tris(2-carboxyethyl)phosphine, 5 mM DTT, pH 7.4. Next, reduced ws-LYNX1 was purified on a SP Sepharose resin (GE Healthcare) equilibrated in 50 mM NaPi, 8 M urea, 5 mM DTT, pH 5.0. The protein was eluted by a gradient of NaCl. DTT and NaCl were removed by gel filtration on a NAP-25 column (GE Healthcare) equilibrated in 50 mM Tris/HCl, 8 M urea, pH 9.5. Refolding of ws-LYNX1 was induced by dissolving of reduced protein in a renaturation buffer (50 mM Tris/HCl, 1.5 M urea, 0.5 M L-Arg, 3 mM GSH, and 0.3 mM GSSG, pH 9.5) to final concentration of 0.1 mg/ml. Renaturation was performed during 3 days at 4 °C. The refolded ws-LYNX1 was analyzed and purified on a reverse-phase C4 HPLC column (4.6 × 250 mm, A300, Jupiter, Phenomenex). For production of ^{15}N -labeled ws-LYNX1, transformed cells were grown on Terrific Broth medium until A_{600} of 0.6. The cells were harvested (2000 × g for 20 min) and resuspended in an equal volume of minimal medium M9 containing $^{15}\text{NH}_4\text{Cl}$ as a nitrogen source, and afterward, gene expression was induced.

NMR Experiments and Spatial Structure Calculation—The NMR investigation was done using 0.5 mM samples of ^{15}N -labeled or unlabeled ws-LYNX1 in 5% D_2O or 100% D_2O at pH 5.3 and 25 °C. NMR spectra were acquired on a Bruker Avance 800 spectrometer equipped with a cryoprobe. ^1H and ^{15}N resonance assignment was obtained by a standard procedure using combination of two- and three-dimensional total correlation spectroscopy (TOCSY) and NOESY spectra (18). The $^3J_{\text{H}-\text{H}}$ and $^3J_{\text{NH}-\text{H}}$ coupling constants were determined using three-dimensional HNHA and HNHB experiments (19). The $^3J_{\text{H}-\text{H}}$ and $^3J_{\text{H}-\text{H}}$ coupling constants were measured using the ACME program (20) in the COSY spectrum in 100% D_2O solution. Spatial structure calculation was performed in the CYANA program (21). Upper interproton distance constraints were derived from NOESY ($\tau_m = 80$ ms) cross-peaks via a “1/ r^6 ” calibration. Torsion angle restraints and stereospecific assignments were obtained from J coupling constants and NOE intensities. Hydrogen bonds were introduced basing on temperature coefficients and deuterium exchange rates of HN protons (supplemental Fig. S2). The disulfide bond connectivity pattern was established on the basis of observed NOE contacts (22) and verified during preliminary stages of spatial structure calculation. In the final rounds of structure calculation, lower distance constraints (3.0 Å), based on the expected cross-peaks but not present in the NOESY spectra, were introduced. The NMR-derived data (atomic coordinates, chemical shifts, and restraints) have been deposited in the Protein Data Bank under accession code 2L03.

Binding of ws-LYNX1 to nAChRs and AChBPs—The binding of ws-LYNX1 to GH₄C1 cells expressing human $\alpha 7$ nAChR, nAChR-enriched *Torpedo californica* membranes, *Aplysia californica* AChBP (Ac-AChBP), and *Lymnaea stagnalis* AChBP (Ls-AChBP) was carried out in competitive experiments with ^{125}I - α -Bgtx as described in Ref. 23. The tested amounts of ws-LYNX1 (from 1 to 30 μM) were preincubated 3 h with the GH₄C1 cells expressing human $\alpha 7$ nAChR (final concentration of toxin-binding sites, 0.4 nM), or nAChR-enriched *Torpedo* membranes (final concentration of toxin-binding sites, 1.25 nM), or the Ls-AChBP, or Ac-AChBP (final concentration of toxin-binding sites 2.4 and 150 nM, respectively). Binding with the GH₄C1 cells and *Torpedo* membranes was carried out in 50 μl of 20 mM Tris/HCl buffer (containing 1 mg/ml of BSA, pH 8.0) and with the AChBPs, in 50 μl of binding buffer (PBS, containing 0.7 mg/ml of BSA and 0.05% Tween 20, pH 7.5), at 25 °C. Next, ^{125}I - α -Bgtx (~2000 Ci/mmol) was added to a final concentration of 0.15–0.35 nM for 5 min followed by filtration of reaction mixture on GF/C filters (Whatman, Maidstone) presoaked in 0.25% polyethylenimine (for cells and membranes) or on double DE-81 filters (Whatman) presoaked in binding buffer (for AChBPs). Unbound radioactivity was removed from the filters by washes (3 × 3 ml) with the respective incubation buffers. Nonspecific binding was determined in the presence of 10 μM α -cobratoxin (α -Cbt; 3-h preincubation).

The binding of ws-LYNX1 to SH-EP1 epithelial cells expressing human $\alpha 4\beta 2$ nAChR was carried out in competitive experiments with [^3H]epibatidine (49 Ci/mmol, Amersham Biosciences) as follows. The tested amounts of ws-LYNX1 (from 1 to

Structure-Function Study of Water-soluble LYNX1

30 μM) were incubated 4 h with SH-EP1 cells (final concentration of epibatidine-binding sites, 0.2 nM) and 2 nM [^3H]epibatidine. Filtration was performed on GF/C filters as mentioned above, and nonspecific binding was determined in the presence of 4 mM nicotine. Competition data were fit using ORIGIN (version 7.5; OriginLab Corp.) to a one-site dose-response curve using the Hill equation.

Binding of ws-LYNX1 to Muscarinic Acetylcholine Receptors—Membranes from CHO cells expressing individual subtypes of muscarinic receptors (for M₁ and M₃, 5 μg of membrane protein; for M₂, M₄, and M₅, 20 μg of membrane protein) were incubated for 60 min at 30 °C in the presence of 150 pM [^3H]NMS without (control) or with 10 μM ws-LYNX1. Incubation was terminated by fast filtration through GF/B filters (Whatman) essentially as described previously (24). Nonspecific binding was determined in the presence of 10 μM atropine.

Electrophysiology—Two-electrode voltage clamp experiments were performed on *Xenopus laevis* oocytes. Oocytes were prepared and injected as described in Ref. 25. Briefly, oocytes were injected with 2 ng of cDNA encoding for human $\alpha 4\beta 2$ (ratio 1:1), $\alpha 3\beta 2$ (ratio 1:1), or $\alpha 7$ nAChRs and utilized 2–3 days later. All recordings were performed with an automated two-electrode voltage clamp robot. Oocytes were clamped at −100 mV and perfused with OR2 (oocyte ringer) containing 82.5 mM NaCl, 2.5 mM KCl, 2.5 mM Ca₂Cl, 1 mM MgCl₂, 5 mM HEPES, and 20 $\mu\text{g}/\text{ml}$ BSA. OR2 was adjusted to pH 7.4. Atropine (0.5 μM) was added to all solutions to block activity of endogenous muscarinic receptors. Acetylcholine and ws-LYNX1 were dissolved in OR2 just before use. Data were digitized and analyzed off-line using MATLAB (Mathworks, Natick, MA).

Computer Modeling of ws-LYNX1·Ls-AChBP Complex—The x-ray structures of Ls-AChBP with nicotine, carbamylcholine, and α -Cbtx (Protein Data Bank codes 1UW6, 1UV6, and 1YI5, respectively) were used for modeling of the ws-LYNX1·Ls-AChBP complex. All 20 NMR structures of ws-LYNX1 were docked independently using both AutoDock (version 4) and HEX (version 4.5) programs. The solutions of the complexes were relaxed and underwent molecular dynamics simulation with GROMACS for 20-ns trajectories as described in Ref. 26 (the OPLS-AA force field was used). Ws-LYNX1 structure was also analyzed by molecular dynamics for 50 ns. The root mean square deviation to starting coordinates did not exceed 2.5 Å.

RESULTS

Expression of ws-LYNX1 in *E. coli*—The structural and functional studies require the milligram quantities of a protein. For obtaining the water-soluble domain of human LYNX1 (amino acid residues 1–73), the production in bacterial *E. coli* cells was chosen, as previous studies reported a successful application of bacterial systems for expression of α -neurotoxins (27). Several approaches, including the expression of thioredoxin-fused protein, secretion of ws-LYNX1 fused with the signal peptide of *E. coli* heat-stable enterotoxin II (STII) (NCBI accession number M35729), and the production in the form of *E. coli* inclusion bodies with subsequent refolding, were tested. Despite the fact that secretion system was the most efficient for production of short-chain and long-chain α -neurotoxins (28), its application

for ws-LYNX1 as well as production in the form of thioredoxin-fused protein (29) were unsuccessful. However, the direct expression into inclusion bodies followed by the refolding (see “Experimental Procedures”) resulted in the milligram scaled production of ws-LYNX1. Interestingly, a similar protocol was previously successfully applied for bacterial production of non-conventional (weak) toxin WTX from *N. kaouthia* venom, which, similarly to LYNX1, contains a fifth disulfide bond in the N-terminal loop (Fig. 1) (17). The yield of refolded ws-LYNX1 and of its ^{15}N -labeled analog was 1.8 and 0.5 mg/l of bacterial culture, respectively.

The homogeneity of the refolded ws-LYNX1 was confirmed by SDS-PAGE, analytical HPLC, and mass spectrometry (supplemental Fig. S1). The measured molecular mass of the recombinant protein (8400 Da) within experimental error coincides with the calculated mass of water-soluble domain of human LYNX1 (amino acids 1–73) with an additional Met residue at the N terminus and five closed disulfide bridges (8399.6 Da, supplemental Fig. S1C). Formation of disulfide bonds for the refolded ws-LYNX1 was additionally confirmed using Ellman’s reagent. CD spectroscopy of the refolded ws-LYNX1 revealed a preferentially β -structural organization (supplemental Fig. S1D).

Spatial Structure of ws-LYNX1 in Comparison with Structures of Other Three-finger Proteins—The spatial structure of ws-LYNX1 was studied by ^1H – ^{15}N NMR spectroscopy in aqueous solution at pH 5.3 (supplemental Fig. S2 and Table S2). The calculated set of 20 ws-LYNX1 structures and the representative structure are shown on Fig. 2. The protein is composed by three prolonged loops (I, II, and III) protruding from the “head” region. The secondary structure of ws-LYNX1 represents two antiparallel β -sheets, one consisting of two strands (Asp³–His⁵ and Pro¹⁷–Arg¹⁹ (loop I)) and another of four strands (Cys⁷–Tyr⁹ (loop I), Tyr²⁶–Thr³⁵ (loop II), Arg³⁸–Val⁴⁶ (loop II), and Ser⁶²–Cys⁶⁷ (loop III)). Almost the whole structure is well defined, except for a part of the third loop (residues Thr⁵²–Ala⁶¹) (Fig. 2B). The residues in this region demonstrate close to random coil values of ^1H chemical shifts and averaged $^3J_{\text{H}^N\text{H}^\alpha}$ coupling constants with magnitudes ~7 Hz. Moreover, no long and medium range NOE contacts were detected for these residues indicating enhanced mobility of this fragment.

The ws-LYNX1 structure is stabilized by four disulfide bonds in the head (Cys⁴–Cys²⁷, Cys²⁰–Cys⁴⁵, Cys⁴⁹–Cys⁶⁶, and Cys⁶⁷–Cys⁷²) and one in the first loop (Cys⁷–Cys¹⁴). These results confirm the disposition of disulfide bonds earlier proposed for LYNX1 (1). Apart from the backbone-backbone hydrogen bonds associated with canonical elements of secondary structure, the head and loops of the protein are stabilized by additional H-bonding and electrostatic interactions (Fig. 2C). For instance, two hydrogen bonds (HN Leu⁷¹–CO Asp³ and HN Asp³–O^{δ1} Asp⁷⁰) control the relative spatial arrangement of N and C termini of the protein. The N-H–N hydrogen bond (HN Asn¹⁶–N^{δ1} His⁵) and salt bridge (Asp³–Arg¹⁹) stabilize the first loop. The hydrogen bond HN Cys⁶⁶–O^{ε1} Glu⁵¹ stabilizes the third loop. In addition, several tight β - and γ -turns present in the tips of the loops I and II and in the head region (supplemental Fig. S2). The comparison of NMR spectra of the ws-LYNX1 measured at pH 5.3 and 7.0 (supplemental Fig. S3) indi-

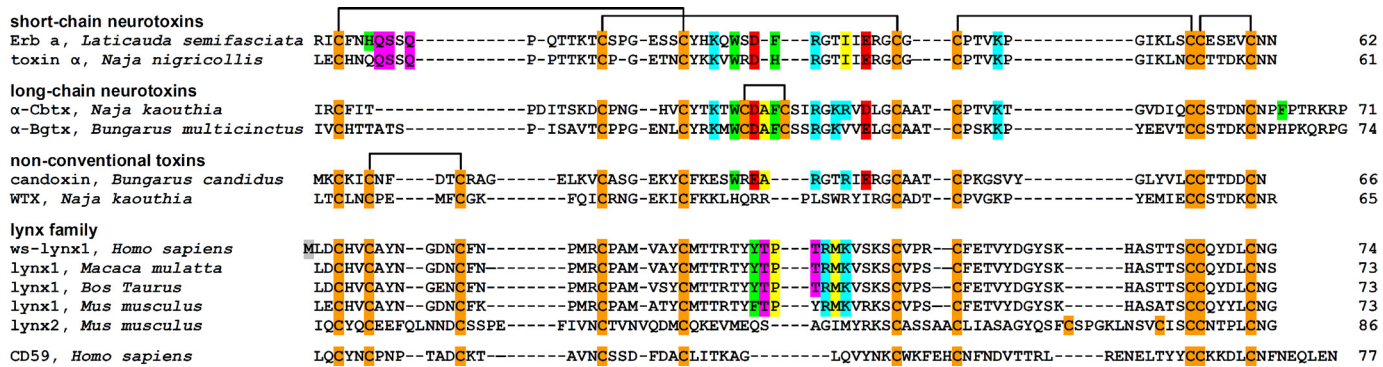


FIGURE 1. Amino acid sequence alignment of ws-LYNX1, other members of LYNX family (shown without GPI consensus sequence at the C terminus), CD59, and three-finger α -neurotoxins from snake venoms (upper panel) and comparison of spatial structures of ws-LYNX1, CD59, candoxin, erabutoxin-a, and α -cobratoxin (lower panel). The sequence data were obtained from Swiss-Prot Protein Database. The artificially introduced Met¹ residue in the ws-LYNX1 sequence is highlighted gray. Cysteine residues are colored in orange, and the disulfide linkages are shown. The atomic coordinates for α -Cbtx, erabutoxin-a, candoxin, and CD59 were taken from the Protein Data Bank (Protein Data Bank codes 2CTX, 1QKD, 1JGK, and 2J8B, respectively). Residues of α -Cbtx and erabutoxin-a important for binding to nAChRs according to mutagenesis data (14, 15), homologous residues in candoxin (16), and corresponding residues in loop II of ws-LYNX1 are shown. Aromatic, hydrophobic, positively charged, negatively charged, and polar residues are colored in green, yellow, blue, red, and magenta, respectively.

cates that the protein has similar spatial structure at neutral and moderately acidic conditions.

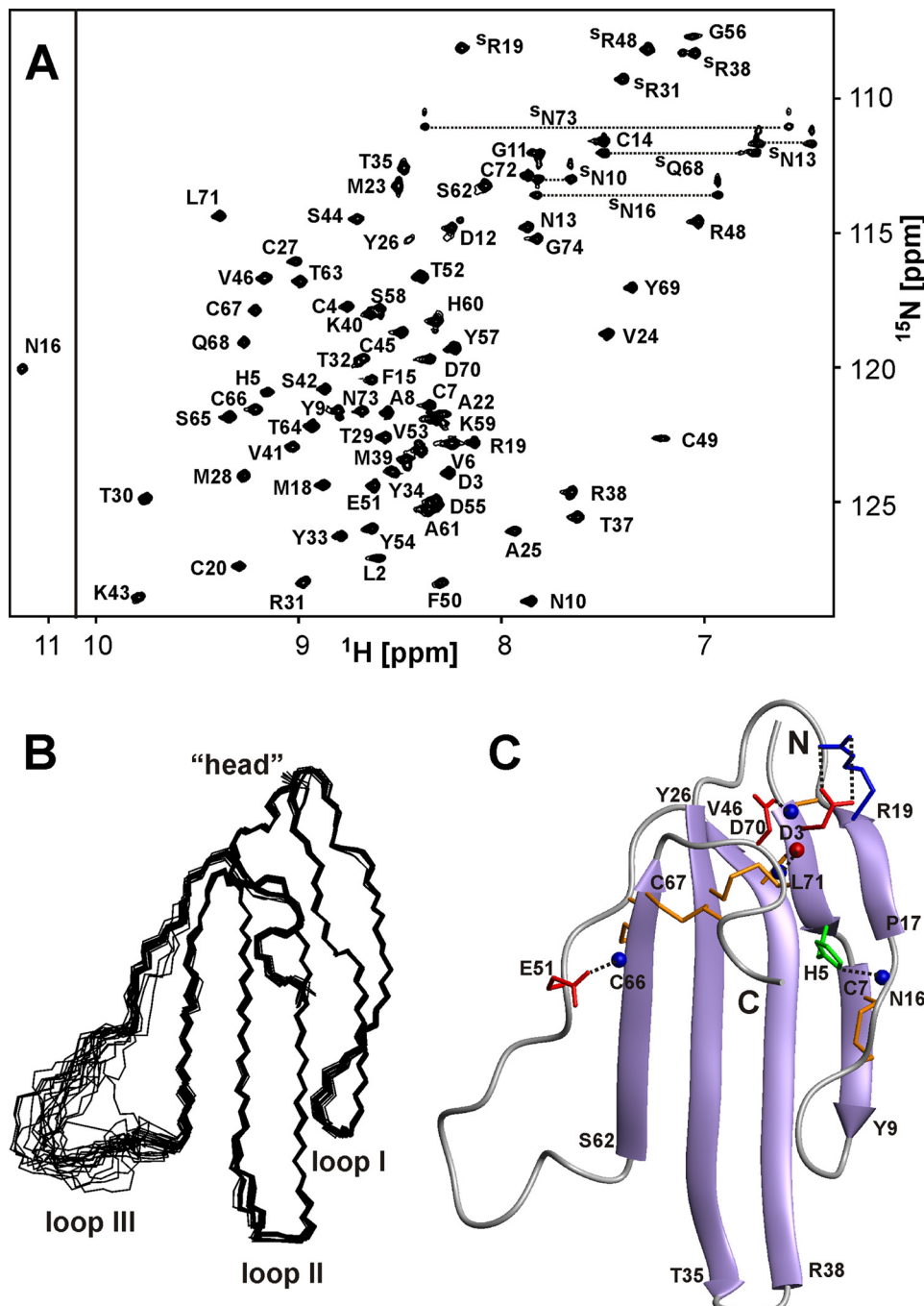
Because LYNX1 targets nAChRs, it is interesting to compare its three-dimensional structure with those of snake venom α -neurotoxins and some nonconventional toxins acting on nAChRs (16, 30, 31). CD59, the complement regulatory protein of the Ly6 family, was included for comparison because the spatial structure is known for its GPI-lacking form (32, 33). Fig. 1 shows a similarity in the overall fold for all these proteins. The fifth disulfide bond in the loop I is common for ws-LYNX1, nonconventional toxins, and CD59. However, a large and mostly disordered loop III is a unique feature of ws-LYNX1; CD59 protein also contains quite long insertion in the loop III, but this element is well structured and adopts an α -helical conformation in crystal and solution (32, 33).

ws-LYNX1 Binding to AChBPs, nAChRs, and Muscarinic AChRs—Previous studies demonstrated LYNX1 effects on the ACh-induced currents in *Xenopus* oocytes and cell lines expressing $\alpha 4\beta 2$ nAChR (1–3). However, it was not possible to quantify the observed activity and measure K_d or EC₅₀ for LYNX1 effects. Here, we measured the binding parameters for ws-LYNX1 interaction with nAChRs as well as with Ac-AChBP and Ls-AChBP, excellent structural models for nAChR ligand-binding domains (34). Because homo-oligomeric AChBPs are most similar to $\alpha 7$ homo-oligomeric nAChR, and as Ls-AChBP

binds α -Bgtx with nanomolar affinity, competition with radioactive α -Bgtx allows the detection of compounds that should bind to $\alpha 7$ nAChR (34, 35). Moreover, compounds that target other nAChR subtypes may also interact with AChBPs, although with a lower affinity (36).

The competition experiments with ¹²⁵I- α -Bgtx yielded an IC₅₀ $\sim 10 \mu M$ for ws-LYNX1 binding to AChBPs (Fig. 3A). Although the affinity is not high, the attempts to crystallize the ws-LYNX1-AChBP complexes were undertaken but still did not yield positive results.⁴ The binding of ws-LYNX1 to AChBPs suggests that it may also bind to nAChRs. Indeed, the presence of tight complexes of LYNX1 and $\alpha 7$ or $\alpha 4\beta 2$ nAChRs was earlier shown by co-immunoprecipitation (1–3). However, in the case of human $\alpha 7$ nAChRs overexpressed in the GH₄C₁ cell line, no competition with α -Bgtx was detected at 30 μM ws-LYNX1 (Fig. 3C). Under the conditions necessary to analyze competition with [³H]epibatidine for binding to $\alpha 4\beta 2$ nAChR in the SH-EP1 epithelial cell line, we achieved the same 30 μM concentration of ws-LYNX1, which did not show any inhibition (Fig. 3D). For comparison, the displacements of these radioactive ligands by α -bungarotoxin and epibatidine, respectively, are shown in these figures.

⁴ P. Rucktoo and T. Sixma, private communication.



Downloaded from www.jbc.org by guest, on March 13, 2013

FIGURE 2. NMR data define the spatial structure of ws-LYNX1 in aqueous solution. *A*, two-dimensional ^1H , ^{15}N -HSQC spectrum of ws-LYNX1 (0.5 mM, pH 5.3, 25 °C). The obtained resonance assignments are shown. The resonances of Asn and Gln NH₂ groups are connected by dotted lines. *B*, the set of the best 20 ws-LYNX1 structures superimposed over the backbone atoms in regions with well defined structure. The three loops and head of the protein are labeled. *C*, ribbon representation of ws-LYNX1 spatial structure. The electrostatic and hydrogen bonding interactions that stabilize the protein fold are shown. The Arg, Asp/Glu, and His side chains participating in salt bridges and hydrogen bonds with backbone amides are in blue, red, and green, respectively. The hydrogen bond H^N Leu⁷¹-CO Asp³ is also shown. Backbone amide and carbonyl groups are shown by blue and red spheres. The disulfide bonds are shown in orange.

Because LYNX2 was co-immunoprecipitated with muscle nAChR (4), we tested ws-LYNX1 binding to the muscle-type nAChR from *T. californica* and found IC₅₀ to be ~30 μM (Fig. 3*B*). Thus, the observed competitions pointed to a possible overlap in ws-LYNX1 and α-neurotoxin binding sites on the surfaces of AChBPs and muscle type nAChR.

The additional disulfide bond in the loop I and micromolar affinity to the muscle type and α7 nAChRs are characteristic for

some nonconventional neurotoxins, e.g. WTX (37). Because WTX binding to muscarinic acetylcholine receptors has been reported recently (38), we tested the interaction of ws-LYNX1 with M₁–M₅ muscarinic receptors. Fig. 3*E* shows that 10 μM ws-LYNX1 had no effect on all tested subtypes, with the exception of the M₃ receptor, for which a statistically significant 15% increase in [³H]N-methylscopolamine (NMS) binding in the presence of ws-LYNX1 was observed. A weak positive allosteric

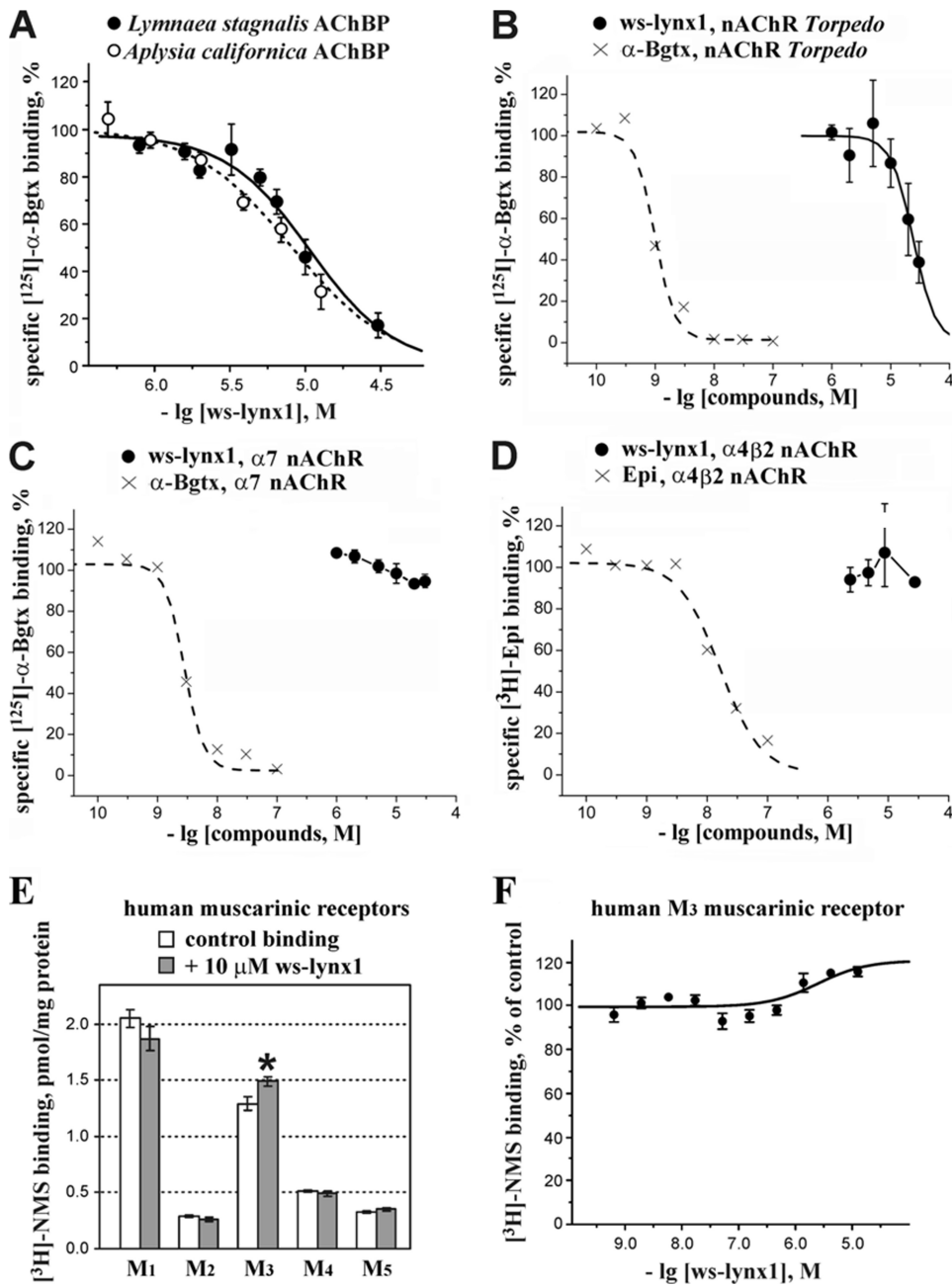


FIGURE 3. Binding of ws-LYNX1 to AChBPs and nicotinic and muscarinic acetylcholine receptors. Competition of ws-LYNX1 with $[^{125}\text{I}]$ - α -Bgtx for binding to Ls-AChBP and Ac-AChBP (A), to membrane-bound nAChR from *T. californica* (B), and to α 7 nAChR in the GH₄C₁ cell line (C). Competition of ws-LYNX1 with $[^3\text{H}]$ epibatidine for binding to α 4 β 2 nAChR in the SH-EP1 cell line is shown in D. For comparison, the displacements of $[^{125}\text{I}]$ - α -Bgtx and $[^3\text{H}]$ epibatidine by unlabeled Bgtx and epibatidine are also shown in these panels. Each point is mean \pm S.E. of three independent experiments. The Hill equation ($y = 100/(1 + ([\text{toxin}]/[\text{IC}_{50}]^{1/\alpha}))$) was fitted to normalized data (% of control binding). The calculated parameters IC_{50} and nH were 10.7 μM and 1.5 for Ls-AChBP, 9.4 μM and 1.2 for Ac-AChBP, and 24 μM and 2.3 for muscle-type nAChR. E, effects of 10 μM ws-LYNX1 on $[^3\text{H}]$ NMS binding at M₁–M₅ human muscarinic receptors expressed in membranes of CHO cells. The asterisk indicates that binding of $[^3\text{H}]$ NMS to the M₃ receptor in the presence of ws-LYNX1 was significantly different from control ($p < 0.05$, according to t test). Each point is mean \pm S.E. of quadruplicates. F, interaction of ws-LYNX1 with $[^3\text{H}]$ NMS binding at muscarinic M₃ receptor. Membranes expressing M₃ muscarinic receptor (5 μg of protein) were incubated in the presence of indicated concentrations of ws-LYNX1 and 108 pm $[^3\text{H}]$ NMS. $[^3\text{H}]$ NMS binding is expressed in percent of control binding in the absence of ws-LYNX1. Each point is mean \pm S.E. of quadruples. The equation ($y = 100 \times ([\text{NMS}] + K_d)/([NMS] + K_d + (K_a + 10^{[\text{ws-lynx1}]})/(K_a + 10^{[\text{ws-lynx1}]})^\alpha)$) was fitted to normalized data (% of control binding). K_d of $[^3\text{H}]$ NMS binding (207 pm) was determined in parallel saturation experiment. Estimated parameters are K_a (equilibrium dissociation constant of ws-LYNX1) 3.0 μM and a factor of cooperativity (α) of 0.8. The correlation coefficient of the fit is 0.8.

interaction (factor of cooperativity $\alpha \sim 0.8$) between ws-LYNX1 and $[^3\text{H}]$ NMS was confirmed in a pseudocompetition experiment at the M₃ receptor (Fig. 3F). The affinity of ws-LYNX1 was relatively low ($K_a \sim 3 \mu\text{M}$) as compared with the reported affinity of WTX ($K_a \sim 0.3 \mu\text{M}$). Nevertheless, the

obtained preliminary data point to a possible existence of non-nAChR molecular targets for LYNX1.

*Electrophysiology Studies and Effect of ws-LYNX1 on Human nAChRs—*Electrophysiological recordings were performed on *Xenopus* oocytes expressing α 4 β 2, α 3 β 2, and α 7 nAChRs in the

Structure-Function Study of Water-soluble LYNX1

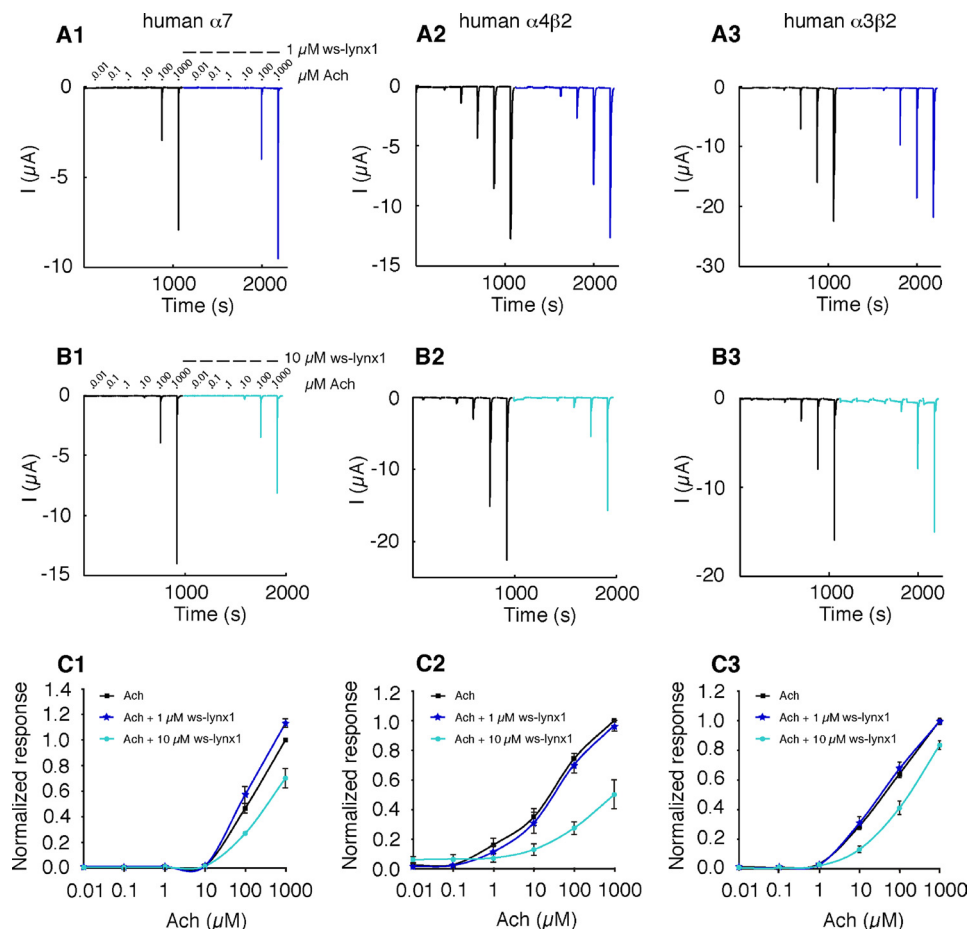


FIGURE 4. Effect of ws-LYNX1 on nAChRs expressed in *Xenopus* oocytes. A1–A3, concentration-response curve for ACh on human $\alpha 7$ (A1), human $\alpha 4\beta 2$ (A2), and human $\alpha 3\beta 2$ nAChRs (A3) in the absence and presence of 1 μM ws-LYNX1. B1–B3, ACh-induced responses on human $\alpha 7$ (B1), human $\alpha 4\beta 2$ (B2), and human $\alpha 3\beta 2$ nAChRs (B3) in the absence and presence of 10 μM ws-LYNX1. C1–C3, ACh-evoked activation curves of the fitted data for human $\alpha 7$ (C1), human $\alpha 4\beta 2$ (C2), and human $\alpha 3\beta 2$ nAChRs (C3) in the absence and presence of 1 and 10 μM ws-LYNX1 ($n = 3–11$). The highest ws-LYNX1 concentration (10 μM) affects the higher ACh-induced responses. At 1 μM ws-LYNX1 an increased response was observed for human $\alpha 7$ nAChR at 1000 μM ACh.

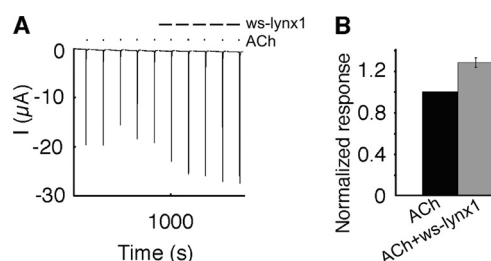


FIGURE 5. Effect of 1 μM ws-LYNX1 on human $\alpha 7$ nAChR expressed in *Xenopus* oocytes. A, five repetitive ACh (1000 μM) responses in the absence and presence of 1 μM ws-LYNX1. B, bar diagram of the data ($n = 6$), 1 μM ws-LYNX1 increases the ACh response.

absence and presence of 1 μM or 10 μM ws-LYNX1. Currents were measured at -100 mV and elicited by different ACh concentrations ranging from 10 nM to 1 mM. Application of 1 μM ws-LYNX1 showed no effect on $\alpha 4\beta 2$ and $\alpha 3\beta 2$; however, a slight enhancement of the ACh-induced currents was observed for $\alpha 7$ nAChR (Fig. 4, A and C). This effect was confirmed in another batch of cells using a single concentration of 1 mM ACh with or without exposure to 1 μM ws-LYNX1 ($n = 6$) (Fig. 5). Contrary to that, the application of 10 μM ws-LYNX1 resulted in inhibition of the ACh-induced currents for all three receptors, but the effect was more profound on $\alpha 4\beta 2$ nAChRs (Fig. 4,

B and C). Interestingly, the blocking effect of ws-LYNX is not suppressed by increasing ACh concentrations but becomes even more visible, especially for $\alpha 4\beta 2$ nAChRs as was earlier observed for the membrane-tethered LYNX1 (2). This suggests that inhibition caused by ws-LYNX1 is probably not competitive. For naturally occurring LYNX1 (although at unknown concentrations), an increase in desensitization rate has been described for $\alpha 4\beta 2$ nAChR (2), but our data did not reveal significant modification of the response time course in the presence of 1 μM or 10 μM ws-LYNX1 for any of receptors tested.

Computer Modeling of ws-LYNX1 Interaction with AChBP—The established NMR structure of ws-LYNX1 made possible the docking of ws-LYNX1 to Ls-AChBP and the comparison with binding modes for three-finger α -neurotoxins. The Ls-AChBP structures, with either loop C in an outward position (as in complex with competitive antagonist α -CbtX) or shifted to the central axis (as in complexes with agonists carbamylcholine and nicotine) (39, 40), were used. The docking and subsequent molecular dynamics studies revealed that the ws-LYNX1 affinity to Ls-AChBP in the latter case was considerably higher (estimated energies of interaction are -239 and -342 kJ/mol/binding site, respectively). Thus, ws-LYNX1 appears to stabilize loop C in the position characteristic for Ls-AChBP complexes with agonists.

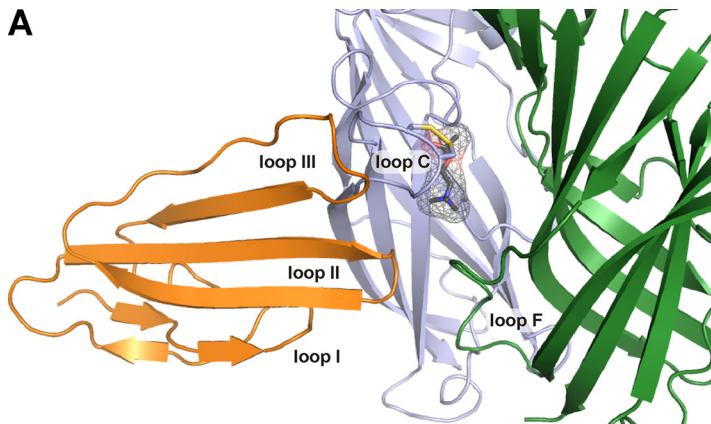
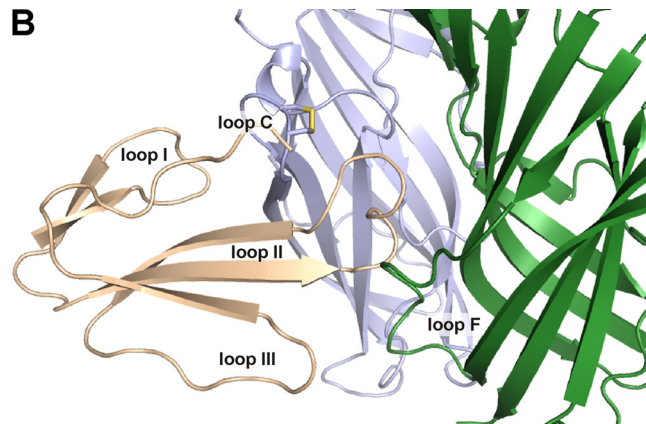
A**B**

FIGURE 6. Model of ws-LYNX1·Ls-AChBP complex (A) in comparison with the x-ray structure of α -Cbtx·Ls-AChBP complex (Protein Data Bank code 1Y15) (B). One subunit of AChBP (principal side of the interface) is in blue; the other (complementary side) is in green. The vicinal disulfide bond in C-loop of AChBP is marked by yellow. Ws-LYNX1 and α -Cbtx are in orange and beige, respectively. An ACh molecule is shown in A using a space-filled representation.

The resulting model for complex ws-LYNX1·Ls-AChBP is shown in Fig. 6A, and the structure of the α -Cbtx·Ls-AChBP complex (39) is given for comparison (Fig. 6B). Similarly to α -neurotoxins, the central loop II of ws-LYNX1 interacts with loop C of the AChBP protomer. At the same time, the model revealed some differences in the binding modes of ws-LYNX1 and α -Cbtx with Ls-AChBP. These include the disposition of the loop C and opposite orientations of ligands; the loop I of ws-LYNX1 is below loop II, and the loop I of α -Cbtx is above.

DISCUSSION

Membrane-tethered proteins LYNX1 and LYNX2 are co-localized with some nAChR subtypes and modulate their activity. The structure-function investigations of these natural GPI-tagged proteins would meet considerable problems, including their production in sufficient amounts, solubilization, and estimation of the effective concentrations. Thus, we focused our study on a recombinant water-soluble analog of LYNX1 that can permit detailed structure-function characterization. Due to expected spatial similarity of LYNX1 with secreted three-finger neurotoxins, we supposed that their action on nAChRs should have some common features and, at least in part, does not require the GPI anchor. Indeed, our NMR study revealed a high degree of structural homology between ws-LYNX1 expressed in *E. coli* and snake venom α -neurotoxins (Fig. 1). Moreover, the comparison of obtained electrophysiological data on ws-LYNX1 with previous investigations of natural membrane-tethered LYNX1 (2) revealed some similarities in their action on nAChRs (see below).

The presented data reveal new facets in the molecular mechanism of LYNX1 action on the nicotinic receptors. One such finding is the observation of competition between ws-LYNX1 and long-chain α -neurotoxin (α -Bgtx) for binding to *Torpedo* nAChR and to AChBPs. The measured binding parameters (Fig. 3, A and B) supplement the earlier co-immunoprecipitation data on binding of LYNX1 or LYNX2 to $\alpha 4\beta 2$, $\alpha 7$, and muscle-type nAChRs (2–4). The observed profound inhibition of ACh-evoked currents by 10 μ M ws-LYNX1 in $\alpha 4\beta 2$ nAChR (Fig. 4) agrees well with the previous proposal that this receptor subtype is possibly the major target for GPI-anchored proto-toxins LYNX1 and LYNX2 (2–4). Fig. 4 shows that 10 μ M ws-

LYNX1 also inhibited (reduced the current amplitude) $\alpha 7$ and $\alpha 3\beta 2$ nAChRs. No substantial effects were observed for $\alpha 7$ nAChR at 10 μ M ACh, but a clear reduction of the current was registered at 100 and 1000 μ M ACh. Interestingly, ws-LYNX1 at 1 μ M had no effect on currents induced in $\alpha 4\beta 2$ and $\alpha 3\beta 2$ nAChRs but significantly increased the current of $\alpha 7$ nAChRs (Fig. 5). These data imply the presence of concentration-dependent effects of ws-LYNX1 on $\alpha 7$ nAChRs resulting in potentiation or inhibition of the current amplitude. It should be noted that attempts to elucidate the concentration dependences were made previously only for the insect analog of LYNX1 by varying the amount of its cRNA introduced into oocytes (41). Moreover, LYNX1 action on $\alpha 3\beta 2$ nAChRs was not reported previously.

Because in binding studies we saw neither inhibition of [³H]epibatidine binding to $\alpha 4\beta 2$ nAChR nor of [¹²⁵I]- α -Bgtx association with $\alpha 7$ nAChR at 30 μ M ws-LYNX1, the effects observed in electrophysiological experiments with 1 and 10 μ M ws-LYNX1 indicate that, at least in part, its activity could arise from binding outside the classical nAChR binding site for agonists/competitive antagonists. This assumption is further supported by the fact that in electrophysiological experiments, the inhibitory effect of ws-LYNX1 becomes even more pronounced at high concentrations of ACh (Fig. 4, C2).

The observed competition between ws-LYNX1 and α -Bgtx for binding to muscle type nAChR and AChBPs suggests that the ws-LYNX1 binding site at least partially overlaps with the α -neurotoxin binding sites on these targets. The differences in the ws-LYNX1 interactions with distinct nAChR subtypes can be compared with those of the three-finger neurotoxins and α -conotoxins: α -Bgtx, a long-chain neurotoxin, binds to the $\alpha 7$ and muscle-type nAChRs, whereas short-chain neurotoxins target only the latter type. The most relevant to our case is the example of α -conotoxin ImII; it has the same potency as α -conotoxin ImI in blocking $\alpha 7$ nAChR but displaces [¹²⁵I]- α -Bgtx much more weakly (42). Moreover, it has been recently shown that binding of α -conotoxin ImII occurs at the classical site for agonists and competitive antagonists on AChBPs and $\alpha 7$ nAChR, whereas at *Torpedo* nAChR, this conotoxin binds mainly beyond this site (23).

The different action modes of ws-LYNX1 and snake neurotoxins can be attributed to considerable differences in the nature of their functional groups brought to the binding sites at the receptor. Fig. 1 depicts α -Cbtx side chains important for interaction with $\alpha 7$ nAChRs (14), whereas those necessary for binding of short-chain α -neurotoxins to muscle-type receptors (15) are shown on erabutoxin-a. The short- and long-chain neurotoxins, together with those nonconventional neurotoxins that block nAChRs with high affinity (e.g. candoxin (16)), have in loop II a combination of aromatic, positively and negatively charged residues (Fig. 1), which possibly determine the targeting of the toxin to the ligand binding pocket on the receptor surface (39, 43). A positively charged residue located in the tip of loop II (Arg^{33} in α -Cbtx and erabutoxin-a or Arg^{35} in candoxin) imitates a positive charge of ACh, thus preventing the simultaneous binding of neurotoxin and the agonist. Ws-LYNX1 does not have such a set of residues and in principle can be targeted to another site on the receptor surface, leaving a possibility for simultaneous ACh binding.

There is another group of three-finger proteins, so-called muscarinic toxins, mostly found in black mamba venoms, which block muscarinic acetylcholine receptors (44). The dual action of a three-finger protein on the nicotinic and muscarinic AChRs was described for WTX, a nonconventional weak neurotoxin from the *N. kaouthia* venom (38). In the present report, we showed the preliminary data about the ws-LYNX1 action on the M_3 subtype of human muscarinic AChR (Fig. 3, E and F), which, in view of the described similarities in the activity of ws-LYNX1 and LYNX1 on the nAChRs, suggest the necessity to check the action of GPI-attached LYNX1 on muscarinic AChRs and other putative targets.

Attaching α -Bgtx, a three-finger neurotoxin, to the membrane via GPI anchor preserved its inhibition of $\alpha 7$ nAChR (45). Our work, on the other hand, shows that the detachment of LYNX1, also a three-finger protein, from the membrane does not destroy its activity. The release of water-soluble forms from GPI-containing proteins due to effects of proteases and phospholipases is well known (46); such forms were detected for CD59 (33) and for uPAR proteins (composed of the prototypical three-finger domains), especially in cancer cells (47, 48). Thus, our results suggest that if membrane-detached LYNX1 arises, some *in vivo* activities similar to those of ws-LYNX1 may be anticipated.

The determined high resolution spatial structure of ws-lynx1 makes it possible to analyze how this molecule, and probably its progenitor LYNX1, recognizes the target. As the highest affinity for ws-LYNX1 was observed in binding to AChBPs, and the x-ray structures for these proteins are known, at the first stage, we confined this analysis to computer modeling of the ws-LYNX1 complex with the *L. stagnalis* AChBP. We have chosen this particular protein because the x-ray structure of its complex with α -Cbtx, a three-finger neurotoxin, is known (39).

The results of docking and molecular dynamics illustrate a general similarity between binding of ws-LYNX1 and α -Cbtx (Fig. 6). However, marked dissimilarities were also identified; α -Cbtx approaches the target with one side of its relatively flat molecule, whereas ws-LYNX1 approaches with the opposite side. In addition, the binding site for ws-LYNX1 overlaps only

partially with that for snake neurotoxin. Contrary to α -Cbtx (Fig. 6), ws-LYNX1 appears to stabilize the loop C of AChBP in position closer to the central axis in a conformation that was observed previously in complexes of AChBPs with agonists (40). In principle, this would even allow a simultaneous binding of ws-LYNX1 and acetylcholine depicted in the model. However, further studies are needed to verify how this model is close to reality and to what extent it is applicable to different nAChR subtypes.

In summary, the results presented here demonstrate that the water-soluble domain of human LYNX1 (ws-LYNX1), obtained by expression in *E. coli*, is an individual protein with the correct primary structure and well defined three-dimensional structure. A high resolution NMR study of ws-LYNX1 demonstrated a three-finger fold well characterized earlier for snake venom neurotoxins. However, the marked differences between ws-LYNX1 and neurotoxins in the conformation of individual loops were revealed. In general, it was shown that ws-LYNX1 provides a good model to elucidate at the molecular level the modulatory effects of LYNX1 on nAChRs. Indeed, we characterized the interaction of ws-LYNX1 with several nAChR subtypes and AChBPs. Our results for the first time demonstrated a concentration dependence of ws-LYNX1 modulatory effects and indicated that the activity of the naturally occurring LYNX1 and its congeners is most probably not restricted to $\alpha 4\beta 2$ nAChR. Determination of the high resolution NMR structure of ws-LYNX1, one of the initial stages of our research in this field, made docking and molecular dynamics analysis of ws-LYNX1 interaction with its targets possible. We hope that future mutagenesis studies, based on the solved spatial structure of ws-LYNX1 and computational models, will shed light on the detailed molecular mechanisms of LYNX1 modulating effects.

Acknowledgments—We are grateful to T. Sixma for the samples of acetylcholine binding proteins, F. Hucho for the membrane-bound nicotinic receptor from *T. californica*, Eli Lilly for the $\text{GH}_4\text{C}1$ line with the overexpressed $\alpha 7$ nicotinic receptor, R. Lukas for the line with $\alpha 4\beta 2$ receptor, and R. V. Tikhonov for assistance in recombinant protein production. Fruitful discussions with I. Ibanez-Tallón are highly appreciated. The computations were performed at the Research Computing Center SKIF-MSU Chebyshev.

REFERENCES

1. Miwa, J. M., Ibanez-Tallón, I., Crabtree, G. W., Sánchez, R., Sali, A., Role, L. W., and Heintz, N. (1999) *Neuron* **23**, 105–114
2. Ibañez-Tallón, I., Miwa, J. M., Wang, H. L., Adams, N. C., Crabtree, G. W., Sine, S. M., and Heintz, N. (2002) *Neuron* **33**, 893–903
3. Miwa, J. M., Stevens, T. R., King, S. L., Caldarone, B. J., Ibanez-Tallón, I., Xiao, C., Fitzsimonds, R. M., Pavlides, C., Lester, H. A., Picciotto, M. R., and Heintz, N. (2006) *Neuron* **51**, 587–600
4. Tekinay, A. B., Nong, Y., Miwa, J. M., Lieberam, I., Ibanez-Tallón, I., Greengard, P., and Heintz, N. (2009) *Proc. Natl. Acad. Sci. U.S.A.* **106**, 4477–4482
5. Chimienti, F., Hogg, R. C., Plantard, L., Lehmann, C., Brakch, N., Fischer, J., Huber, M., Bertrand, D., and Hohl, D. (2003) *Hum. Mol. Genet.* **12**, 3017–3024
6. Tsuji, H., Okamoto, K., Matsuzaka, Y., Iizuka, H., Tamiya, G., and Inoko, H. (2003) *Genomics* **81**, 26–33
7. Moriwaki, Y., Watanabe, Y., Shinagawa, T., Kai, M., Miyazawa, M., Okuda,

- T., Kawashima, K., Yabashi, A., Waguri, S., and Misawa, H. (2009) *Neurosci. Res.* **64**, 403–412
8. Arredondo, J., Chernyavsky, A. I., Jolkovsky, D. L., Webber, R. J., and Grando, S. A. (2006) *J. Cell. Physiol.* **208**, 238–245
 9. Song, P., Sekhon, H. S., Fu, X. W., Maier, M., Jia, Y., Duan, J., Proskosil, B. J., Gravett, C., Lindstrom, J., Mark, G. P., Saha, S., and Spindel, E. R. (2008) *Cancer Res.* **68**, 4693–4700
 10. Hruska, M., Keefe, J., Wert, D., Tekinay, A. B., Hulce, J. J., Ibañez-Tallon, I., and Nishi, R. (2009) *J. Neurosci.* **29**, 14847–14854
 11. Tsetlin, V. (1999) *Eur. J. Biochem.* **264**, 281–286
 12. Nirthanian, S., and Gwee, M. C. (2004) *J. Pharmacol. Sci.* **94**, 1–17
 13. Tsetlin, V. I., and Hucho, F. (2004) *FEBS Lett.* **557**, 9–13
 14. Antil-Delbeke, S., Gaillard, C., Tamiya, T., Corringer, P. J., Changeux, J. P., Servent, D., and Ménez, A. (2000) *J. Biol. Chem.* **275**, 29594–29601
 15. Pillet, L., Tréneau, O., Ducancel, F., Drevet, P., Zinn-Justin, S., Pinkasfeld, S., Boulain, J. C., and Ménez, A. (1993) *J. Biol. Chem.* **268**, 909–916
 16. Nirthanian, S., Charpartier, E., Gopalakrishnakone, P., Gwee, M. C., Khoo, H. E., Cheah, L. S., Bertrand, D., and Kini, R. M. (2002) *J. Biol. Chem.* **277**, 17811–17820
 17. Lyukmanova, E. N., Shulepko, M. A., Tikhonov, R. V., Shenkarev, Z. O., Paramonov, A. S., Wulfson, A. N., Kasheverov, I. E., Ustich, T. L., Utkin, Y. N., Arseniev, A. S., Tsetlin, V. I., Dolgikh, D. A., and Kirpichnikov, M. P. (2009) *Biochemistry* **74**, 1142–1149
 18. Wuthrich, K. (1986) *NMR of Proteins and Nucleic Acids*, John Wiley and Sons, New York
 19. Bax, A., Vuister, G. W., Grzesiek, S., Delaglio, F., Wang, A. C., Tschudin, R., and Zhu, G. (1994) *Methods Enzymol.* **239**, 79–105
 20. Delaglio, F., Wu, Z., and Bax, A. (2001) *J. Magn. Reson.* **149**, 276–281
 21. Güntert, P. (2004) *Methods Mol. Biol.* **278**, 353–378
 22. Arseniev, A. S., Kondakov, V. I., Maiorov, V. N., and Bystrov, V. F. (1984) *FEBS Lett.* **165**, 57–62
 23. Kasheverov, I. E., Zhmak, M. N., Fish, A., Rucktooa, P., Khruschov, A. Y., Osipov, A. V., Ziganshin, R. H., D'hoedt, D., Bertrand, D., Sixma, T. K., Smit, A. B., and Tsetlin, V. I. (2009) *J. Neurochem.* **111**, 934–944
 24. Jakubik, J., El-Fakahany, E. E., and Dolezal, V. (2006) *Mol. Pharmacol.* **70**, 656–666
 25. Hogg, R. C., Bandelier, F., Benoit, A., Dosch, R., and Bertrand, D. (2008) *J. Neurosci. Methods* **169**, 65–75
 26. Mordvintsev, D. Y., Polyak, Y. L., Kuzmin, D. A., Levtsova, O. V., Tourleigh, Y. V., Utkin, Y. N., Shaitan, K. V., and Tsetlin, V. I. (2007) *Comput. Biol. Chem.* **31**, 72–81
 27. Lyukmanova, E. N., Shulepko, M. A., Shenkarev, Z. O., Dolgikh, D. A., and Kirpichnikov, M. P. (2010) *Russian J. Bioorg. Chem.* **36**, 137–145
 28. Lyukmanova, E. N., Shenkarev, Z. O., Schulga, A. A., Ermolyuk, Y. S., Mordvintsev, D. Y., Utkin, Y. N., Shoulepko, M. A., Hogg, R. C., Bertrand, D., Dolgikh, D. A., Tsetlin, V. I., and Kirpichnikov, M. P. (2007) *J. Biol. Chem.* **282**, 24784–24791
 29. Lyukmanova, E. N., Shulga, A. A., Arsenieva, D. A., Pluzhnikov, K. A., Dolgikh, D. A., Arseniev, A. S., and Kirpichnikov, M. P. (2004) *Russian J. Bioorg. Chem.* **30**, 25–34
 30. Betzel, C., Lange, G., Pal, G. P., Wilson, K. S., Maelicke, A., and Saenger, W. (1991) *J. Biol. Chem.* **266**, 21530–21536
 31. Nastopoulos, V., Kanellopoulos, P. N., and Tsernoglou, D. (1998) *Acta Crystallogr. D Biol. Crystallogr.* **54**, 964–974
 32. Leath, K. J., Johnson, S., Roversi, P., Hughes, T. R., Smith, R. A., Mackenzie, L., Morgan, B. P., and Lea, S. M. (2007) *Acta Crystallogr. Sect. F Struct. Biol. Cryst. Commun.* **63**, 648–652
 33. Fletcher, C. M., Harrison, R. A., Lachmann, P. J., and Neuhaus, D. (1994) *Structure* **2**, 185–199
 34. Rucktooa, P., Smit, A. B., and Sixma, T. K. (2009) *Biochem. Pharmacol.* **78**, 777–787
 35. Celie, P. H., Kasheverov, I. E., Mordvintsev, D. Y., Hogg, R. C., van Nierop, P., van Elk, R., van Rossum-Fikkert, S. E., Zhmak, M. N., Bertrand, D., Tsetlin, V., Sixma, T. K., and Smit, A. B. (2005) *Nat. Struct. Mol. Biol.* **12**, 582–588
 36. Dutertre, S., Ulens, C., Büttner, R., Fish, A., van Elk, R., Kendel, Y., Hopping, G., Alewood, P. F., Schroeder, C., Nicke, A., Smit, A. B., Sixma, T. K., and Lewis, R. J. (2007) *EMBO J.* **26**, 3858–3867
 37. Utkin, Y. N., Kukhtina, V. V., Kryukova, E. V., Chiodini, F., Bertrand, D., Methfessel, C., and Tsetlin, V. I. (2001) *J. Biol. Chem.* **276**, 15810–15815
 38. Mordvintsev, D. Y., Polyak, Y. L., Rodionov, D. I., Jakubik, J., Dolezal, V., Karlsson, E., Tsetlin, V. I., and Utkin, Y. N. (2009) *FEBS J.* **276**, 5065–5075
 39. Bourne, Y., Talley, T. T., Hansen, S. B., Taylor, P., and Marchot, P. (2005) *EMBO J.* **24**, 1512–1522
 40. Celie, P. H., van Rossum-Fikkert, S. E., van Dijk, W. J., Brejc, K., Smit, A. B., and Sixma, T. K. (2004) *Neuron* **41**, 907–914
 41. Liu, Z., Cao, G., Li, J., Bao, H., and Zhang, Y. (2009) *J. Neurochem.* **110**, 1707–1714
 42. Ellison, M., McIntosh, J. M., and Olivera, B. M. (2003) *J. Biol. Chem.* **278**, 757–764
 43. Dellisanti, C. D., Yao, Y., Stroud, J. C., Wang, Z. Z., and Chen, L. (2007) *Nat. Neurosci.* **10**, 953–962
 44. Servent, D., and Fruchart-Gaillard, C. (2009) *J. Neurochem.* **109**, 1193–1202
 45. Ibañez-Tallon, I., Wen, H., Miwa, J. M., Xing, J., Tekinay, A. B., Ono, F., Brehm, P., and Heintz, N. (2004) *Neuron* **43**, 305–311
 46. Montuori, N., and Ragno, P. (2009) *Front. Biosci.* **14**, 2494–2503
 47. Lomholt, A. F., Hoyer-Hansen, G., Nielsen, H. J., and Christensen, I. J. (2009) *Br. J. Cancer* **101**, 992–997
 48. Rasch, M. G., Lund, I. K., Almasi, C. E., and Hoyer-Hansen, G. (2008) *Front. Biosci.* **13**, 6752–6762

RESEARCH PAPER

Negative cooperativity in binding of muscarinic receptor agonists and GDP as a measure of agonist efficacy

J Jakubík¹, H Janíčková¹, EE El-Fakahany² and V Doležal¹

¹Institute of Physiology Academy of Sciences of the Czech Republic, Prague, Czech Republic, and

²Division of Neuroscience Research in Psychiatry, University of Minnesota Medical School, Minneapolis, MN, USA

Correspondence

Jan Jakubík, Institute of Physiology, AV ČR, v.v.i., Vídeňská 1083, 142 20 Praha, Czech Republic. E-mail: jakubik@biomed.cas.cz

Re-use of this article is permitted in accordance with the Terms and Conditions set out at http://wileyonlinelibrary.com/onlineopen#OnlineOpen_Terms

Keywords

muscarinic acetylcholine receptors; agonist efficacy; GDP binding

Received

17 June 2010

Revised

23 August 2010

Accepted

22 September 2010

BACKGROUND AND PURPOSE

Conventional determination of agonist efficacy at G-protein coupled receptors is measured by stimulation of guanosine-5'-γ-thiotriphosphate (GTPγS) binding. We analysed the role of guanosine diphosphate (GDP) in the process of activation of the M₂ muscarinic acetylcholine receptor and provide evidence that negative cooperativity between agonist and GDP binding is an alternative measure of agonist efficacy.

EXPERIMENTAL APPROACH

Filtration and scintillation proximity assays measured equilibrium binding as well as binding kinetics of [³⁵S]GTPγS and [³H]GDP to a mixture of G-proteins as well as individual classes of G-proteins upon binding of structurally different agonists to the M₂ muscarinic acetylcholine receptor.

KEY RESULTS

Agonists displayed biphasic competition curves with the antagonist [³H]-N-methylscopolamine. GTPγS (1 μM) changed the competition curves to monophasic with low affinity and 50 μM GDP produced a similar effect. Depletion of membrane-bound GDP increased the proportion of agonist high-affinity sites. Carbachol accelerated the dissociation of [³H]GDP from membranes. The inverse agonist N-methylscopolamine slowed GDP dissociation and GTPγS binding without changing affinity for GDP. Carbachol affected both GDP association with and dissociation from G_{i/o} G-proteins but only its dissociation from G_{s/olf} G-proteins.

CONCLUSIONS AND IMPLICATIONS

These findings suggest the existence of a low-affinity agonist-receptor conformation complexed with GDP-ligated G-protein. Also the negative cooperativity between GDP and agonist binding at the receptor/G-protein complex determines agonist efficacy. GDP binding reveals differences in action of agonists versus inverse agonists as well as differences in activation of G_{i/o} versus G_{s/olf} G-proteins that are not identified by conventional GTPγS binding.

Abbreviations

CHO cells, Chinese hamster ovary cells; GDP, guanosine diphosphate; GTPγS, guanosine-5'-γ-thiotriphosphate; NMS, N-methylscopolamine

Introduction

Almost 900 genes of the human genome encode several thousands of G-protein coupled receptors (GPCRs). GPCRs thus represent the largest family of receptors. The heterotrimeric guanine nucleotide-binding proteins (G-proteins) function to transduce signals from these receptors to effector systems including enzymes, such as adenylyl cyclase and phospholipase C and ion channels. Binding of an agonist to a GPCR induces conformational changes in the receptor protein that enable the receptor to promote guanosine diphosphate (GDP) release from the α -subunit of interacting heterotrimeric G-proteins ($G\alpha$) (Wess, 1997) and formation of a high-affinity complex with guanine nucleotide-free $G\alpha$ (Kent *et al.*, 1980). The $G\alpha$ subunit dissociates from the agonist-receptor- $G\alpha$ complex upon binding of GTP and releases free $G\alpha$ with bound GTP and $\beta\gamma$ dimer, both of which are involved in regulation of the activity of various effector systems.

The biological activity of an agonist is a product of both affinity and efficacy. While affinity of an agonist for a receptor is strictly given by free binding energy, agonist efficacy in transducing a signal across the cell membrane depends on time-ordered complex conformational changes involving interactions among agonist, receptor, G-protein and guanine nucleotides. These interactions and the resulting conformational changes are less well characterized. In their pioneering work, De Lean *et al.* (1980) reported that GDP did not affect the efficacy of β -adrenoceptor agonists at G_s G-protein-coupled receptors. However, it has been repeatedly demonstrated that GDP affects binding of agonists at G_i G-protein coupled GPCRs (Florio and Sternweis, 1989; Tota and Schimerlik, 1990), muscarinic agonists decrease GDP binding (Haga *et al.*, 1986; Shiozaki and Haga, 1992) and accelerate its dissociation (Ferguson *et al.*, 1986). Although the structural basis for many steps in the G-protein nucleotide cycle have been clarified over the past decade, the precise mechanism for receptor-mediated G-protein activation (GDP-GTP exchange) remains incompletely defined largely because of difficulties in obtaining crystals of receptor G-protein complexes for X-ray diffraction analysis (Johnston and Siderovski, 2007; Oldham and Hamm, 2008).

The aim of our study was to investigate in detail the mechanisms that determine efficacy of agonists at individual classes of G-proteins coupled to M_2 muscarinic acetylcholine receptors in natural membrane environments. We performed detailed analyses of allosteric interactions between guanine nucleotides and four structurally distinct agonists exhibiting different potencies and efficacies at the M_2 receptor expressed in Chinese hamster ovary (CHO) cells. We showed that the efficacy of these agonists in stimulation of GTP binding correlates with the magnitude of negative cooperativity with GDP binding to the receptor G-protein complex. These data suggest that the decrease in GDP affinity due to acceleration of its dissociation plays a key role in determining agonist efficacy at the muscarinic M_2 receptor. We suggest that measurements of GDP binding provide additional information on receptor activation to that obtained from GTP binding assays. Most importantly, it reveals differences in the action of agonists and inverse agonists that are not observable in GTP binding studies.

Methods

Cell culture and membrane preparation

Chinese hamster ovary cells stably transfected with the human M_2 muscarinic receptor gene (CHO- M_2 cells) were kindly donated by Professor T.I.Bonner. Cell cultures and crude membranes were prepared as described previously (Jakubík *et al.*, 2006). Briefly, cells were grown to confluence in 75 cm^2 flasks in Dulbecco's modified Eagle's medium supplemented with 10% fetal bovine serum and 2×10^6 cells were subcultured to 100 mm Petri dishes. Medium was supplemented with 5 mM butyrate for the last 24 h of cultivation to increase receptor expression. Cells were detached by mild trypsinization on day 5 after subculture. Detached cells were washed twice in 50 mL of phosphate-buffered saline and 3 min centrifugation at $250\times g$. Washed cells were suspended in 20 mL of ice-cold incubation medium (100 mM NaCl, 20 mM Na-HEPES, 10 mM MgCl₂; pH = 7.4) supplemented with 10 mM EDTA and homogenized on ice by two 30 s strokes using Polytron homogenizer (Ultra-Turrax; Janke & Kunkel GmbH & Co. KG, IKA-Labortechnik, Staufen, Germany) with a 30 s pause between strokes. Cell homogenates were centrifuged for 30 min at $30\,000\times g$. Supernatants were discarded, pellets resuspended in fresh incubation medium and centrifuged again. Resulting membrane pellets were kept at -20°C until assayed within a maximum of 10 weeks.

Preparation of GDP-less membranes

Membrane-bound GDP was removed by mild denaturation (Ferguson *et al.*, 1986). Membranes were incubated for 3 h in 1 M ammonium sulphate at 4°C , centrifuged and resuspended in incubation medium containing 20% glycerol for 1 h to allow renaturation. Then they were again centrifuged, resuspended in incubation medium, and used for experiments.

Equilibrium radioligand binding experiments

All radioligand binding experiments were optimized and carried out as described earlier (Jakubík *et al.*, 2006). Briefly, membranes were incubated in 96-well plates at 30°C in the incubation medium described above that was supplemented with freshly prepared dithiotreitol at a final concentration of 1 mM. Incubation volume was 200 μL or 800 μL for [³H]N-methylscopolamine (NMS) saturation experiments. Approximately 30 and 10 μg of membrane proteins per sample were used for [³H]NMS and [³⁵S]GTP γ S binding respectively. NMS binding was measured directly in saturation experiments using six concentrations (30 pM to 1000 pM) of [³H]NMS for 1 h. Depletion of radioligand was smaller than 20% for the lowest concentration. For calculations, radioligand concentrations were corrected for depletion. Agonist binding was determined in competition experiments with 1 nM [³H]NMS. Membranes were first pre-incubated 60 min with agonists and guanine nucleotides, if applicable, and then incubated with [³H]NMS for additional 120 min. Non-specific binding was determined in the presence of 10 μM NMS. Equilibrium [³H]GDP binding was measured after 5 h incubation. Non-specific binding was determined in the presence of 50 μM GDP. Agonist stimulated [³⁵S]GTP γ S binding was measured in

a final volume of 200 µL of incubation medium with 500 pM of [³⁵S]GTPγS and 50 µM GDP for 20 min at 30°C after 60 min pre-incubation with GDP and agonist. Non-specific binding was determined in the presence of 1 µM unlabelled GTPγS. Incubations were terminated by filtration through Whatman GF/F glass fibre filters (Whatman, Maidstone, UK) using a Tomtech Mach III cell harvester (Perkin Elmer, Norwalk, CT, USA). Filters were dried in vacuum for 1 h at 80°C and then solid scintillator Meltilex A was melted on filters (105°C, 90 s) using a hot plate. The filters were cooled and counted in Wallac Microbeta scintillation counter.

Kinetic experiments

Kinetics of [³⁵S]GTPγS binding at GDP-less membranes was measured in a final volume of 200 µL at 30°C. Association of 1 nM [³⁵S]GTPγS with GDP-less membranes was measured after 20 min pre-incubation with buffer or carbachol ± 50 µM GDP. Dissociation of [³⁵S]GTPγS was initiated by 1 µM GTPγS alone or in mixture with carbachol after 90 min pre-incubation of GDP-less membranes with 1 nM [³⁵S]GTPγS ± 50 µM GDP. Kinetics of [³H]GDP binding at G_{i/o} and G_{s/olf} G-proteins was measured using scintillation proximity assay (SPA) (DeLapp *et al.*, 1999) essentially as described earlier (Jakubík *et al.*, 2006). Association of 500 nM [³H]GDP was measured after 20 min pre-incubation of GDP-less membranes with buffer or carbachol. Dissociation of [³H]GDP was started by addition of 50 µM GDP alone or in mixture with carbachol after prelabelling GDP-less membranes with 500 nM [³H]GDP for 180 min at 30°C. Dissociation was stopped by cooling and solubilization of samples by adding Nonidet P-40 to final concentration of 1% for 15 min. Primary polyclonal rabbit IgG antibody against α subunit of G_{i/o} or G_{s/olf} G-proteins in final dilution 1:1000 was then added and samples were incubated on ice for 60 min. Afterwards, 50 µL aliquots of anti-rabbit IgG coated scintillation beads were added (Amersham Bioscience, Buckinghamshire, UK; 500 mg of beads was resuspended in 40 mL of incubation buffer) and incubation continued for another 3 h. Trapped α subunits were pelleted at 4°C and 1500× g for 15 min and counted using SPA protocol in Wallac Microbeta scintillation counter.

Data analysis

In general binding data were analysed as described previously (Jakubík *et al.*, 2006). Data were preprocessed by Open Office 2.3 (<http://www.openoffice.org>) and subsequently analysed by Grace 5.1.18 (<http://plasma-gate.weizmann.ac.il/Grace>) and statistic package R (<http://www.r-project.org>) on Mandriva distribution of Linux.

The following equations were fitted to data:

Saturation of radioligand binding

$$y = B_{\text{MAX}} \times x / (x + K_D) \quad (\text{Eqn } 1)$$

y, binding of radioligand at free concentration of radioligand x; B_{MAX}, maximum binding capacity; K_D, equilibrium dissociation constant.

Concentration-response

$$y = 1 + (E_{\text{MAX}} - 1) / (1 + (EC_{50}/x)^{nH}) \quad (\text{Eqn } 2)$$

y, radioactivity in the presence of agonist at concentration x normalized to radioactivity in the absence of agonist; E_{MAX},

maximal increase by agonist; EC₅₀, concentration of agonist producing 50% of maximal effect; nH, Hill coefficient.

Interference with [³H]NMS or [³H]GDP binding

$$y = 100 \times (1 - x^{nH} / (IC_{50} + x)^{nH}) \quad (\text{Eqn } 3)$$

$$y = (100 - f_{\text{low}}) \times (1 - x / (IC_{50\text{high}} + x)) + f_{\text{low}} \times (1 - x / (IC_{50\text{low}} + x)) \quad (\text{Eqn } 4)$$

y, binding of radioligand at a concentration of displacer x normalized to binding in the absence of displacer; IC₅₀, concentration causing 50% decrease in binding; nH, Hill coefficient; f_{low}, percentage of low affinity sites; IC_{50high}, concentration causing 50% decrease in binding to high affinity sites; IC_{50low}, concentration causing 50% decrease in binding to low affinity sites. Both equations were fitted to data and the one giving better fit determined by F-test was used. Equilibrium dissociation constant of displacer (K_i) was calculated according to Cheng and Prusoff (Cheng and Prusoff, 1973).

Rate of association

$$y = B_{\text{eq}} \times [1 - \exp(-1 \times k_{\text{obs}} \times x)] \quad (\text{Eqn } 5a)$$

$$y = B_{\text{eq1}} \times (1 - \exp(-1 \times k_{\text{obs1}} \times x)) + B_{\text{eq2}} \times [1 - \exp(-1 \times k_{\text{obs2}} \times x)] \quad (\text{Eqn } 5b)$$

y, binding of radioligand at time x; k_{obs}, k_{obs1}, k_{obs2}, observed rates of association; B_{eq}, B_{eq1}, B_{eq2}, equilibrium binding.

Rate of radioligand dissociation

$$y = 100 \times e^{(-k_{\text{off}} \times x)} \quad (\text{Eqn } 6a)$$

$$y = (100 - f_2) \times e^{(-k_{\text{off1}} \times x)} + f_2 \times e^{(-k_{\text{off2}} \times x)} \quad (\text{Eqn } 6b)$$

y, binding of radioligand at time x normalized to time 0; k_{off}, k_{off1}, k_{off2}, rate constants; f₂, percentage of sites with rate constant k_{off2}.

Allosteric interaction of radioligand

Allosteric interaction between a radioligand and an allosteric modulator was analysed according to the ternary complex model (Ehlert, 1988).

$$y = \frac{[D] + K_D}{[D] + \frac{K_D \times (K_A + x)}{K_A + x / \alpha}} \quad (\text{Eqn } 7)$$

y, binding of radioligand in the presence of ligand A at concentration x normalized to the absence of ligand A; [D] concentration of radioligand; K_D, equilibrium dissociation constant of radioligand; K_A, equilibrium dissociation constant of ligand A; α, factor of cooperativity between radioligand and ligand A.

Allosteric interaction between GDP and agonist binding

Allosteric interaction between GDP and agonist binding was analysed according to the ternary complex model with agonists competing with radioligand (Jakubík *et al.*, 1997).

$$\gamma = \frac{[D] + K_D}{[D] + \frac{K_D \times ([A] \times (K_A + x/\beta) + K_I \times (K_A + x))}{K_I \times (K_A + x/\alpha)}} \quad (\text{Eqn 8})$$

γ , binding of radioligand ($[^3\text{H}]NMS$) in the presence of GDP at concentration x normalized to the absence of GDP; $[D]$ concentration of radioligand; K_D , equilibrium dissociation constant of radioligand; $[A]$, concentration of agonist; K_I , equilibrium dissociation constant of high affinity agonist binding form Eqn 3; K_{A_0} , equilibrium dissociation constant of allosteric ligand (GDP); α , factor of cooperativity between radioligand and allosteric ligand from Eqn 7 (always 1); β , factor of cooperativity between allosteric ligand and agonist.

Materials

The radioligands $[^3\text{H}]NMS$ ($[^3\text{H}]GDP$), $[^3\text{S}]GTP\gamma S$ and anti-rabbit IgG-coated scintillation proximity beads were from Amersham (UK). Rabbit polyclonal antibodies against C-terminus of G-protein ($G_{i/o}$, C-10, and $G_{s/o/f}$, C-18) were from Santa Cruz Biotechnology (Santa Cruz, CA, USA). Carbachol, dithiotreitol, EDTA, GDP, GTP γS , NMS chloride and pilocarpine were from Sigma (St. Louis, MO, USA). Oxotremorine was from RBI (Natick, MA, USA) and Nonidet P-40 was from USB Corporation (Cleveland, OH, USA). Furmethide was kindly donated by Dr Shelkovnikov (University of St. Petersburg, Russia). Nomenclature of receptors and G-proteins follows Alexander *et al.* (2009).

Results

General characterization of crude membranes

Experiments were performed on membranes of CHO-M₂ cells stably expressing 1.4 ± 0.2 pmol of binding sites for $[^3\text{H}]NMS$ chloride per mg of membrane protein. The equilibrium dissociation constant (K_D) of $[^3\text{H}]NMS$ was 512 ± 32 pM (mean \pm SEM, $n = 4$, measurements on cells from independent seedings). Total binding of $[^3\text{S}]GTP\gamma S$ to crude membranes was 123 ± 18 pmol per mg of protein out of which 74 ± 11 pmol was to $G_{i/o}$, 21 ± 3 pmol to $G_{q/11}$ and 16 ± 3 pmol to $G_{s/o/f}$ G-proteins respectively (means \pm SEM, $n = 3$).

Carbachol, furmethide, oxotremorine and pilocarpine concentration dependently stimulated binding of $[^3\text{S}]GTP\gamma S$ (Figure 1, Table 1). Carbachol and furmethide induced similar maximal increase of $[^3\text{S}]GTP\gamma S$ binding (threefold and 3.1-fold increase respectively) with half-effective concentrations (EC_{50}) of 12.3 and 7.0 μM respectively. Oxotremorine and pilocarpine were more potent ($EC_{50} = 1.0$ and 1.2 μM respectively) but less efficacious ($E_{\max} = 2.8$ and 1.6-fold increase respectively). The rank order of efficacy was: furmethide = carbachol > oxotremorine > pilocarpine, with a ranking of potency of: oxotremorine = pilocarpine > furmethide = carbachol. Carbachol had no effect on $[^3\text{S}]GTP\gamma S$ binding at wild-type (non-transfected) CHO cells.

Influence of guanine nucleotides on the affinity of agonists

Affinity of agonist binding was assessed indirectly in competition experiments with 1 nM of the muscarinic radioligand $[^3\text{H}]NMS$ (Figure 2). Competition curves were biphasic and

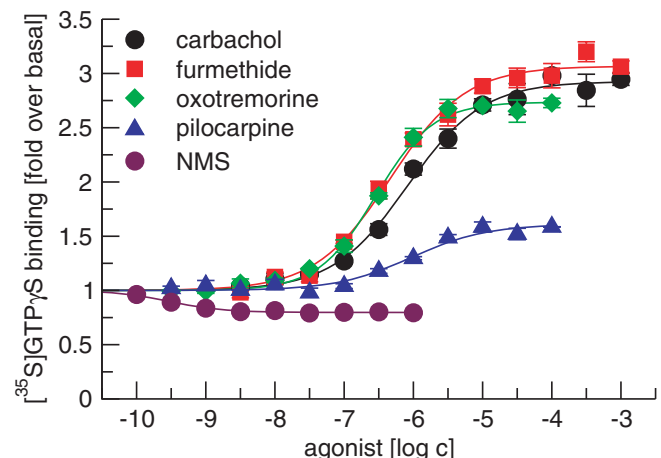


Figure 1

Stimulation of $[^3\text{S}]guanosine-5'-\gamma$ -thiophosphate (GTP γS) binding by agonists. $[^3\text{S}]GTP\gamma S$ binding to membranes stimulated by increasing concentrations (abscissa, log M) of agonists carbachol, furmethide, oxotremorine, pilocarpine and antagonist N-methylscopolamine (NMS) is expressed as fold over basal (ordinate). Data are mean \pm SEM of values from three experiments performed in quadruplicate. Curves were fitted using Equation 2 and results of fits are shown in the Table 1.

displayed a similar proportion (50 to 66%) of low-affinity binding sites for all agonists but different affinities for both high- and low-affinity binding sites (Table 2). High-affinity binding ranged from 12 nM for oxotremorine to 120 nM for carbachol and low-affinity binding from 580 nM for oxotremorine to 9 μM for carbachol. Competition curves between $[^3\text{H}]NMS$ and agonists in the presence of 1 μM GTP γS expectedly became monophasic for all agonists (Figure 2) with calculated equilibrium inhibition constants (K_I) corresponding to the low-affinity K_I in the absence of GTP γS . Similarly, 50 μM GDP present during competition measurements (Figure 2) also converted curves to monophasic ones with K_I corresponding to that in the presence of GTP γS and the low-affinity K_I in the absence of added nucleotides (Figure 2, Table 2).

In order to explore the effects of added GDP on agonist binding, we reduced membrane-bound native GDP by inducing its dissociation under slightly denaturing conditions, washing and renaturing as described in *Methods*. Competition curves remained biphasic (Figure 2) but the proportion of low-affinity sites decreased fivefold to sevenfold compared with membranes before treatment (Table 2). Low-affinity K_I of agonists corresponded to the low-affinity K_I under control conditions. High-affinity K_I values were significantly lower for carbachol and oxotremorine (twofold and fourfold respectively) and not changed for oxotremorine and pilocarpine.

Characterization of GDP-depleted membranes

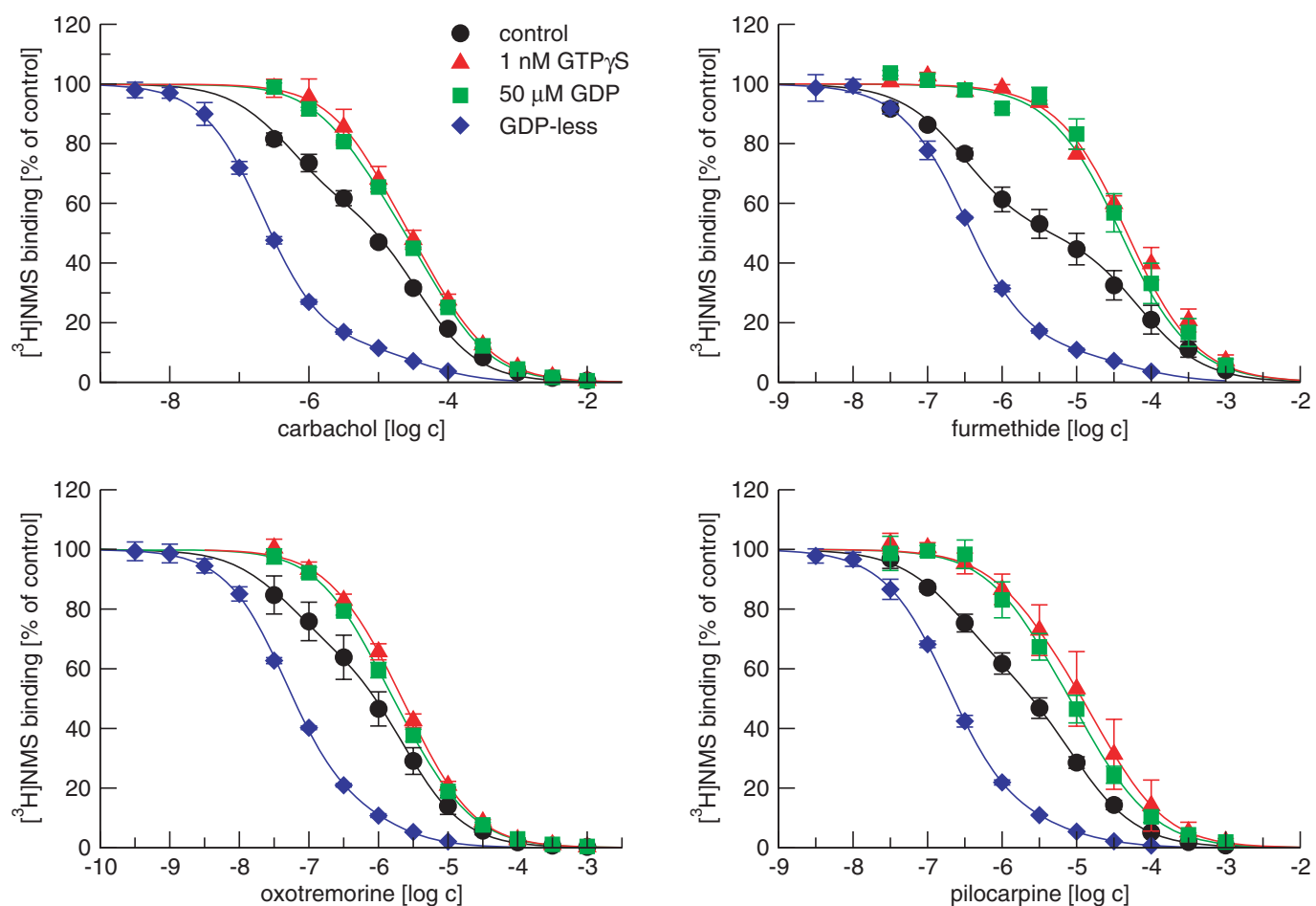
In comparison with crude membranes, depletion of GDP did not change the affinity for $[^3\text{H}]NMS$ (498 ± 29 pM) but increased the number of binding sites per mg of protein to 24 ± 3 pmol (mean \pm SEM, $n = 4$). On the other hand, total binding of $[^3\text{S}]GTP\gamma S$ per mg of protein fell to 28 ± 2 pmol

Table 1Parameters of agonist-stimulated [³⁵S]GTP γ S binding to membranes from M₂ CHO cells

	pEC₅₀	E_{MAX} [fold over basal]	nH
Carbachol	4.91 ± 0.04*	3.01 ± 0.07	0.81 ± 0.05
Furmethide	5.15 ± 0.05	3.12 ± 0.08	0.82 ± 0.05
Oxotremorine	5.99 ± 0.04**	2.78 ± 0.06*	0.92 ± 0.03
Pilocarpine	5.93 ± 0.08**	1.59 ± 0.06***	0.98 ± 0.03

Constants and Hill coefficients (nH) were obtained by fitting Equation 2 to data from individual experiments shown in Figure 1. Half-effective molar concentration of agonists is expressed as negative logarithm (pEC₅₀) and maximal stimulation (E_{MAX}) as fold increase over basal binding. Data are means ± SEM of values from three individual experiments performed in quadruplicate. *P < 0.05, significantly different from furmethide; **P < 0.01, significantly different from carbachol and furmethide; ***P < 0.001, significantly different from all other agonists by ANOVA and Tukey's test.

CHO cells, Chinese hamster ovary cells; GTP γ S, guanosine-5'- γ -thiotriphosphate.

**Figure 2**

Effects of guanine nucleotides on competition between agonists and [³H]N-methylscopolamine (NMS) binding. Binding of 1 nM [³H]NMS to membranes in the presence of increasing concentrations (abscissa, log M) of the agonists carbachol (upper left), furmethide (upper right), oxotremorine (lower left) and pilocarpine (lower right) is expressed as per cent of control binding in the absence of agonist. Data are shown for binding to crude membranes (control); binding to crude membranes in the presence of 50 μ M guanosine diphosphate (GDP); binding to crude membranes in the presence of 1 μ M guanosine-5'- γ -thiotriphosphate (GTP γ S); and binding to GDP-less membranes. Data are mean ± SEM of values from three experiments performed in quadruplicate. Curves were fitted using Equations 3 and 4. Results of fits are shown in Table 2.

Table 2

Effects of guanine nucleotides on binding parameters of muscarinic agonists

		Carbachol	Furmethide	Oxotremorine	Pilocarpine
Control	pK _i high	6.92 ± 0.08	7.12 ± 0.09	7.93 ± 0.07	7.19 ± 0.08
	pK _i low	5.04 ± 0.08	4.78 ± 0.08	6.24 ± 0.07	5.65 ± 0.08
	f _{low} [%]	59 ± 11	50 ± 9	66 ± 8	58 ± 9
+1 μM GTPγS	pK _i	5.13 ± 0.05	4.76 ± 0.05	6.26 ± 0.04	5.54 ± 0.06
+50 μM GDP	pK _i	5.19 ± 0.06	4.77 ± 0.05	6.38 ± 0.04	5.67 ± 0.05
GDP-less membranes	pK _i high	7.27 ± 0.08*	7.77 ± 0.08**	7.95 ± 0.07	7.33 ± 0.07
	pK _i low	4.99 ± 0.09	4.87 ± 0.09	6.49 ± 0.08	5.69 ± 0.10
	f _{low} [%]	12 ± 4**	9.6 ± 3.8**	13 ± 4**	7.9 ± 3.2**

Equilibrium inhibition constants K_i and percentages of low affinity sites were obtained by fitting Equations 3 and 4 to data from individual experiments shown in Figure 2. K_i values of agonists are expressed as negative logarithms of molar concentration (pK_i). f_{low} is the fraction of receptors in the low-affinity state. Data are means ± SEM of values from three independent experiments performed in quadruplicate. *P < 0.05; **P < 0.01, significantly different from corresponding control membranes by t-test.

GDP, guanosine diphosphate.

Table 3Rate constants of [³⁵S]GTP-γS binding in GDP-less membranes

	k_{obs} [h⁻¹]	B_{eq} [fmol·μg⁻¹ protein]	k_{off} [h⁻¹]
GDP-less membranes	4.35 ± 0.15	5.66 ± 0.22	0.324 ± 0.013
+100 μM carbachol	4.33 ± 0.17	5.70 ± 0.25	0.327 ± 0.014
50 μM GDP	1.34 ± 0.14*	1.21 ± 0.12*	0.334 ± 0.012
+100 μM carbachol	3.98 ± 0.14** ^a	4.85 ± 0.19** ^a	0.322 ± 0.012
+100 nM NMS	1.01 ± 0.08 ^a	1.20 ± 0.11	0.343 ± 0.009

Constants were obtained by fitting Equations 5a or 6a as appropriate to data from individual experiments shown in Figure 3. k_{obs}, association rate constant; B_{eq}, binding at equilibrium; k_{off}, dissociation rate constant. Data are means ± SEM of values from three independent experiments performed in quadruplicate. *P < 0.01; significantly different from control (GDP vs. GDP-less, with vs. without carbachol) and ^aP < 0.05; significantly different from control without ligand by t-test.

GDP, guanosine diphosphate; GTPγS, guanosine-5'-γ-thiotriphosphate; NMS, N-methylscopolamine.

out of which 18 ± 1 pmol was to G_{i/o}, 3.5 ± 0.5 pmol to G_{q/11} and 4.6 ± 0.6 pmol to G_{s/olf} G-proteins respectively (means ± SEM, n = 3).

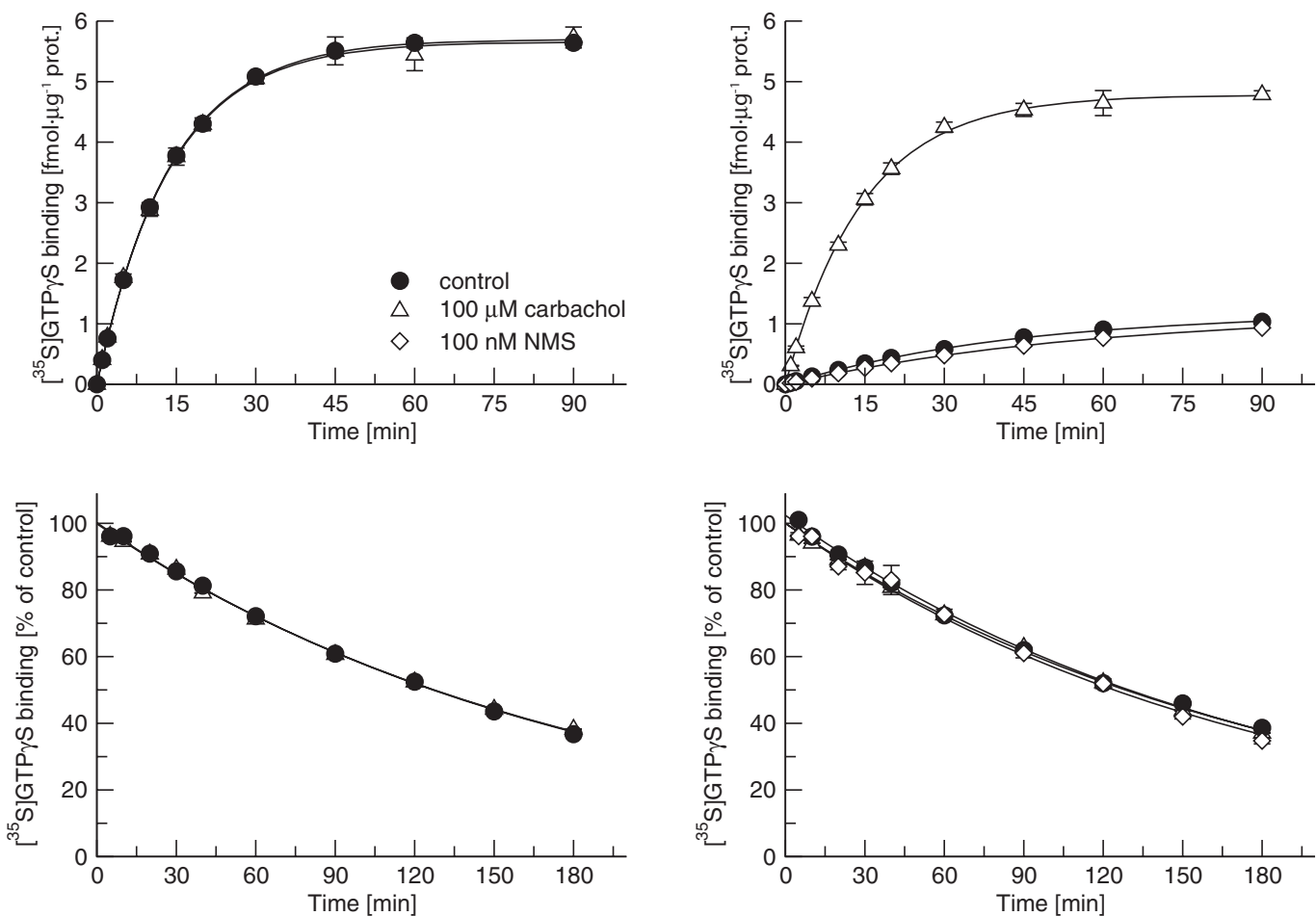
Kinetics of [³⁵S]GTPγS binding to membranes

Measurements of 1 nM [³⁵S]GTPγS binding kinetics were carried out on GDP-depleted membranes without (Figure 3, left) or with added 50 μM GDP (Figure 3, right). As shown in Table 3, addition of GDP slowed down the rate of association 3.2-fold, decreased equilibrium binding 4.7-fold, but did not change the rate of dissociation (Figure 3, Table 3). A saturating concentration of carbachol (100 μM) did not change kinetics of [³⁵S]GTPγS binding in the absence of GDP (Figure 3, left, open circles). In the presence of GDP, carbachol had no effect on the rate of dissociation of [³⁵S]GTPγS but accelerated the rate of association 2.6-fold and increased equilibrium binding fourfold (to 92 and 90% of that in the absence of GDP respectively). In the presence of GDP, the inverse agonist NMS slowed the association of [³⁵S]GTPγS by

25% and, similarly to carbachol, did not change dissociation kinetics (Table 3).

Kinetics of [³H]GDP binding to membranes

Measurements of 500 nM [³H]GDP binding kinetics (Figure 4) were carried out on GDP-less membranes in the absence or in the presence of 10 μM or 100 μM carbachol or 0.1 μM NMS. Association of [³H]GDP was biphasic with an observed association rate (k_{obs slow}) of 0.010 min⁻¹ for 44% of sites and k_{obs fast} of 0.063 min⁻¹ for the rest. Ten μM carbachol decelerated association of the slower fraction sevenfold while it slowed down that at the faster fraction by only twofold. Carbachol (100 μM) brought further slowing down of both the slower and faster fractions to 0.00024 min⁻¹ and 0.013 min⁻¹ respectively. Dissociation of [³H]GDP was also biphasic with dissociation rate constants k_{off slow} 0.85 min⁻¹ for 40% of sites and k_{off fast} 0.073 min⁻¹ for the rest. Carbachol accelerated [³H]GDP dissociation from the faster fraction more than 100-fold at both concentrations while the rate at the slower fraction was

**Figure 3**

Kinetics of [³⁵S]guanosine-5'-γ-thiophosphate (GTPγS) binding to membranes. Time course of association of 1 nM [³⁵S]GTPγS with (top row) and dissociation from (bottom row) GDP-less membranes. Binding was carried out either in the absence (left graphs) or presence (right graphs) of 50 μM GDP in the absence or presence of 100 μM carbachol or 100 nM N-methylscopolamine (NMS). Data are presented as mean ± SEM of values from three experiments performed in quadruplicate. Curves were fitted using Equations 5 (association) or 6 (dissociation). Results of fits are shown in the Table 3.

reduced threefold and fourfold at 10 and 100 μM carbachol, respectively.

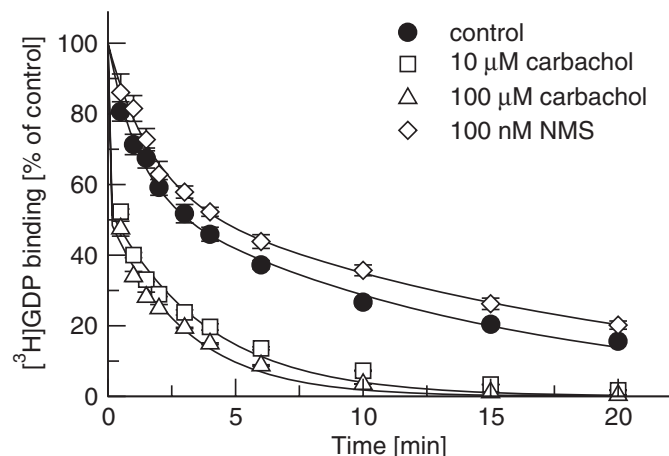
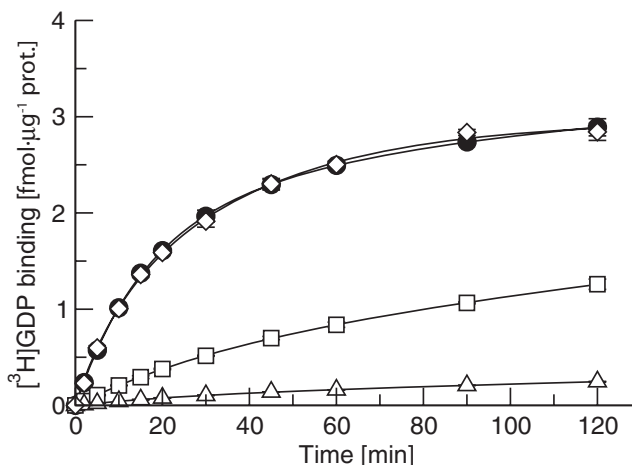
Allosteric interactions between GDP and agonists

Carbachol-induced changes in GDP kinetics confirmed allosteric interactions between GDP and carbachol. In order to quantify allosteric interactions between GDP and agonists, their affinities to free receptor-G-protein complex had to be known. Affinity of GDP was determined in equilibrium binding of [³H]GDP to GDP-less membranes in homologous competition (Figure 5 left) and saturation (Figure 5 right) experiments. Homologous competition curves of 1 μM and 5 μM [³H]GDP were monophasic with Hill coefficient equal to 1 and IC₅₀ values 4.48 (95% interval of confidence 3.93–5.02) and 8.55 (95% interval of confidence 7.62–9.59) μM, respectively, giving K_D for [³H]GDP of 3.49 μM. In accordance with competition experiments, saturation binding of GDP-less membranes with 0.3 to 10 μM [³H]GDP displayed K_D of 3.47

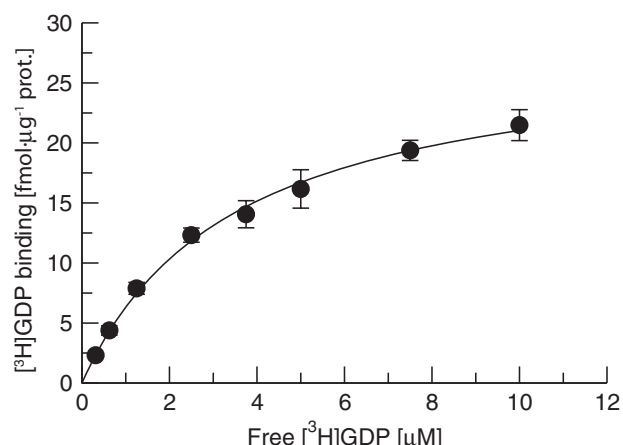
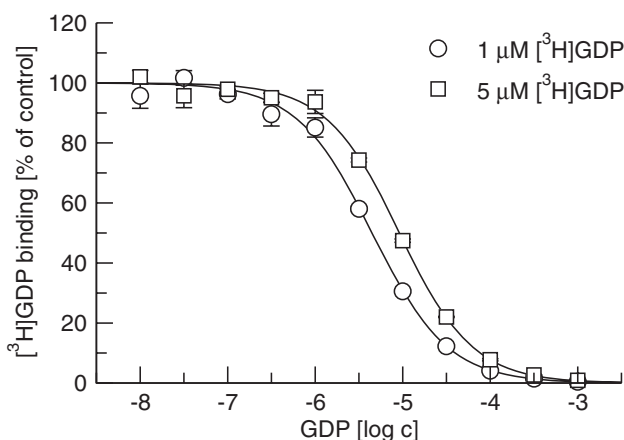
± 0.03 μM and B_{MAX} of 28 ± 3 fmol of binding sites per μg of protein.

In the first set of experiments to quantify the magnitude of allosteric interactions between GDP and agonists, the binding of [³H]GDP at fixed 10 μM concentration and increasing concentrations of tested agonists was measured in competition-like experiments (Figure 6). While the inverse agonist NMS did not affect [³H]GDP binding, all the tested agonists decreased it. Fitting Eqn 7 to data using all four agonists gave the same equilibrium dissociation constant for [³H]GDP (pK_A 5.51 ± 0.05; mean ± SD; n = 12). Factors of cooperativity α between binding of [³H]GDP and carbachol, furmethide, oxotremorine and pilocarpine were (expressed as pα) -2.3 ± 0.2, -2.4 ± 0.3, -1.8 ± 0.1 and -1.4 ± 0.1 (mean ± SEM., n = 3) respectively.

In the second set of experiments determining the magnitude of allosteric interactions between GDP and agonists, we employed [³H]NMS as a tracer because of the high cost of [³H]GDP and difficulties in quantifying negative cooperativity

**Figure 4**

Kinetics of $[^3\text{H}]$ GDP binding to membranes. Time course of association 500 nM $[^3\text{H}]$ GDP with (left) and dissociation from (right) GDP-less membranes in the absence or presence of 10 μM or 100 μM carbachol or 100 nM N-methylscopolamine (NMS). Data are expressed as mean \pm SEM of values from three experiments performed in quadruplicate. Curves were fitted using Equations 5 (association) or 6 (dissociation).

**Figure 5**

Equilibrium binding of $[^3\text{H}]$ GDP to membranes. Left: Homologous competition of GDP (abscissa, log M concentration of GDP) with 1 μM and 5 μM $[^3\text{H}]$ GDP binding (ordinate, percent of control binding). Right: $[^3\text{H}]$ GDP saturation binding (abscissa, concentration in μM ; ordinate, $[^3\text{H}]$ GDP binding in $\text{fmol}\cdot\mu\text{g}^{-1}$ protein). Data are presented as mean \pm SEM of values from three experiments performed in quadruplicate. Curves were fitted using Equations 1 and 3 as appropriate.

between GDP and full agonist (carbachol, furmethide) binding. The magnitude of negative cooperativity between agonists and GDP in these experiments was derived from a decrease in displacement of $[^3\text{H}]$ NMS binding by a fixed concentration of tested agonist by increasing concentrations of GDP in GDP-less membranes. In the absence of agonist, GDP had no effect on $[^3\text{H}]$ NMS binding (Figure 7). Eqn 7 could not be fitted to the data and the factor of cooperativity α between $[^3\text{H}]$ NMS and GDP is thus equal to 1. Agonists competed with $[^3\text{H}]$ NMS and diminished its binding (Figure 7). GDP allosterically reduced the affinity for agonists that was manifested as an increase in $[^3\text{H}]$ NMS binding. Factors of cooperativity β between GDP and agonists were calculated by fitting Eqn 8 to the data shown in Figure 7. GDP diminished the affinity of the

full agonists furmethide and carbachol 250-fold and 200-fold, respectively, while the affinity of the partial agonists oxotremorine and pilocarpine was reduced only 60-fold and 25-fold respectively. Estimated affinity for GDP was 3.2 μM ($\text{pK}_A = -5.49 \pm 0.03$; mean \pm SEM.; $n = 12$) for all fits.

Agonist stimulation of $[^3\text{S}]$ GTP γ S binding to individual G-proteins

Binding of $[^3\text{S}]$ GTP γ S to individual subclasses of G-proteins was measured in SPAs (Figure 8). As expected, all tested agonists stimulated binding of $[^3\text{S}]$ GTP γ S to Gi/o G-proteins with higher potency than to G_{s/off} and G_{q/11} G-proteins (Table 4). The rank order of potencies was oxotremorine = pilocarpine > furmethide > carbachol at all tested G-protein subclasses

(except no stimulation of [³⁵S]GTPγS binding by oxotremorine at G_{q/11} was detected). Agonists were also more efficacious in stimulating [³⁵S]GTPγS binding at G_{i/o} G-proteins than at the other two G-protein classes. The rank order of agonist efficacies to stimulate [³⁵S]GTPγS binding varied among G-protein classes and was as follows: furmethide = carbachol = oxotremorine > pilocarpine at G_{i/o}, carbachol = furmethide > oxotremorine > pilocarpine at G_{s/o/f}, and carbachol > furmethide > pilocarpine > oxotremorine at G_{q/11}.

Kinetics of [³H]GDP binding to individual subclasses of G-proteins

Kinetics of 500 nM [³H]GDP binding at individual subclasses of G-proteins measured in SPA is shown in Figure 9.

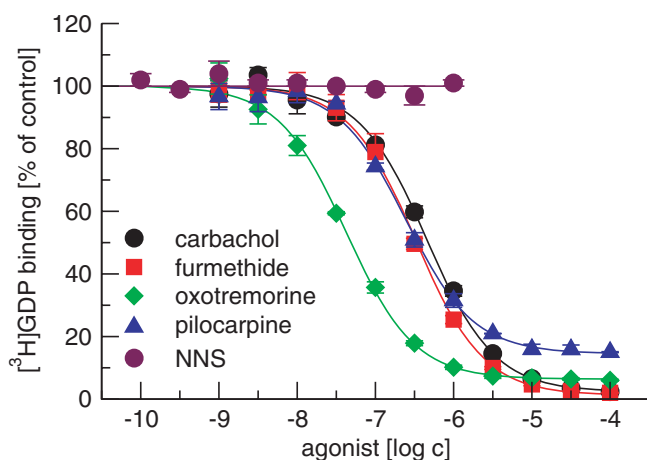


Figure 6

Direct measurement of allosteric interactions between agonists and [³H]GDP at membranes. The magnitude of allosteric interactions between agonists (carbachol, furmethide, oxotremorine, pilocarpine) or antagonist [N-methylscopolamine (NMS)] and GDP was measured directly as changes in equilibrium binding of 10 μM [³H]GDP to GDP-less membranes in the presence of increasing ligand concentration (abscissa, log M). Data are expressed as mean ± SEM of values from three experiments performed in quadruplicate. Curves were fitted using Equation 7.

Table 4

Parameters of [³⁵S]GTPγS binding to G_{i/o}, G_{s/o/f} and G_{q/11} subtypes of G-proteins

	G _{i/o} pEC ₅₀	E _{MAX}	G _{s/o/f} pEC ₅₀	E _{MAX}	G _{q/11} pEC ₅₀	E _{MAX}
carbachol	5.11 ± 0.06	2.89 ± 0.06	4.25 ± 0.06	1.82 ± 0.05	4.37 ± 0.02	1.61 ± 0.02
furmethide	5.34 ± 0.10	2.95 ± 0.09	4.76 ± 0.03*	1.70 ± 0.02	4.72 ± 0.06*	1.20 ± 0.01*
oxotremorine	6.03 ± 0.05**	2.72 ± 0.05	5.13 ± 0.04**	1.53 ± 0.01**	n.c.	n.c.***
pilocarpine	5.95 ± 0.06**	1.52 ± 0.05***	5.05 ± 0.05**	1.10 ± 0.01***	4.95 ± 0.05**	1.08 ± 0.01***

Constants and Hill coefficients (nH) were obtained by fitting Equation 2 to data from individual experiments shown in Figure 1. Half effective molar concentration of agonists is expressed as negative logarithm (pEC₅₀) and maximal stimulation (E_{MAX}) as fold increase over basal binding. Data are means ± SEM of values from three individual experiments performed in quadruplicate. *P < 0.05, significantly different from carbachol; **P < 0.01, significantly different from carbachol and furmethide; ***P < 0.001, significantly different from all other agonists by ANOVA and Tukey's test.

GTPγS, guanosine-5'-γ-thiotriphosphate; n.c., no convergence.

Association of [³H]GDP with the G_{i/o} subclass of G-proteins that preferentially couple with the M₂ receptors was biphasic (Figure 9, top left) with twice as many sites with fast (k_{obs1} = 0.055 min⁻¹) as with slow (k_{obs2} = 0.011 min⁻¹) association kinetics (Table 5). Carbachol converted the association curve to become monophasic and decreased equilibrium binding 1.8-fold and ninefold at 10 and 100 μM concentrations respectively. Carbachol (100 μM) slowed down the association of [³H]GDP 12-fold in comparison to fast sites or 10-fold in comparison to mono-exponential fit of association data under control conditions (in the absence of carbachol) (k_{obs} = 0.042 ± 0.005 min⁻¹; B_{eq} = 2.8 ± 0.3 fmol·μg·prot⁻¹; mean ± SEM; n = 3). Dissociation curves were biphasic in the absence as well as in the presence of carbachol with 36 to 38% of slow binding sites. Carbachol accelerated the dissociation rate to a similar extent from both slow and fast sites. Acceleration was 6.3–6.5-fold by 10 μM carbachol and eightfold by 100 μM carbachol respectively (Figure 9, lower left; Table 5).

Muscarinic M₂ receptors also couple non-preferentially with the G_{s/o/f} and G_{q/11} subclasses of G-proteins. We therefore attempted to determine the influence of carbachol on the kinetics of [³H]GDP binding at these two other major G-protein subclasses. Unlike the results obtained for the G_{i/o} subclass, association and dissociation curves of [³H]GDP binding with G_{s/o/f} were monophasic in the absence as well as in the presence of carbachol (Figure 9, right column). Carbachol had no effect on [³H]GDP binding association rate, accelerated [³H]GDP dissociation rate 1.8-fold and threefold, and decreased equilibrium binding 1.9-fold and 8.1-fold at 10 and 100 μM carbachol respectively (Figure 9, top right, Table 5). We were not able to determine the kinetics of [³H]GDP binding at G_{q/11} subclass of G-proteins due to extremely fast on and off rates.

Allosteric interactions between GDP and agonists at individual subclasses of G-proteins

Effects of agonists on equilibrium binding of 10 μM [³H]GDP to individual subclasses of G-proteins was measured in SPA (Figure 10, Table 6). All agonists decreased [³H]GDP binding to G_{i/o} (Figure 10, upper left) and G_{s/o/f} (Figure 10, upper right)

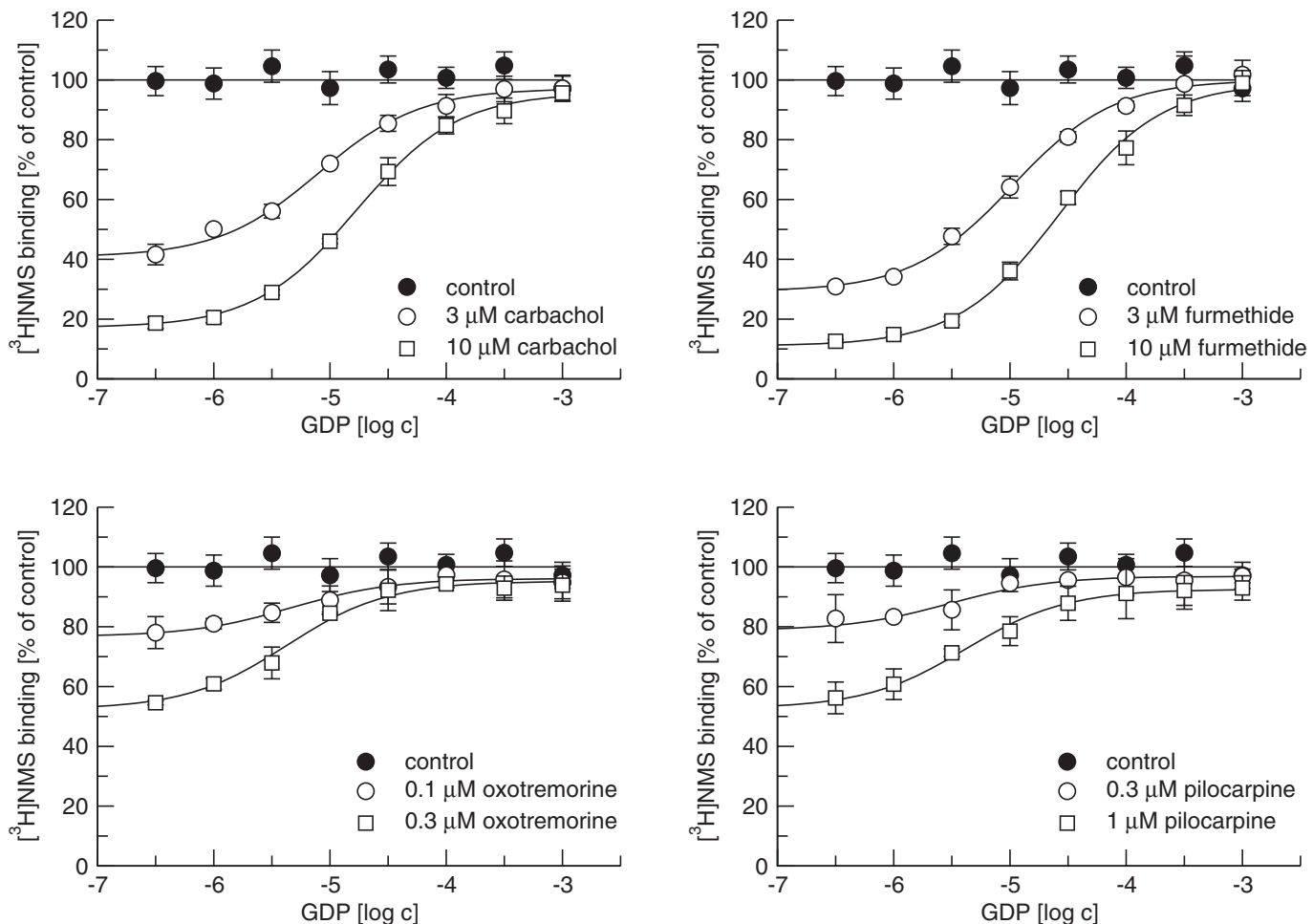


Figure 7

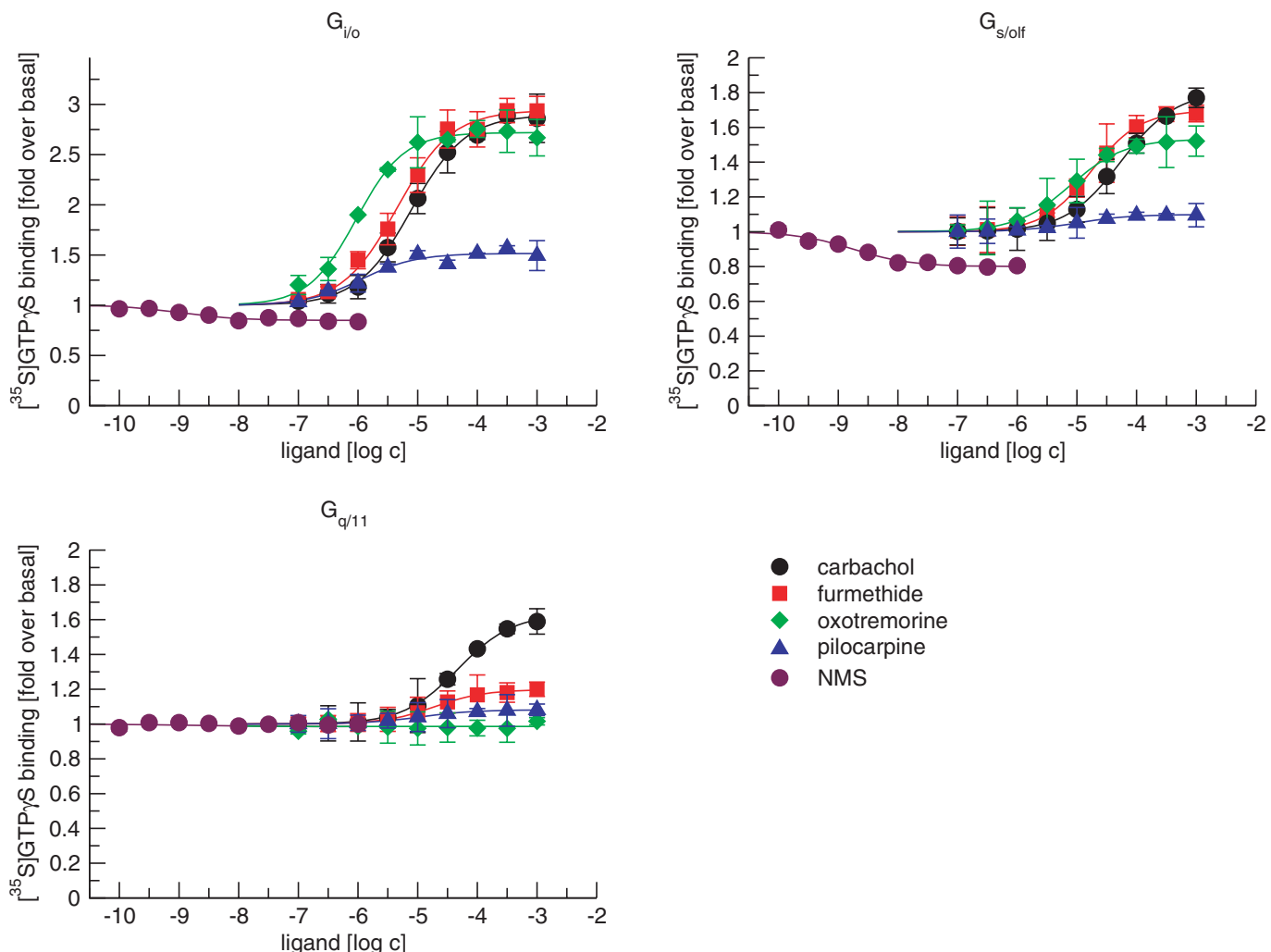
Indirect measurement of allosteric interactions between agonists and GDP at membranes. The magnitude of allosteric interactions between agonists (carbachol, upper left; furmethide, upper right; oxotremorine, lower left; pilocarpine, lower right) and GDP was measured indirectly as changes in equilibrium binding of 1 nM [³H]N-methylscopolamine (NMS) to GDP-less membranes in the presence of a fixed concentration of agonist and increasing concentrations of GDP (abscissa, log M). Binding of 1 nM [³H]NMS in the absence of agonist is also shown (control). Carbachol and furmethide were used at 3 and 10 μM, oxotremorine at 0.1 and 0.3 μM, and pilocarpine at 0.3 and 1 μM. Data are presented as mean ± SEM of values from three experiments performed in quadruplicate. Curves were fitted using Equations 7 ([³H]NMS alone) or 8 ([³H]NMS in the presence of agonist).

G-proteins. Oxotremorine (Figure 10), unlike all other agonists, had no effect on [³H]GDP equilibrium binding to G_{q/11} (Figure 10, lower panel) G-proteins. The rank order of factors of cooperativity between [³H]GDP and agonist binding varied among G-protein classes and was as follows: furmethide = carbachol = oxotremorine > pilocarpine at G_{i/o}, carbachol = furmethide > oxotremorine > pilocarpine at G_{s/olf}, and carbachol > furmethide > pilocarpine > oxotremorine at G_{q/11} (Table 6).

Discussion

Conventional determination of agonist efficacy of G-protein coupled receptors often utilizes measurements of agonist-induced activation of GTPγS binding. We analysed the role of

GDP (the second guanine nucleotide that binds to G-proteins) in the process of activation of the M₂ muscarinic acetylcholine receptors and tested whether changes in its binding could serve as a possible measure of agonist efficacy. The muscarinic agonists studied here differ in structure as well as affinity and efficacy to stimulate GTPγS binding via the M₂ muscarinic receptor (Figure 1). Binding studies show that GTPγS decreases the affinity of agonists as reported previously for the majority of, if not all, GPCRs (Wess, 1997). The decrease in agonist affinity is generally interpreted as being due to disintegration of the receptor/G-protein complex and the liberation of the signalling GTPγS-ligated G-protein α-subunit and complex of βγ subunits (Johnston and Sidrovska, 2007). In accordance with previous findings (Haga *et al.*, 1986; Florio and Sternweis, 1989; Tota and Schimerlik, 1990; Shiozaki and Haga, 1992) our data demonstrate that at

**Figure 8**

Stimulation of $[^{35}\text{S}]$ guanosine-5'- γ -thiotriphosphate (GTP γ S) binding to $G_{i/\text{lo}}$, $G_{s/\text{olf}}$ and $G_{q/11}$ G-proteins by agonists. $[^{35}\text{S}]$ GTP γ S binding to $G_{i/\text{lo}}$ (upper left), $G_{s/\text{olf}}$ (upper right), and $G_{q/11}$ (lower row) G-proteins stimulated by increasing concentrations (abscissa, log M) of agonists carbachol, furmethide, oxotremorine and pilocarpine or antagonist N-methylscopolamine (NMS) is expressed as fold over basal (ordinate). Data are presented as mean \pm SEM of values from three experiments performed in quadruplicate. Curves were fitted using Equation 2 and results of fits are shown in the Table 4.

the muscarinic M₂ receptors GDP also decreases agonist affinity. In addition, we found that reduction of membrane-bound GDP increases the proportion of high-affinity binding sites for all agonists to a similar extent (Figure 2). Adding GDP back to GDP-less membranes reduces agonist affinity (Figure 7). These findings are consistent with the existence of an agonist low-affinity conformation of the receptor that is complexed with GDP-ligated G-protein, in addition to the agonist low-affinity conformation of receptor that is uncoupled from G-protein upon binding of GTP (Abdulaev *et al.*, 2006).

Although the affinity of agonists at the low-affinity binding state is similar in the presence of either GDP or GTP γ S, kinetics of guanine nucleotides binding provide evidence that the molecular mechanisms of modulation of agonist affinity is different. The ability of carbachol to accelerate dissociation and decelerate association of GDP

(Figure 4) proves the existence of allosteric interaction between agonist and GDP on the receptor/G-protein complex. On the other hand, the inability of agonists to change the kinetics of GTP γ S binding in the absence of GDP (Figure 3, left column; Table 3) is in concert with data obtained in a reconstituted system (Florio and Sternweis, 1989) and the commonly accepted concept that the GTP γ S-ligated G α subunit dissociates from receptor (Johnston and Siderovski, 2007) and therefore the kinetics of GTP γ S binding cannot be allosterically regulated by agonists. Receptor-mediated acceleration of GTP γ S association in the presence of GDP (Figure 3, upper row; Table 3) is a consequence of accelerated GDP dissociation, while in the absence of GDP the speed of GTP γ S binding (irrespective of presence or absence of agonist) is already maximal. Lack of effect of agonists on the rate of GTP γ S dissociation in both the presence and absence of GDP (Figure 3, lower row; Table 3) further supports the

Table 5Effects of carbachol on the kinetics of [³H]GDP binding to G_{i/o} and G_{s/off} G-proteins

		Control	10 µM carbachol	100 µM carbachol
G _{i/o}	k _{obs1} [min ⁻¹]	0.055 ± 0.003	0.0056 ± 0.0003**	0.0044 ± 0.0002**
	B _{eq1} [fmol·µg ⁻¹ protein]	2.1 ± 0.2	1.7 ± 0.2**	0.35 ± 0.03**
	k _{obs2} [min ⁻¹]	0.011 ± 0.006		
	B _{eq2} [fmol·µg ⁻¹ protein]	1.1 ± 0.1		
	k _{off1} [min ⁻¹]	0.35 ± 0.03	2.2 ± 0.2**	2.8 ± 0.3**
	k _{off2} [min ⁻¹]	0.040 ± 0.004	0.26 ± 0.03**	0.32 ± 0.03**
	f ₂ [%]	37 ± 5	38 ± 4	36 ± 5
	k _{obs} [min ⁻¹]	0.031 ± 0.003	0.030 ± 0.003	0.031 ± 0.003
	B _{eq} [fmol·µg ⁻¹ protein]	0.81 ± 0.04	0.43 ± 0.02**	0.10 ± 0.01**
G _{s/off}	k _{off} [min ⁻¹]	0.067 ± 0.007	0.12 ± 0.01**	0.20 ± 0.02**

Association rate constants (k_{obs}), equilibrium binding (B_{eq}), dissociation rate constants (k_{off}) and percentages (f₂) of populations were obtained by fitting Equations 6a and 6b or 7a and 7b as appropriate to data from individual experiments shown in Figure 9. Values from better fits are shown. Data are means ± SEM of values from three independent experiments performed in triplicates. **P < 0.01, significantly different from control in the absence of carbachol by t-test.

GDP, guanosine diphosphate.

Table 6Parameters of [³H]GDP binding to G_{i/o}, G_{s/off} and G_{q/11} subtypes of G-proteins

	G_{i/o} pK_A	pα	G_{s/off} pK_A	pα	G_{q/11} pK_A	pα
Carbachol	6.90 ± 0.06	-2.3 ± 0.2	6.87 ± 0.06	-1.2 ± 0.1	6.87 ± 0.02	-0.85 ± 0.09
Furmethide	7.13 ± 0.05	-2.4 ± 0.2	7.10 ± 0.05	-1.0 ± 0.1	7.17 ± 0.06	-0.32 ± 0.05
Oxotremorine	7.93 ± 0.05	-2.1 ± 0.2	7.97 ± 0.05	-0.78 ± 0.08	n.c.	n.c.
Pilocarpine	7.23 ± 0.06	-0.94 ± 0.08	7.19 ± 0.07	-0.24 ± 0.04	7.25 ± 0.08	-0.16 ± 0.03

Equilibrium dissociation constants (K_A) of agonists and factors of cooperativity (α) between agonists and [³H]GDP binding are expressed as negative logarithms. Constants were obtained by fitting Equation 7 to data from individual experiments shown in Figure 10. Data are means ± SEM of values from three independent experiments performed in quadruplicates.

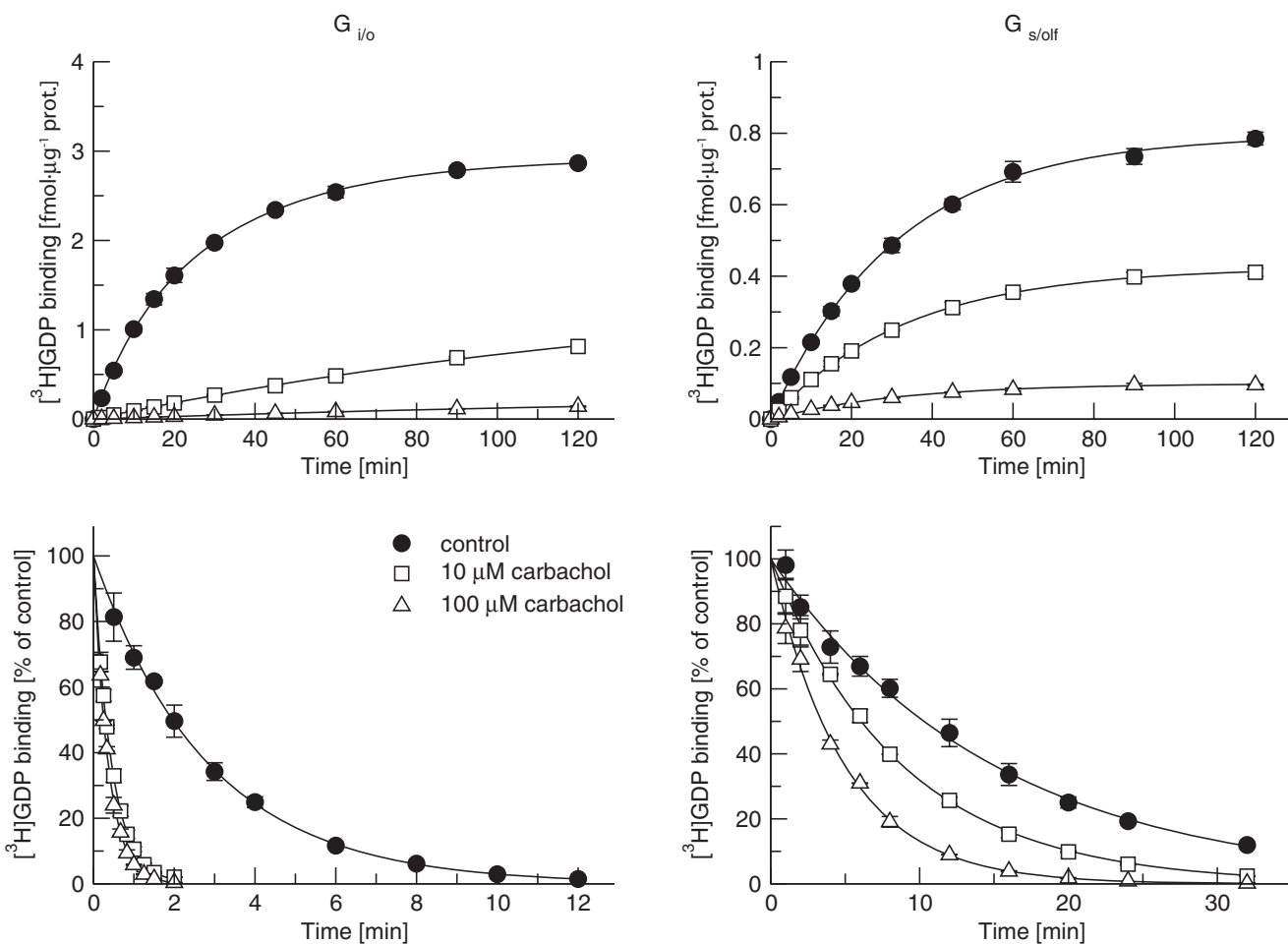
GDP, guanosine diphosphate.

notion that, under our experimental conditions, the G_α subunit with bound GTP_γS is not in physical contact with the receptor.

Agonist-induced allosteric acceleration of GDP dissociation from the G_α subunit strongly implies involvement of this mechanism in regulating the strength (efficacy) of agonist signal transmission to intracellular second messenger pathways. Despite multiple lines of evidence for allosteric interaction between agonist and GDP on receptor-G-protein complex the magnitude of these allosteric interactions has not been quantified so far. Our present data show that the magnitude of negative cooperativity between the four tested agonists displaying different potencies and efficacies, and GDP binding (Figure 6) demonstrate that full agonists (carbachol, furmethide) display significantly stronger negative cooperativity than partial agonists (oxotremorine, pilocarpine). The magnitude of negative cooperativity correlates with agonist efficacy in stimulating

GTP_γS binding to membranes (furmethide ≥ carbachol > oxotremorine > pilocarpine) (Figure 11). Interestingly, 30 years ago Birdsall *et al.* (1978) showed that agonist efficacy correlates with the ratio of agonist high- and low-affinity binding. Our results confirm these observations and provide a plausible interpretation. Agonist high-affinity binding takes place at a receptor-G-protein complex free of GDP and low-affinity binding occurs at a complex with GDP-ligated G-protein that is low due to negative cooperativity in binding of agonist and GDP. The stronger the negative cooperativity (more negative pα in our experiments) is, the higher the agonist efficacy and the lower the agonist affinity is in the low-affinity binding state. Thus, agonist efficacy correlates with the difference in affinities of the agonist high and low-affinity binding states.

In addition to inhibition of adenylyl cyclase (G_i-mediated), activation of non-preferential G-proteins is associated with strong stimulation of adenylyl cyclase and

**Figure 9**

Kinetics of ³H]GDP binding to G_{i/o} and G_{s/olf} G-proteins. Association of 500 nM ³H]GDP with G_{i/o} (top left) and G_{s/olf} (top right) and dissociation of 500 nM ³H]GDP from G_{i/o} (bottom left) and G_{s/olf} (bottom right) subclasses of G-proteins was measured by scintillation proximity assay as described in Methods. GDP-less membranes were pre-incubated for 20 min with either buffer or 10 μM or 100 μM carbachol. Then, 500 nM ³H]GDP was added and association terminated by filtration at the indicated times (abscissa, min). ³H]GDP binding (ordinate) is expressed as fmol per μg of protein. In dissociation measurements, GDP-less membranes were equilibrated for two hours in the presence of 500 nM ³H]GDP. Dissociation was then initiated by the addition of 50 μM GDP alone or in combination with carbachol at 10 μM or 100 μM and terminated at indicated times (abscissa, min). ³H]GDP binding (ordinate) is expressed as per cent of binding at the beginning of dissociation. Data are expressed as mean ± SEM of values from three experiments performed in triplicate. Curves were fitted using Equations 5a and 5b (association) or 6a and 6b (dissociation). Results of fits are shown in Table 5.

relatively weak effects on accumulation of inositol phosphates (G_q-mediated) by muscarinic M₂ receptors was observed repeatedly (Ashkenazi *et al.*, 1987; Burford *et al.*, 1995; Jakubík *et al.*, 1996; Michal *et al.*, 2001; 2007). In SPAs, fumethide, carbachol and pilocarpine stimulated GTPγS binding to preferential G_{i/o} as well as non-preferential G_{s/olf} and G_{q/11} G-proteins. In contrast, oxotremorine stimulated GTPγS binding only to G_{i/o} and G_{s/olf} G-proteins (Figure 8, Table 4). Different orders of efficacies at individual G-protein classes can be explained by the concept of agonist specific conformations (Kenakin, 2003), where individual agonists induce different receptor conformations that differ in the ability to activate individual classes of G-proteins.

In agreement with an allosteric mode of action, affinities of GDP for the G α subunits calculated from interactions with

all of the tested agonists are the same (between 2.9 and 3.4 μM; Figures 6, 7 and 10) and correspond well to published values (Thomas *et al.*, 1993) as well as results of ³H]GDP kinetics (Figures 4 and 9; Tables 3 and 5) and ³H]GDP saturation binding (Figure 5). Thus, changes in GDP affinity or kinetics are good measures of agonist efficacy at the G_{i/o}-coupled M₂ muscarinic receptor. In practice, being the first step next to receptor activation, ³H]GDP binding appears to be a more direct measure of receptor activation than GTPγS binding or second messenger levels in case of M₂ receptors, and this may be so at other G_{i/o} coupled GPCRs. However, this assay requires laborious preparation of membranes free of GDP. Agonist induced changes in GTPγS binding were demonstrated in fused G_α/β₂-adrenoceptors where agonist efficacy was well reflected by changes in the kinetics of GTPγS binding (Wenzel-Seifert and Seifert, 2000; Seifert *et al.*, 2001).

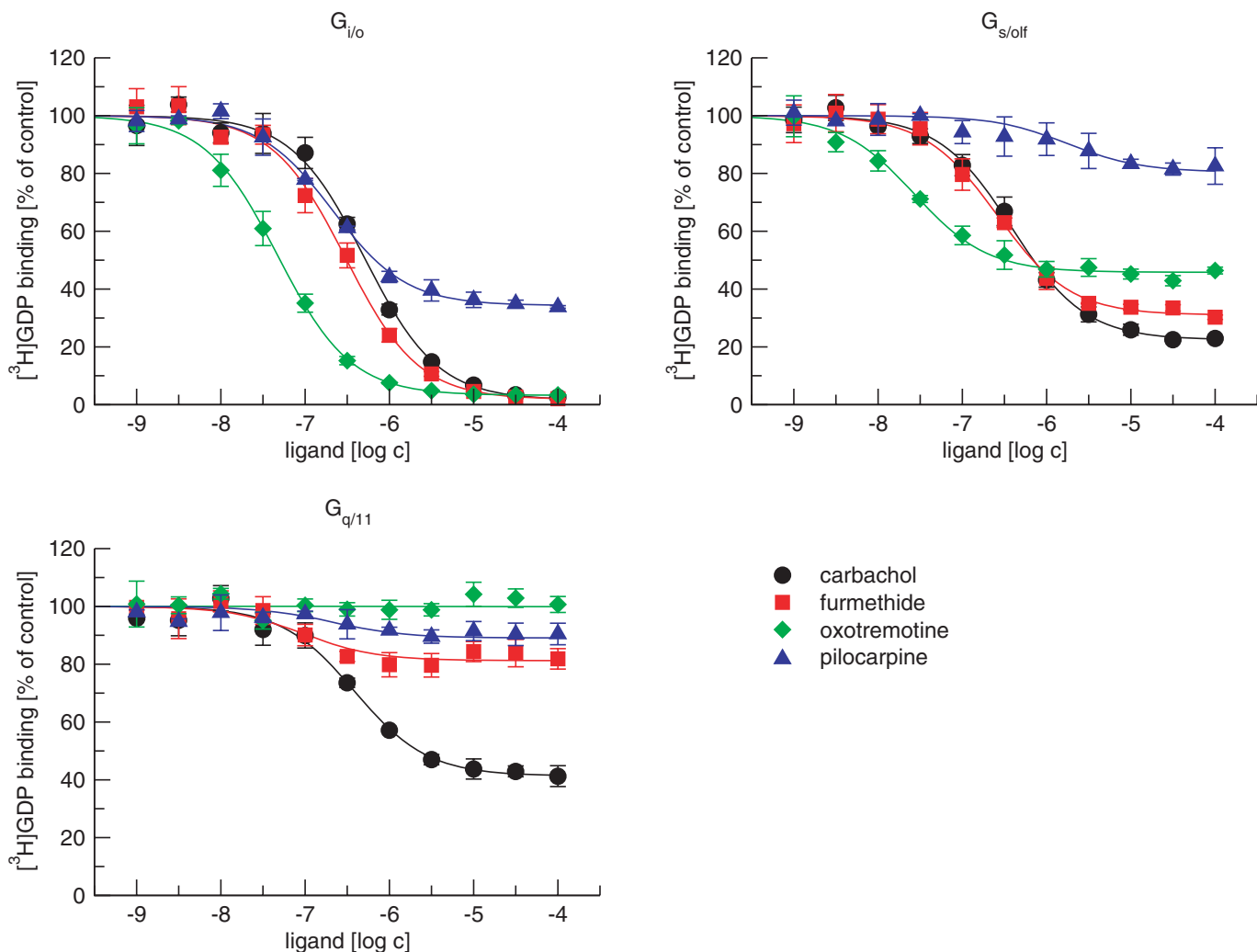


Figure 10

Allosteric interactions between agonists and [³H]GDP at individual G-proteins. The magnitude of allosteric interactions between agonists (carbachol, furmethide, oxotremotine, pilocarpine) and [³H]GDP was measured directly as changes in equilibrium binding of 10 μM [³H]GDP to G_{i/o} (upper left), G_{s/off} (upper right) or G_{q/11} (lower row) G-proteins in the presence of increasing ligand concentration (abscissa, log M) via scintillation proximity assay as described in Methods. Data are presented as mean ± SEM of values from three experiments performed in quadruplicate. Curves were fitted using Equation 7. Results of fits are shown in the Table 6.

However, in concert with the involvement of agonist-induced decrease in GDP affinity in G-protein activation, GDP differentially and concentration-dependently influenced relative efficacies of partial agonists in increasing GTPγS binding (Wenzel-Seifert and Seifert, 2000). In accordance with previous findings (Florio and Sternweis, 1989), agonists at M₂ receptors under our experimental conditions do not change the kinetics of GTPγS binding in the absence of GDP (Figure 3). Thus, while a change in the kinetic of GTPγS binding is a good measure of activation of physically coupled G-protein/β₂-adrenoceptors, kinetics of GDP binding seem to be a closer measure in case of M₂ muscarinic receptors and likely in other GPCR. Another drawback of GTPγS binding measurements is their dependence on the concentration of GDP that strongly affects outcome of the experiments (Figure 3). Also, unlike GDP binding, GTPγS concentra-

response curve has to be measured under non-equilibrium conditions (Figure 3).

The data presented here show some interesting aspects of the process of receptor activation. NMS was reported as an inverse agonist at the M₂ receptor (Jakubík *et al.*, 1995; Burstein *et al.*, 1997) and behaved as inverse agonist under our experimental conditions (Figures 1 and 8). Although positive cooperativity in binding with GDP would be expected, our data show that the cooperativity between NMS and GDP is neutral (Figures 6 and 7) and NMS only slightly slows down GDP dissociation (Figure 4 right), implying different mechanisms underlying the inverse agonist nature of NMS. One possible explanation may be that NMS stabilizes the receptor in the ground state (inactive conformation) (Hulme *et al.*, 2003) that leads to reduction of spontaneous transition of the ligand-free receptor to an active state and slower rate of GDP

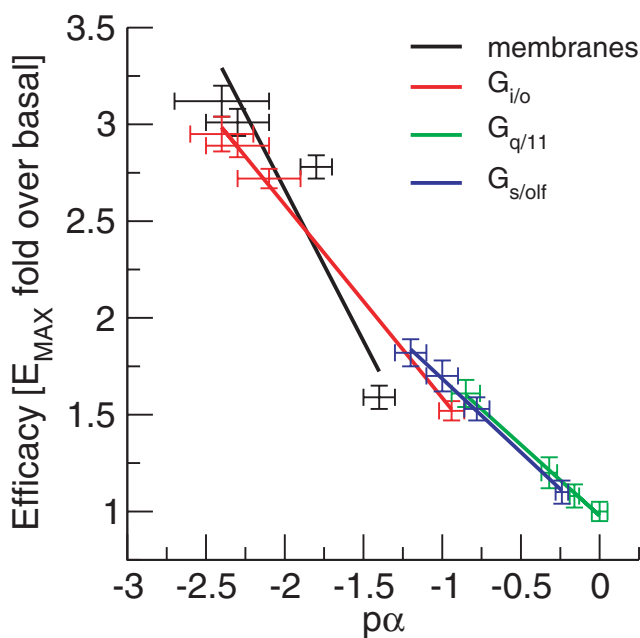


Figure 11

Correlation of binding cooperativity between agonist and GDP with maximal stimulation of [³⁵S]guanosine-5'-γ-thiotriphosphate (GTPγS) binding by agonist. Values of maximum of [³⁵S]GTPγS binding (E_{MAX}) to membranes, $G_{i/o}$, $G_{s/olf}$ and $G_{q/11}$ (Tables 1 and 4) are plotted against the negative logarithms of the factor of binding cooperativity between agonist and GDP ($p\alpha$) (results of Figure 6 and Table 6). Lines: 2D (Deming) linear regression of the data.

dissociation. Significantly, this difference in mechanisms of agonism and inverse agonism cannot be revealed by measurement of GTPγS binding.

The second interesting aspect of our study is derived from data shown in Figure 9 that illustrates that carbachol slows down association of GDP with $G_{i/o}$ G-proteins but does not change the rate of association of GDP with $G_{s/olf}$ G-proteins. These data suggest that interaction of the M₂ receptor with preferential $G_{i/o}$ G-proteins differs from that with non-preferential $G_{s/olf}$ G-proteins. One possible explanation is that $G_{i/o}$ G-proteins precouple to M₂ receptors while $G_{s/olf}$ do not (Shea and Linderman, 1997; Hein *et al.*, 2005), where precoupling gives an agonist a chance to influence GDP association while collision coupling does not. However, demonstration of this difference in coupling requires further detailed analysis. Again, this difference in kinetics at $G_{i/o}$ and $G_{s/olf}$ classes of G-proteins cannot be revealed by measurement of GTPγS binding.

In conclusion, we have demonstrated that the negative cooperativity between GDP and agonist binding played a key role in signal transduction via the M₂ receptor. Agonist-induced low-affinity conformation of the $\text{G}\alpha$ G-protein subunit for GDP leads to accelerated dissociation of bound GDP that in turn accelerates binding of GTP and G-protein activation. Thus, stronger negative cooperativity between a given agonist and GDP binding leads to a bigger shift of the GDP/GTP affinity ratio resulting in a higher rate of GTP

binding and agonist efficacy. Our data demonstrated benefits of GDP binding measurements that can reveal mechanistic differences that are not apparent in measurements of GTP binding, as was demonstrated in case of inverse agonists versus agonists or $G_{i/o}$ versus $G_{s/olf}$ G-proteins. Measurements of GDP binding therefore provide additional information beyond that obtained from GTP binding measurements.

Acknowledgements

This work was supported by Project AV0Z 50110509, the grants of the Grant Agency of the Czech Republic 305/09/0681, the Grant Agency of the Czech Academy of Sciences IAA500110703, and the Ministry of Education, Youth and Sports, Czech Republic LC554, and NIH grant NS25743.

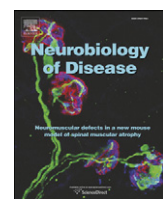
Conflicts of interest

None.

References

- Abdulaev NG, Ngo T, Ramon E, Brabazon DM, Marino JP, Ridge KD (2006). The receptor-bound "empty pocket" state of the heterotrimeric G-protein alpha-subunit is conformationally dynamic. *Biochemistry* 45: 12986–12997.
- Alexander SPH, Mathie A, Peters JA (2009). Guide to receptors and channels (GRAC). 4th edn. *Br J Pharmacol* 158 (Suppl. 1): S1–S254.
- Ashkenazi A, Winslow JW, Peralta EG, Peterson GL, Schimerlik MI, Capon DJ *et al.* (1987). An M₂ muscarinic receptor subtype coupled to both adenylyl cyclase and phosphoinositide turnover. *Science* 238: 672–675.
- Birdsall NJ, Burgen AS, Hulme EC (1978). The binding of agonists to brain muscarinic receptors. *Mol Pharmacol* 14: 723–736.
- Burford NT, Tobin AB, Nahorski SR (1995). Differential coupling of m₁, m₂ and m₃ muscarinic receptor subtypes to inositol 1,4,5-trisphosphate and adenosine 3',5'-cyclic monophosphate accumulation in Chinese hamster ovary cells. *J Pharmacol Exp Ther* 274: 134–142.
- Burstein ES, Spalding TA, Brann MR (1997). Pharmacology of muscarinic receptor subtypes constitutively activated by G proteins. *Mol Pharmacol* 51: 312–319.
- Cheng Y, Prusoff WH (1973). Relationship between the inhibition constant (K_I) and the concentration of inhibitor which causes 50 per cent inhibition (I_{50}) of an enzymatic reaction. *Biochem Pharmacol* 22: 3099–3108.
- DeLapp NW, McKinzie JH, Sawyer BD, Vandergriff A, Falcone J, McClure D *et al.* (1999). Determination of [³⁵S]guanosine-5"-O-(3-thio)triphosphate binding mediated by cholinergic muscarinic receptors in membranes from Chinese hamster ovary cells and rat striatum using an anti-G protein scintillation proximity assay. *J Pharmacol Exp Ther* 289: 946–955.

- De Lean A, Stadel JM, Lefkowitz RJ (1980). A ternary complex model explains the agonist-specific binding properties of the adenylate cyclase-coupled beta-adrenergic receptor. *J Biol Chem* 255: 7108–7117.
- Ehlert FJ (1988). Estimation of the affinities of allosteric ligands using radioligand binding and pharmacological null methods. *Mol Pharmacol* 33: 187–194.
- Ferguson KM, Higashijima T, Smigel MD, Gilman AG (1986). The influence of bound GDP on the kinetics of guanine nucleotide binding to G proteins. *J Biol Chem* 261: 7393–7399.
- Florio VA, Sternweis PC (1989). Mechanisms of muscarinic receptor action on Go in reconstituted phospholipid vesicles. *J Biol Chem* 264: 3909–3915.
- Haga K, Haga T, Ichiyama A (1986). Reconstitution of the muscarinic acetylcholine receptor. Guanine nucleotide-sensitive high affinity binding of agonists to purified muscarinic receptors reconstituted with GTP-binding proteins (Gi and Go). *J Biol Chem* 261: 10133–10140.
- Hein P, Frank M, Hoffmann C, Lohse MJ, Bünenmann M (2005). Dynamics of receptor/G protein coupling in living cells. *EMBO J* 24: 4106–4114.
- Hulme EC, Lu ZL, Saldanha JW, Bee MS (2003). Structure and activation of muscarinic acetylcholine receptors. *Biochem Soc Trans* 31: 29–34.
- Jakubík J, Bačáková L, el-Fakahany EE, Tuček S (1995). Constitutive activity of the M1-M4 subtypes of muscarinic receptors in transfected CHO cells and of muscarinic receptors in the heart cells revealed by negative antagonists. *FEBS Lett* 377: 275–279.
- Jakubík J, Bačáková L, Lisá V, el-Fakahany EE, Tuček S (1996). Activation of muscarinic acetylcholine receptors via their allosteric binding sites. *Proc Natl Acad Sci U S A* 93: 8705–8709.
- Jakubík J, Bačáková L, El-Fakahany EE, Tuček S (1997). Positive cooperativity of acetylcholine and other agonists with allosteric ligands on muscarinic acetylcholine receptors. *Mol Pharmacol* 52: 172–179.
- Jakubík J, El-Fakahany EE, Doležal V (2006). Differences in kinetics of xanomeline binding and selectivity of activation of G proteins at M(1) and M(2) muscarinic acetylcholine receptors. *Mol Pharmacol* 70: 656–666.
- Johnston CA, Siderovski DP (2007). Receptor-mediated activation of heterotrimeric G-proteins: current structural insights. *Mol Pharmacol* 72: 219–230.
- Kenakin T (2003). Ligand-selective receptor conformations revisited: the promise and the problem. *Trends Pharmacol Sci* 24: 346–354.
- Kent RS, De Lean A, Lefkowitz RJ (1980). A quantitative analysis of beta-adrenergic receptor interactions: resolution of high and low affinity states of the receptor by computer modeling of ligand binding data. *Mol Pharmacol* 17: 14–23.
- Michal P, Lysíková M, Tuček S (2001). Dual effects of muscarinic M(2) acetylcholine receptors on the synthesis of cyclic AMP in CHO cells: dependence on time, receptor density and receptor agonists. *Br J Pharmacol* 132: 1217–1228.
- Michal P, El-Fakahany EE, Doležal V (2007). Muscarinic M2 receptors directly activate Gq/11 and Gs G-proteins. *J Pharmacol Exp Ther* 320: 607–614.
- Oldham WM, Hamm HE (2008). Heterotrimeric G protein activation by G-protein-coupled receptors. *Nat Rev Mol Cell Biol* 9: 60–71.
- Seifert R, Wenzel-Seifert K, Gether U, Kobilka BK (2001). Functional differences between full and partial agonists: evidence for ligand-specific receptor conformations. *J Pharmacol Exp Ther* 297: 1218–1226.
- Shea L, Linderman JJ (1997). Mechanistic model of G-protein signal transduction. Determinants of efficacy and effect of precoupled receptors. *Biochem Pharmacol* 53: 519–530.
- Shiozaki K, Haga T (1992). Effects of magnesium ion on the interaction of atrial muscarinic acetylcholine receptors and GTP-binding regulatory proteins. *Biochemistry* 31: 10634–10642.
- Thomas TC, Schmidt CJ, Neer EJ (1993). G-protein alpha o subunit: mutation of conserved cysteines identifies a subunit contact surface and alters GDP affinity. *Proc Natl Acad Sci U S A* 90: 10295–10298.
- Tota MR, Schimerlik MI (1990). Partial agonist effects on the interaction between the atrial muscarinic receptor and the inhibitory guanine nucleotide-binding protein in a reconstituted system. *Mol Pharmacol* 37: 996–1004.
- Wenzel-Seifert K, Seifert R (2000). Molecular analysis of beta(2)-adrenoceptor coupling to G(s)-, G(i)-, and G(q)-proteins. *Mol Pharmacol* 58: 954–966.
- Wess J (1997). G-protein-coupled receptors: molecular mechanisms involved in receptor activation and selectivity of G-protein recognition. *FASEB J* 11: 346–354.



Functional cholinergic damage develops with amyloid accumulation in young adult APPswe/PS1dE9 transgenic mice

Eva Machová^a, Vladimír Rudajev^a, Helena Smyčková^a, Henna Koivisto^b, Heikki Tanila^{b,c}, Vladimír Doležal^{a,*}

^a Institute of Physiology CAS, Vídeňská 1083, 14220 Prague 4, Czech Republic

^b A. I. Virtanen Institute, University of Kuopio, P.O.Box 1627, 70211 Kuopio, Finland

^c Department of Neurology, Kuopio University Hospital, P.O.Box 1777, 70211 Kuopio, Finland

ARTICLE INFO

Article history:

Received 4 June 2009

Revised 3 December 2009

Accepted 26 December 2009

Available online 4 January 2010

Keywords:

Alzheimer's disease

Transgenic APPswe/PS1dE9 mice

Acetylcholine release

Muscarinic neurotransmission

Brain cortex

Hippocampus

Striatum

G-proteins

ABSTRACT

We investigated the functional characteristics of pre- and postsynaptic cholinergic transmission in APPswe/PS1dE9 double transgenic mice at a young age (7–10 weeks) before the onset of amyloid plaque formation and at adult age (5–6 months) at its onset. We compared brain slices from cerebral cortex and hippocampus with amyloid deposits to slices from striatum with no amyloid plaques by 6 months of age. In young transgenic mice we found no impairments of preformed and newly synthesized [³H]-ACh release, indicating intact releasing machinery and release turnover, respectively. Adult transgenic mice displayed a significant increase in preformed [³H]-ACh release in cortex but a decrease in hippocampus and striatum. The extent of presynaptic muscarinic autoregulation was unchanged. Evoked release of newly synthesized [³H]-ACh was significantly reduced in the cortex and hippocampus but unchanged in the striatum. Carbachol-induced G-protein activation in cortical membranes displayed decreased potency but normal efficacy in adult animals and no changes in young animals. These results indicate that functional pre- and postsynaptic cholinergic deficits are not present in APPswe/PS1dE9 transgenic mice before 10 weeks of age, but develop along with β-amyloid accumulation in the brain.

© 2009 Elsevier Inc. All rights reserved.

Introduction

The characteristic post-mortem morphological finding in Alzheimer's disease (AD) is the presence of senile plaques comprising β-amyloid peptides as their main constituent and neurofibrillary tangles in the cerebral cortex and hippocampus. However, these pathological changes are also found in post-mortem brains of elderly persons with no history of clinical symptoms of the disease (Snowdon, 2003). The primary event in the pathogenesis of AD is considered to be increased production of noxious β-amyloid fragments composed of 39–43 amino acids. The biologically active form of β-amyloid consists of soluble oligomers (Haass and Steiner, 2001; Klein et al., 2001) that appear in the brain earlier than amyloid plaques and neurofibrillary tangles.

In rare familial cases of AD overproduction of β-amyloid fragments is due to known defects in amyloid precursor protein (APP), presenilin 1, or presenilin 2 genes (Selkoe, 2001). However, the reason for increased production of β-amyloid is unknown in the sporadic form of the disease that represents the overwhelming majority of cases. Original neurochemical findings in Alzheimer's

disease brains pointed out disturbances of acetylcholine metabolism (Bowen et al., 1976; Davies and Maloney, 1976; Perry et al., 1977a,b; Sims et al., 1980, 1981; Francis et al., 1985 and 1999) and led to formulation of the "cholinergic hypothesis" of Alzheimer's disease (Bartus et al., 1982). Since then, a large body of evidence has accumulated either in support of or questioning this hypothesis (Bartus, 2000). The crucial question is whether disturbances of cholinergic mechanisms are present and play a role at the beginning of the pathogenesis of AD or simply reflect a general neurodegeneration that afflicts many neurotransmitter systems in the late or terminal stage of the disease. This is a very important issue because in addition to the involvement of muscarinic neurotransmission in cognitive functions, stimulation of M₁ and M₃ subtypes of muscarinic receptors leads to non-amyloidogenic cleavage of the amyloid precursor protein (Buxbaum et al., 1992; Nitsch et al., 1992). We have recently demonstrated in the cerebral cortex of a transgenic APPswe/PS1dE9 mouse model of AD (Jankowsky et al., 2004) a reduction of vesicular acetylcholine transporter protein levels and a functional decline of muscarinic neurotransmission (Machová et al., 2008). These deficits were already apparent in 7-month-old transgenic animals and deteriorated further with aging. APPswe/PS1dE9 mice demonstrate appearance of plaques at about 4 months of age (Shemer et al., 2006) and manifest cognitive deficits between 10–15 months of age (Savonenko et al., 2005; Minkeviciene et al., 2008).

* Corresponding author. Fax: +420 296442488.

E-mail address: dolezal@biomed.cas.cz (V. Doležal).

Available online on ScienceDirect (www.sciencedirect.com).

Cholinergic neurotransmission depends on the ability of cholinergic nerve terminals to synthesize, store and release acetylcholine (ACh), and on the ability of postsynaptic cells to adequately respond to released ACh. Our objective was to determine the functional integrity of cholinergic terminals in young (7–10 weeks) and adult (5–6 months) APPswe/PS1dE9 mice, i.e. before and at an early stage of amyloid pathology. We performed two types of *ex vivo* experiments on cortical, hippocampal and striatal slices. In the first set of experiments we investigated the release of previously stored (preformed) ACh and its presynaptic autoregulation. These experiments tested the releasing machinery and function of muscarinic inhibitory autoreceptors. In the second set of experiments we estimated the capacity to maximally release newly synthesized ACh that is additionally limited by the supply of substrates for ACh synthesis and loading of ACh to synaptic vesicles. In addition, we probed the capacity of the ACh analog carbachol in activating muscarinic receptors/G-protein coupling in cortical membranes that show age and transgene-dependent deterioration in mice between 7 and 17 months of age (Machová et al., 2008).

Methods

Animals

The APPswe/PS1dE9 founder mice were obtained from the Johns Hopkins University, Baltimore, MD, USA (D. Borchelt and J. Jankowsky, Dept. of Pathology) and a colony was established at the University of Kuopio as described previously (Machová et al., 2008). The housing conditions (National Animal Center, Kuopio, Finland and Animal Facility of the Institute of Physiology, v.v.i. in Prague, Czech republic) were controlled (temperature 22 °C, light from 07:00 to 19:00; humidity 50–60%), and fresh food and water were freely available. Female transgenic mice and littermate controls were transported to Prague by air and left to accommodate for at least 2 weeks before experiments. Two age groups of mice were used, young (7–10 weeks) and adult (5–6 months). The experiments were conducted according to the Council of Europe (Directive 86/609) in accordance with the Declaration of Helsinki.

Release of preformed ACh

Cortical, hippocampal, and striatal slices were prepared from 5- to 6-month-old female mice using McIlwain tissue chopper set at a width of 0.35 mm. Tissues (brain cortex from left hemisphere, left and right striatum, and left and right hippocampus) were dissected and chopped in two perpendicular directions. Superfusion experiments were done essentially as described previously (Lazareno et al., 2004; Machová et al., 2007). Brain slices were loaded with [³H] choline (Amersham, UK; SRA 82 Ci/mmol) in Krebs buffer (in mM: NaCl 138; KCl 3; CaCl₂ 1.2; MgCl₂ 1; NaH₂PO₄ 1.2; NaHCO₃ 25; glucose 10; saturated with mixture of 5% CO₂/95% O₂; final pH adjusted to 7.4) for 30 min, washed in superfusion medium, and loaded to a superfusion apparatus (Brandel, USA). Superfusion medium contained 10 μM hemicholinium-3 to prevent re-uptake of labeled choline. In experiments on striatal slices 500 nM domperidone (RBI, USA) was included in superfusion medium to prevent dopamine D₂ receptor-mediated inhibition of acetylcholine release (Doležal et al., 1992). Slices were superfused at a rate of 0.5 ml/min and 4-min fractions were collected after 1 h washout of free radioactive substances. The release of [³H]-ACh was evoked by mild field electrical stimulation (sixty 2-ms rectangular monopolar pulses, 1 Hz, 25 mA) at the beginning of the third, ninth and fifteenth fractions denoted S₁, S₂, and S₃, respectively. These conditions do not induce autoinhibition of the release by endogenous ACh. The first stimulation was always control. The second stimulation was in the presence of 10 μM carbachol to maximally

stimulate autoinhibition and the third stimulation in the presence of 1 μM atropine to prevent any stimulation of presynaptic muscarinic autoreceptors.

Release of newly synthesized ACh

The release of newly synthesized [³H]-ACh was done as described previously (Doležal and Tuček, 1991). Briefly, brain slices were preincubated in Krebs buffer containing 2 μM choline and 50 μM paraoxon to irreversibly inhibit cholinesterases for 1 h and then washed three times to remove paraoxon. Slices were then separated into duplicate incubation vials and incubated for 60 min in 0.3 ml of normal Krebs buffer or depolarizing Krebs buffer with 50 mM KCl (at the expense of NaCl to maintain isoosmolarity) containing 2 μM choline, 1 μM atropine, and [³H]choline (1 μCi/ml). In case of striatal slices incubation medium also contained 500 nM of the dopamine D₂ receptor antagonist domperidone, both during preincubation and incubation. Preincubations and incubations were at 37 °C. At the end of incubation tissues and media were separated by centrifugation (2 min, 400 g). Tissues were extracted into 0.3 ml of 10% trichloroacetic acid. Concentrations of [³H]-ACh in incubation media and tissue trichloroacetic acid extracts were determined as described (Doležal and Tuček, 1991). Trichloroacetic acid was removed from tissue extracts with ether. Two 0.1 ml aliquots were taken from each extract and medium. One of them was incubated with choline oxidase (0.2 U; Sigma) to remove choline and the other with choline oxidase plus acetylcholinesterase (type V, 2 IU; Sigma) to remove both choline and ACh. Final volume of 0.2 ml was made up with 100 mM Tris buffer (final concentration 50 mM and pH 8). After 20 min at 37 °C, 0.2 ml of sodium tetraphenylboron dissolved in butyronitrile (10 mg/ml) was added, the mixture was vigorously shaken for 1 min, the organic phase was separated by centrifugation, and the radioactivity in 0.1 ml aliquots of organic layer was measured. The radioactivity corresponding to [³H]-ACh was calculated as the difference between the radioactivities recovered in the organic phases from the two samples.

GTP-γ³⁵S binding

Determinations of carbachol-stimulated GTP-γ³⁵S binding as a postsynaptic marker of cholinergic transmission were done in membranes prepared from right hemisphere cortices. They were homogenized on ice in 1.5 ml of buffer containing 100 mM NaCl, 10 mM Mg Cl₂, 20 mM Hepes, 10 mM EDTA, and pH 7.4 using a glass homogenizer. Homogenates were centrifuged at 30 000 g and 4 °C for 30 min. Supernatants were then collected, membrane pellets were resuspended in 1.5 ml of the same buffer without EDTA, and again centrifuged under the same conditions. Supernatants were removed and pooled with previous ones. Crude membrane pellets and supernatants were stored in –80 °C until assayed. Pooled supernatants were used to confirm increase in concentration of soluble amyloid β_{1–40} and amyloid β_{1–42} in transgenic animals.

Muscarinic receptor-induced activation of G-proteins was determined as an increase of GTP-γ³⁵S binding to membranes caused by the muscarinic receptor agonist carbachol, essentially as described earlier (Jakubík et al., 2006; Machová et al., 2008). Briefly, 50 μl aliquots of membranes containing 10 μg protein were incubated for 15 min at 30 °C in 150 μl of reaction buffer containing 100 mM NaCl, 10 mM Mg Cl₂, 20 mM Hepes, 1 mM DTT, 50 μM GDP, and the muscarinic agonist carbachol at a concentration range 300 nM–100 μM. After this preincubation, 50 μl aliquots of GTP-γ³⁵S (Perkin Elmer, USA; SRA 1250 Ci/mmol) were added to give a final concentration of 500 pM and incubation continued for another 60 min. Total content of G-proteins in membranes was determined as GTP-γ³⁵S binding in the absence of GDP. Aliquots of membrane suspension containing 5 μg of protein were incubated for 60 min

under the same conditions. Nonspecific binding was assessed in the presence of 10 μM unlabeled GTP. Incubations were terminated by rapid vacuum filtration through Whatman GF/F filters using Tomtec harvester Mach III (USA). Radioactivity retained on filters was measured with Wallac Microbeta counter (Finland).

Miscellaneous

Choline concentration in the incubation medium was assayed using Amplex Red Acetylcholine/Acetylcholinesterase Assay Kit from Molecular Probes (USA) according to manufacturer's instructions.

Immunohistochemistry of β-amyloid deposits was done on 30 μm coronal sections from 9-week- and 7-month-old transgenic mice using mouse anti-human Aβ4-9 antibody (6E10; Senetek, St. Louis, USA) essentially as described earlier (Machová et al., 2008).

Determinations of amyloid β₁₋₄₀ and amyloid β₁₋₄₂ in supernatants were done using human/rat/mouse specific ELISA kit from Wako Chemicals (USA) according to manufacturer's instruction.

Proteins were determined by Peterson's modification (Peterson, 1977) of the Lowry's method.

Presentation of data and statistical analysis

Data are expressed as means ± SEM. Statistical evaluations were done using Prism 5 (GraphPad Software Inc., USA).

Chemicals

All chemicals were from Sigma (Czech Republic) unless indicated otherwise.

Results

Results of superfusion experiments are summarized in Fig. 1 and Table 1. In control mice, the first electrical stimulation (S1, control stimulation in the absence of drugs) evoked similar release of [³H]-ACh in cortex (young 1.48 ± 0.21 and adult 1.56 ± 0.09% of tissue content) and hippocampus (young 1.07 ± 0.08 and adult 1.36 ± 0.13%) but significantly higher release in adult striatum (young 2.74 ± 0.38 and adult 5.39 ± 0.33%; p < 0.001 by t-test). There were no significant differences in the evoked [³H]-ACh release between young control and transgenic animals. In contrast, the evoked release was significantly increased in cortex (by 24%), and significantly decreased in hippocampus (by 32%) and striatum (by 47%) in adult transgenic mice. Carbachol significantly inhibited evoked [³H]-ACh release in all three brain regions in control and transgenic mice of both age groups and atropine fully prevented this effect. Similarly, the extent of presynaptic autoregulation of [³H]-ACh release (mediated by M₂ muscarinic receptors in cortex and hippocampus, and by M₄ muscarinic receptors in striatum) estimated as a ratio S3 (the release in conditions of blocked autoreceptors by atropine) / S2 (inhibited release due to maximal activation of autoreceptor by carbachol) was not changed in any brain region and age group. The loading of brain slices with [³H] choline and its conversion to [³H]-ACh (Table 2) were determined after a 30-min incubation followed by 1 h washing in the presence of hemicholinium-3 that prevented any new synthesis of [³H]-ACh during washing. Incorporation of radioactivity did not differ between control and transgenic mice of either age group in any of the tested brain regions. The tissue content of [³H]-ACh expressed in dpm/μg protein was significantly higher in adult mice than young mice in all tissues except hippocampus from transgenic animals. However, relative incorporation of radioactivity into [³H]-ACh did not differ between control and transgenic mice in any of the brain regions in both age groups. The relative incorporation of radioactivity into [³H]-ACh was highest in striatum (range 83.8–85.0%) and significantly lower in cortex (range 69.5–74.5%) and hippocampus (range 68.2–73.9%).

Potassium depolarization significantly increased the release of newly synthesized [³H]-ACh formed during incubation in slices from all brain regions and age groups (Fig. 2). In young transgenic mice, neither basal release nor potassium depolarization evoked release of newly synthesized [³H]-ACh was changed compared to corresponding controls. In contrast, both basal and potassium depolarization evoked release in cortex and hippocampus were significantly reduced in adult transgenic mice (by 40% and 37% in cortex and by 36% in hippocampus, respectively; p < 0.05, paired t-test). Neither resting nor stimulated [³H]-ACh release was changed in striatum. The content of [³H]-ACh in slices at the end of incubation in both resting and depolarizing conditions (Table 3) did not differ between control and transgenic mice in all examined brain regions of both age groups. The observed changes in [³H]-ACh release were not due to unequal liberation of endogenous choline during incubation that would result in unequal dilution of radioactive tracer. As shown in Table 3, the concentration of free extracellular choline at the end of incubation did not differ between tissue samples from control and transgenic mice of corresponding age. However, slices prepared from adult animals liberated more choline than those from young animals during incubation in all examined tissues. This increase in choline release was significant in all tissue incubated in resting conditions and in control hippocampus and striatum incubated in depolarizing conditions.

Next we verified changes in muscarinic receptor/G-protein coupling in membranes from cerebral cortex. In line with our previous findings (Machová et al., 2008) we observed about 5-fold (from 2.1 ± 0.6 to 10.0 ± 1.0 μM, p < 0.01 by t-test) rightward shift of the concentration-response curve of carbachol-stimulated GTP-γ³⁵S binding in cortical membranes of adult transgenic animals with no change in maximal binding (Table 4). This shift of the concentration-response curve was not present in young transgenic mice. Basal binding of GTP-γ³⁵S, E_{max} of carbachol-stimulated GTP-γ³⁵S binding and total G-protein content were all significantly smaller in adult mice than in young mice but did not differ between control and transgenic mice of the same age.

In the last set of experiments we estimated age-related changes in buffer-soluble Aβ₁₋₄₀ and Aβ₁₋₄₂ (Table 5). Concentrations of Aβ₁₋₄₀ and Aβ₁₋₄₂ were already significantly increased in young transgenic mice (7 times and 12 times, respectively). Concentrations of Aβ₁₋₄₀ were the same in young and adult control mice and increased only by about 38% (from 176.1 to 242.9 pmol/mg protein) with age in transgenic mice. In contrast, concentrations of Aβ₁₋₄₂ increased with age by about 257% (from 3.3 to 11.8 pmol/mg protein) in control mice and by about 503% (from 39.9 to 240.6 pmol/mg protein) in transgenic mice. These changes in buffer-soluble β-amyloid concentrations resulted in an age-dependent decrease in Aβ₁₋₄₀/Aβ₁₋₄₂ ratios from 7.5 to 1.8 in control and from 4.4 to 1.0 in transgenic mice. Despite significant increases in buffer-soluble Aβ₁₋₄₀ and Aβ₁₋₄₂ concentrations, all brain regions in young transgenic mice were free of visible β-amyloid deposits (Fig. 3). In contrast, adult transgenic mice displayed apparent amyloid plaque deposition in the cortex and hippocampus, while the striatum still remained free of amyloid plaques.

Discussion

The main finding of our experiments is the significant decrease of evoked release of newly synthesized ACh in cortical and hippocampal slices dissected from adult (5- to 6-month-old) transgenic APPswe/PS1dE9 mice at the age when they start to demonstrate amyloid pathology but no cognitive deficits (Savonenko et al., 2003 and Savonenko et al., 2005; Shemer et al., 2006; Machová et al., 2008; Minkeviciene et al., 2008). Reduction of the evoked ACh release correlated with a sharp increase in soluble Aβ₁₋₄₂ concentration and

decrease in $A\beta_{1-40}/A\beta_{1-42}$ ratio. Experiments on young (7 to 10-week-old) transgenic mice indicate that the observed changes are not inborn but gradually develop in parallel with increasing

concentrations of soluble β -amyloid. In concert with our previous findings in 7-month-old transgenic mice (Machová et al., 2008) we also observed comparable decrease in potency but not efficacy of

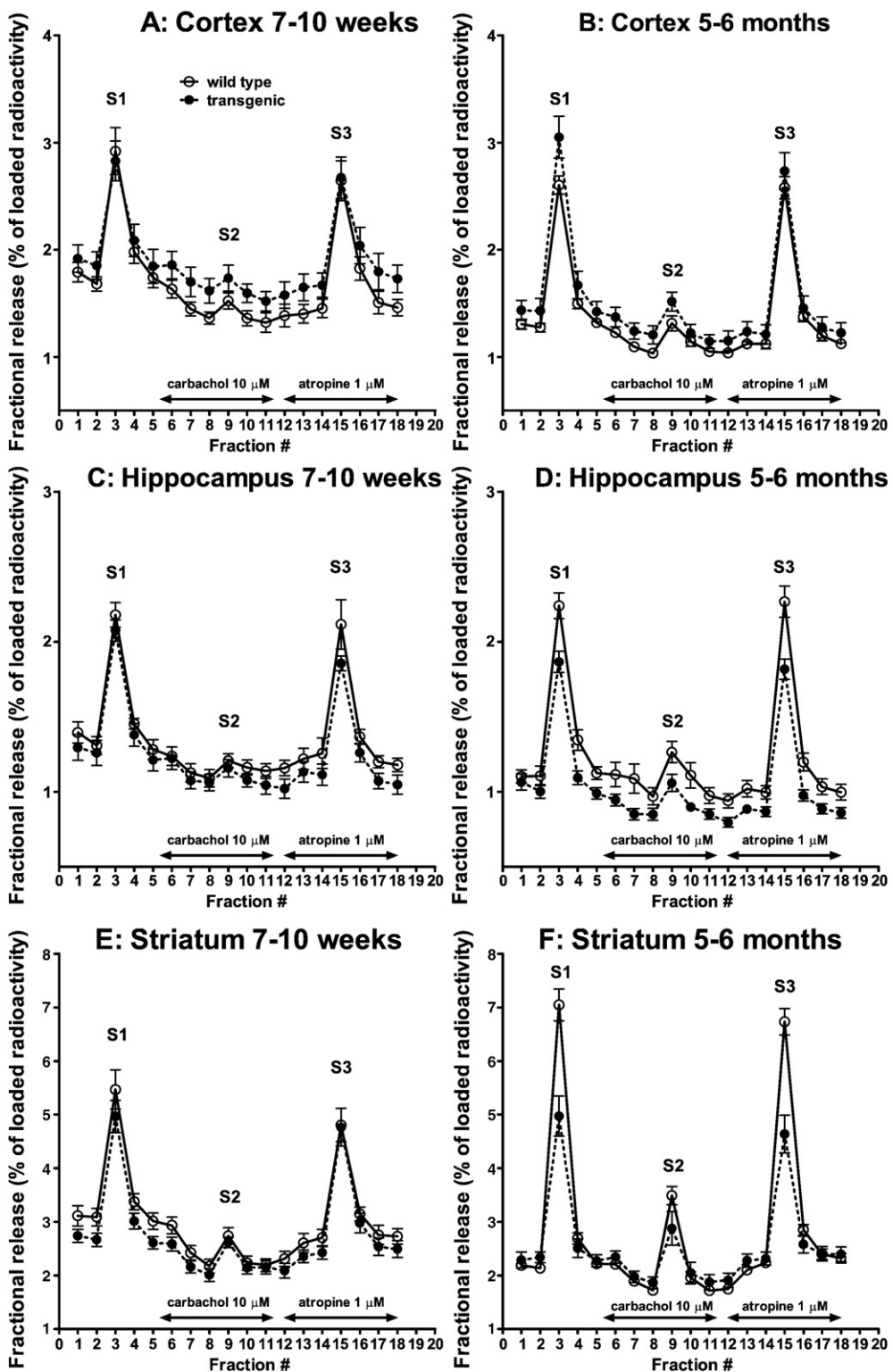


Fig. 1. Electrical stimulation-evoked release of preformed [^3H]-ACh from brain slices. Brain slices from control and transgenic mouse cortex (A, B), hippocampus (C, D), and striatum (E, F) dissected from 7–10 weeks (A, C, E) or 5–6 months (B, D, F) mice were loaded with [^3H]-Choline and then superfused as described in Methods. The release of radioactivity (ordinate) is expressed as percentage of tissue content of radioactivity present in tissue at the beginning of respective collection period (abscissa). The evoked release of radioactivity represents [^3H]-ACh while basal output of radioactivity consists of a mixture of [^3H]-ACh and other labeled substances. The first stimulation was in control conditions, the second in the presence of $10 \mu\text{M}$ carbachol to maximally stimulate muscarinic autoreceptors, and the third in the presence of $1 \mu\text{M}$ atropine to block presynaptic autoregulation of release. Values of stimulated release of [^3H]-ACh, basal outflow of radioactivity, number of observations, and statistical evaluation of the data are shown in Table 1.

Table 1Electrical stimulation-evoked [³H]-ACh release and resting outflow of radioactivity from brain slices of control and transgenic animals.

	Cortex		Hippocampus		Striatum	
	Control	Transgenic	Control	Transgenic	Control	Transgenic
7–10 weeks						
S1: Control	1.48 ± 0.21	1.22 ± 0.12	1.07 ± 0.08	1.00 ± 0.06	2.74 ± 0.38	2.70 ± 0.38
S2: Carbachol	0.20 ± 0.02	0.19 ± 0.03	0.14 ± 0.01	0.13 ± 0.02	0.61 ± 0.09	0.60 ± 0.10
S3: Atropine	1.51 ± 0.20	1.25 ± 0.11	1.06 ± 0.11	0.94 ± 0.06	2.49 ± 0.31	2.78 ± 0.38
B1: Control	1.68 ± 0.07	1.85 ± 0.13	1.31 ± 0.06	1.26 ± 0.08	3.09 ± 0.16	2.67 ± 0.12
B2: Carbachol	1.36 ± 0.06	1.62 ± 0.12	1.09 ± 0.06	1.06 ± 0.05	2.17 ± 0.13	2.01 ± 0.12
B3: Atropine	1.45 ± 0.09	1.67 ± 0.11	1.26 ± 0.10	1.11 ± 0.07	2.70 ± 0.16	2.43 ± 0.13
ratio S2/S1	0.15 ± 0.02	0.16 ± 0.02	0.14 ± 0.01	0.12 ± 0.02	0.24 ± 0.02	0.22 ± 0.02
ratio S3/S1	1.06 ± 0.09	1.06 ± 0.07	0.96 ± 0.06	0.96 ± 0.06	0.94 ± 0.05	1.04 ± 0.02
ratio S3/S2	7.74 ± 0.74	7.76 ± 1.15	7.45 ± 0.96	8.74 ± 0.89	4.80 ± 1.07	5.32 ± 0.62
(n)	10	10	10	10	10	10
5–6 months						
S1: Control	1.56 ± 0.09	1.94 ± 0.12*	1.36 ± 0.13	0.93 ± 0.06*	5.39 ± 0.33	2.87 ± 0.39*
S2: Carbachol	0.34 ± 0.08	0.36 ± 0.04	0.49 ± 0.11	0.22 ± 0.04*	2.01 ± 0.23	1.18 ± 0.27*
S3: Atropine	1.60 ± 0.10	1.73 ± 0.13	1.40 ± 0.12	1.00 ± 0.07*	4.95 ± 0.24	2.50 ± 0.29*
B1: Control	1.29 ± 0.04	1.46 ± 0.11	1.10 ± 0.07	1.01 ± 0.05	2.14 ± 0.05	2.34 ± 0.10
B2: Carbachol	1.03 ± 0.03	1.22 ± 0.08	0.99 ± 0.06	0.86 ± 0.04	1.72 ± 0.06	1.86 ± 0.11
B3: Atropine	1.13 ± 0.04	1.27 ± 0.08	0.99 ± 0.05	0.88 ± 0.03	2.24 ± 0.07	2.31 ± 0.12
ratio S2/S1	0.21 ± 0.05	0.19 ± 0.02	0.37 ± 0.08	0.27 ± 0.05	0.43 ± 0.05	0.43 ± 0.05
ratio S3/S1	1.04 ± 0.05	0.89 ± 0.05	1.08 ± 0.07	1.10 ± 0.06	0.88 ± 0.04	0.94 ± 0.06
ratio S3/S2	6.85 ± 1.19	5.82 ± 0.72	4.24 ± 0.44	5.63 ± 0.89	2.48 ± 0.28	2.49 ± 0.24
(n)	17	17	16	18	14	14

Data are derived from experiments shown in Fig. 1. Electrical stimulation-evoked release of preformed [³H]-ACh (S1–S3; calculated as described in Methods) and resting outflow of radioactivity (B1–B3; outflow in fractions immediately preceding S1, S2, and S3, respectively, i.e. fractions F2, F8 and F14) are expressed in percent of tissue content of radioactivity in control conditions (S1, B1), in the presence of 10 μM carbachol (S2, B2), and in the presence of 1 μM atropine (S3, B3), respectively. Ratios S2/S1, S3/S1, and S3/S2 indicate degree of muscarinic autoinhibition, reversibility by antagonist, and overall extent of muscarinic autoregulation, respectively. Values are mean ± SEM of indicated number of individual values from five 7–10 weeks old mice and six (cortex and hippocampus) or five (striatum) 5–6 months old mice.

* p < 0.05; significantly different from corresponding non-transgenic controls by t-test; n, number of observations.

carbachol to activate muscarinic receptors in cerebral cortex membranes also in 5 to 6-month-old mice. Similarly to the evoked ACh release, the impairment of muscarinic receptor/G-protein coupling was not present in young mice. Findings of reduced evoked ACh release and potency of the acetylcholine analog carbachol in stimulating muscarinic receptors lend further support to early involvement of cholinergic transmission in the pathogenesis of AD (Sims et al., 1980; Sims et al., 1981; Bartus et al., 1982; Francis et al., 1985, 1999; Doležal and Kašparová, 2003; Perry et al., 2003; Goto et al., 2008). The decrease of evoked release of newly synthesized ACh in cortex and hippocampus could stem from a reduced ability to synthesize ACh, damage of the releasing machinery, or slowing of loading of newly synthesized ACh into synaptic vesicles. A distinct pattern of changes in individual studied brain regions (decrease of potassium-evoked release in cortex and hippocampus but not in striatum, no effect on resting hippocampal and striatal release) is not consistent with a general mechanism. The present results point to the impairment of ACh transport to synaptic vesicles. The content of

labeled ACh found in slices from control and transgenic animals incubated in conditions of maximally stimulated release was the same in all brain regions. A limited supply of substrates for ACh synthesis (choline or acetylcoenzyme A) or reduced capacity of choline acetyltransferase to synthesize ACh would lead in addition to a decrease of its content in slices. A further observation supporting an involvement of vesicular acetylcholine transporter is the decrease of “resting acetylcholine release” in cortical slices. Unlike in hippocampal slices, basal acetylcholine release in cortical and striatal slices involves a detectable component of evoked release due to spontaneous firing (Doležal and Wecker, 1991; Doležal and Tuček, 1991). Cortex and hippocampus in rodents as well as in humans receive cholinergic innervation from basal forebrain cholinergic neurons while cholinergic system in striatum is mainly composed of intrinsic cholinergic interneurons. However, unlike in humans, rodent cortex also contains interneurons (Mesulam et al., 1983; Mesulam, 2004) that may be responsible for the disparity of resting liberation between cortex and hippocampus. Our observations demonstrate differences in transgenic animals between the evoked release of newly synthesized ACh in striatum and cortex induced by both potassium depolarization and natural spontaneous activity. These observations provide plausible evidence for the functional significance of decreased vesicular acetylcholine transporter protein levels in cortex that we previously reported in 7-month-old APPswe/PS1dE9 mice (Machová et al., 2008). Another factor explaining the decrease of evoked release of newly synthesized ACh in cortex and hippocampus but not in striatum is the robust difference in the rate of amyloid accumulation in these brain regions. While manifest amyloid plaque burden was present in cortex and hippocampus by 7 months of age, we found only occasional plaques in striatum at this age (although they appear at an older age).

Control release of previously stored ACh in the absence of muscarinic ligands (denoted S1) evoked by mild electrical stimulation differed between control and transgenic mice in adult, but not young, animals in all tested brain areas. However, it was not influenced

Table 2Incorporation of ³H-choline to acetylcholine during loading.

	Control 7–10 weeks	Transgenic 7–10 weeks	Control 5–6 months	Transgenic 5–6 months
³ H-ACh in tissue (dpm/μg protein)				
Cortex	88.3 ± 9.7	85.9 ± 10.7	188.4 ± 21.0*	157.7 ± 22.5*
Hippocampus	149.5 ± 12.7	165.3 ± 23.6	314.2 ± 52.5*	229.2 ± 50.4
Striatum	470.2 ± 48.8	438.5 ± 42.7	1193 ± 97*	1055 ± 69*
³ H-ACh in tissue (% of incorporated radioactivity)				
Cortex	74.5 ± 5.9	73.6 ± 7.1	70.8 ± 2.6	69.5 ± 2.4
Hippocampus	73.3 ± 3.8	72.0 ± 4.5	73.9 ± 2.3	68.2 ± 4.8
Striatum	84.3 ± 0.8	83.8 ± 1.3	85.0 ± 2.0	85.0 ± 2.6

Values of ³H-ACh loading shown as means ± S.E.M. of five observations are expressed in dpm/μg protein (upper part) or in percent of incorporated radioactivity (lower part).

* p < 0.05; significantly different from corresponding young animals by t-test. There are no significant difference between control and transgenic animals of the same age.

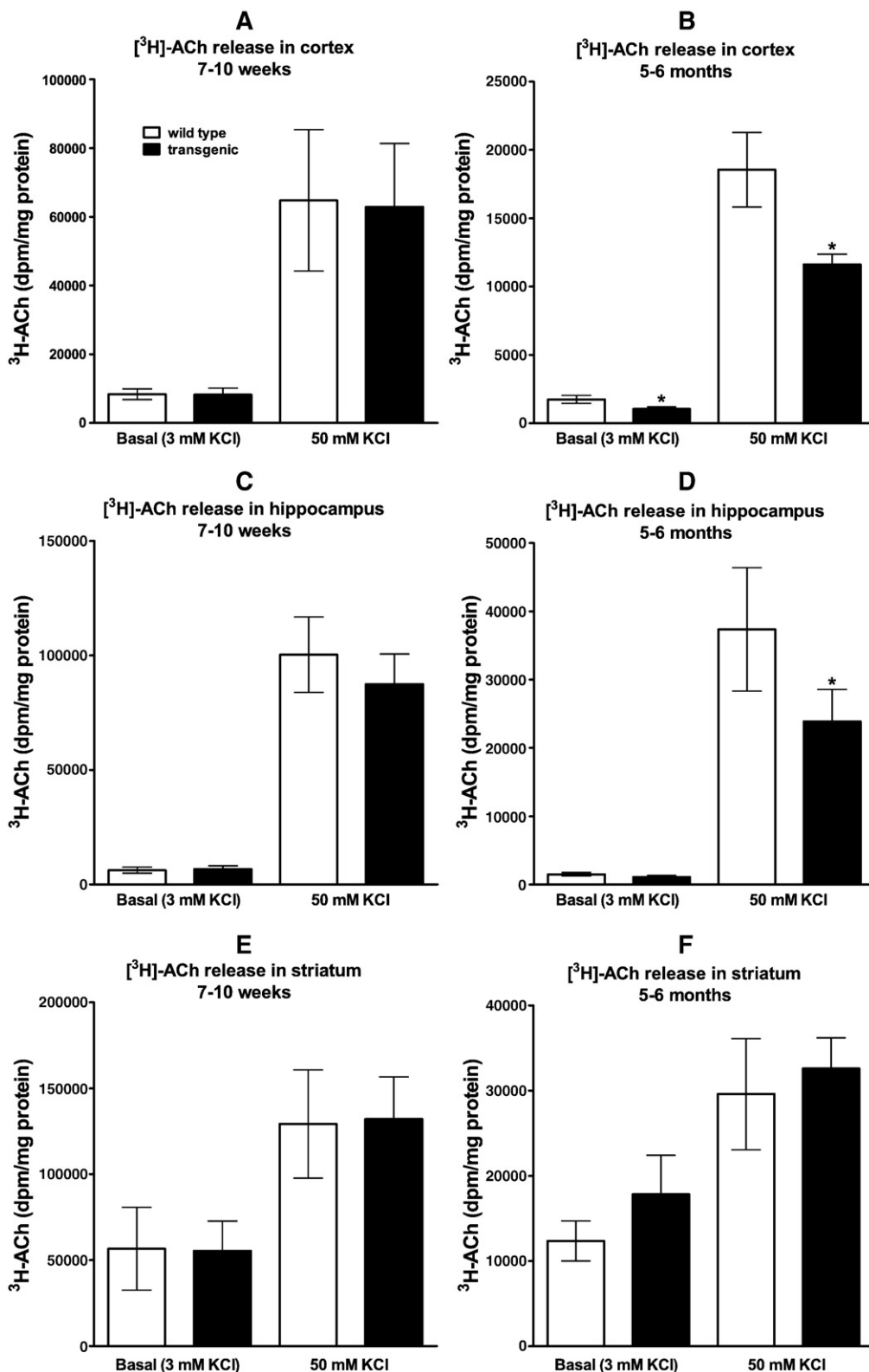


Fig. 2. Potassium depolarization-evoked release of newly synthesized [³H]-ACh from brain slices of control wild-type and transgenic mice. Brain slices were equilibrated in control medium containing the cholinesterase inhibitor paraoxon and then incubated in medium without paraoxon containing 2 μM [³H]-choline, 1 μM atropine, and either 3 mM or 50 mM potassium chloride for 30 min. [³H]-ACh release (ordinate: dpm/mg protein*30 min) from cortex, hippocampus, and striatum in 7–10 weeks old (A, C, E) and 5–6 months old (B, D, F) control (open columns) and transgenic (closed columns) is shown as means ± SEM from five experiments on randomly paired (control-transgenic) animals. *, p < 0.05; significantly different from non-transgenic littermates by paired t-test.

uniformly. The release was significantly reduced in hippocampus (by 32%) and striatum (by 47%) but significantly increased in cortex (by 24%). The evoked release of ACh in this experimental setup depends

on the operation of the releasing machinery and on extracellular regulatory influences but not on events connected with ACh synthesis and storage. Opposite changes in evoked ACh release in cortex on the

Table 3Tissue content of ^3H -ACh and concentration of choline in medium after incubations in the presence of $[^3\text{H}]$ choline.

	wt 7–10 weeks	tg 7–10 weeks	wt 5–6 months	tg 5–6 months
<i>^3H-ACh in tissue after incubation (dpm/μg protein)</i>				
Cortex 3 mM K+	12928 \pm 2276	13402 \pm 2350	10614 \pm 2109	10168 \pm 1824
Hippocampus 3 mM K+	20715 \pm 4355	17904 \pm 3271	17483 \pm 2724	15776 \pm 3556
Striatum 3 mM K+	73390 \pm 12690	73326 \pm 12690	58674 \pm 11469	80533 \pm 17620
Cortex 50 mM K+	8030 \pm 1776	9436 \pm 2375	3773 \pm 544	4145 \pm 689
Hippocampus 50 mM K+	12770 \pm 3240	12814 \pm 2805	7943 \pm 946	7792 \pm 880
Striatum 50 mM K+	16326 \pm 3918	16042 \pm 4997	9502 \pm 1085	15989 \pm 6069
<i>Choline concentration in medium after incubation (μM)</i>				
Cortex 3 mM K+	2.21 \pm 0.26	2.36 \pm 0.28	3.93 \pm 0.38*	4.09 \pm 0.38*
Hippocampus 3 mM K+	1.43 \pm 0.27	1.58 \pm 0.29	2.40 \pm 0.12*	2.97 \pm 0.25*
Striatum 3 mM K+	0.94 \pm 0.11	0.98 \pm 0.16	2.58 \pm 0.41*	2.26 \pm 0.38*
Cortex 50 mM K+	2.56 \pm 0.44	2.54 \pm 0.38	3.68 \pm 0.45	3.90 \pm 0.53
Hippocampus 50 mM K+	1.35 \pm 0.16	1.98 \pm 0.38	2.49 \pm 0.18*	2.92 \pm 0.43
Striatum 50 mM K+	1.44 \pm 0.24	1.40 \pm 0.19	3.15 \pm 0.48*	2.80 \pm 0.58

Tissue content of ^3H -ACh (in dpm/ μg protein) and choline concentration at the end of incubations are expressed as means \pm SEM of values obtained in five experiments shown in Fig. 2.* $p < 0.05$; significantly different from corresponding 7–10 weeks old mice by t-test. There are no significant difference between control and transgenic animals of the same age.

one hand and in striatum and hippocampus on the other hand (Table 1) that are not connected with changes of ACh loading (Table 2) are not consistent with a general impairment of the releasing machinery. Regional differences in the extent of cholinergic functional changes likely reflect different rate of amyloid deposition and associated neuropathology in different brain regions. Degeneration of monoaminergic axon terminals has been recently demonstrated in APPswe/PS1dE9 mice at the age of 12 months and loss of noradrenergic and serotonergic neurons at 18 months (Liu et al., 2008). The loss of noradrenergic and serotonergic terminals was more robust in somatosensory cortex than in hippocampus (Liu et al., 2008). In contrast, loss of striatal dopaminergic terminals in this mouse model has been reported only at 17 months of age and is unaccompanied by neuron loss in substantia nigra (Perez et al., 2005; Liu et al., 2008). By and large, the extent of monoaminergic neurodegeneration in different brain regions corresponds to the extent of amyloid plaque burden, being highest in cortex followed by hippocampus and an order of magnitude less in striatum (Fig. 3). Moreover, monoaminergic neurodegeneration appears to proceed faster in APPswe/PS1dE9 mice than cholinergic neuropathology, because significant loss of acetylcholinesterase positive terminals occurs only at \sim 19 months of age in APPswe/PS1dE9 mice and is equally robust in hippocampus as in somatosensory cortex (Savonenko et al., 2005). To link neurodegenerative changes in monoaminergic neurons to observed functional changes in the ACh neurotransmission may appear far-fetched since all these lesions occur much later than

changes in ACh release we demonstrated. However, functional disorders as those we demonstrated for muscarinic receptors/G-protein coupling (Machová et al., 2008; Table 4) may concern also other G-protein coupled receptors that mediate postsynaptic actions of various transmitters. Presumed changes in potency and efficacy of various monoaminergic transmitters in stimulating presynaptic receptors on cholinergic terminals or receptors located on cell bodies in case of cortex and striatum in our experiments might explain changes of preformed evoked ACh release.

Signal transduction via muscarinic receptors is reduced in membranes prepared from cortical tissue of Alzheimer brain (Tsang et al., 2005) or cortical membranes from transgenic mouse models of AD (Machová et al., 2008; Table 4). The evoked release of ACh is modulated by presynaptic muscarinic autoreceptors (Bymaster et al., 2003) and various heteroreceptors (Starke, 1987; Raiteri, 2006). In knockout mice, muscarinic M₂ and M₄ receptors were shown to play an important role in the *in vivo* homeostasis of hippocampal acetylcholine release and in cognition (Tzavara et al., 2003). The M₂ muscarinic receptors act as presynaptic inhibitory autoreceptors in cortex and hippocampus while the M₄ receptors do the task in striatum (Doležal and Tuček, 1998; Zhang et al., 2002; Lazarenko et al., 2004). We examined whether impairment of muscarinic receptor coupling affects functioning of these two muscarinic autoreceptor subtypes. Application of the muscarinic agonist carbachol in a saturating concentration reduced cortical ACh release in adult transgenic mice to the same extent as in wild-type animals while in

Table 4Parameters of carbachol-stimulated GTP- $\gamma^{35}\text{S}$ binding in cerebral cortex membranes.

	EC ₅₀ (μM)	Basal binding (fmol/mg protein)	E _{max} (fmol/mg protein)	Total G-proteins (pmol/mg protein)
Membranes from 7–10 weeks old animals				
Wild type	2.72 \pm 0.59 (6)	616.9 \pm 67.0 (6)	280.2 \pm 11.3 (6)	5.8 \pm 0.5 (4)
Transgenic	4.14 \pm 0.88 (7)	805.5 \pm 60.3 (7)	286.8 \pm 22.2 (7)	5.6 \pm 0.2 (5)
Membranes from 5–6 months old animals				
Wild type	1.96 \pm 0.44 (4)	187.0 \pm 17.0 [#] (5)	95.4 \pm 19.3 [#] (4)	3.9 \pm 0.1 [#] (3)
Transgenic	7.85 \pm 1.53 ^{*#} (5)	249.9 \pm 37.2 [#] (5)	119.0 \pm 10.4 [#] (5)	3.9 \pm 0.5 [#] (3)

Results are mean \pm SEM of data obtained in cerebral cortex membranes prepared from number of mice indicated in parentheses.* $p < 0.05$; significantly different from age-matched wild type mice by t-test.† $p < 0.05$; significantly different from corresponding 7–10 weeks old mice by t-test.

Table 5Concentration of buffer soluble amyloid β_{1-40} and amyloid β_{1-42} in cerebral cortex.

	$A\beta_{1-40}$ (pmol/mg protein)	$A\beta_{1-42}$ (pmol/mg protein)
7–10 weeks old animals		
Wild type	24.7 ± 4.9	3.3 ± 0.3
Transgenic (n)	176.1 ± 15.3*	39.9 ± 3.0*
5–6 months old animals		
Wild type	21.3 ± 2.5	11.8 ± 1.0#
Transgenic (n)	242.9 ± 15.6*#	240.6 ± 16.6*#

Results normalized to total protein content are mean ± SEM of values obtained in high-speed supernatants of cerebral cortex homogenates prepared from number of mice indicated in parentheses.

* p < 0.05; significantly different from non-transgenic control mice by t-test.

p < 0.05; significantly different from corresponding 7–10 weeks old mice by t-test.

transgenic hippocampus and striatum the reduction was larger than in wild-type slices. Nevertheless, the extent of autoregulation when expressed as the ratio "the release in the presence of atropine (blocked autoreceptors)/the release in the presence of carbachol (activated autoreceptors)" was the same in controls and transgenic animals in all three brain areas (ratios S3/S2 in Table 4). As already mentioned, stimulation of GTP binding by muscarinic receptors is impaired in this transgenic mouse line (Machová et al., 2008; Table 4). Our results exploiting a functional assay on intact tissue *ex vivo* demonstrate that this impairment, in line with results of muscarinic receptor stimulation of GTP-γ³⁵S binding, does not affect the maximal response mediated by M₂ and M₄ receptors that preferentially utilize G_{i/o} G-protein signaling pathway but as mentioned in previous paragraph may reduce potency of ACh in autoinhibiting its own release.

In summary, we employed two experimental paradigms to probe ACh release in native tissue *ex vivo*. In the first set of experiments we addressed ACh release induced by electrical stimulation and its autoregulation in isolation from upstream events involving synthesis and storage of ACh. We found a significant increase in evoked cortical ACh release and a significant decrease in striatum and hippocampus from transgenic animals. These changes are probably due to adaptive changes and may be related to regional differences in monoaminergic terminals regulating ACh release. The maximal extent of muscarinic autoregulation of ACh release (mediated by M₂ receptors in cortex

and hippocampus, and by M₄ receptors in striatum) was preserved in all brain areas in transgenic animals. In the second set of experiments we examined the extent of maximal ACh release evoked by potassium depolarization under conditions that also involve ACh synthesis and storage as limiting steps. The significant decrease of evoked ACh release in cortex and hippocampus but not in striatum with no change of tissue ACh content indicates a reduction of ACh loading to synaptic vesicles. We did not find any of these changes in tissues from young transgenic mice. These results demonstrate impaired operation of cholinergic synapses in cortex and hippocampus of transgenic APPswe/PS1dE9 mice that develop at an early stage of amyloid-β accumulation.

Acknowledgments

This work was supported by Project AV0Z50110509 and by Grants IAA500110703, MSMT CR LC554, and EU FP7 project LipiDiDiet GA No 211696.

References

- Bartus, R.T., 2000. On neurodegenerative diseases, models, and treatment strategies: lessons learned and lessons forgotten a generation following the cholinergic hypothesis. *Exp. Neurol.* 163, 495–529.
- Bartus, R.T., Dean, R.L., Beer, B., Lippa, A.S., 1982. The cholinergic hypothesis of geriatric memory dysfunction. *Science* 217, 408–414.
- Bowen, D.M., Smith, C.B., White, P., Davison, A.N., 1976. Neurotransmitter-related enzymes and indices of hypoxia in senile dementia and other abiotrophies. *Brain* 99, 459–496.
- Buxbaum, J.D., Oishi, M., Chen, H.I., Pinkas-Kramarski, R., Jaffe, E.A., Gandy, S.E., Greengard, P., 1992. Cholinergic agonists and interleukin 1 regulate processing and secretion of the Alzheimer beta/A4 amyloid protein precursor. *Proc. Natl. Acad. Sci. U. S. A.* 89, 10075–10078.
- Bymaster, F.P., McKinzie, D.L., Felder, C.C., Wess, J., 2003. Use of M1–M5 muscarinic receptor knockout mice as novel tools to delineate the physiological roles of the muscarinic cholinergic system. *Neurochem. Res.* 28, 437–442.
- Davies, P., Maloney, A.J., 1976. Selective loss of central cholinergic neurons in Alzheimer's disease. *Lancet* 2, 1403.
- Doležal, V., Kašparová, J., 2003. Beta-amyloid and cholinergic neurons. *Neurochem. Res.* 28, 499–506.
- Doležal, V., Tuček, S., 1991. Positive and negative effects of tacrine (tetrahydroaminoacridine) and methoxytacrine on the metabolism of acetylcholine in brain cortical prisms incubated under "resting" conditions. *J. Neurochem.* 56, 1207–1215.
- Doležal, V., Tuček, S., 1998. The effects of brucine and alcuronium on the inhibition of ³H-acetylcholine release from rat striatum by muscarinic receptor agonists. *Br. J. Pharmacol.* 124, 1213–1218.
- Doležal, V., Wecker, L., 1991. Modulation of acetylcholine release from rat striatal slices: interaction between 4-aminopyridine and atropine. *J. Pharmacol. Exp. Ther.* 258, 762–766.
- Doležal, V., Jackisch, R., Hertting, G., Allgaier, C., 1992. Activation of dopamine D1 receptors does not affect D2 receptor-mediated inhibition of acetylcholine release in rabbit striatum. *Naunyn Schmiedebergs Arch. Pharmacol.* 345, 16–20.
- Francis, P.T., Palmer, A.M., Sims, N.R., Bowen, D.M., Davison, A.N., Esiri, M.M., Neary, D., Snowden, J.S., Wilcock, G.K., 1985. Neurochemical studies of early-onset Alzheimer's disease. Possible influence on treatment. *N. Engl. J. Med.* 313, 7–11.
- Francis, P.T., Palmer, A.M., Snape, M., Wilcock, G.K., 1999. The cholinergic hypothesis of Alzheimer's disease: a review of progress. *J. Neurol. Neurosurg. Psychiatry* 66, 137–147.
- Goto, Y., Niidome, T., Hongo, H., Akaike, A., Kihara, T., Sugimoto, H., 2008. Impaired muscarinic regulation of excitatory synaptic transmission in the APPswe/PS1dE9 mouse model of Alzheimer's disease. *Eur. J. Pharmacol.* 583, 84–91.
- Haass, C., Steiner, H., 2001. Protofibrils, the unifying toxic molecule of neurodegenerative disorders? *Nat. Neurosci.* 4, 859–860.
- Jakubik, J., El-Fakahany, E.E., Doležal, V., 2006. Differences in kinetics of xanomeline binding and selectivity of activation of G proteins at M1 and M2 muscarinic acetylcholine receptors. *Mol. Pharmacol.* 70, 656–666.
- Jankowsky, J.L., Fadale, D.J., Anderson, J., Xu, G.M., Gonzales, V., Jenkins, N.A., Copeland, N.G., Lee, M.K., Younkin, L.H., Wagner, S.L., Younkin, S.G., Borchelt, D.R., 2004. Mutant presenilins specifically elevate the levels of the 42 residue beta-amyloid peptide *in vivo*: evidence for augmentation of a 42-specific gamma secretase. *Hum. Mol. Genet.* 13, 159–170.
- Klein, W.L., Kraft, G.A., Finch, C.E., 2001. Targeting small Abeta oligomers: the solution to an Alzheimer's disease conundrum? *Trends Neurosci.* 24, 219–224.
- Lazarenko, S., Doležal, V., Popham, A., Birdsall, N.J., 2004. Thiochrome enhances acetylcholine affinity at muscarinic M4 receptors: receptor subtype selectivity via cooperativity rather than affinity. *Mol. Pharmacol.* 65, 257–266.
- Liu, Y., Yoo, M.-J., Savonenko, A., Stirling, W., Price, D.L., Borchelt, D.R., Mamounas, L., Lyons, W.E., Blue, M.E., Lee, K.K., 2008. Amyloid pathology is associated with progressive monoaminergic neurodegeneration in a transgenic mouse model of Alzheimer's disease. *Neurobiol. Dis.* 28 (51), 1385–1384.

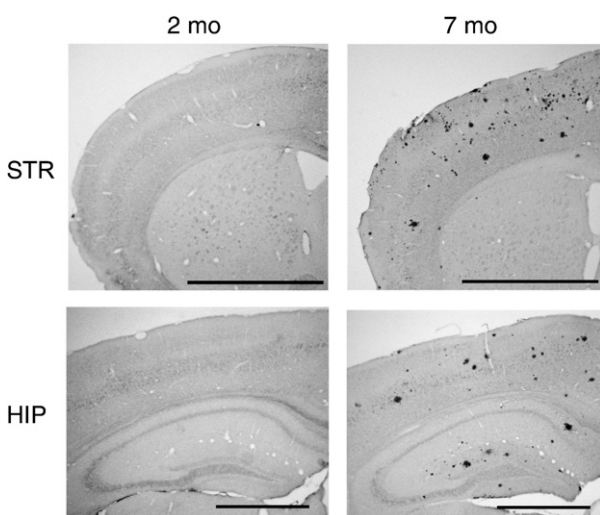


Fig. 3. Immunohistochemical staining for human specific β-amyloid (6E10) in cortex and striatum (upper row) and hippocampus (lower row) of young (9 weeks) and adult (7 months) APPswe/PS1dE9 mice. The scale bar is 1.0 mm. Note virtual absence of staining in all regions of young transgenic mice and in striatum of adult mice.

- Machová, E., Jakubík, J., El-Fakahany, E.E., Doležal, V., 2007. Wash-resistantly bound xanomeline inhibits acetylcholine release by persistent activation of presynaptic M(2) and M(4) muscarinic receptors in rat brain. *J. Pharmacol. Exp. Ther.* 322, 316–323.
- Machová, E., Jakubík, J., Michal, P., Oksman, M., Iivonen, H., Tanila, H., Doležal, V., 2008. Impairment of muscarinic transmission in transgenic APPswe/PS1dE9 mice. *Neurobiol. Aging* 29, 368–378.
- Mesulam, M.M., 2004. The cholinergic innervation of the human cerebral cortex. *Prog. Brain Res.* 145, 67–78.
- Mesulam, M.M., Mufson, E.J., Wainer, B.H., Levey, A.I., 1983. Central cholinergic pathways in the rat: an overview based on an alternative nomenclature (Ch1-Ch6). *Neuroscience* 10, 1185–1201.
- Minkeviciene, R., Ihälainen, J., Malm, T., Matilainen, O., Keksa-Goldsteine, V., Goldsteins, G., Iivonen, H., Leguit, N., Glennon, J., Koistinaho, J., Banerjee, P., Tanila, H., 2008. Age-related decrease in stimulated glutamate release and vesicular glutamate transporters in APP/PS1 transgenic and wild-type mice. *J. Neurochem.* 105, 584–594.
- Nitsch, R.M., Slack, B.E., Wurtzman, R.J., Crowdon, J.H., 1992. Release of Alzheimer amyloid precursor derivatives stimulated by activation of muscarinic acetylcholine receptors. *Science* 258, 304–307.
- Perez, S.E., Lazarov, O., Koprich, J.B., Chen, E.Y., Rodriguez-Menendez, V., Lipton, J.W., Sisodia, S.S., Mufson, E.J., 2005. Nigrostriatal dysfunction in familial Alzheimer's disease-linked APPswe/PS1DeltaE9 transgenic mice. *J. Neurosci.* 25, 10220–10229.
- Perry, E.K., Gibson, P.H., Blessed, G., Perry, R.H., Tomlinson, B.E., 1977a. Neurotransmitter enzyme abnormalities in senile dementia. Choline acetyltransferase and glutamic acid decarboxylase activities in necropsy brain tissue. *J. Neurol. Sci.* 34, 247–265.
- Perry, E.K., Perry, R.H., Blessed, G., Tomlinson, B.E., 1977b. Necropsy evidence of central cholinergic deficits in senile dementia. *Lancet* 1, 189.
- Perry, E.K., Kilford, L., Lees, A.J., Burn, D.J., Perry, R.H., 2003. Increased Alzheimer pathology in Parkinson's disease related to antimuscarinic drugs. *Ann. Neurol.* 54, 235–238.
- Peterson, G.L., 1977. A simplification of the protein assay method of Lowry et al. which is more generally applicable. *Anal. Biochem.* 83, 346–356.
- Raiteri, M., 2006. Functional pharmacology in human brain. *Pharmacol. Rev.* 58 (2), 162–193.
- Savonenko, A., Xu, G.M., Melnikova, T., Morton, J.L., Gonzales, V., Wong, M.P., Price, D.L., Tang, F., Markowska, A.L., Borchelt, D.R., 2005. Episodic-like memory deficits in the APPswe/PS1dE9 mouse model of Alzheimer's disease: relationships to beta-amyloid deposition and neurotransmitter abnormalities. *Neurobiol. Dis.* 18, 602–617.
- Savonenko, A.V., Xu, G.M., Price, D.L., Borchelt, D.R., Markowska, A.L., 2003. Normal cognitive behavior in two distinct congenic lines of transgenic mice hyperexpressing mutant APP SWE. *Neurobiol. Dis.* 12, 194–211.
- Selkoe, D.J., 2001. Alzheimer's disease: genes, proteins, and therapy. *Physiol. Rev.* 81, 741–766.
- Shemer, I., Holmgren, C., Min, R., Fulop, L., Zilberman, M., Sousa, K.M., Farkas, T., Hartig, W., Penke, B., Burnashev, N., Tanila, H., Zilberman, Y., Harkany, T., 2006. Non-fibrillar beta-amyloid abates spike-timing-dependent synaptic potentiation at excitatory synapses in layer 2/3 of the neocortex by targeting postsynaptic AMPA receptors. *Eur. J. Neurosci.* 23, 2035–2047.
- Sims, N.R., Bowen, D.M., Smith, C.C., Flack, R.H., Davison, A.N., Snowden, J.S., Neary, D., 1980. Glucose metabolism and acetylcholine synthesis in relation to neuronal activity in Alzheimer's disease. *Lancet* 1, 333–336.
- Sims, N.R., Bowen, D.M., Davison, A.N., 1981. [¹⁴C]acetylcholine synthesis and carbon ¹⁴C dioxide production from [^{U-}¹⁴C]glucose by tissue prisms from human neocortex. *Biochem. J.* 196, 867–876.
- Snowdon, D.A., 2003. Healthy aging and dementia: findings from the Nun Study. *Ann. Intern. Med.* 139, 450–454.
- Starke, K., 1987. Presynaptic alpha-autoreceptors. *Rev. Physiol. Biochem. Pharmacol.* 107, 73–146.
- Tsang, S.W., Lai, M.K., Kirvell, S., Francis, P.T., Esiri, M.M., Hope, T., Chen, C.P., Wong, P.T., 2005. Impaired coupling of muscarinic M(1) receptors to G-proteins in the neocortex is associated with severity of dementia in Alzheimer's disease. *Neurobiol. Aging* 27, 1216–1223.
- Tzavara, E.T., Bymaster, F.P., Felder, C.C., Wade, M., Gomeza, J., Wess, J., McKinzie, D.L., Nomikos, G.G., 2003. Dysregulated hippocampal acetylcholine neurotransmission and impaired cognition in M2, M4 and M2/M4 muscarinic receptor knockout mice. *Mol. Psychiatry* 8, 673–679.
- Zhang, W., Basile, A.S., Gomeza, J., Volpicelli, L.A., Levey, A.I., Wess, J., 2002. Characterization of central inhibitory muscarinic autoreceptors by the use of muscarinic acetylcholine receptor knock-out mice. *J. Neurosci.* 22, 1709–1717.